THE UNIVERSITY
of EDINBURGH

Stabilisation of hepatocyte phenotype using synthetic materials

Baltasar Lucendo Villarin

MRes

University of Edinburgh

2015

This dissertation is submitted for the degree

of Doctor of Philosophy

Declaration

This thesis is the result of my work and includes nothing that is the outcome of work done in collaboration, except where indicated in the text.

The work in this thesis has not been submitted for any other degree or professional qualification.

Baltasar Lucendo Villarin

Abstract

Primary human hepatocytes are a scare resource with limited lifespan and variable function which diminishes with time in culture. As a consequence, their use in tissue modelling and therapy is restricted. Human embryonic stem cells (hESC) could provide a stable source of human tissue due to their self-renewal properties and their ability to give rise to all the cell types of the human body. Therefore, hESC have the potential to provide an unlimited supply of hepatocytes. To date, the use of hESCs-derived somatic cells is limited due to the undefined, variable and xeno-containing microenvironment that influences the cell performance and life span, limiting scale-up and downstream application. Therefore, the development of highly defined cell based systems is required if the true potential of stem cell derived hepatocytes is to be realised. In order to replace the use of animal derived culture substrates to differentiate and maintain hESCs-derived hepatocytes, an interdisciplinary approach was employed to define synthetic materials, which maintain hepatocyte-like cell phenotype in culture. A simple polyurethane, PU134, was identified which improved hepatocyte performance and stability when compared to biological matrices. Moreover, the synthetic polymer was amenable to scale up and demonstrated batch-to-batch consistency. I subsequently used the synthetic polymer surface to probe the underlying biology, identifying key modulators of hepatocyte-like cell phenotype. This resulted in the identification of a novel genetic signature, MMP13, CTNND2 and THBS2, which was associated with stable hepatocyte performance. Importantly, those findings could be translated to two hESC lines derived at GMP. In conclusion, hepatocyte differentiation of pluripotent stem cells requires a defined microenvironment. The novel gene signature identified in this study represents an example of how to deliver stable hESCs-derived hepatocytes.

Lay Summary

Current animal and cellular hepatocyte models present limitations that make them unsuitable for clinical and toxicological applications. In the other hand, pluripotent stem cells under the correct stimuli can generate any cell type found in the human body including hepatocytes, the mayor cell type found in the liver. The ability to generate renewable sources of human hepatocytes has enormous potential to improve human health and wealth. One major obstacle to the routine deployment of stem cell-derived cells is their instability in culture due to the use of animal-derived culture substrates. To tackle this issue, I combined a synthetic polymer culture surface, polyurethane 134, previously identified as a surface that supports and promotes the generation of hepatocytes from pluripotent stem cells, with an animal-free and clinical grade hepatocyte differentiation approach to obtain stem cell-derived hepatocytes. This defined system represents a platform that permits informative and mechanism analysis of liver biology. The aim of this project is to understand how the synthetic polymer stabilise the pluripotent stem cell derived hepatocytes. From this study, I identified genes associated with stable hepatocyte function. Moreover, these findings were successfully translated to clinical grade human pluripotent stem cells. These findings hold a potential to manufacture stable clinical grade stem cell derived hepatocytes.

Table of Contents

List of figures and tables

Abbreviations

AFM	Atomic Force Microscopy
AFP	Alpha fetoprotein
Alb	Albumin
APC	Allophycocyanin
BAL	Bio-artificial Liver
bFGF	Basic Fibroblast Growth Factor
BMP	Bone Morphogenic Protein
BSA	Bovine Serum Albumin
C/EBP	CCAAT - Enhancer Binding Protein
Ca^{2+}	Calcium
CK19	Cytokeratin 19
CM	Conditioned Media
CTGF	Connective Tissue Growth Factor
CYP	Cytochrome P450
DAPI	4‘,6-diamino-2-phenylindole
DMEM	Dulbecco’s Modified Eagle's medium
DMSO	Dimethyl sulfoxide
DNA	Deoxyribonucleic acid
EB	Embryoid Bodies
E-Cad	E-Cadherin
ECL	Enhanced Chemiluminescence
ECM	Extracellular Matrix
EDTA	Ethylenediaminetetraacetic acid
EGF	Epithelial Growth Factor
EHS	Engelbreth-Holm-Swarm
FACS	Fluorescence Activated Cell Sorting

FBS	Foetal Bovine Serum
FGF	Fibroblast Growth factor
FITC	Fluorescein Isothiocyanate
Fox	Forkhead Box
GMP	Good Manufacture Practise
hESC	Human Embryonic Stem Cell
HGF	Hepatocyte Growth Factor
HLC	Hepatocyte-like cell
HNF	Hepatocyte Nuclear Factor
hPSC	Human Pluripotent Stem Cells
HRP	Horse Radish Peroxidase
HTP	High Throughput
ICM	Inner cell mass
iPSC	induce Pluripotent Stem Cells
KOSR	Knock-Out Serum Replacement
L15	Leibovitz's L-15 media
LETF	Liver-specific Transcription Factor
MAPK	RAS/MAP Kinase Pathway
MEF	Mouse embryonic fibroblast
MG	Matrigel™
MMP	Metalloproteinase
MT	mTeSR1™
OC	One-cut
Oct-4	Octamer 4
OSM	Oncostatin M
PAS	Peptide-acrylate Surface (PAS)
PBS	Phosphate Buffered Saline
PBS/T	Phosphate Buffered Saline/Tween
PCR	Polymerase Chain Reaction

PDGF	Platelet-derived Growth Factor
PE	R-Phycoerythrin
PI3K/AKT	Phosphoinositide 3-Kinase
PMEDSAH	2-(methacryloyloxy) ethyl dimethyl-(3-sulfopropyl) ammonium hydroxide
Prox1	Prospero Homeobox 1
PU134	Polyurethane 134
RNA	Ribonucleic acid
SD	Standard deviation
SEM	Scanning Electron Microscopy
siRNA	Small Interference Ribonucleotide acid
SNP	Single Nucleotide Polymorphism
Sox	SRY-box containing gene
SSEA	Stage-specific embryonic antigen
STM	Septum Transversum Mesenchyme
TF	Transcription Factor
TGFβ	Transforming Growth Factor-β
TIMPs	Tissue Inhibitors of Metalloproteinases
TRA	Keratan Sulfate Antigen
Wnt3a	Wingless-type MMTV integration site family, member 3a
ZO-1	Zona Ocludens-1
α-SMA	Alpha-Smooth Muscle

Acknowledgements

I would like to give thanks to all the people that during my life and especially in the last few years have helped me, not only in completing this thesis, but also in becoming a better person.

Firstly, I would like to thank MRC for providing the founding which allowed me to undertake this research. I also wish pass on my gratitude to my first supervisor Dr Dave Hay, for his support and guidance during my research, for always being approachable and sympathetic and especially for helping me to get the best out of myself in Science. In addition, I would like to acknowledge the help from my second supervisor, Prof Stuart Forbes, for keeping an eye out for and always making sure my research was going in the right direction.

My gratitude should also be registered to Prof Mark Bradley for providing me with the equipment, resources and suggestions to perform this study. Thanks also to Dr Jeffrey Wattson, from Chemistry department, for his positive input and generosity.

To Dr Teresa Bellon Heredia, for trusting me during and after my dissertation, which provided me with invaluable lab experience.

During this research I have had the good fortune to receive help and support from people at the Centre for Regenerative Medicine. To Dr Paul Travers for all his help and suggestions before and during my thesis; I will always be grateful to him. To Daga, for all her help during these years and bearing with me during my ups and downs; to Claire Medine, for all her teaching, support and good vibes during all these years; and especially to Kate Cameron, for making the lab a more human place to work; for all her help, support, suggestions and friendship during all these years, even well before the thesis.

I also would like to thanks my close people in Edinburgh that made life away from home an enriching experience. To Julio, for his patience with me, for all the adventures in the Highlands and abroad and for his care; to David, for his friendship, for the Fridays omelettes that kept me sane; to Pablo, for being an example of perseverance and overcoming, for transferring all his optimism to me. To Mike, for

his unconditional friendship, his good heart, his support and his encouragement, for reminding me that there was light at the end of the tunnel; to Ana, for sharing crazy runs in the hills, for her support and faith, not only in my thesis but also in life; to Gra, for her generosity, for her pizzas and yummy camp grub, for the bicycle trips, for being how she is. To Max, Ima, Oli, Truji, Irene, Ruth,… for making Edinburgh a better place to life.

I would also like to thank my friends in Spain. Despite the distance I always have them on my mind. To my loved friends Simon, Sergio and Chapiss I would not understand life without them. We grew up together and part of what I am is because of them. To Guille, Cafu and Rayo, for their friendship and support. To my university friends; to Dani, for the good times at the university in Madrid, for being an exemplar in science, for all his encouragement and for being there despite the distance; to Sara, for her persistence, her faith in me and for always being on my side. I consider all of you part of my family.

Especial thanks to my family for all their support. To my brother Alfredo, for being the first person to tell me about Science and instil a passion for it in me; to my mother, one of the most important persons in my life; for bringing me up, for fighting to give me a good education, for all her effort and encouragement, for prioritizing my well-being to her own. To my father and grandfather; despite the fact that you are longer here you inspire me, and I would not have made it without your efforts; wherever you are I hope I have made you proud. You are both shining examples of the kind of man I want to be.

Last but not least, thank you Amee. You have stood beside me during all these challenging years, for being so understanding, for all your help and support, for taking care of me, for growing up together at my side, part of this work is yours. And for more that I cannot express on paper.

Publications

The following papers were published during the course of my study for the degree of Doctor of Philosophy. The findings of this thesis are included, in part, in these publications; however, others are part of research collaborations:

Articles

- Polymer suppoted directed differentiation reveals a unique gene signature predicting stable hepatocyte performance. **Villarin BL**, Cameron K, Szkolnicka D, Rashidi H, bates N, Klimber SJ, Flint O, Forbes SJ, Iredale JP, Bradley M, Hay DC. Adv Healthc Mater. 2015 June 24. doi: 10.1002/adhm.201500391.
- Gene networks and transcription factor motifs defining the differentiation of stem cells into hepatocyte-like cells. Godoy P, Schmidt-Heck W, Natarajan K, **Lucendo-Villarin B,** Szkolnicka D, Asplund A, Bjorquist P, Widera A., Stoeber R, Campos G, Hammad S, Sachinidis A, Chaudhari U, Damm G, Weiss TS, Nussler A, Synnergren J, Edlund K, Küppers-Munther B, Hay D, Hengstler JG. J Hepatol. 2015 May 25. pii: S0168-8278(15)00340-2. doi: 10.1016/j.jhep.2015.05.013.
- Modulating innate immunity improves hepatitis C virus infection and replication in stem cell-derived hepatocytes. Zhou X, Sun P, **Lucendo-Villarin B**, Angus AG, Szkolnicka D, Cameron K, Farnworth SL, Patel AH, Hay DC. Stem Cell Reports. 2014 May 29; 3(1):204-14. doi: 10.1016/j.stemcr.2014.04.018.
- Stabilizing hepatocellular phenotype using optimized synthetic surfaces. **Lucendo-Villarin B**, Cameron K, Szkolnicka D, Travers P, Khan F, Walton JG, Iredale JP, Bradley M, Hay DC. J Vis Exp. 2014 Sep 26;(91):51723. doi: 10.3791/51723.
- Accurate prediction of drug-induced liver injury using stem cell-derived populations. Szkolnicka D, Farnworth SL, **Lucendo-Villarin B,** Storck C, Zhou W, Iredale JP, Flint O, Hay DC. Stem Cells Transl Med. 2014 Feb;3(2):141-8. doi: 10.5966/sctm.2013-0146.
- Deriving functional hepatocytes from pluripotent stem cells. Szkolnicka D, Farnworth SL, **Lucendo-Villarin B**, Hay DC. Curr Protoc Stem Cell Biol. 2014 Aug 1;30:1G.5.1-1G.5.12. doi: 10.1002/9780470151808.sc01g05s30.
- Developing high-fidelity hepatotoxicity models from pluripotent stem cells. Medine CN, **Lucendo-Villarin B**, Storck C, Wang F, Szkolnicka D, Khan F, Pernagallo S, Black JR, Marriage HM, Ross JA, Bradley M, Iredale JP, Flint O, Hay DC. Stem Cells Transl Med. 2013 Jul;2(7):505-9. doi: 10.5966/sctm.2012-0138
- Pluripotent stem cell-derived hepatocytes: potential and challenges in pharmacology. Szkolnicka D, Zhou W, **Lucendo-Villarin B**, Hay DC. Annu Rev

Pharmacol Toxicol. 2013;53:147-59. doi: 10.1146/annurev-pharmtox-011112-140306.

- Maintaining hepatic stem cell gene expression on biological and synthetic substrata. **Lucendo-Villarin B**, Khan F, Pernagallo S, Bradley M, Iredale JP, Hay DC. Biores Open Access. 2012 Jan;1(1):50-3. doi: 10.1089/biores.2012.0206.
- Robust generation of hepatocyte-like cells from human embryonic stem cell populations. Medine CN, **Lucendo-Villarin B**, Zhou W, West CC, Hay DC. J Vis Exp. 2011 Oct 26;(56):e2969. doi: 10.3791/2969.

Book Chapters

- Serum- Free Directed Differentiation of Human Embryonic Stem Cells to Hepatocytes. Cameron, K., **Lucendo-Villarin, B**., Szkolnicka, D., and Hay, DC. Methods in Molecular Biology: Protocols in In Vitro Hepatocyte Research. 2015. http://www.springer.com/in/book/
- Cell Matrix Interactions in Liver Development and Disease. **Lucendo Villarin B** and Hay DC. Advances in Medicine and Biology, Volume 46, 2012

Front Covers

- Villarin, B Lucendo., Cameron, K., Szkolnicka, D., Rashidi, H., Bates, N., Kimber, SJ., Flint, O., Forbes, SJ., Iredale, JP., Bradley M. et al. Polyurethane: Stable Cell Phenotype Requires Plasticity: Polymer Supported Directed Differentiation Reveals a Unique Gene Signature Predicting Stable Hepatocyte Performance. Adv Healthc Mater. 2015. 4(12):1819.

CHAPTER ONE

GENERAL INTRODUCTION

1.1 Human embryonic stem cells

Human embryonic stem cells (hESCs) are pluripotent cells which give rise to all somatic cell types found in the body. hESCs represent a real alternative to generate unlimited amount of somatic cells. hESCs possess two properties that make them ideal candidates: the unlimited self-renew ability that allows them to make identical copies of themselves without developing chromosomal abnormalities or undergoing growth arrest, and the pluripotency capacity to differentiate into any cell of the human body (Cai *et al*., 2006; Hoffman and Carpenter, 2005; Vazin and Freed, 2010). In addition, the known genetic background of the cells allows the obtaining of the desire cell type with a known and stable genotype. These characteristics make hESCs a valuable tool with different applications, including understanding the complex mechanism involved during the development of specialised cells and establishment of organ structures, drug discovery, predictive toxicology and regenerative medicine (Greenhough *et al*., 2010; Rippon and Bishop, 2004).

1.1.1 hESC derivation

Human embryonic stem cells (hESCs) are derived from the inner cell mass of blastocyst stage embryos (Thomson, 1998). The formation of a diploid zygote, known as blastocyst, results from the fertilisation of an egg. The blastocyst consists on an inner layer of cells called the embryoblast that develops into the embryo; and an outer layer of cells called trophoblast which will eventually give rise to the placenta, chorion and the umbilical cord. Pioneers studies in mouse ESCs and in culturing techniques developed in non-human ESC lines (Josephson *et al*., 2006; Thomson *et al*., 1996), lead to the generation of human ESC lines by Thompson and colleagues (Thomson, 1998) and Reubinoff and colleagues (Reubinoff *et al*., 2000). The hESC lines generated retained their pluripotency, were kariotypically normal,

and upon injection into immunodeficient mouse they generated germ layers containing cell from the three germ layers.

Isolation of the ICM has been traditionally performed using two different techniques: immunosurgery and mechanical dissection. Immunosurgery requires the use of animal-derived products that prevent the use of the hESCs in transplantation therapies; while mechanical and enzymatical isolation do not required these animal-derived products, obtaining hESCs at a suitable grade for clinical applications.

However, the use of the ICM at the blastocyst stage involves ethical issues. In order to avoid these issues, different groups tried to isolate cells at the morula or blastomere stage with variable success rates, obtaining hESCs with inefficient differentiation capacity (Klimanskaya *et al*., 2006; 2007; Strelchenko *et al*., 2004). This issue was resolved by Chung and collaborators by supplementing the culture media with laminin, mimicking the stem cell niche (Chung *et al*., 2008).

1.1.2 Characterisation of hESCs

hESCs are characterized using an array of stem cell specific markers including; the expression of the ES specific transcription factors Sox 2 (Avilion *et al*., 2003), Octamer binding protein 4 (Oct-4) (Pesce *et al*., 1999; Schöler *et al*., 1989) and Nanog (Chambers *et al*., 2003; Mitsui *et al*., 2003); the cell surface markers including the globoseries glycolipid antigen designated stage specific embryonic antigens (SSEA)-4 (Kannagi *et al*., 1983); the keratin sulphate related antigens (or tumour recognition antigens) TRA -1-60 and TRA-1-81 (Andrews *et al*., 1984) and their morphology. hESC morphology *in vitro* is characterized by the display of tightly packed colonies with well-defined edges and a high nucleus to cytoplasm ratio with a pronounced nucleoli (Pera *et al*., 1999).

Different from human somatic cells, hESCs display an unlimited life span independently from genetic alterations or inactivation of tumour suppressor

pathways (Brandenberger *et al*., 2004; Rosler *et al*., 2004). However, prolonged maintenance *in vitro* can lead to karyotypic abnormalities in processes similar to the tumorigenic events that occurs *in vivo* (Baker *et al*., 2007; Draper *et al*., 2003; Mitalipova *et al*., 2005). Therefore, different techniques including giemsa-stained karyotyping (Campos *et al*., 2009), DNA microarrays, short tandem repeat analysis, fluorescent in situ hybridization and whole genome single nucleotide polymorphism (SNP) can also be employed to confirm the precise hESC signature within the population (Brimble *et al*., 2005; Josephson *et al*., 2006; Mitalipova *et al*., 2005). The pluripotency ability of the hESCs confers them with the capacity to differentiate to cell types of the three primary germ layers; ectoderm, mesoderm and endoderm; and cell types derived from these primary germ layers, including from ectoderm neurons (Schuldiner *et al*., 2001) and keratinocytes (Guenou *et al*., 2009), from the mesoderm skeletal muscle (Abujarour *et al*., 2014), cardiomyocytes (Kehat *et al*., 2001) and hematopoietic cells (Chadwick *et al*., 2003), and from the endoderm liver (Hay *et al*., 2008a), lung (Wong *et al*., 2012) and pancreas (Cho *et al*., 2012).

1.1.3 In vitro growth and maintenance of hESCs

A successful hESC culture requires the maintenance of indefinite self-renewal properties. Mouse embryonic fibroblasts (MEFs) were firstly used to support propagation of hESCs in the undifferentiated stage (Reubinoff *et al*., 2000). Since then, in order to move to a xeno-free hESC culture system various approaches using human-derived cell types have been used, including feeder cells derived from fallopian tube epithelium (Bongso *et al*., 1994), foetal foreskin, muscle (Amit *et al*., 2004; Richards *et al*., 2002), bone marrow (Cheng *et al*., 2003) or amniotic epithelium (Gumbiner *et al*., 1996).

If hESCs are to be employed in clinical or therapeutic applications, generation of fully defined culture systems are required. As a result, great efforts were put in developing fully defined systems. Xu and colleagues (Xu *et al*., 2001) developed a

feeder free culture condition using Matrigel™, a matrix secreted by Engelbreth-Holm-Swarm (EHS) mouse sarcoma cells, but still in the presence of a culture media conditioned by embryionic fibroblast cells supplemented with basic fibroblast growth factor (bFGF). Subsequently, different approaches have been successfully applied on maintaining hESC pluripotency on recombinant proteins including, vitronectin (Braam *et al*., 2008), laminin (Rodin *et al*., 2010) or a combination or laminin 521 and E-Cadherin (Rodin *et al*., 2014), resulting in improved hESC cultures.

In addition to culture substrate optimisation, studies have focused on identifying the secreted factors released by the feeder layers responsible for the maintenance of the hESC pluripotent state. Overall, studies have shown the following proteins to be essential for sustaining undifferentiated proliferation of hESCs in serum-free media: high concentrations of bFGF, Activin A, transforming growth factor beta-1 (TGFβ-1) and the bone morphogenic protein (BMP) repressor Noggin (Levine *et al*., 2005; Wang *et al*., 2005; Beattie *et al*., 2005; Pera *et al*., 2004). In order to standardise the hESC culture techniques, companies have released to the market defined xeno-free media, being StemPro® (Invitrogen) and mTeSR1™ (Stem Cell Technologies) the most effective (Hannoun *et al*., 2010). Recently, the new fully defined E8™ media has been shown to promote efficient self-renewal and differentiation of hESCs and iPSCs (Chen *et al*., 2011).

Despite all the advances made in developing feeder-free and serum-free defined conditions for maintenance of hESCs, a deeper understanding of the mechanism involved in the stabilisation and maintenance of the pluripotency in hESCs is still required.

1.1.4 Methods for expansion of hESCs

The high self-renewal capacity of hESCs, which is dependent on the culture conditions and the hESC line itself, involves the necessity of performing frequent passages and transfers to freshly prepare substrate upon confluency. The cells can

be mechanically, enzymatically or chemically disaggregated, using collagenase IV, dispase, trypsin or EDTA (Chen *et al*., 2011; Hoffman and Carpenter, 2005; Mei *et al*., 2010). The potential clinical applications of the hESCs require the use of recombinant animal-free enzymes such as human collagenase (Crook *et al*., 2007), which has shown to be equally successful. However, there are disadvantages associated with either method. While mechanical passaging is labour intensive and cannot be accurately reproduced; enzymatic or chemical passaging can damage cells by the removal of important surface proteins or ions and have been linked to genetic abnormalities (Brimble *et al*., 2005; Draper *et al*., 2003; Mitalipova *et al*., 2005; Shirahashi *et al*., 2004). Different alternatives have been proposed as a solution to avoid genetic instability including bulk passaging and single cell dissociation (Ellerström *et al*., 2006). As such, manufacturing of a robust and reliable large-scale expansion of undifferentiated hESCs requires the development of an automated approach (Joannides *et al*., 2006).

1.1.5 The hESC microenvironment

Stem cells are surrounded by their specific microenvironment *in vivo*, composed of cells, cytokines, and extracellular matrix (ECM). Cell-to-microenvironment interactions trigger the activation of various cell functions; including proliferation, self-renewal, differentiation and maintenance of the undifferentiated state of the cells (Joddar *et al*., 2014). As such, mimicking the niche and the cell natural environment are required for the maintenance of the 'stemness'. For this purpose, the use of biological-derived substrates represents an attractive approach. For example, Melkoumian and colleagues reported that conjugation of components of the extracellular matrix including, vitronectin, laminin, fibronectin and bone sialoprotein to a peptide-acrylate surface (PAS) retained hESC specific properties. The resulting cells were efficiently differentiated into functional cardiomyocytes in a scalable manner (Melkoumian *et al*., 2010). In addition to the use of biological derived substrates for the maintenance of the 'stemness', researches have focused on developing strategies involving the use of synthetic polymers, either alone or in

combination with biological-derived substrates, to simulate the hESC microenvironment. Villa-Diaz and colleagues described a synthetic polymer, poly [2-(methacryloyloxy) ethyl dimethyl-(3-sulfopropyl) ammonium hydroxide] (PMEDSAH) that supported long term self-renewal and pluripotency of undifferentiated hESCs when cultured in a number of serum containing and serum-free media (Villa-Diaz *et al*., 2010). The structure–function relationship between material properties and biological performances was highlighted by Mei and colleagues as they showed that combination of vitronectin with high-acrylate content polymers could successfully maintain the pluripotency properties and colony formation of the hESCs for a prolonged period of time (Mei *et al*., 2010). Hydrogels, structures composed of cross-linked and hydrophilic polymer scaffolds which expand into an ECM-like gel state when exposed to water, have been also employed in hESC cultures. A synthetic polymer hydrogel made by crosslinking acrylic acids and acrylate peptides with an independently tuned matrix stiffness and ligands density was found to support short term hESC self-renewal (Li *et al*., 2006). Zhan and colleagues described a synthetic thermoresponsive acrylate based hydrogel that supported long term hESC growth and pluripotency, involving reagent free dissociation passaging in response to a reduction in ambient temperature (Zhang *et al*., 2013).

Despite that most of the hESC culture conditions rely on two-dimensional surfaces, different research have shown that three-dimensional cultures provide a more accurate culture environment for hESCs, leading to improved maintenance of pluripotency, proliferation and cell survival (Yim and Leong, 2005). A study performed on mouse ESCs using a synthetic polyamide matrix scaffold mimicking the basement membrane, demonstrated that Nanog expression was enhanced by activation of the GTPase Rac and the subsequent induction of the phosphoinositide 3-kinase pathway (PI3K), that resulted in a gain in proliferative ability (Nur, 2005). To date, a hyaluronic acid (HA) hydrogel has been shown to replicate major components of the ECM abundant in embryos and stem cells niches, maintaining hESCs in undifferentiated state while preserving their differentiation abilities (Gerecht *et al*., 2007).

1.2 Reprograming and programing

Somatic adult cells represent an alternative source to hESCs to obtain tissue specific cell types. This can be achieved by two different strategies; either by reprograming somatic adult cells into induced pluripotent stem cells (iPSCs) prior to their differentiation into specific cell types; or by directly reprograming adult somatic cells to another type of cell in a process known as transdifferentiation. The use of adult somatic cells to obtain differentiated cell types represents a promising alternative for downstream applications; including disease modelling, drug discovery and personalised cell therapies as it reduces the complications associated with the immune-rejection. Moreover, the use of adult somatic cells overcomes the controversy associated with the ethical issues associated to the origin of hESCs (Chakraborty *et al*., 2010).

1.2.1 iPSCs

Induced pluripotent stem cells (iPSCs), like hESCs, possess the capacity to self-renew and differentiate into any cell type of the adult body. Different techniques have been developed to reprogram cells to a pluripotent state. Gurton and colleagues, pioneers in these reprograming techniques, employed somatic cell nuclear transfer (SCNT) to obtain totipotent cells by earing lineage-specific signatures in the nuclei of a somatic cell. Despite that this approach has been successfully employed in mouse cells; it has not been reported in humans. Fusion of somatic cells with pluripotent cells represents another approach employed to obtain pluripotent cells. Still, the karyotyping abnormalities of the resulting cells limit their use (Yamanaka and Blau, 2010).

The limitations of these techniques were overcome by employing a new strategy developed by Yamanaka and colleagues, in which mouse embryonic fibroblasts (MEFs) and adult mouse tail-tip fibroblasts were reprogrammed to induce pluripotent stem cells (iPSCs). The authors employed retrovirus-mediated transfection of a core of transcription factors known as the Yamanaka factors;

namely POU5F1 (Oct 4), SOX2, KLF4 and c-Myc (Takahashi and Yamanaka, 2006), subsequently reported in human adult fibroblasts (Takahashi *et al*., 2007). While the resulting mouse iPSCs generated were able to form embryoid bodies as well as teratomas containing all three germ layers, when cells were injected into a donor mouse blastocyst they could not form chimeric mice, the most thorough test of pluripotency. This issue was solved by using Nanog to select reprogramed cells instead of FbX15, a gene expressed during co-expression of the Yamanaka factors (Okita *et al*., 2007).

The trasnfection of the reprograming factors into the terminally differentiated somatic cells can be done by two types of methods accordingly to the integration of the viral vector into the host cell genome: integrating viral vector systems and integrating free vectors systems. Integrating viral vector systems such as retroviral and lentiviral transduction are highly efficient (Brambrink *et al*., 2008; Stadtfeld *et al*., 2008; Takahashi *et al*., 2006; Touboul *et al*., 2010). However, these techniques possess the risk of tumour formation. Non integrating methods include the use of viral vectors such as Adeno virus (dsDNA) and Senday virus (RNA) (Takahashi *et al*., 2006; Touboul *et al*., 2010), transfer of plasmids containing reprograming factors (Yu *et al*., 2009), direct delivery of reprograming proteins by fusing them with a cell penetrating peptide (Kim *et al*., 2009) or the use of self-replicating RNA replicon (Yoshioka *et al*., 2013). Recently, it has been shown that iPSCs can be generated from a variety of terminated somatic cell populations including pancreatic cells, keratinocytes, ESCs derived hematopoietic cells and primary human hepatocytes (Liu *et al*., 2010; Okita and Yamanaka, 2010).

1.2.2 Transdifferentiation

Transdifferentiation, like reprograming of adult somatic cells, represents a promising approach to obtain different cell types. Transdifferentiation possesses advantages to the use of iPSCs. The process is faster and more efficient, reducing

the risk of pluripotency-associated tumorigenesis and immunogenicity, recently identified in iPSCs (Zhao *et al*., 2011).

Traditional methods of transdifferentiation of somatic cells into another cell type have relied in the expression of single transcription factor (TF) or a core of tissue specific TFs. Transient expression of a single TF has been successfully applied in transdifferentiating different cell types, including fibroblasts into myoblast by ectopic expression of MyoD (Davis *et al*., 1987; Huang *et al*., 2011), pancreatic cells into hepatocytes by inducing the expression of C/EBPβ (Shen *et al*., 2000) or a reciprocal transition between myeloid cells and megakaryocytes induced by the expression of GATA1 (Pang *et al*., 2011). However, the use of a single TF to induce transdifferentiation is restricted to certain cell lineages.

Therefore, researches successfully explored the possibility of employing several tissue specific TFs to transdifferentiate somatic cells into different cell types of the three germ layers. For example, human and mouse fibroblasts have been converted into functional neurons (Pang *et al*., 2011; Pfisterer *et al*., 2011; Vierbuchen *et al*., 2010), macrophages-like cells, hepatocyte-like cells (Huang *et al*., 2011) and cardiomyocyte-like cells (Ieda *et al*., 2010). In addition, other types of somatic cells have been transdifferentiated using lineage specific transcription factors; including pancreatic exocrine cells to obtain beta-cells (Zhou *et al*., 2008) and mesoderm to cardiac myocytes (Takeuchi *et al*., 2009). However, the use of these lineage specific transcription factors does not allow isolation, expansion and characterisation of the reprogrammed cells, limiting their use in clinical applications.

As such, combinations of iPSC transcription factors (iPSC-TFs) with cell-type-specific signals represent an alternative to directly generate differentiated cells from somatic cells. This technology possesses advantages compared with conventional iPSC reprograming processes, which are generally slow, involving several steps with low efficiency, which results in populations of pluripotent cells displaying unstable epigenetics. In addition to the use of iPSC-TF, direct conversion of somatic cells into the desire cell type requires efficient differentiation approaches of pluripotent cells

into terminated differentiated cells. This technology has been successfully applied to directly transdifferentiate fibroblasts to cardiac (Efe *et al*., 2011), neural (Kim *et al*., 2009) and blood progenitor cells (Szabo *et al*., 2010).

1.3 Current sources of hepatocytes

Currently, freshly isolated primary human hepatocytes represent the current gold standard model to study human hepatocyte biology *in vitro* and recapitulate the functional response of the liver, especially for studies to predict *in vivo* drug metabolism and clearance (Hewitt *et al*., 2007; Obach, 2009). While primary hepatocytes offer significant functional benefits, the methods employed to isolate and culture hepatocytes represent a limitation for their use. Collagenase digestion followed by a series of density-gradient centrifugation steps represents the most effective and standardise method to isolate primary hepatocytes from intact liver tissues (LeCluyse *et al*., 2005). However, during the initial stages of isolation, primary hepatocytes undergo a process of dedifferentiation denoted by changes in cell morphology, structure, polarity, a drastic decrease in liver specific gene expression and liver specific functions, including CYP-activity and albumin production (Bader *et al*., 1992; Dunn *et al*., 1989; LeCluyse, 2001; LeCluyse *et al*., 1996; Nelson *et al*., 1982), in a process referred as dedifferentiation, which represents an important limitation for the use of primary hepatocytes. In an effort to extend culture longevity, both in terms of liver specific functions and basic cellular functionality, a number of approaches have been developed; including adjustment of the culture medium and the extracellular matrix, changes in the cell culture format and culturing hepatocytes with other cell types (Griffith and Swartz, 2006; LeCluyse, 2001; LeCluyse *et al*., 1996; Meng *et al*., 2010). Despite advantages observed with certain approaches, the scarcity, low proliferative capacity and quality still hinder the use of human hepatocytes in the study of the human biology and toxicity studies (Fox and Strom, 2008). As a result, low quality fragments displaying high levels of phenotypic variation are frequently used for research, which leads to difficulties in reliably studying human hepatocyte biology. As a

consequence, alternative models are used, including human cell lines, progenitor cells from adult liver and animal liver models.

Hepatocarcinoma derived cell lines and immortalised human hepatocyte cell lines have been widely used in an attempt to enhance cell availability. In contrast to primary cell cultures, human tumour-derived cell lines, including the well characterised hepatocellular carcinoma derived cell lines HepG2 and HepaRG (Guillouzo *et al*., 2007), are not restricted to a limited number of cell divisions (Mees *et al*., 2009; Shay and Wright, 2005). Therefore, they represent a ready available and scalable resource of cells that can generate relevant data to humans. However, the differentiated cellular characteristics, genomic instability (Wong *et al*., 2000), their cancerous nature and incomplete expression of metabolic enzymes of these cells makes them an unreliable cell source to be used in therapy, human biology studies and toxicology test (Brandon *et al*., 2003; Richert, 2006; Rodríguez-Antona *et al*., 2002; Takahashi *et al*., 2006). As such, researches have focused on immortalising human primary hepatocytes (Allen *et al*., 2001). For this purpose different techniques, including transfecting cells with the simian virus 40 Tantigen (SV 40 Tantigen) (Li *et al*., 2005; Schippers *et al*., 1997), lipofectamine mediated co-transfection of albumin promoter regulated constructs (Werner *et al*., 1999) and retrovirus mediate transfer of oncogenes (Kobayashi *et al*., 2003) have been employed. However, the risks of tumorigenic effects and possible damages in the DNA regulatory transfected regions have not been explored in much detail, limiting their use in downstream applications.

Hepatoblast and hepatic progenitor cells, the resident stem cell population of the liver, are cell capable of differentiating into both cholangiocytes and hepatocytes (Herrera *et al*., 2006; Rogler, 1997). However, their low number and limited proliferative capacity make them difficult to isolate, expand and purify, limiting their use (Alison *et al*., 2007; Fiegel *et al*., 2006; Vessey and la M. Hall, 2001).

As an alternative to human *in vitro* models, porcine, rodent and other animal hepatocytes have been widely applied in developmental and preclinical studies.

However, their lack of predictability, the presence of xeno-contaminants and high phenotypic variations make them an inaccurate and unreliable substitute for human hepatocytes as they do not accurately mimic the mechanisms found in humans (Behnia *et al*., 2000; Guillouzo, 1998). As such, there is an urgent need for reliable and predictable *in vitro* hepatocyte models.

1.4 Liver development

Human liver development is a complex process that requires an extensive network of signals from the extracellular matrix and nearby mesoderm, acting in a time- and/or dose- dependent manner. However, to truly appreciate the potential of the hESCs in downstream applications including regenerative medicine and studying of the human body development, it is important to understand the origin and function of these cells during human development.

1.4.1 Mammalian embryonic development

Following fertilisation of an egg the resulting single cell, known as zygote, undergoes a series of divisions resulting in a cluster of 4-16 smaller cells called the morula (Hardy *et al*., 1989), which is surrounded by a glycoprotein membrane called the zona pellucida (Biswas and Hutchins, 2007). As the development progresses the cells of the morula, known as blastomere, continue to divide forming a central fluid cavity called the blastocoel (Hardy and Spanos, 2002) that contains a cell mass known as blastocyst. The blastocyst, in early embryo development, consists of an outer layer of cells known as trophectoderm and an inner cell mass (ICM) developed from the primitive blastocyst (figure 1A) (Johnson *et al*., 1986). Embryonic stem cells can be isolated from the ICM at this developmental stage. By the time of implantation, the ICM separates from the trophoblast forming a cavity known as amniotic cavity. Differentiation of the inner cell mass originates two specialized cell types, hypoblast and epiblast cells, surrounding the amniotic cavity (figure 1B)

(Gardner and Rossant, 1979). While the hypoblast will form the yolk sac, all tissues in the adult body will developed from the epiblast (Rossant, 2008).

The next step in the development, known as gastrulation, involves the formation from the epiblast of a thick ridge of cells called the primitive streak (PS). Exposure of the cells to signalling pathways such as Activin/Nodal, BMPs, FGFs and Wnt will induce the cells to migrate towards or inwards the primitive streak, resulting in the formation of the three germ layers. These three layers of cells, ectoderm, mesoderm and endoderm, will form all of the cells types found in the adult body (figure 1C) (Lawson *et al*., 1991).

1.4.2 Hepatic Endoderm Specification

During the migration of the newly specified endoderm through the primitive streak, the embryo undergoes a series of movements and rotations causing the endoderm to become the innermost layer (Lawson and Pedersen, 1987). In parallel to the migration process, the endodermal cells continue to expand eventually forming the anterior, posterior and lateral domains, converging on each other to form a closed primitive gut tube (figure 1D). The primitive tube is subdivided into three domains: foregut, midgut and hindgut (figure 1E). As development continues the hindgut domain develops into the large intestine, the midgut into the small intestine, while the foregut produces the thyroid, oesophagus, lungs, liver, pancreas, the biliary tree and stomach.

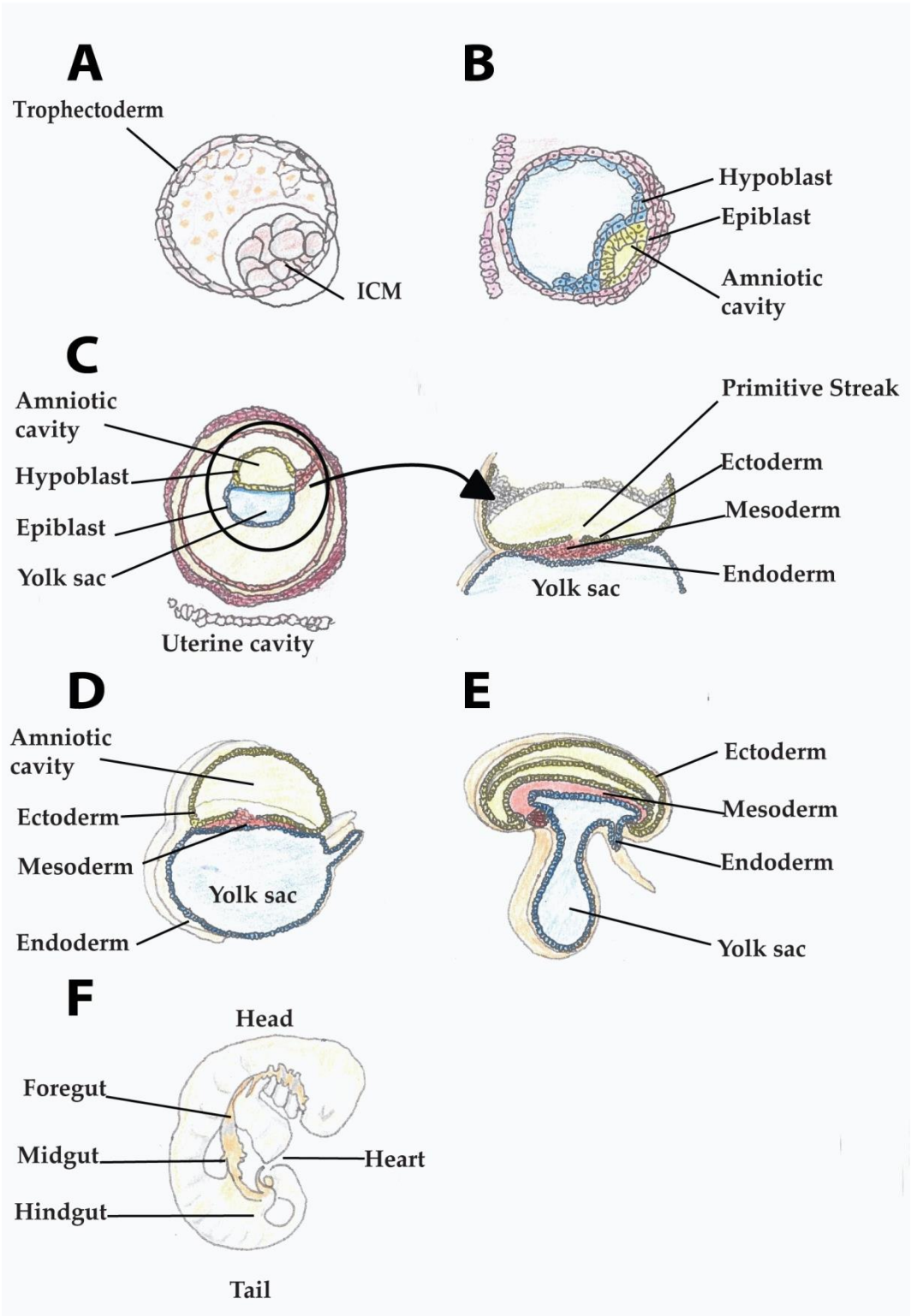

Figure 1. Early mammalian gut development. (A) Fertilisation of an egg and subsequent cell divisions result in the formation of the blastocyst, which consist of an outer layer of trophectoderm and an inner cell mass, which (B) flattens into a flattened disk made up of two cell layers: the epiblast and the hypoblast surrounding the amniotic cavity. (C) Gastrulation follows soon after implantation and begins with the formation of the primitive streak, formed by the rearrangement and movement of

the epiblast, which results in the formation of the three embryonic germ layers, and (D-E) the differentiation into the ectoderm, mesoderm, and endoderm. (F) As development progresses the endoderm layer expands forming a primitive gut tube with distinct foregut, midgut and hindgut domains. Modified from Gieseck *et al*., 2001.

Fate-mapping experiments in mouse embryos at embryonic day 8.0 of gestation (e8.0) have revealed the presence of three distinct domains of hepatic progenitor cells: two lateral paired domains and a third ventral midline domain of the foregut from where the liver originates (Tremblay and Zaret, 2005; Zaret and Grompe, 2008). At this stage, albumin, alpha-fetoprotein and transthyretin are expressed in a portion of the ventral endoderm, representing the first molecular evidence of the liver development (Agarwal *et al*., 2008; Hay *et al*., 2008a). Migration of the lateral domains towards the midline and fusion with the ventral domain initiates the closure of the foregut, resulting in a single prehepatic domain lying adjacent to the developing heart at e9.0 and in close apposition to regions of lateral plate mesoderm, which will ultimately generates the mesothelial cells of the proepicardium and septum transversum.

Previous studies in chick, frog, mouse and zebrafish models revealed that coordinate signalling of fibroblast growth factor (FGF) -1 and -2 from the developing cardiac mesoderm, and bone morphogenetic proteins (BMP) -2 and -4 from the septum transversum mesenchyme (STM) are critical in hepatic induction (Calmont *et al*., 2006; Jung, 1999; Rossi *et al*., 2001).

The main source of FGFs is the developing cardiac mesoderm (Deutsch *et al*., 2001; Serls *et al*., 2005), playing a critical role in the induction of hepatic cells (Gualdi *et al*., 1996). The FGF-mediated hepatic cell fate specification is evolutionarily highly conserved and acts in a concentration dependent manner (Cheng *et al*., 2003; Shin *et al*., 2007). During liver development, the morphogenetic changes observed result in the distancing between the hepatic endoderm and the cardiac mesoderm (Jung, 1999). Consequently, the concentration of FGFs decreases, inhibiting the differentiation into an anterior fate such as the lungs. FGF concentration gradients

induce varied vital responses for synchronizing developmental events (Serls *et al*., 2005). Cultures of ventral endoderm in the presence of absence of different members of the FGF family demonstrated that FGF1 and FGF2 can induce the expression of the characteristic marker of hepatic cell fate albumin (Gualdi *et al*., 1996; Jung, 1999). The use of signalling inhibitors on embryo tissue explants and whole-embryo cultures revealed that the FGF signalling activates the RAS/MAP kinase pathway (MAPK) ERK1 and ERK2 (Bottcher, 2005; Corson, 2003; Schlessinger, 2004) and the phosphoinositide 3-kinase pathway (PI3K/AKT). While ERK is involved in enhancing hepatic gene expression and nascent hepatocyte stability, PI3K/AKT pathway activation seems to be involved in the hepatic growth (Calmont *et al*., 2006).

Proliferation and complete differentiation of the nascent hepatic endoderm require the signalling molecules members of the transforming growth factor beta (TGFβ) superfamily, secreted by the septum transversum mesenchyme, the bone morphogenic protein (BMP) -2 and -4. BMP2 and BMP4 cooperate with FGF signalling to encourage hepatic competence and specification of the primitive endoderm via GATA4, a GATA zinc finger transcription factor (Huang *et al*., 2008). DNA foot-printing analyses of the transcriptional regulatory elements controlling the onset of albumin expression during hepatic development revealed bounding of GATA4 and the transcription factor Forkhead box (Fox) A at the gene promoter (Bossard and Zaret, 1998), making it accessible to additional transcription factors such as hepatocyte nuclear factor 1 (HNF1) and CCAAT-enhancer binding protein beta (C/EBPβ), resulting in the transcriptional activation of albumin.

Binding of BMP -2 and -4 to the constitutively active serine/threonine kinase type II receptors induces the phosphorylation of the Gly-Ser (GS) domains in the kinase type I receptors, leading to their activation. The receptor complex subsequently phosphorylates Smad1, Smad5 and Smad8, which is then able to complex with Smad4, regulating the gene transcription in the nucleus (Heldin *et al*., 1997; Shi and Massagué, 2003).

The WNT signalling pathway is also implicated during the onset of the hepatic development. However, contrary to the clear inductive role for FGF and BMP signalling, the contribution of WNT signalling is complex, contributing differently depending on the developmental stage (McLin *et al*., 2007). At early somite stages, WNT signalling displays repressive effects in the posterior endoderm inhibiting the expression of Hhex, an essential transcriptional regulator of hepatic development; in the anterior endoderm, the expression of WNT antagonists relives the expression of Hhex, promoting the commitment of the endoderm to a hepatic fate. Following specification, WNT signalling appears to promote liver bud growth and differentiation in multiple systems including *Xenopus*and zebrafish (Goessling *et al*., 2008; Shin *et al*., 2007).

1.4.3 Formation of the Hepatic Bud from Hepatic Endoderm

1.4.3.1Proliferation and Migration

Liver bud originates from the newly specified ventral endodermal cells, called at this stage hepatoblast. The liver bud, at e9.5, begins to thicken as the cells transit from a simple cuboidal to a pseudostratified columnar epithelium (Bort *et al*., 2006), expressing hepatocyte genes; including albumin, alpha-fetoprotein and hepatocyte nuclear factor 4α (HNF4α); all of them considered indicators of early hepatic fate (Lemaigre and Zaret, 2004; Zaret and Grompe, 2008). Between e9.0 and e9.5, the laminin and collagen IV -rich basal layer surrounding the developing hepatic endoderm breaks down (Zaret, 2002; Zhao and Duncan, 2005) and the hepatoblasts delaminate and migrate into the STM to form the nascent liver bud (Bort *et al*., 2006; Margagliotti *et al*., 2008; Medlock and Haar, 1983; Shiojiri and Sugiyama, 2004). This process is controlled by an extensive network of transcription factors involved in cell migration and adhesion; including Hhex, Prox-1 and the Onecut factor 1 (OC-1, also known as HNF6α) and Onecut-2 (HNF6β).

The expression of the homeobox transcription factor Hhex, a transcription factor critical for proliferation and migration of endoderm cells beyond cardiogenic mesoderm, is required to ensure cell pseudostratification (Bort, 2004; Bort *et al*., 2006). Transactivation of this factor is induced by GATA4 and/or GATA6 (Denson *et al*., 2000; Watt *et al*., 2007; Zhao *et al*., 2005), being the latest required to maintain the differentiation state of the hepatoblast (Zhao and Duncan, 2005). Hepatoblast delamination is controlled by the homeodomain transcription factor Prox1. The prospero-related homeobox 1 (Prox1) is involved in degrading the basal matrix surrounding the liver bud, promoting the hepatoblast delamination and migration from the surrounding basal layer into the STM (Sosa, 2000), a process involving a downregulation in the expression of E-Cadherin (Bort *et al*., 2006; Medlock and Haar, 1983). Onecut factors OC-1 and OC-2 are involved in the morphogenesis and expansion of the liver primordium by controlling a gene network involved in cell adhesion and hepatoblast migration (Margagliotti *et al*., 2007). This gene network regulates the expression of extracellular matrix (ECM) proteins and ECM remodelling enzymes, such as the matrix metalloproteinases (MMPs) -14, expressed in the hepatic progenitors, and MMP-2, expressed predominantly in the surrounding mesenchyme (Margagliotti *et al*., 2007; Medico *et al*., 2001; Papoutsi *et al*., 2007). Endothelial precursor cells lie between the developing hepatic epithelium and the STM. The close contact with blood vessels persists as hepatoblasts migrate into the stroma. Null mutations in the vascular endothelial growth factor receptor gene Vegfr-2 (also known as Flk-1) result in embryos lacking endothelial cells with liver buds failing to delaminate (Matsumoto, 2001). In addition, inhibition of angiogenesis represses liver bud growth in culture, suggesting that endothelial cells provide important paracrine and physical factors which promote hepatoblast migration and proliferation.

1.4.3.2 Liver Bud Growth

Paracrine signals from surrounding and hepatic mesenchyme induce a tremendous liver bud growth between days e9.5 and e15. Coordinate signalling from FGF8, via

PI3K pathway, and BMP4 (Jung, 1999; Rossi *et al*., 2001; Sekhon *et al*., 2004), in conjunction with Wnt/β-catenin signalling, promotes hepatic growth (McLin *et al*., 2007;; Monga *et al*., 2003).

Hepatocyte growth factor (HGF), a potent mitogen expressed by mesenchymal cells, is needed in hepatoblast migration (Deutsch *et al*., 2001; Medico *et al*., 2001; Michalopoulos and Bowen, 1993), in part by activating the small GTPase Arf6 (Suzuki *et al*., 2006). HGF binding to the tyrosine kinase receptor c-Met expressed in the neighbouring epithelial cells (Iida *et al*., 2003; Ishikawa *et al*., 2001), and TGFβ signalling activation via Smad2/Smad3 pathway (Weinstein *et al*., 1994) are also required for the stimulation of hepatoblast proliferation (Birchmeier *et al*., 2003; Bladt *et al*., 1995; Moumen *et al*., 2007; Sachs *et al*., 2000; Schmidt *et al*., 1995). Data suggest that HGF and TGFβ signalling act in parallel converging on β1-integrin, regulating and controlling hepatic architecture (Weinstein *et al*., 1994). In addition, FGF and HGF signalling stimulate many of the same intracellular kinase cascades, including MAPK and PI3K pathways, and both have been reported to stimulate the activity of β-catenin in the liver bud, suggesting crosstalk with the Wnt pathway (Berg *et al*., 2007; Monga *et al*., 2003; Sekhon *et al*., 2004). β-catenin, best known as a mediator of the canonical Wnt signalling pathway, is predominantly expressed at the periphery of the developing liver lobes, which correspond with growth zones. β-catenin interacts with c-Met in hepatocytes and upon HGF binding, it is translocated to the nucleus (Monga *et al*., 2003). Also, FGF-10, secreted by myofibroblastic cells, controls the activation of β-catenin stimulating the proliferation of hepatoblast (Berg *et al*., 2007).

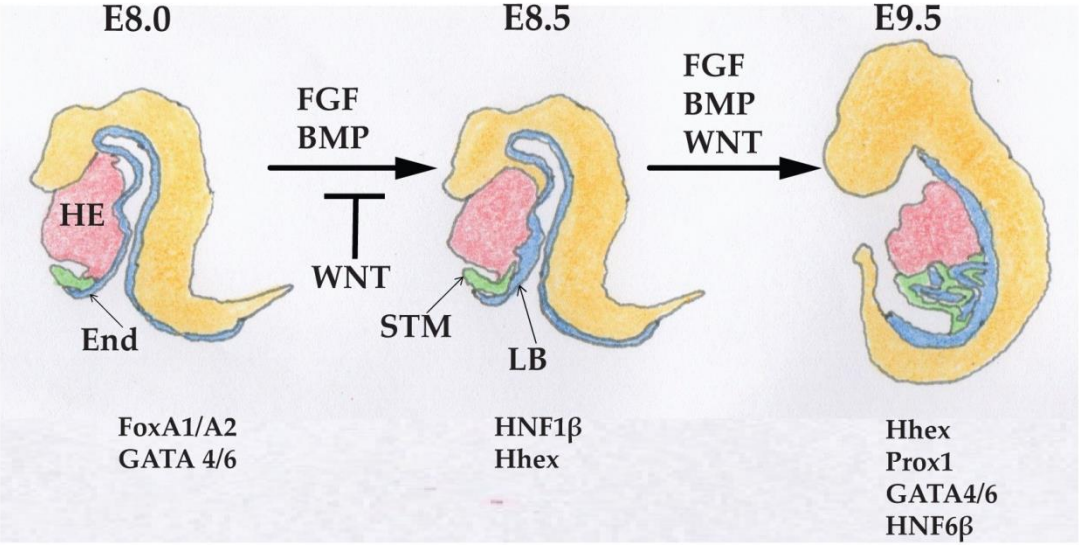

Figure 2. Hepatic endoderm specification. The illustration reflects the onset of liver parenchyma cells indicating signalling molecules and transcription factors important in the process. Wnt signalling, at early stages in the differentiation process, promotes posterior endoderm identity and must be inhibited anteriorly by local Wnt antagonist expression for the progression of the liver development. At late stages, Wnt signalling acts in parallel with FGF and BMP signalling, driving hepatic specification, expansion and differentiation. Days refer to mouse development. Foregut endoderm (End; blue), heart (HE; red), liver bud (LB; blue), septum transversum parenchyme (STM; green). Modified from Duncan *et al*., 2005.

1.4.4 Hepatocyte Specification

When the liver buds out of the endoderm, soon after mesenchyme invasion, around e13 in mouse development, the bipotential hepatoblasts soon face a decision to differentiate into either hepatocytes or cholangiocytes, also known as biliary epithelial cells.

The decision to differentiate into hepatocytes (AFP+/albumin+) or cholangiocytes (cytokeratin (CK)-19+) (Jung, 1999) requires the correct balance of a complex cell signalling network acting in a gradient manner. The localisation of the hepatoblast within the developing liver determines the differentiation of the cells. While hepatoblasts surrounding the liver parenchyma differentiate into hepatocytes, cholangiocytes will originate from hepatoblasts found at the portal mesenchymal (Lemaigre and Zaret, 2004).

Previous studies have revealed that a gradient of Activin and TGFβ has a crucial role in the hepatocyte specification. The gradient in the expression of both factors is negatively modulated by the transcription factors Onecut-1 and Onecut-2 (Clotman, 2005), favouring the hepatocyte differentiation. This pathway acts in coordination with Jagged-Notch pathway in supporting biliary differentiation (McCright *et al*., 2002; Tanimizu, 2004).

1.4.5 Hepatocyte Maturation

Soon after hepatoblasts fate the decision to differentiate into hepatocytes, additional signals from haematopoietic cells such as the cytokine oncostatin M (OSM), act in combination with hepatocyte growth factor (HGF), regulating hepatocyte maturation in a process that goes even after birth.

Oncostatin M, a member of the interleukine-6 (IL-6) family, by binding the gp130 membrane receptor promotes morphological maturation into polarized epithelium via K-ras and E-cadherin (Matsui *et al*., 2002; Michalopoulos *et al*., 2003; Suzuki *et al*., 2003; Tan *et al*., 2008), through the JAK/Stat3 signalling pathway (Ito *et al*., 2000; Kamiya *et al*., 1999). The hepatocyte growth factor, HGF, promotes the organisation of hepatocytes into cord-like structures by regulating the expression of diphosphate-ribosylation factor 6 (ARF6), an enzyme involved in actin cytoskeleton remodelling. In addition, some evidences suggest that TNFα, via activation of the transcription nuclear factor κB (NF-κB), balances HGF and OSM activity, inhibiting maturation and maintaining the proliferative capacity of foetal hepatocytes, thus allowing the liver to grow to the appropriate size before differentiating (Kamiya and Gonzalez, 2004). TNFα repression after birth is necessary to obtain fully mature hepatocytes expressing cytochrome P450 genes (Hart *et al*., 2009).

During maturation, the liver-enriched transcription factors including C/EBPα, HNF1α, HNF3α-γ, nuclear hormone receptors and HNF4α, act in a complex inter-regulatory network to control hepatocyte gene expression (Cheng *et al*., 2006; Odom, 2004; Qu *et al*., 2007). HNF4α expression strongly correlates with

hepatocyte cell phenotype (Bulla, 1997; Späth and Weiss, 1997), playing an essential role in hepatocyte function by regulating a cascade of essential transcription factors involved in the correct development of the foetal liver architecture (Chen *et al*., 1994; Li *et al*., 2000). Data suggests that HNF4α binds to the promoters of nearly half of the genes expressed in the mouse liver (Odom, 2004), including genes encoding cell adhesion and functional proteins important in hepatocyte epithelial structures (Konopka *et al*., 2007; Satohisa *et al*., 2005). Previous observations suggest that HNF4α could induce expression of HNF1α (Taraviras *et al*., 1994). HNF1α and C/EBPα expression, which is induced by HGF (Soriano *et al*., 1995; Tomizawa *et al*., 1998) are essential to ensure complete hepatocyte maturation and metabolic hepatic functions (Pontoglio *et al*., 1996; Wang *et al*., 1995).

HNF4α and Wnt signalling, among other factors, are involved in the liver metabolic zonation, which begins after birth (Jungermann and Katz, , 1989). Based on the expression of a number of metabolism-regulating genes, within the hepatic lobule a periportal zone from a pericentral zone can be distinguished. HNF4α induces the expression of certain metabolic related genes in the pericentral zone. Null HNF4α livers display the same expression of such metabolic genes in both zones; periportal and pericentral zone (Stanulović *et al*., 2007). Equally, Wnt signalling is involved in the regulation of the metabolic zonation, whereas its receptor β-catenin is expressed in the perivenous area, and the β-catenin negative regulator APC is expressed in periportal hepatocytes (Benhamouche *et al*., 2006).

1.5 Liver architecture

The acquisition of the correct tissue architecture within the organs is crucial in order to ensure a normal body function. The liver is the largest internal organ, compromising one fiftieth of the total weight of the adult body. The liver exhibits both endocrine and exocrine properties. Endocrine functions include secretion of hormones, clotting factors and serum proteins such as albumin, which condition the

blood; while the generation and secretion of bile and drug metabolism are the major exocrine function.

The basic structural unit of the liver is the liver lobule, which displays a polygonal structure with a central vein localised in the centre of the lobule and a portal triad consisting on the hepatic artery, bile duct and hepatic portal vein. The basic functional unit of the liver is called acinus. The acinus is formed by plates or cords of hepatocytes, generally one cell thick in mammals, radiating from the central vein and lined by sinusoidal capillaries. Blood enters the lobule via the portal triad of vessel, flows through the parenchyma and exists via the central vein. This flow creates a chemical gradient and distinct microenvironments (Gebhardt and Baldysiak, 2007; Ugele *et al*., 1991) which divides the acinus into three zones accordingly to their function. The periportal zone or zone 1, responsible for oxidative metabolism, gluconeogenesis and ureagenesis; the pericentral zone or zone 3, responsible for glycolysis, liponeogenesis and metabolism of xenobiotics; and a mid-lobular region or zone 2 that displays a mixture of zone 1 and zone 3 functions (Turner *et al*., 2011).

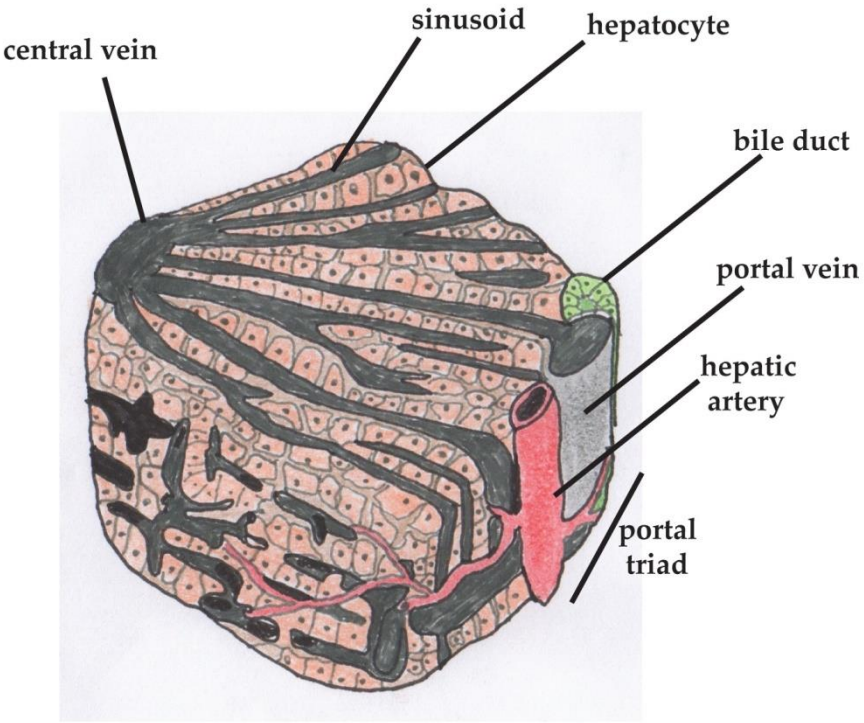

Figure 3. Liver architecture. Illustration showing overall structure of a portion of a liver lobule. Modified from Si-tayeb *et al*., 2010.

The cells comprising the liver can be divided into two categories: parenchymal cells and non-parenchymal cells. The parenchymal fraction consists on hepatocytes, the major cell type of the liver, making up to 80% of the total liver volume and 60% of the total cell population in the liver. The non-parenchymal fraction includes bile duct epithelial cells, liver sinusoidal endothelial cells, hepatic stellate cells and Kupffer cells.

Hepatocytes are highly differentiated epithelial cells that perform the major functions associated with the liver, including protein, fat, steroids and xenobiotics metabolism. The hepatocyte morphology is characterised by the possession of a cuboidal shape with one or more nuclei, with polyploidy cells, 4N or 8N, increasing in number from zone 1 to zone 3 (Deutsch *et al*., 2001) and a prominent nucleoli. Hepatocytes display abundant mitochondria with Golgi complexes adjacent to the bile canaliculi and the cytoplasm is rich in rough and smooth endoplasmic

reticulums, which are indicative of the hepatocyte secretory nature and enzymes of the phase I and phase II drug metabolism, respectively.

The non-parenchymal cells display important roles in the regulation of the hepatic growth and functions, including the production of growth factors and other mediators of cellular function. Liver sinusoidal endothelial cells (LESC) are thin and elongated cells located in the hepatocyte basolateral surface, delimiting a space known as Space of Disse or perisinusoidal space. Their plasma membrane possesses abundant fenestrations that increase the contact between the hepatocytes and the circulating blood, allowing the diffusion of small substances to the hepatocytes (Cogger *et al*., 2010). Hepatic stellate cells (HSC), also known as Ito cells, are found embracing the endothelial cells in the Space of Disse. These cells are involved in the sinusoid contractility, matrix remodelling and hepatocyte proliferation during liver regeneration by secreting cytokines, including HFG, TGFα and EGF (Friedman, 2008). In addition, HSC are responsible for the increase deposition of extracellular matrix observed during the progression of liver cirrhosis, which can be resolved by the action of cytokines secreted by the resident macrophages of the liver, with a mesenchymal origin, the Kupper cells (Jaeschke, 2007).

The hepatic progenitor cells (HPC) are the epithelial cells that line the bile ducts. Hepatoblasts are found in a compartment contained within the canals of Hering. These canals represent the smallest and most peripheral branches of the biliary tree connecting the bile canalicular system with the interlobular ducts (Gaudio *et al*., 2009). Under normal circumstances HPC display a relatively low proliferation rate. However, upon continuous damage or severe loss of the epithelial cells of the liver, HPC are activated and expand from the canals of Hering to the pericentral zone, giving rise to mature hepatocytes or cholangiocytes (Forbes *et al*., 2002).

Epithelial organs possess two domains on opposite surface of an epithelial sheet, the apical (luminal) and basolateral (blood-facing) domains. However, hepatocytes possess two basolateral domains interfacing with the sinusoidal microvasculature on opposite sides of the single cell layers or plates known as sinusoidal domains and

an apical domain, lying between the lateral domains of opposing epithelial cells forming the canalicular domain. The canalicular domain forms a belt like structure around the periphery of each hepatocyte that, by interconnecting with canaliculi from adjacent cells, forms a network of small tubular compartments terminating at the portal triad and interconnecting with bile ducts via the canals of Hering, eventually draining into the common bile duct and the gall bladder. Both surfaces display different biochemical characteristics critical for maintaining normal hepatic function (Chapman and Eddy, 1989): the basolateral domains of the hepatocytes are responsible for the exchange of metabolites with the blood and establish interactions with the ECM providing support and anchorage for the cells; and the apical domain is responsible for the transport of bile acids and detoxification products into the canaliculus that surrounds the hepatocyte (Decaens *et al*., 2008).

The extracellular matrix (ECM) of the liver is found in the Space of Disee, between the hepatocytes and the liver sinusoidal endothelial cells. It has an important role in directing and maintaining both architecture and phenotypic gene expression of liver cells. The ECM is a thin layer which composition varies in a gradient manner, paralleled by those of soluble signals. Generally, the ECM in the liver consists mostly of fibronectin, proteoglycans and collagens, mainly type I and minor quantities of types III, IV, V, and VI (Martinez, 1995), favouring a rapid bidireccional exchange of macromolecules between plasma and hepatocytes. In addition, the niche of the hepatic progenitor cells is rich in laminins (Lorenzini *et al*., 2010).

1.6 Generation of *in vitro* hepatocyte-like cells from pluripotent stem cells or somatic cells

Different sources of hepatocytes, including primary hepatocytes, hepatocyte cell lines and non-human derived hepatocytes have been employed to satisfy the current high demand. Although the use of these sources is widely extended, they possess limitations restricting their use in downstream application. Primary hepatocytes, although considered the current 'gold standard', display an instable

phenotype. In addition, the scarcity and quality of the available primary human hepatocytes restrict their use (Gómez-Lechón *et al*., 2010; Hewitt and Lechón, 2007). Hepatocarcinoma derived cell lines and immortalised human hepatocytes display a genomic instability and incomplete expression of hepatocyte specific functions (Wong *et al*., 2000). Non-human hepatocytes show a high phenotypic variation, the risk of xeno-contaminants and the difficulty to translate the findings to the human hepatocyte biology, which prevent their use as a reliable replacement for human hepatocytes (Behnia *et al*., 2000; Guillouzo, 1998).

Therefore, there is an urgent need for reliable and predictable *in vitro* hepatocyte models. As such, the self-renewal and pluripotent nature of pluripotent stem cells in combination with efficient hepatocyte differentiation approaches make them an ideal and reliable source of human hepatocytes. Moreover, the knowledge gained from reprograming somatic cells into pluripotent stem cells can be successfully applied to directly transdifferentiate somatic cells into another cell type, confers the somatic cells with the capacity of becoming a potential source of hepatocytes to be used in downstream applications.

Discoveries in the mechanism of the liver development along with the emergence of pluripotent stem cell technologies have allowed the improvement of existing differentiation protocols to obtain hepatocyte-like cells (HLCs) from pluripotent stem cells and somatic cells, in processes that mimic the patterns and stages observed during embryologic development. The protocols developed generally used two different strategies, either cellular aggregation strategies via embryoid body formation or differentiation in a monolayer culture.

1.6.1 Differentiation via Embryoid Bodies (EBs)

In an attempt to mimic the cell-to-cell and the cell-to-ECM interactions observed during development *in vivo*, researches developed protocols involving aggregation strategies through the formation of three-dimensional structures called embryoid bodies (EBs). Embryoid bodies result from the spontaneous differentiation of

aggregated ES cells in suspension or using low adhesion specialized plates. EBs are characterized by the expression of markers from the three embryonic germ layers.

Lavon and colleagues developed a strategy to isolate cells primed towards the endoderm fate from suspension cultures of hESCs-derived EBs, using hESCs labelled with a reporter gene expressed under the control of a hepatocyte specific promoter (albumin-eGFP). The resulting isolated cells grown as a monolayer in the presence of a media supplemented with bFGF, displayed enhanced expression of albumin, suggesting that hepatic cells developed *in vivo* in a niche next to the cardiac mesodermal cells (Lavon *et al*., 2004). The effect of different components of the extracellular matrix (ECM) in hepatic differentiation was tested by several groups. Schwartz and colleagues observed an improvement in the gene expression of endodermal markers in hESCs-derived EBs on collagen I coated plates in the presence of FGF4 and HGF (Schwartz and Linehan, 2005). Sirahashi and colleagues highlighted the importance that the culture conditions, including medium, substrates, foetal bovine serum (FBS) and growth and differentiation factors possess in the hepatocyte differentiation of both, human and mouse ESc (Shirahashi *et al*., 2004). Baharvand and colleagues revealed that three-dimensional cultures enhanced hepatocyte differentiation when compared with two-dimensional cultures as 3D resembles more closely the *in vivo* environment (Baharvand *et al*., 2006).

Despite the initial promising findings, the stochastic and spontaneous differentiation that EBs undergo result in heterogeneous population of different cells lineages with poor hepatocyte differentiation efficiency. To address this issue, research have focused in developing differentiation protocols in a stepwise manner resembling the processes observed during liver development *in vivo* in an EB independent manner.

1.6.2 Direct differentiation of hESC into hepatocyte-like cells (HLC)

There are a big number of differentiation protocols for deriving functional hepatocyte-like cells from hESC in a step-wise manner, using animal derived matrices including, collagen, gelatin or Matrigel™ as basement membrane. Most of the available differentiation protocols try to mimic the hepatogenesis processes that occur during development *in vivo*, consisting in different steps; priming of the hESC towards definitive endoderm prior to hepatic endoderm induction and followed by inducing hepatocyte maturation in the hepatic endoderm generated. The resulting HLCs are characterized using a number of specific assays, including gene and protein expression, urea production, cytochrome P450 activity, serum protein production and glycogen storage. However, the exact approach varies between laboratory groups.

1.6.2.1 Endoderm specification

The existing protocols to induce endoderm differentiation on an EB independent manner tried to mimic the processes that occur during development *in vivo*.

D'Amour and colleagues developed an efficient differentiation protocol to derived hESCs into definitive endoderm using high concentrations of Activin A (D'Amour *et al*., 2005). Activing A mimics nodal signalling, a member of the transforming growth factor-β (TGFβ) superfamily that plays a critical role in the initiation of the development of the endoderm during gastrulation (Green and Smith, 1990). Treatment with Activin A resulted in over 80% of the cells expressing the endoderm marker Sox 17 and FoxA2 (Cereghini, 1996; Cirillo *et al*., 2002). Ishii and colleagues studied the endoderm differentiation under the presence of several factors including HGF, BMP4, FGF4 and ATRA (all-trans-retinoic acid) on different extracellular matrix components. They found that sequential addition of Activin A and HGF on Matrigel coated dishes produced higher yield of AFP positive cells (Ishii *et al*., 2008).

The WNT signalling pathway is also implicated during the onset of the hepatic development. Studies in the role of Wnt and β-catenin signalling during the differentiation and proliferation of pre-hepatic endodermal cells have led to improvements in the endoderm specification from hESCs (Burke *et al*., 2006; Fletcher *et al*., 2008; McLin *et al*., 2007). Hay and colleagues studied the expression of Wnt signalling during liver development. Their findings reveal the importance of Wnt3a signalling in Primitive Streak (PS) and endoderm development. Wnt3a expression during liver development during the first trimester is restricted to the portal system, while in the second trimester it is also detected in the liver parenchyma suggesting a potential role in early hepatogenesis. By applying this knowledge, they found that a treatment of Activin A in combination with Wnt3a leaded to a more rapid and enhanced endodermal differentiation that resulted in more functional HLCs (Hay *et al*., 2008a).

1.6.2.2 Hepatic specification and differentiation

Cai and colleagues developed a differentiation protocol that mimicked the *in vivo* situation. After priming hESCs towards definitive endoderm employing Activin A, they generated hepatic endoderm by treating cells with FGF4 and BMP2. The resulting cells were differentiated towards HLCs in a two-stage differentiation strategy. The hepatic endoderm was committed to the hepatocyte fate by using a media supplemented with HGF, followed by a hepatocyte maturation induced by OSM and dexomethasone. The resulting cells expressed a range of adult liver markers including CYP7A1, CYP3A4 and CYP2B6, tyrosine aminotransferase, tryptophan oxigenase2, phosphoenolpyruvate carboxykinase (PEPCK). Moreover, the authors detected hepatocyte functions including albumin secretion, glycogen storage and inducible cytochrome P450 activity. Interestingly, these cells were susceptible to hepatitis C virus HCV infection (Cai *et al*., 2007).

Agarwal and colleagues employed FGF4 and HGF to promote hepatic specification on hESCs-derived endoderm cultured on collagen I coated wells. Following this,

hepatocyte differentiation and maturation of the endoderm-derived cells was induced using a combination of BSA, FGF4, HGF, OSM and dexamethasone, obtaining HLCs expressing a number of hepatocyte specific markers including albumin, alpha-fetoprotein (AFP), CYP3A4 and CYP7A1. Hepatocyte functions including glycogen storage and albumin secretion were detected. In addition, cells were injected in a damaged mouse liver, reporting expansion and repopulation of the liver (Agarwal *et al*., 2008).

Brolen and colleagues demonstrated that induction of definitive endoderm with Activin A and FGF2 excluded the extraembryonic differentiation of hESCs. Following hepatic specification using combinations of BMP2 and -4 with FGF1, -2 and -4, hepatocyte maturation was induced employing a cocktail of different factors including EGF, insulin, transferrin, ascorbic acid, FGF4, HGF, dexomethasone, dimethyl sulfoxide (DMSO) and OSM. They successfully applied this differentiation protocol to three different hESC lines. The resulting HLCs displayed hepatic functions including, urea secretion, glycogen storage and cytochrome P450 activity (Brolén *et al*., 2009).

Basma and colleagues reported a differentiation approach involving an initial EB formation step. The hESCs-derived EBs were plated on matrigel and treated with Acticin A and FGF2. Hepatic specification and maturation was induced using HGF and DMSO, followed by a treatment with dexamethasone. Enrichment of the HLC population was performed employing FACS sorting for ASGPR positive cells, a specific feature of mature hepatocytes; obtaining HLC population with comparable function to adult hepatocytes. Furthermore, engraftment of the enriched population of cells after the splenic injection was observed, displaying proliferation and secretion of functional liver-specific proteins (Basma *et al*., 2009).

Touboul and colleagues obtained hepatic progenitor cells from hESCs-derived definitive endoderm cells by applying a treatment with FGF10, retinoic acid and SB431542, a pharmacological inhibitor of activin/nodal pathway. The authors suggested that retinoic acid plays an important role in hepatic specification, which is

synergized by FGF10 and Wnt signalling. The generated bipotential progenitor cells could be efficiently differentiated into cholangiocytes displaying structural and functional similarities to bile duct cells in normal liver (Dianat *et al*., 2014). Hepatocyte differentiation was induced using FGF4, HGF and EGF, generating HLCs that, post-injection, successfully engrafted in a mouse liver secreting human albumin (Touboul *et al*., 2010).

Hay and colleagues induced hepatic specification from hESCs-derived endodermal cells by supplementing the media with DMSO, an organosulfur compound that induces the acetylation of the histones. Hepatocyte differentiation was induced employing a serum containing media supplemented with HGF and OSM. The resulting HLCs were capable of repopulating a damage liver of a mouse, displaying biliary duct-like structures, parenchymal hepatocyte markers and myofibroblast markers (Hay *et al*., 2008a). Furthermore, engrafted cells still secreted human serum albumin three months post-transplantation (Payne *et al*., 2010).

1.6.3 Hepatocyte differentiation of iPSCs

The self-renewal and pluripotent properties displayed by induce pluripotent stem cells (iPSCs) make them an attractive cell source to generate HLCs. In addition, the possibility to obtain autologous iPSCs makes them an ideal source of somatic cells to be used in disease modeling and transplantation. The existent hepatocyte differentiation protocols of hESCs have been successfully fine-tuned to generate HLCs from iPSCs.

Si-Tayeb and colleagues described a four step differentiation protocol in low oxygen to obtain functional HLCs with no differences compared with hESCs-derived HLCs regarding to morphological features, mRNA fingerprint and integration into the mouse hepatic parenchyma *in vivo* (Si-Tayeb *et al*., 2010).

The differentiation protocol developed by Hay and colleagues was successfully translated into iPSC technology by Sullivan and colleagues. The authors successfully

differentiated three iPSC lines, obtaining HLCs displaying cytochrome P450 activity and secreting liver specific protein including albumin, alpha-fetoprotein and fibronectin (Sullivan *et al*., 2009).

Song and colleagues applied a multi-phasic differentiation approach of iPSC to obtain HLCs which displayed liver cell markers and liver related functions including urea production, albumin secretion and cytochrome P450 activity comparable with hESCs-derived HLCs (Song *et al*., 2009).

Despite the encouraging outcomes, most of the current hepatocyte differentiation approaches deliver somatic cells in two dimensional cell cultures displaying many typical hepatocyte characteristics. While these attributes are promising, they lack in mimicking the three dimensional *in vivo* microenvironment (Yim and Leong, 2005), as demonstrated by a low cellular polarity or limited functionality under standard culture conditions for certain toxicity testing. In order to overcome this issue, researches have focused on developing differentiation strategies employing three dimensional *in vitro* platforms including spheroids culture plates and bioreactors.

As such, Takayama and colleagues developed a three-dimensional spheroid culture system to obtain hESC- and iPSC-derived HLCs that predicted sensitively drug-induced hepatotoxicity (Takayama *et al*., 2013). Vosough and colleagues described a stirred-suspension bioreactor culture to obtain iPSC-derived HLCs that, post-transplantation into the spleens of a mouse with liver injury, successfully engrafted with cells displaying expression of different liver specific enzymes and secreted albumin (Vosough *et al*., 2013). Sivertsson and colleagues compared the efficiency in the differentiation towards the hepatocyte lineage of hESCs between a two-dimensional culture system and a three-dimensional bioreactor system, suggesting an improvement in the hepatic differentiation when the three dimensional system was applied (Sivertsson *et al*., 2012). While these approaches marked significant progress, their complexity and/or undefined nature limited a large scale development of the technology.

1.6.4 Hepatocyte differentiation from somatic cells-transdifferentiation

The knowledge acquired from reprograming somatic cells into induced pluripotent stem cells (iPSCs) indicated that somatic cells could be directly reprogramed or transdifferentiated into another cell type. As such, this knowledge has been applied to successfully transdifferentiate mouse and more recently human fibroblast into HLCs.

Sekiya and colleagues transfected mouse embryonic and adult fibroblast with HNF4α plus FoxA1, -A2 or -A3 successfully obtaining induced HLCs (iHLCs) expressing hepatocyte functions such as glycogen storage and uptake of low-density lipoproteins (LDL). In addition, the resulting cells displayed features of hepatocyte polarization including the canalicular membrane protein multidrug resistance-associated protein (Mrp 2), the basolateral membrane protein Mrp4 and the tight junction protein ZO-1. Moreover, post-injection in a fumarylacetoacetate hydrolase-deficient mouse liver, cells successfully engrafted and reconstituted the hepatic tissue, and despite they stopped proliferating after 2 months, cells responded to a two-thirds partial hepatectomy (Sekiya and Suzuki, 2011).

Another independent study performed by Huang and colleagues, employed mouse tail fibroblast as starting cell population, and using lentivirus expression of GATA4, HNF1α and Fox3, they observed that inactivated $p19^{Arf}$ was a requirement to overcome the proliferative limitation of the cells. The resulting population of iHLCs expressed hepatocyte genes and proteins including albumin, AFP, HNF4α and cytochrome P450 enzymes specific to mature hepatocytes. In addition, iHLC were capable of metabolizing toxicological compounds. Moreover, these cells were successfully transplanted *in vivo* and repopulated the livers of mice with acute liver failure (fumarylacetoacetate-hydrolase-deficient mice), rescuing more than half of the recipients (Huang *et al*., 2011).

Moreover, recently the same group reported successful reprograming of human fibroblast into iHLC by lentivirus expression of FoxA1, HNF1α and HNF4α. The

resulting iHLCs expressed hepatocyte genes and displayed functional characteristic of mature hepatocytes, including biliary drug clearance and cytochrome P450 activity. In addition, upon transplantation into fumarylacetoacetate-dehydrolase-deficient mice, iHLCs restored the liver function (Huang *et al*., 2014).

Despite all the recent advantages made in the field, most of the current differentiation approaches to obtain HLC from pluripotent stem cells and somatic cells rely on the use animal derived matrices, which suffer from batch-to-batch variation and instability, influencing the reproducibility and phenotypic stability of the cells. As such, it is necessary to identify synthetic matrices that can ensure the delivery of reliable and stable HLCs without compromising their functional capacities.

1.7 Biomaterials in stem cell technology.

Since the derivation of human embryonic stem cells (hESCs) from the inner cell mass of blastocyst embryos research has put great efforts in using these cells in clinical and research applications. Traditionally, human pluripotent stem cells (hPSCs) have been cultured *in vitro* employing feeder layers such as mouse embryonic fibroblast (MEFs) or extracellular matrices such as matrigel. These matrices successfully maintain the undifferentiated and pluripotent state of the cells by secreting or providing essential cytokines and growth factors to the culture media, such as TGFβ and activin A, and extracellular matrices (ECM) such as laminins (Xu *et al*., 2001). However, these matrices display inconsistencies in the expression and secretions of these factors and pathogenic and immunogenic contaminations that can influence the cell function and phenotype (Mallon *et al*., 2006). As such, the use of these cells in downstream applications such as treatment of human diseases, or interpretation of mechanistic studies designed to understand the biology of the PSCs and their relation with the surrounding cells and microenvironments is limited (Brafman *et al*., 2009). Consequently, in an attempt to overcome these limitations, researches have focused on developing xeno-free,

chemically defined substrates (biomaterials) that efficiently replace the use of animal-derived culture substrates in hPSC cultures. As such, different strategies have been developed, including; recombinant proteins such as collagens, vitronectin and laminins (Braam *et al*., 2008; Brafman *et al*., 2010; Rodin *et al*., 2014; 2010); synthetic peptides such as GAGs (glycosaminoglycans) and heparin binding peptides (Klim *et al*., 2010), and synthetic polymers.

Synthetic polymers are a type of biomaterials. Broadly, biomaterials can be classified into polymers, metals, ceramics and composites. Polymers, physical networks made out of monomers subunits, have gained the attention of the stem cell field due to their physical properties including their inert nature, diverse composition, their extensive forms and their capacity to interact with other synthetic or recombinant derived substrates, all of which make them attractive substrates for clinical and research applications.

Due to the anchorage-dependent nature of the pluripotent stem cells, synthetic materials employed in the culture of hPSCs must allow cell adhesion, spreading and colony formation while maintaining the genetic stability, self-renewal and pluripotent state of the cells for a high number of passages (Villa-Diaz *et al*., 2013). Cell polarity has also been demonstrated to maintain the undifferentiated state of hPSC. For example, the cell adhesion molecule E-Cadherin is co-expressed with other typical undifferentiated markers, including the cell surface markers SSEA-4, TRA-1-60 and TRA-1-81 as well as pluripotency factors Oct-4, Nanog and Sox2 (Li et al., 2012). In addition, these materials require being compatible with the sterilisation treatment of the culture plates, being cost-effective and having the potential to be scaled-up for commercial purpose.

1.7.1 Polymers in pluripotent stem cell cultures

Several materials have been combined with polymers and employed as stem cell culture substrates, including peptide, protein-based systems and biomolecules, with promising results in the maintenance of hPSC cultures (Gao *et al*., 2009; Mei *et al*.,

2010). However, the presence of peptides or recombinant proteins can increase the cost of the substrates, possess risk of xeno-contaminant, batch-to-batch variations and have the risk of going under degradation from the metalloproteinases secreted by the cell cultures, all of which compromise the cell performance (Villa-Diaz *et al*., 2013). As such, attention has focussed on developing fully synthetic substrates for the maintenance of PSCs.

Poly [2-(methacryloyloxy) ethyl dimethyl-(3-sulfopropyl) ammonium hydroxide] (PMEDSAH) represents one of the most extended synthetic substrates studied in the maintenance of PSC. It has been shown to successfully support long-term culture of several hESC and iPSC (Villa-Diaz *et al*., 2010). Aminopropylmethacrylamide (APMAAm) represent another example of synthetic substrate that has been successfully employed in the long-term maintenance of undifferentiated PSCs, by promoting the adsorption of different proteins presented in the culture media, mainly bovine serum albumin (BSA), which was identified as an essential component to promote cell adhesion (Irwin *et al*., 2011). The importance of media protein adsorption in the maintenance of PSCs was also revealed by Mei and colleagues, by identifying a polymer generated from monomers with high acrylate content that displays the capacity of fixing vitronectin from the culture media to promote colony formation, revealing the importance of physical parameters of the polymers including wettability, surface topography and surface chemistry (Mei *et al*., 2010).

Although synthetic polymers represent a more economical and stable approach to culture hPSCs, these platforms are still applied in 2D systems, which limit the mimicking of the three dimensional *in vivo* cell-to-cell and cell-to-ECM interactions. As such, different approaches have been employed to emulate a three dimensional culture system, including the use suspension cultures, bioreactors and hydrogels.

Amit and colleagues developed a free serum culture media supplemented with IL6RIL6 (interleukin-6 receptor interleukin-6 fusion protein) that supported long-term aggregated cultures of hPSCs in suspension while maintaining their

pluripotency abilities (Amit *et al*., 2010). Steiner employed similar approach and obtained suspension cultures of hPSCs that maintained their pluripotency capacity by using a neurobasal media supplemented with serum replacement and ECM components (Steiner, 2010). Despite the culture improvements observed in this system, the complexity of the media employed and the dependence on biological derived components for both, the media and cell passaging, represent a limitation for their use. As such, the use of hydrogels, that due to their physical properties can be easy tuned in two or three dimensional topography, have been explored as hPSC culture substrates, including hyaluronic acid (Liu *et al*., 2012), polyacrylamide-based (Brafman *et al*., 2009) and amino-propylmethacrylamide hydrogels (Irwin *et al*., 2011). Of interest, Zhan and colleagues identified a thermoresponsive and animal free passaging acrylate based hydrogel for the maintenance of PSCs compatible with the use of serum-free defined media, which represents a hallmark in the possession of defined and animal free culture system of hPSCs (Zhang *et al*., 2013).

1.7.2 Polymers in stem cell differentiation

During cell differentiation, the nature of the microenvironment plays a critical role in guiding stem cell specification towards the desire cell fate. Therefore, the use of well-defined synthetic cell microenvironments that mimic the stem cell niche *in vivo* represents an important step towards a well-defined and scalable cell culture system for applications. There are several examples of polymers either alone or in combination with peptides that have been employed in promoting the differentiation of PSCs into cells of the three germ layers while revealing the insights of developmental cues. For example, neural differentiation has been achieved by combining polycacrilamides hydrogels combined with glycosaminoglycans (GAG)-binding peptides which favored the attachment and neural differentiation of hESCs in the absence of neurogenic factors by only tuning the mechanical properties of the underlying matrix, which have revealed the importance of mechanical cues to control the differentiation of pluripotent stem cells (Musah *et al*., 2012). Also, these synthetic platforms have been employed to immobilize growth factors and

adhesion molecules to the culture substrate promoting neural differentiation (Yang *et al*, 2014). The polymer technology has also allowed the identification of key extracellular membrane receptors, namely integrins, involved in the differentiation into early mesodermal fate (Li *et al*., 2011). In addition to elucidate early developmental signals, polymers can also replace differentiation factors. Gelatin methacylate-based matrices have shown to promote osteogenic differentiation in the absence of typical osteoinductive factors, both on 2D surfaces and 3D scaffolds (Kang *et al*., 2014).

Polymers, both alone or in combination with proteins or peptides, have been also applied to promote hepatocyte differentiation of PSCs, and have been used to explore mechanistic processes of hepatogenesis. As such, Yamazoe and colleagues observed that hepatocyte differentiation from hESCs was promoted in the presence of a three dimensional polyamide nanofiber that induces the continuous activation of Rac 1, a protein involved in the remodeling of the cytoskeleton (Yamazoe *et al*., 2013). Hydrogels have been also employed in studying hepatocyte differentiation. Malinen and colleagues employed a three dimensional system made out of nanofibrillar cellulose and hyaluraonan-gelatin hydrogel to differentiate the HepaRG liver progenitor cells towards hepatocytes, revealing the importance of cell density in hepatocyte differentiation efficiency (Malinen *et al*., 2014). Another study performed by Takayama and colleagues combined stage-specific transient overexpression of hepatocyte-related transcription factors and a spheroid culture plate (Nanopillar Plate) to perform hepatocyte differentiation of hPSCs, obtaining hepatocytes that responded to hepatotoxic compounds. However, the complexity of the differentiation approach and the requirement of matrigel in the culture substrate represent a limitation for large-scale manufacturing (Takayama *et al*., 2013). More recently, Celiz and colleagues employed high-throughput technology to perform an extensive screening to identify a synthetic polymer substrate that supported both hPSC culture and differentiation into the three germ layers in a defined environment. From this screening they identified one in particular, HPhMA-*co*-HEMA, which resulted from the polymerization of 5 (*N*-(4-

hydroxyphenyl)methacrylamide) and poly(2-hydroxyethyl methacrylate) (polyHEMA) that supported both, maintenance of undifferentiated hPSCs and their differentiation capacity into cells of the three germ layers, providing a robust platform for the large-scale production of stem cell derived somatic cells for clinical and research applications (Celiz *et al*., 2015).

1.7.3 Polymer screening approaches

Identification of new biomaterials compatible with the desired biological application or biological response represents a slow and time consuming process. To overcome this issue, high throughput or combinatorial polymer based approaches to polymer synthesis, fabrication and screening have been developed.

Menger and colleagues pioneered in employing high throughput technology to identify new organic catalysts with phosphatase activity (Menger *et al*., 1995). In parallel, Brocchini and colleagues employed this technology to create a library of structural related polymers by combination of monomers (Brocchini *et al*., 1997). Polymer libraries possess the potential to increase the number of polymeric candidate materials for any specific application and systematize the study of existent correlations between polymer structure, material properties and performance. Refining of the technique was subsequently developed by Boussie and colleagues by deposition and analysis of polymer spots on a surface, resulting in the possession of microarrays compromising a large number of polymers (Boussie and Devenney, 2004). The technology was further translated to the biology field by Meredith and colleagues, who generated a polymer microarray employing variations in temperature during polymer synthesis on a glass slide, to identify polymer hits that increased alkaline phosphatase expression in osteoblasts (Meredith and Sormana, 2003) (Meredith *et al*, 2003). How and colleagues applied this technology to identify DNA delivery systems for cell transfection using a microarray containing polymers with high DNA binding affinity (How *et al*., 2004). The polymer microarray was synthetized employing the contact printing technique,

which automatized the mixing process of the monomers forming the polymer in a process in which physical parameters are highly regulated, therefore ensuring a high reproducibility between experiments. Anderson and colleagues translated this technology to the stem cell field. The authors identified polymer hits that supported hESC attachment and promoted epithelial differentiation from a polymer microarray compromising 1728 different acrylate-based polymer candidates (Anderson *et al*., 2004).

Subsequently, polymer arrays have been applied in a number of applications including, synthesis of scaffold libraries for screening cell–material interactions in a three dimensional format (Yang *et al*., 2008), identification of polymers that enable adhesion and proliferation of a suspension cell line (Pernagallo *et al*., 2008) and identification of thermoresponsive polymer hydrogels for cellular capture, proliferation and release upon temperature reduction with applications to several cell types (Zhang *et al*., 2009). As such, the possession of a defined culture system for the culturing and differentiation of hPSC will undoubtedly provide information on novel mechanisms of action with the possibility of developing stable culture of somatic cells for clinical, therapeutic and research applications.

1.8 The objectives of the thesis

The thesis initially focuses on establishing a serum-free hepatocyte differentiation approach from hESCs compatible with the use of the polyurethane 134 (PU134) as a culture substrate. The culture system was used as a platform to study the mechanism of action of the PU134 in stabilising the hepatocyte phenotype observed on cells under the defined conditions and identifying key genes involved in this stabilisation process. The final investigation was carried out by translating the findings to clinical grade hESC lines.

CHAPTER 2

MATERIALS AND METHODS

2.1 Materials and solutions

2.1.1 Cell culture media

Table 1. Cell media culture employed.

Cell line	Growth media	Media supplements	Supplier
Human embryonic stem cells	Condition media	10ng basic fibroblast growth facto(bFGF)	R & D System
	mTeSR1™	N/A	Stem Cell technologies
Mouse Embryonic Fibroblast	Dulbecco's modified Eagle's medium (DMEM)	20% KnockOut Serum Replacement 1% Glutamax 1% Non-Essential Aminoacids 0.1mM β-Mercaptoethanol	All Life Technologies
Embyoid Bodies	Knock-Out DMEM	20% FBS 1% Glutamax 1% Penicillin Streptomycine	All Life Technologies
hESCs-derived Hepatic Endoderm	Advanced RPMI 1640	B27 100 ng/ml Activin A 50 ng/ml Wnt3a 1% Penicillin/ Streptomycine	Life Technologies R & D System Peprotech Life Technologies
	SR/DMSO	20% Knock Out Serum Replacement 0.5% Glutamax 1% Non-Essential Aminoacids 0.1mM β-Mercaptoethanol 1% Penicillin Streptomycine 1% DMSO	All Life Technologies Sigma Aldrich
	Leibovitz L-15 Medium	8.3% Tryptose phospate broth 8.3% FBS 10 µM hydrocortisone 21-hemisuccinate 1 µM Insulin (bovine pancreas) 1% L-glutamine 0.2% Ascorbic Acid 1% Penicillin Streptomycine	Sigma Aldrich Life Technologies Sigma Aldrich Sigma Aldrich Life Technologies Sigma Aldrich Life Technologies

	HepatoZYME™ medium	1% Glutamax 10 µM hydrocortisone 21-hemisuccinate 1% Penicillin Streptomycine	Life Technologies Sigma Aldrich Life Technologies

2.1.2 Antibodies

Table 2. Antibodies used for immunostaining.

Primary Antibodies			
Antibody	**Host**	**Dilution**	**Supplier**
Alpha-fetoprotein	Mouse Mono	1/500	Abcam
Muscle Actin	Mouse Mono	1/200	DAKO
β-tubulin III	Mouse Mono	1/1000	Sigma-Aldrich
Octamer 4	Rabbit Poly	1/200	Abcam
Nanog	Rabbit Poly	1/200	Abcam
Sox 17	Goat Poly	1/500	R&D Systems
HNF4α	Rabbit Poly	1/100	Santa Cruz
GATA 4	Goat Poly	1/200	R&D Systems
GATA 6	Goat Poly	1/200	R&D Systems
Cytokeratin 19	Mouse Mono	1/50	DAKO
Albumin	Mouse Mono	1/200	Sigma
Vimentin	Mouse Mono	1/200	DAKO
Ki67	Mouse Mono	1/400	DAKO
CYP3A	Sheep Poly	1/500	University of Dundee*
CYP2D6	Sheep Poly	1/200	University of Dundee*
E-Cadherin	Mouse Mouse	1/200	Abcam
OZ-1	Mouse Mouse	1/200	Abcam
IgG	Mouse Mouse	1/400	DAKO
IgG	Rabbit Poly	1/400	DAKO
IgG	Sheep Poly	1/400	DAKO

IgG	Goat Poly	1/400	DAKO
Secondary Antibodies			
Anti-Rabbit 488	Donkey	1/400	Life Technologies
Anti-Mouse 488	Rabbit	1/400	Life Technologies
Anti-Mouse 568	Goat	1/400	Life Technologies
Anti-Sheep 488	Donkey	1/400	Life Technologies
Anti-Goat 488	Rabbit	1/400	Life Technologies
Anti-Goat 568	Rabbit	1/400	Life Technologies
Anti-Rabbit 568	Donkey	1/400	Life Technologies

***** Kind gift of Dr R. Hay, College of Life Science, University of Dundee, Dundee, UK.

Table 3. Antibodies used for FACS.

Antibody	**Conjugated**	**Type**	**Dilution**	**Supplier**
SSEA-1	FITC	Mouse IgM	1/50	Biolegend
SSEA-4	PE	Mouse IgG	1/50	Biolegend
TRA-1-60	PE	Mouse IgM	1/50	Biolegend
TRA-1-81	Alexa Fuor® 647	Mouse IgM	1/50	Biolegend

Table 4. Antibodies used for Western Blot

Antibody	**Host**	**Dilution**	**Supplier**
HNF4α	Rabbit Poly	1/100	Santa Cruz
Albumin	Mouse Mono	1/100	Sigma
β-actin	Mouse Mono	1/10000	Sigma
Anti-mouse IgG HRP	Goat	1/1000 (ALB 1/2000)	R&D Systems
Anti-rabbit IgG HRP	Swine	1/3000	R&D Systems

2.1.3 Oligonucleotides

All custom design primers were purchased from Applied Biosystems.

Table 5. Oligonucleotides used in this study

Gene	Primer
Octamer 4	Hs00742896 – s1
Nanog	Hs02387400 – g1
Sox17	Hs00751752 – s1
Alpha-fetoprotein	Hs01040607_m1
Sox 9	Hs01001343_g1
EpCAM	Hs00158980_m1
HNF1β	Hs01001604 – m1
HNF3β	Hs00232764 – m1
cytokeratin 19	Hs00761767_s1
Prox 1	Hs00896294_m1
Albumin	Hs00910225 – m1
HNF4α	Hs01023298 – m1
E-Cadherin	Hs01023894_m1
CYP3A4	Hs00604506 – m1
Vimentin	Hs00185584_m1
ADAMTS13	Hs00260148_m1
CTNND2	Hs00181643_m1
NCAM 1	Hs00941830_m1
THBS2	Hs01568063_m1
MMP10	Hs00233987_m1
MMP13	Hs00233992_m1
GAPDH	Hs02758991_g1

2.1.4 Small-interference RNAs

Table 6. siRNAs used in the study

Gene	Part number	UniGene ID
NCAM	s9294	Hs.503878
CTNND2	s3728	Hs.314543
THBS2	s8865	Hs.2258
MMP10	s224726	Hs.371147
MMP13	s8874	Hs.2936

2.2 Mammalian cell culture and differentiation

All cell culture reagents were GIBCO® products supplied by Life Technologies (UK) unless stated otherwise. Corning (UK) supplied the plastic ware utilised throughout the cell culture. Cell culture media employed in this thesis are described in Table 1

2.2.1 Human embryonic stem cell culture

2.2.1.1 Gradual transition of hESCs to MT

The human embryonic stem cell H9, hESCs H9, was maintained on Matrigel™ (BD Biosciences, UK) coated plastic ware with mouse embryonic fibroblast Conditioned Media (CM) (R&D systems) supplemented with 10 ng/ml of bFGF (Prepotech, USA) on a mouse feeder layer (VH Bio Ltd, UK) before being transferred into mTeSR1™ (MT) (Stem Cell Technologies, UK). The cells were split at 1:3 ratio and allowed to settle down overnight. They were transferred into 75:25 ratio of CM to MT for 48 hours, followed by 50:50, 25:75 and finally 100% MT.

2.2.1.2 Culturing hESCs

hESCs H9 were cultured for over 30 passages on Matrigel™ coated 6 well plates were fed with 3 ml of MT. The media in the plates was changed daily. The cells were incubated at 37 ^{o}C in 5% (v/v) CO_2, 95% (v/v) air, for optimal growth. The hESCs Man 11 and Man 12 were always cultured in mTeSR1™ media and maintained for over 30 passages on Matrigel™ coated 6 well plates, and no gradual transition from MEF-CM to MT media was performed.

2.2.1.3 Passaging hESCs

hESCs were split at a ratio of 1:3 using collagenase IV (Life Technologies) diluted in KO-DMEM at a 200U/ml . The existing media was aspirated off, and the cells were washed once with PBS (Sigma-Aldrich). 1 ml of collagenase was added and cells incubated at 37 ^{o}C for about 5 minutes until the edges of the colonies rounded up. The enzymatic solution was aspirated off and the cells were washed once with PBS. 3 ml of fresh media was added to the cells and they were subsequently scrapped off and triturated 1-2 times before transferring 1 ml into a new plate containing 2 m of fresh media for a 1:3 split.

2.1.1.4 Freezing and thawing hESCs

The freezing mix used consisted of knock-out serum replacement and 10% dimethyl sulfoxide (DMSO). At 80-90% confluence, hESCs cultured on a mouse embryonic fibroblast layer in CM, were scrapped off, placed into a 15 ml tube, and centrifuged at 1,000 rpm for 5 minutes. The supernatant was aspirated and the cells were resuspended in 0.5 ml of the freezing mix and transferred to liquid nitrogen.

The cells were routinely thawed by placing the cryotube in a water bath at 37 ^{o}C. The hESCs H9 were then taken up in 1 ml of CM and were resuspended in 6 ml CM and centrifuged at 1,000 rpm for 10 minutes. The supernatant was aspirated and the cells were resuspended in 3 ml of CM containing bFGF and place into a feeder

layer on Matrigel™ coated well. The supernant of ESCs Man 11 and Man 12, after centrifugation, was aspirated and the cells were resuspended in 3 ml of MT.

2.2.2 Embroid body formation

Embroid bodies (EBs) can be generated with hESCs when they are at about 80-90% confluent. The media was aspirated off and the cells were washed once with PBS. 4 ml of EB media was added. The cells were scraped off using a cell scraper. The full 4 ml containing hESCs were placed in low cluster plates to promote cell aggregation. The EBs were fed with fresh EB media every other day for 7 days until the EBs were defined and vacuolated. The EBs were then transferred to 0.5% gelatine coated chamber slides (BD Biosciences, UK). The plate down EBs were allowed to differentiate spontaneously for 14 days and fed every other day with EB media. After 14 days the differentiated cells were fixed with 100% ice cold methanol (Sigma Aldrich) at -20 ^{o}C for 30 min. Post fixation, cell monolayers were washed twice with PBS at room temperature, and were stained using antibodies for the three germ layers (Fletcher *et al*., 2008).

2.2.3 Hepatic differentiation of hESCs

2.2.3.1 Hepatoblast specification of hESC

hESCs were cultured and propagated on propagated on Matrigel™ coated plates with mTeSR1™. Hepatic differentiation was initiated when hESC reached a confluence level of approximately 30-40%, by replacing the culture media with priming medium RPMI 1640-B27 supplemented with 10 ng/ml activin A and 50 ng/ml Wnt3a. The cells were cultured in priming medium for 3 days (the medium was replaced every 24 hours) and final priming medium with Activin A and Wnt3a was made up fresh each day. After 72 hours the media was replaced by specification medium SR/DMSO for 5 days (the medium was replaced every 48 hours).

2.2.3.2 Hepatocyte maturation of hESCs

For experiments no involving replating of the cells, hepatocyte maturation of the hESCs-derived hepatoblasts was induced at day 8 in the differentiation process. Cells were cultured either on the presence of the serum containing maturation medium L-15 or the serum-free medium HepatoZYME™-SFM medium (Life Technologies), both supplemented with 10 ng/ml hHGF (Peprotech) and 20 ng/ml OSM, for 9 days (L-15 medium) or 13 days (HepatoZYME™-SFM medium). The medium was changed every 48 hours. Maturation and maintenance medium with hHGF and OSM was made up fresh each day.

2.2.3.3 Hepatic endoderm replating and hepatocyte maturation of hESCs

For experiments involving replating of the cells on Matrigel™ or polyurethane 134 (PU134) surfaces, cell were maintained on HepatoZYME-SFM media supplemented with 10 ng/ml HGF (Peprotech) and 20 ng/ml OSM (R&D Systems) for 24 hours (day 9). Then, the existing media was aspirated off and cells were washed once with 3ml PBS without calcium chloride and magnesium chloride (Invitrogen). The existing PBS was washed off and replaced with 1 ml of TrypLE™ (Life Technologies) followed by an incubation at 37 ^{o}C for about 5 minutes until cells started to round up. The enzymatic solution was aspirated off and the cells were washed once with 3 ml of PBS. 3 ml of fresh medium HepatoZYME™-SFM medium supplemented with 5% KO-SR, 20 ng/ml hHGF, 40 ng/ml of OSM and 10 ng/ml of EGF (Prepotech) was added to the cells. The cells were subsequently scrapped off and triturated 1-2 times before transferring into a new Matrigel™ or polymer PU134 coated surface; using a 1,2:1 split ratio when 48 well plate format was used; or 1,5:1 split ratio when 24 well plate format was used. The medium was replaced after 48 hours for HepatoZYME™-SFM medium supplemented with 5% KO-SR, 10 ng/ml hHGF and 20 ng/ml OSM for up to 23 days. Matrices made out of the major components of the extracellular matrix were purchased from BD Biosciences (Becton, Dickinson and Company, Biosciences, san Diego, CA), with splitting conditions and media as described above.

Maturation and maintenance medium with HGF and OSM was made up fresh each day.

2.3 Characterisation of hESCs, hESCs-derived hepatic endoderm and hESCs-derived HLCs

2.3.1 Immunofluorescence

hESC, hESCs-derived hepatic endoderm and hESCs-derived HLCs were fixed in 100% ice-cold methanol (Sigma-Aldrich) at -20°C for 30 min (cells can then be stored in PBS at 4 ^{o}C and stained at a later date). Post fixation, cell monolayers were washed three times with PBS, 5 minutes each wash at room temperature. PBS-0.1% Tween (PBS/T) containing 10% BSA was used to block the cells for 1 hour at room temperature. The serum was removed and the respective primary antibody diluted in 1% BSA (made up in PBS/T) was added and incubated at 4°C overnight with agitation (For primary antibody details, see Table 2). The cells were washed 3 times with PBS/T at room temperature, 5 minutes each wash. Following this, the cells were incubated with the appropriate secondary antibody diluted in PBS/T / 1% BSA for 1 hour at room temperature in the dark with agitation (For secondary antibody details, see Table 2). The cells were washed three times with PBS/T. Following this, wells were incubated with DAPI (1:1000) (Sigma-Aldrich) for 20 minutes at room temperature following manufacturer's instructions. Following this, media was removed, and wells with cells at different stages in the differentiation approach were subsequently mounted with 50 µl of PermaFluor aqueous mounting medium (Thermo Scientific). Well containing hESCs-derived hepatocytes replated on Matrigel™ or PU134 coated surface were placed on a glass slide containing with 50 µl of PermaFluor aqueous mounting medium. In all cases, wells were stored at 4 ^{o}C in the dark.

2.3.1.1 Imaging and acquisition

All images were collected using a Zeiss Axio Observed Z1 microscope, with LD Plan-Neofluar objectives lenses (Carl Zweiss Ltd, Welwiyn garden City, UK). The microscope was couple to a Zeiss AxioCamMR3 camera. The image acquisition and processing software used was Zeiss Axiovison Rel 4.8 and Axiovision version 4.7.1.0, respectively. All images were collected at room temperature.

2.3.2 Fluorescence activated cell sorting

Fluorescence activated cell sorting (FACS) was used to confirm the cells surface marker expression of hESCs cultured in MT. hESC were washed once with 3ml PBS without calcium chloride and magnesium chloride**.** The existing PBS was washed off and 1 ml of TrypLE™ was added to the cells for 7 minutes, until cells lifted as single cells. Single hESCs were harvested and resuspended in FACS-PBS (PBS supplemented with 0.1% BSA and 0.1% sodium azide), counted, and resuspended at 1 x 10^6 cells/ml for use. Aliquots of 1 x 10^5 cells were incubated for 30 minutes at 4 ^oC with the fluorochrome conjugated antibodies (For antibody details, see Table 3). Cells were then washed once with PBS, removing any unbound antibody, and spun down at 1,500 rpm for 10 minutes. Following centrifugation, cells were resuspended in 100 µl of FACS-PBS. Binding of the conjugated antibody was detected using the optimum concentration (determined by titration) of an appropriate fluorochrome conjugated isotype specific antibody. Unstained cells were used as controls.

Dead and apoptotic cells along with debris were not included in the analysis. This was carried out by using an electronic live gate on forward scatter and side scatter parameters. Data for 20,000-50,000 “live” events were acquired for each sample using a FACS Calibur Flow Cytometry System (Becton, Dickinson and Company, Biosciences, San Diego, CA) equipped with a 488-nm laser and analysed using FlowJo software version 7.6.5. (Threestar, Inc., San Carlos, CA).

2.3.3 ELISA assay

HepatoZYME™-SFM medium was added to the cells at different points in the differentiation and incubated for 24 hours at 37 ^{o}C in 5% (v/v) CO_2, 95% (v/v) air. The supernatants were collected after 24 hours and could be store at -80 ^{o}C for later use. Presence of albumin in the media was detected using commercial available microwell plates pre-coated with immobilized human anti albumin antibodies (Alpha Diagnostic Intl. Inc., San Antonio, USA). The supernatant were diluted 1:3 or 1:10 on the Working Sample Diluent and pipetted into the wells in duplicate followed by one hour incubation at room temperature accordingly to manufacturer's instructions. Following this, microwells were washed four times with Working Wash Solution and an anti-human albumin HRP conjugated diluted on Working Sample Diluent was added to the microwells, followed by incubation at room temperature for 30 minutes. Subsequently, the microwells were washed 5 times using Working Wash Solution, and the substrate for the HRP enzyme TMB, was added and incubated for 15 minutes in the dark. Stop Solution was added to each well in order to stop the enzyme reaction, and the plates were read at 450 nm with a reference wavelength of 630 nm using a FLUOstart Omega plate reader (BMG LabTech, Germany). Tissue culture media incubated for 24 hours at 37 ^{o}C, diluted 1:3 or 1:10 was used as a negative control. The data was then normalised to per ml per 24 hours per mg protein as determined by the BCA Assay (Pierce, UK).

2.3.4 Cytochrome P450 assays

hESC-derive HLCs at different time points were incubated with the luciferin conjugated specific CYP3A (1:40) and CYP1A2 (1:50) substrate (P450 P-Glo® Luminescent Kit, Promega, UK) for 5 hours at 37 ^{o}C. The tissue culture media was used as a negative control. The supernatant were then collected and could be stored at -80 ^{o}C for later use. The Luciferin detection reagent was reconstituted by mixing the buffer into the bottle containing the lyophilised Luciferin detection reagent. 50 µl of the supernatant sample was mixed with 50 µl of the detection

reagent in a white 96 well plate and incubated at room temperature in the dark for 20 minutes. The relative levels of basal activity were measure using a luminometer (POLARstar optima). Unless indicated, units of activity were expressed as relative light units per ml per mg protein (RLU/ml/mg) as determined by the BCA Assay.

2.3.5 Drug toxicity on the cells

2.3.5.1 Cytochrome P450 induced drug toxicity-BMS compounds

hESCs-derived hepatocytes maintained on either matrigel or PU134 coated surfaces were incubated at day 17 post-replating with compounds metabolised by specific P450s - BMS-827278 and BMS-835981. BMS compounds stock solution was prepared by dissolving in DMSO to a concentration of 50 mM. Stock solution was diluted on the final maturation media to a final concentration of 50 µM and applied to the cells for 72 hours at 37 ^{o}C in 5% CO_2 without replacing the media. Control cultures did not receive the BMS compounds but had their media supplemented with the appropriate vehicle.

ATP levels within the cells were used as a measure of cell viability at 72 hours post treatment using CellTiter-Glo® (Promega, UK) following the manufacturer's instructions. The CellTiter-Glo® Reagent was reconstituted by mixing the CellTiter-Glo® Buffer into the bottle containing the lyophilized CellTiter-Glo® Substrate. CellTiter-Glo® Reagent and culture media was mixed at a 1:1 ratio and the media on the cells was replace with this solution. The solution without cells was used as a negative control. The content was mixed for 2 minutes on an orbital shaker to induce cell lysis, and the plate was incubated at room temperature for 10 minutes to stabilize luminescent signal. Following this, 100 µl of media was placed in a white 96 well plate. Basal luminescence was measured using a luminometer (POLARstar optima) and units of activity were expressed as relative light units (RLU). Every sample had two replicates.

2.3.5.2 Cytochrome P450 activity drug inducibility

hESCs-derived HLCs maintained on either matrigel or PU134 coated surfaces were incubated at Day 18 post-replating, for 48 hours, with compounds that induce the activity of specific P450s, CYP1A2 and CYP3A. Stock solution of phenobarbital (Sigma-Aldrich) was prepared at a concentration of 1 M in PBS and diluted in fresh maturation media to a final concentration of 1 mM or 2 mM. Dexamethasone (Sigma-Aldrich), prepared to a stock concentration of 2 mM in DMSO; and rifampicin (Sigma-Aldrich), prepared to a stock concentration of 10 mM or 20 mM in H_2O, were diluted together in fresh maturation media to a final concentration of 2 µM dexamethasone and 10 µM or 20 µM of rifampicin. Media containing drug inducers was changed on a daily basis. Control cultures did not receive the drug inducers, but had their medium changed daily which was supplemented with the appropriated vehicle, either PBS or DMSO and H_2O. The activity of CYP3A and CYP1A2 was measured using the luciferin conjugated specific CYP 3A (1:40) and CYP1A2 (1:50) substrate (P450 P-Glo® Luminescent Kit, Promega, UK) for 5 hours at 37 ^{o}C. pGlo technology and activity was measured on a luminometer (POLARstar optima). Units of activity were expressed as relative light units/ml/mg protein (RLU/ml/mg), as determined by the BCA Assay.

2.4 Molecular techniques

2.4.1 RNA isolation and extraction

RNA isolation was performed using RNAeasy® Mini Kit (Qiagen, UK) accordingly to manufacturer's instructions. The cells of interest were washed with PBS and resuspended in 350 µl of lysis buffer (buffer RTL, RNEasy MiniKit, Qiagen) containing β-mercaptoethanol (Gibco, UK). The cells were collected and placed in a 1.5 ml eppendorf (store at -80 ^{o}C for later use if required). Lysis was performed using a vortex for 30 seconds before addition of an equal volume of 70 % Ethanol. The suspension was transferred to an RNeasy Spin Column placed in a collection tube.

After centrifugation at 10,000 rpm for 20 seconds, flow through was discarded and 700 µl Buffer RW1 was added followed by centrifugation at 10,000 rpm for 20 seconds, discarding flow through. Following this, 500 µl of Buffer RPE was added. After centrifugation (10,000 rpm, 30 seconds), 500 µl buffer RPE was added followed by centrifugation at 10,000 rpm for 2 minutes. Then the RNeasy Spin Column was transferred to a new collection tube and centrifuged at 16,000 rpm for 1 minute. The spin column was placed into an RNAse free 1.5 mL tube and 100 µl RNAse free H_2O was added to the membrane. After 3 minutes incubation at room temperature, the tube was centrifuged at 10,000 rpm for 1 minute and store at -80 ^{o}C for later use. All RNA and DNA sequences were quantified using the Nanodrop, concentration and purity were measured.

2.4.2 Reverse transcription (RT)

Reverse transcription (RT) was carried out using the QuantiTect Reverse Transcription Kit (Qiagen), accordingly to manufacturer's instructions. Up to 1 µg of RNA was reverse transcribed. Genomic DNA contamination was performed by adding 7 µl of gDNA Wipeout Buffer to the purified RNA and RNase-free water up to 14 µl. The reaction was incubated at 42 ^{o}C for 5 minutes and then place on ice. 1 µl Quantiscript Reverse Transcriptase, 4 µl 5x Quantiscript RT Buffer and 1 µl RT Primer Mix were added to the reaction and incubate at 42 ^{o}C for 30 minutes, followed by a 95 ^{o}C heat treatment for 5 minutes and finally cool to 4 ^{o}C for 5 minutes.

2.4.3 Quantitative polymerase chain reaction (qPCR)

The resulting cDNA was used for further analysis. Quantitative real-time PCR (qPCR) was carried out using the Taqman Fast Advance Mastermix and appropriate primers (Applied Biosystems). Each qPCR reaction was set up using 0.5 µl of specific primers, (for primer details see Table 5), 5.5 µl of Taqman Fast Advance Mastermix and 5.5 µl of nuclease free water containing 12 ng of cDNA per reaction. Each sample was run

in triplicate. The qPCR reaction consisted of an initial denaturation step at 95 ^{o}C for 10 minutes followed by 40 cycles of denaturation at 95 ^{o}C and annealing/extension at 60 ^{o}C for 1 minute in conjunction with the manufacturer's instructions. qPCR was used to investigate the expression of specific genes within the cells. This is defined as qPCR and utilises cDNA as the template. The samples were analysed using Roche LightCycler 480 Real-Time PCR System and data analysis was performed using Roche LightCycler 480 Software (version 1.5) in the form of cycle threshold (Ct) values. This value represents the point at which fluorescence intensity generated in the PCR reaction reaches a set threshold above the background signal. Relative expression was calculated by the ΔΔCt method (Schmittgen and Livak, 2008) and normalised to GAPDH and expressed as relative expression over the control sample. Quantitative PCRs were run in triplicate. Levels of significance were measured by student's *t-test*.

$$\text{Ratio} = \frac{(\text{E})_{\text{Target}}^{\Delta\text{Target Ct (Ct control}-\text{Ct sample)}}}{(\text{E})_{\text{Housekeeping}}^{\Delta\text{Housekeeping Ct (Ct control}-\text{Ct sample)}}}$$

Where the E_{Target} and $E_{Housekeeping}$ are the PCR amplification efficiencies (calculated from the standard curve) of the real-time PCR reactions for the gene of interest and housekeeping gene, respectively. Δ Target Ct (Ct control – Ct sample) is the difference in Ct value of the gene target between the control and test samples. Δ Housekeeping Ct (Ct control – Ct sample) is the difference in Ct of the housekeeping gene between the control and test samples. This equation presents the expression of the gene of interest in the test sample relative to the control sample.

2.4.4 PCR array

Reverse transcription (RT) of RNA samples used on the PCR array were performed using RT^2 First Strand Kit (Quiagen, UK), and RT^2 Profiler PCR array (Qiagen) was used to analyze the gene expression.

cDNA was synthesized using the RT^2 First Strand Kit (Quiagen) according to the manufacturer's instructions. For each condition, equal amounts of purified RNA from a triplicate were pulled together to make 900 ng of RNA. Genomic DNA elimination was performed by adding to the RNA 84µl of Buffer GE and RNase-free water up to 20 µl. The reaction was incubated at 42 ^{o}C for 5 minutes and then place on ice. 16 µl of 5x Buffer BC3, 4 µl of Control P2, 8 µl of RE3 Reverse Transcriptase Mix and 12 µl of RNase-free water were added to the reaction and incubate at 42 ^{o}C for 15 minutes, followed by a 95 ^{o}C heat treatment for 5 minutes. Prior to PCR Array analysis, 182 µ of RNase-free water was added to each reaction, gently mixed by pipetting up and down several times and placed on ice until PCR array immediately was performed.

Real time PCR reactions were performed using RT^2 Profiler PCR array (Qiagen, UK) in a 384-well optical plates. A master mix consisting on 1,300 µl of 2x RT2 SYBR Green Mastermix, 1,096 µl of RNase-free water and 204 µl of cDNA synthesis reaction was prepared. Following this 10 µl of the master mix reaction was added to each well of the RT^2 Profile PCR Array. Real-time reactions were conducted on an ABI 7900HT (Applied Biosystems) and consisted of an initial denaturation step at 95 ^{o}C for 5 minutes followed by 40 cycles of denaturation at 95 ^{o}C and anneling/extension at 60 ^{o}C for 1 minute. Results were PCR reactions were performed in duplicate for each target gene. The gene expression was analysed by RT^2 Profiler PCR array Data Analysis version 5.0 (Qiagen) in the form of cycle threshold (Ct) values. This value represents the point at which fluorescence intensity generated in the PCR reaction reaches a set threshold above the background signal. Relative expression was calculated by the ΔΔCt method (Liva and Schmittgen, 2001) and normalised against

the average Ct values of 5 housekeeping genes (β2M, HPRT1, ACTβ, GAPDH and RPLP0).

2.4.5 Transfection of the cells

hESCs-derived hepatocytes maintained on PU134 coated surfaces in a 48 well plate format were transfected at Day 13 post-replating with commercial available Silencer® Select siRNAs (Life Technologies), containing sequences to specifically reduce the expression of the candidate genes identified in the PCR array using Lipofectamine® 2000 (Invitrogen) and Opti-MEM® I Reduced Serum Medium (Life Technologies) following manufacturer's instructions. For siRNA details refer to table 6.

The siRNA were diluted in the Opti-MEM Medium to a final concentration of 160 µM (16 pmol of siRNA representing 214 ng of siRNA). The reaction was incubated for 5 minutes at room temperature. Following this, equal amount of Opti-MEM medium containing Lipofectamine® 2000 (10 µl of Lipofectamine® 2000 per 1 µg of genetic material) was added to the mixture, obtaining a final siRNA concentration of 80µM. The reaction was incubated for 20 minutes at room temperature in order to allow the formation of the lipofectamin-genetic material complex. Subsequently, the existing media presented on the wells was removed and the mixture was added drop wise. Accordingly to manufacturer's instructions, the media was incubated for 5 hours at 37 ^{o}C and replaced for fresh maturation media supplemented with factors and antibiotic free. The procedure was repeated 24 hours later. Cells and supernatant were collected at Day 15 post-replating for further analysis. Each condition was done in triplicates. Two different Scramble siRNA controls (Silencer® Select Negative Controls No. 1 and No.2 siRNA, parts number 4390843 and 4390846, respectively) were performed and results were analyzed as one group.

2.4.6 SNP analysis

H9 were maintained in mTeSR1™ for at least three passages before cells were harvested and genomic DNA was collected for SNP and karyotyping analysis. Collection of genomic DNA was performed using Gen Elute® Mammalian Genomic DNA Miniprep (Sigma Aldrich), accordingly to manufacturer's instructions. The existing media was aspirated off and cells were washed once with 3ml PBS without calcium chloride and magnesium chloride (Invitrogen). The existing PBS was washed off and replaced, and 1 ml of TrypLE™ (Life Technologies) was added and incubated at 37 ^{o}C for about 5 minutes until cells started to round up. The resulting suspension cell culture was spun down at 1,500rpm for 5 minutes and the media was removed completely. Following this, the cell pellet was resuspended using 200 µl of Resuspension Solution and mix thoroughly. 20 µl of the Protein K solution was added to the sample, followed by 20 µl of Lysis Solution C. The mix was then vortexed thoroughly and incubated for 10 minutes at 70 ^{o}C In parallel, 500 µl of the Colum Preparation Solution was added to the pre-assembled GenElute Miniprep Binding Column and centrifuged at 10,000 rpm for 1 minute. The flowthrough liquid was discarded. 200 µl of 100% ethanol was added to the lysate and mixed thoroughly by vortexing 10 seconds obtaining and homogeneous solution. Following this, the lysate was transferred to the treated binding column and centrifuged for 1 minute at 8,000 rpm, discarding the collection tube containing the flow-through liquid and then the binding column was placed in a new 2 mL collection tube. A second wash was applied to the binding column by adding 500 µl of Wash Solution and centrifuged for 3 minutes at 10,000 rpm, discarding the collection tube containing the flowthrough liquid and then, the binding column was placed in a new 2 mL collection tube. DNA elution was performed by adding 200 µL of the Elution Solution directly into the centre of the binding column, followed by 1 minute centrifugation at 8,000 rpm for 1 minute. The elute contained pure genomic DNA that was stored at 4 ^{o}C until it was shipped for analysis to an external company. The SNP and karyotyping analysis were performed using Illumina GenomeViewer software.

2.5 Protein biochemistry techniques

2.5.1 Cellular protein extraction

Cells grown in different plate wells format were lysed in 150 µl of RIPA buffer (Millipore) with proteinase and phosphatase inhibitors at 1% final concentration (Sigma-Aldrich). The cell extract was span for 15 minutes at 10,000 rpm at 4 ^{o}C in a microcentrifuge, and the supernatant was transferred to a new 1.5 ml eppendorf tube.

2.5.2 Measuring protein concentration

The Pierce BCA (bicinchoninic acid) protein assay kit (Thermo Fisher Scientific, UK) was used to quantify the protein concentration in the cell protein extract samples. Protein extracts were diluted 1:2 using nuclease free water (5 µl of sample extract and 5 µl of water) in a 96 well plate, each sample was pipette in triplicate. Reagents A and B were mixed at a 1:50 ratio and a volume of 200 µl was transferred into each sample well in addition to wells containing bovine serum albumin standards ranging from 20-2,000 µg/ml, as per manufacturer's instructions. The plate was incubated at room temperature for 10 minutes and the absorbance was read at 562 nm. The protein concentrations were calculated by linear extrapolation using the standard curve generate from the protein standards.

2.5.3 SDS-NuPAGE® polyacrilamie gel electroforesis

The SDS NuPage® gel electrophoresis (SDS-PAGE) was used to separate proteins of varying molecular weights. The Xcell SureLock® Mini-Cell System (Life Technologies, UK) was used with 4-12% Bis-Tris pre-cast polyacrylamide gels (Life Technologies, UK). 20 µg of each sample was denatured at 70 ^{o}C for 10 minutes in 4x NuPAGE® LDS Sample Buffer (Life Technologies). Once the gel was fitted in the chamber, the tank was filled with 1x NuPAGE® MES-SDS running buffer in addition to 0.5 ml of NuPAGE® Antioxidant (Life Technologies, UK) in the inner chamber. The samples

were loaded, including SeeBlue® Plus2 Pre-Stained Standard (Invitrogen). A current of 200 V was applied and the samples were run for approximately 1 hour. The gels containing proteins were carefully removed from the cassette and were used in western blotting.

2.5.4 Western immunoblotting

2.5.4.1 Protein transfer

Western blotting was used to detect the presence of specific proteins in samples extracts using XCell SureLock® Mini-Cell system, as per manufacture's instruction. Proteins were separated via SDS-PAGE followed by subsequently transfer from the polyacrylamide gel to the Polyvinylidene fluoride (PVDF) membrane, that prevents protein cross over if the transfer time was over run and provides long-term durability (Millipore, UK). The membrane was then probed with antibodies specific to the target protein. The transfer sack was assembled in the following order from cathode to anode: 2x sponge; filter paper soaked in 1x NuPAGE® Transfer Buffer; SDS-PAGE gel; PVDF membrane pre-soaked in methanol and then transfer buffer on top of the gel; filter paper soaked in transfer buffer; 3x sponge, and the beginning sequence was repeated for a second gel. It is vital that the membrane is positioned accurately between the gel and the anode as the samples and current will be moving in that direction. The stack was assembled andn the XCell Blot II module and was tightly sealed and placed into the transfer SureLock® tank containing 1x transfer buffer and 0.25 ml antioxidant in the inner chamber and cold water in the outer chamber. A constant current of 160 mA was applied for 90 minutes.

2.5.4.2 Immunoblotting

Once the proteins have been successfully transferred onto the PVDF membrane, the membrane was blocked to prevent non-specific antibody binding. The membrane was blocked in 10 ml of Odyssey Blocking Buffer (LI-COR Biosciences Ltd, UK) for 1 hour with gentle agitation at room temperature. The primary antibody was added

to 3 ml of Odyssey Blocking Buffer at the appropriated dilution of the antibody, and incubated overnight at 4 ^{o}C with gentle agitation. Unbound antibody was removed by three, 5-minute washes with 50 ml of 0.1% PBS Tween (PBST). A horseradish peroxidase (HRP)-conjugated secondary antibody was diluted in 10 ml of Odyssey Blocking Buffer at the appropriated dilution, and incubated for 1 hour with gentle agitation at room temperature. Unbound antibody was, once again, removed by three 5- minute washes with 50 ml of PBST. For antibody details refer to Table 4.

2.5.4.3 Enhanced Chemiluminescence (ECL)

The proteins of interest were detected using enhanced chemiluminescence (ECL), the HRP substrate reacts with the conjugated HRP group present on the secondary antibody specifying the target protein. Protein bands were visualised using the Pierce Enhanced Chemiluminiscence Reagent Kit (Pierce, UK). Peroxidase Buffer and the Luminol/Enhancer Solution was mixed at a 1:1 ratio and spotted on to the membrane (2 ml for each membrane), ensuring it was evenly spread. The membrane was exposed to Odyssey™ Fc Imaging System (LI-COR Biosciences Ltd, UK) for the appropriated length of time, typically 1-10 minutes.

2.6 Synthesis and production of polyurethane 134 (PU134)

Synthesis and identification of the monomer PHNAGAD and the polyurethane 134 (PU134) as a suitable polymer with desirable properties for the culture of HLC was was perfomed by Hay and colleagues, including Prof Mark Bradley, and it is described in Hay *et al*., 2011.

2.6.1 Synthesis of PHNAGAD

PHNGAD (Poly[1,6-hexanodiol/neopentyl glycol/di(ethylene glycol)-alt-adipic acid]diol) was synthesized by applying a heat treatment to the monomers 1,6-hexanediol, di(ethylene glycol) (Sigma Aldrich) and neopentyl glycol (Sigma Aldrich) at 40 ^{o}C for 48 hr in a vacuum oven to remove any residual water. The mix was

allowed to cold down to room temperature under vacuum. Following this, 22 mmol of each monomer and 55 mmol of adipic acid (Sigma Aldrich) were added to a two-necked round bottom flask connected to a Dean-Stark apparatus. The whole assembly was placed under a vacuum and the glassware was gently heated at 40 ^{o}C for 6 hr, in order to avoid any moisture absorption during the addition of the chemical into the flask. Then, 0.055 mmol of the catalyst titanium (IV) butoxide (Sigma Aldrich) was added via syringe drop wise. The reaction mixture was stirred at 180 ^{o}C, under an N_2 atmosphere, and residual water was collected in the Dean-Stark trap. Finally, the product was allowed to cool to room temperature. For schematic representation refer to Figure 4.

2.6.2 Synthesis of PU134

The synthesis of the polyurethane 134, PU134, was started by mixing one equivalent of the polyol PHNGAD (Mn~1,800 Da, 3.2 mmol) with two equivalents (6.4 mmol) of 4'4-Methylenebis (phenyl isocyanate) (Sigma Aldrich) in 12ml of anhydrous N,N-Dimethylformamide (Sigma Aldrich). The reaction mixture was stirred at 70 ^{o}C, under an N_2 atmosphere. Following this, the catalyst titanium (IV) butoxide (0.8% wt) was added, via syringe, drop wise. After 1 hour, one equivalent (3.2 mmol) of the chain extender 1,4-butanediol (Sigma Aldrich) was added. Then, the temperature was increased at 90 ^{o}C and the mixture was stirred for 24 hr under an N_2 atmosphere. Following the reaction, the polyurethane was collected by precipitation by adding hexane (Sigma Aldrich), drop wise into the reaction solution until the precipitation occurred. Subsequently, the solution was centrifuged at 5300 x g for 5 min. The supernatant was decanted and dried off at 40 ^{o}C in a vacuum oven until the solvent evaporated (Mn PU134~1235 Da). For schematic representation refer to Figure 5. Various analytical techniques were employed to characterised the final product; including, gel permeation chromatography, NMR, FTIR, spectroscope and differential scanning calorimeter, ensuring the oolecular weight distribution and the functional groups of the polymer.

2.7 Production of PU134 coated surfaces

2.7.1 Preparation of PU134 solutions

Preparation of the solutions of PU134 on the different solvents were performed by dissolving PU134 into a glass bottle containing a number of solvents: chloroform, a combination of chloroform and toluene in 1:1 ratio, tetrahydrofuran, and combination of tetrahydrofuran and dichloromethane in 1:1 ratio (Sigma Aldrich), to a final concentration of 2%. Following this, the solution was shaken vigorously for 20 min at room temperature using a shaker (Edmun Bühler, Germany) at 200 mot/min, until the solution became homogeneous and no precipitate was observed.

2.7.2 Coating of culture surfaces with PU134

The surfaces (glass slides) were coated with the different PU134 solutions by placing the glass slide on the spin coater (Specialty Coating System, USA). 50 µl of the PU134 solution was applied to the 15 mm in diameter surface using a pipette. The volume of PU134 solution was adjusted accordingly for the required coverslip size keeping the volume to surface ratio proportional. Subsequently, the surface was spun for 7 sec at 23 x g, allowing the obtaining of a polymer coated layer of 1 to 1.25µm of thickness. Following this, PU134 coated surfaces were vacuum dried at room temperature for at least 24 hr before sterilisation.

2.7.3 Irradiation of PU134 coated surfaces

2.7.3.1 Gamma-irradiation

Gamma- irradiation of PU134 coated surfaces were performed by applying a dose of 10 Grays using a laboratory irradiator (CIS Biointernational, France) for 12 min.

2.7.3.2 UV- irradiation

UV- irradiation PU134 coated surfaces were performed by using a 30W, UVC bulb (ESCO, UK) with a wavelength between 290nm and 100nm for 16 min each side.

2.7.4 Scanning Electron Microscopy

Samples that were used for Scanning Electron Microscopy, SEM, were firstly gold coated prior to the SEM acquisition. Gold coating was carried out by sputtering for 200 sec in an atmosphere of 5 x 10^{-1} millibars of pressure in a Bal-Tec Sputter Coater SCD 050 (Capovani Brothers Inc. NY, USA). Subsequently, samples were examined with a Philips XL30CP Scanning Electron Microscopy at an accelerating voltage of 20 kV in secondary electron imaging mode.

2.7.5 Atomic Force Microscopy

An atomic force microscope DimensionV Nanoscope VEECO (VEECO, Instruments Inc, NY, USA) was used to scan the polymer surface within an area 20 μm × 20 μm. The scan rate ranged from 1.32 Hz to 1.60 Hz, and the height values of the surface were obtained with a resolution of 512 × 512 pixels in the scanned region. The root mean square (RMS or Rq) of all the spots in the hit array was calculated through the NanoScope analysis software (VEECO version 1.20) by using the average of height deviations taken form the mean image data place, expressed as:

$$Rq = \sqrt{\frac{\sum(Z_i - Z_i)^2}{N}}$$

Where Zi is the current Z value and N is the number of points within the given area.

The deviation or mean surface roughness (Ra) of the image was calculated using,

$$\mathrm{Ra} = 1/\mathrm{L} \int_0^{\mathrm{L}} \mathrm{IZ(x)Idx}$$

Where Z (x) is the function that describes the surface profile analysed in terms of height (Z) and position (x) of the sample over the evaluation length “L”. Ra represents the mean value of the surface relative to the centre plane.

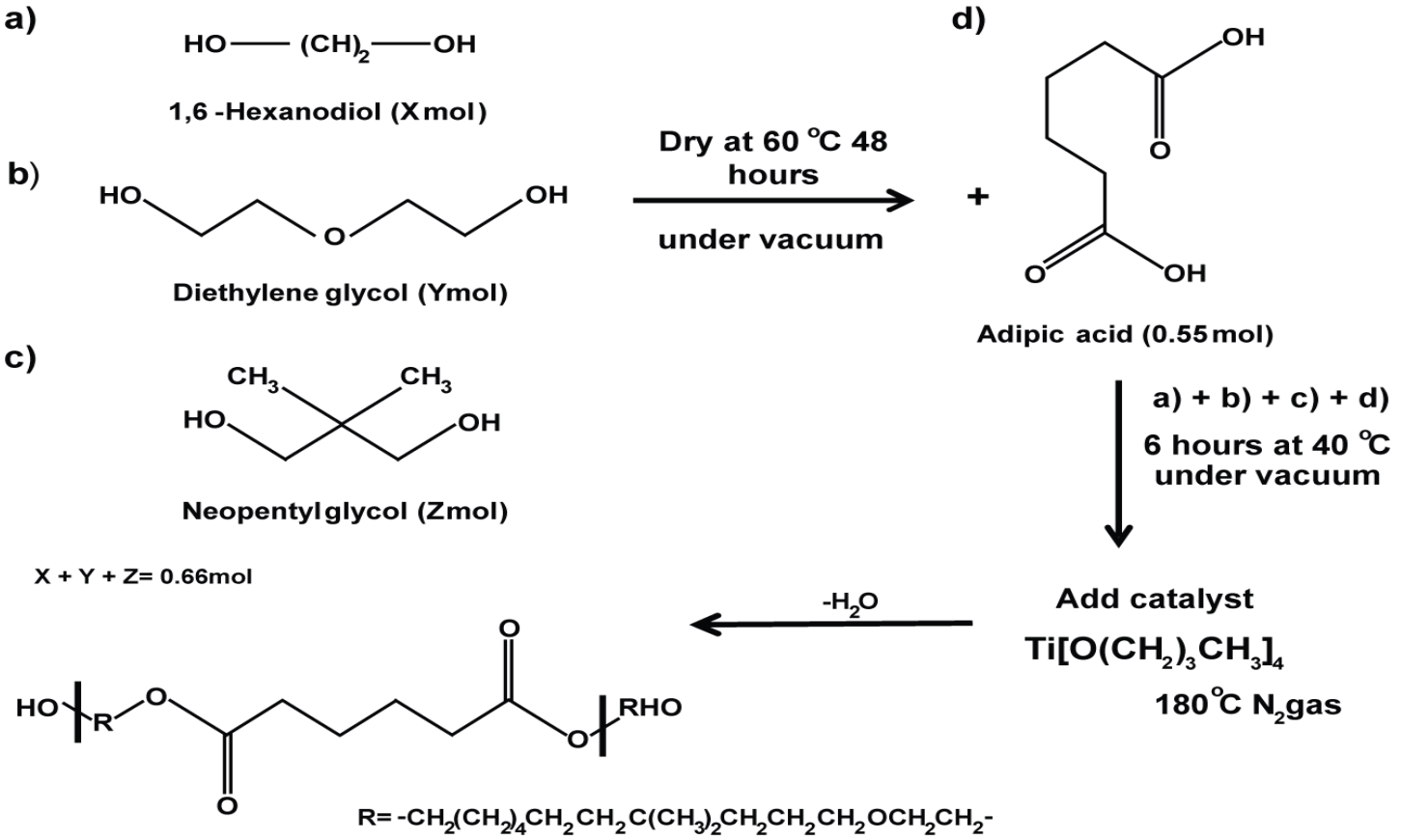

Figure 4. Schematic representation of the synthesis of PHNAGD. PHNAGD was prepared by the reaction of 1,6-Hexanodiol, diethylene glycol, neoppentyl glycol and adipic acid. PHNAGD, Poly[1,6-hexanodiol/neopentyl glycol/di(ethylene glycol)-alt-adipic acid]diol.

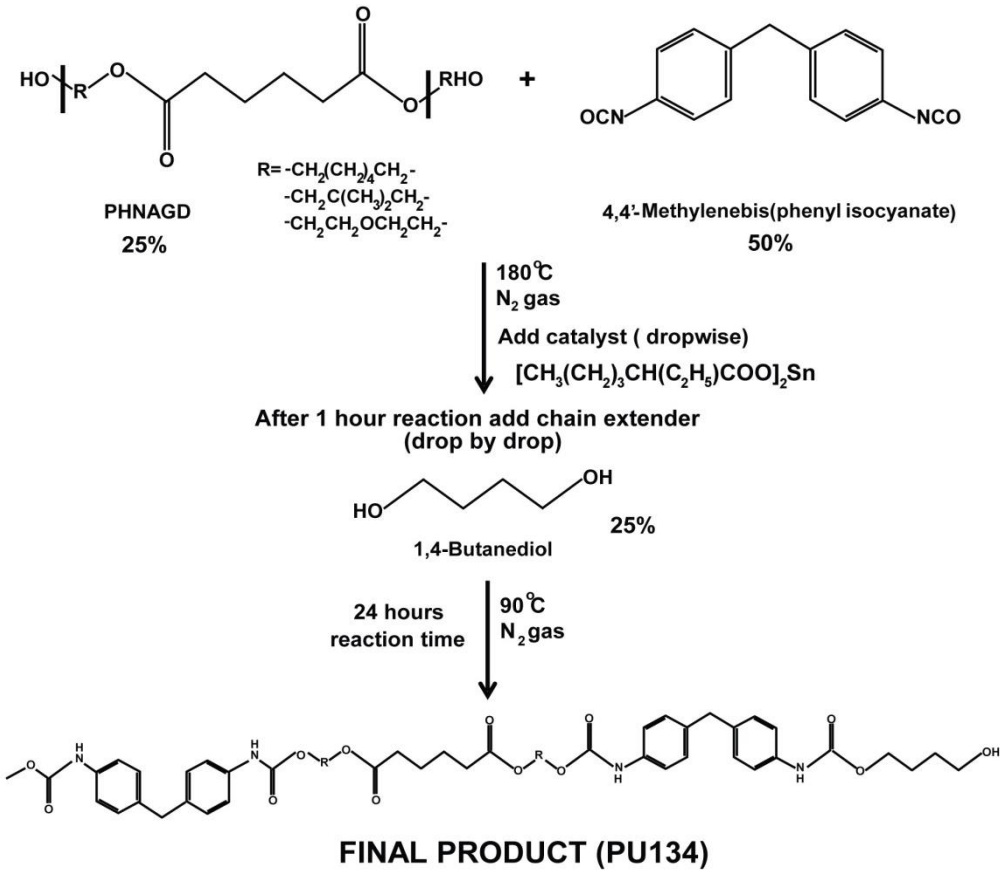

Figure 5. Schematic representation of the synthesis of polyurethane 134. PU134 was prepared by the reaction of 1.0 equivalent of a PHNGAD with 2.0 equivalent of a 4,4′-Methylenebis(phenyl isocyanate), followed by the addition of 1.0 equivalent of a 1,4-butanediol chain extender.

CHAPTER THREE

DEFINING hESCs PLURIPOTENCY AND THEIR DIFFERENTIATION INTO HEPATOCYTES

3.1 Introduction

3.1.1 hESCs

3.1.1.1 Properties of hESCs

Human embryonic stem cells (hESCs) possess two attributes that make them ideal candidates to provide an inexhaustible supply of somatic cells (Wobus and Boheler, 2005): the capacity for self-renewal and the ability to differentiate into cell types from all three germ layers (Pera *et al*., 1999; Semb, 2006). This two attributes make hESCs a potential source of unlimited amount of cells of known genotype background for clinical and biological downstream applications, including disease modeling, drug toxicity, predictive toxicology and cell based therapies (Greenhough *et al*., 2010; Rippon and Bishop, 2004; Vazin and Freed, 2010).

hESCs are isolated from the inner cell mass of blastocyst stage embryos that are not suitable for human implantation (Peura *et al*., 2006; Reubinoff *et al*., 2000; Thomson, 1998). The blastocyst formation occurs after the fertilization of an egg and the formation of the diploid zygote during early embryogenesis. The blastocyst possesses two layers; the outer cell layer, known as the trophoblast, which forms the supporting tissue for the developing embryo and the inner cell layer, referred as the embryoblast or inner cell mass (ICM), that retains the ability of differentiate into all cell types of the embryo body (Cai *et al*., 2006; Hoffman and Carpenter, 2005; Vazin and Freed, 2010). The establishment of hESC lines begins with the dissociation of the ICM from the embryo body, which is performed by different techniques including immunosurgery, mechanical or enzymatic dissection. Subsequent culture of the isolated cells permits the establishment of hESC lines (Semb, 2006).

3.1.1.2 Characterization of hESCs

Undifferentiated hESCs form tightly packed colonies that are typically multi-layered, with well-defined colony borders. They display a high nucleus to cytoplasm ratio

and a prominent nucleoli (Pera *et al*., 1999). hESCs are also defined by the expression of a number of stem cell specific markers, including the transcription factors Octamer 4 (Oct-4) (Pesce *et al*., 1999; Schöler *et al*., 1989), Nanog (Chambers *et al*., 2003; Mitsui *et al*., 2003) and Sox 2 (Avilion *et al*., 2003); the cell surface the globoseries glycolipid antigen 4 or stage specific embryonic antigen (SSEA)-4 (Kannagi *et al*., 1983) and the keratin sulphate related antigens TRA-1-60 and TRA-1-81 (Andrews *et al*., 1984); and absence of hESC negative markers such as lactoreries oligosaccharide antigen SSEA-1 (Kannagi *et al*., 1983).

Like human somatic cells, hESCs display an unlimited life span independently from genetic alterations or inactivation of tumour suppressor pathways (Rosler *et al*., 2004). However, prolonged maintenance *in vitro* can lead to the acquisition of karyotypic abnormalities in processes similar to tumorigenic events observed *in vivo* (Baker *et al*., 2007; Draper *et al*., 2003; Mitalipova *et al*., 2005). Therefore, different techniques including sequencing single nucleotide polymorphism (SNP) and karyotyping are frequently performed to ensure the correct hESC genetic signature within the population and no major mutations occurred (Campos *et al*., 2009). DNA microarrays, short tandem repeat analysis and fluorescent *in situ* hybridization can also be applied to ensure the correct hESC signature within the population (Brimble *et al*., 2005; Josephson *et al*., 2006; Mitalipova *et al*., 2005). The pluripotency nature of the hESCs can be measured by testing their abilities to form all three germ layers *in vitro* (Cai *et al*., 2006; Hannoun *et al*., 2010; Mallon *et al*., 2006). Expression of specific proteins defines each germ layer. Alpha-fetoprotein (AFP) defines endoderm, the mesoderm is usually defined by the presence of alpha-smooth muscle actin (α-SMA) and the ectoderm stains positive for β-tubulin (Hannoun *et al*., 2010). hESCs have also been directly differentiated into cell types of the three germ layers including hepatocytes, cardiomiocytes, neural precursor cells and pancreatic beta-cells (Hay *et al*., 2008a; Kaufman and Thomson, 2002; Kehat *et al*., 2001; Niebruegge *et al*., 2008; Trounson, 2006).

3.1.1.3 hESC culture conditions

hESCs represent an ideal candidate to obtain somatic cells for the study of human biology, *in vitro* modelling and cell based therapy. For this purpose, maintenance of the pluripotent and self-renewal properties of hESCs requires defined and optimized culture systems. The use of monolayers of mitotically inactive mouse embryonic fibroblast (MEFs) feeder cells represents the most common and effective method of maintaining hESCs *in vitro*, as they provide extra-cellular matrix attachment and growth factors required to support undifferentiated proliferation of the hESCs (Ilic, 2006; Vazin and Freed, 2010). However, the use of MEFs in the culture system presents some disadvantages, including the presence of xeno-contaminants, lack of definition and variability between batches of cells (Mallon *et al*., 2006), all of which limit the scale up and application of the cells. In order to create xeno-free hESC culture environments, human feeders have replaced the use of animal feeders (Amit *et al*., 2004). However, the high variability, limited sourcing and the impure hESC population associated with the use of feeders can alter the accuracy of the derived product (Mallon *et al*., 2006). These observations suggest that the development of fully defined culture systems is required if hESCs are to be employed in clinical or therapeutic applications.

Xu and collage were pioneer in establishing a feeder free hESC culture system. They employed Matrigel™ as a basement membrane to provide to the culture with the extra cellular matrix attachment and growth factors required for the maintenance of hESCs (Xu *et al*., 2001). Matrigel is a membrane preparation extracted from a murine Engelbreth-Holm-Swarm (EHS) sarcoma composed of a myriad of ECMs, growth factors and xenobiotics. Despite the improvements observed under this culture condition, this feeder free system still requires the employment of a culture media conditioned by MEFs (CM), supplemented with basic fibroblast growth factor (bFGF) (Braam *et al*., 2008). To tackle this issue, a number of companies released xeno-free and defined culture media. The most popular media used to date include StemPro® (Invitrogen) and mTeSR1™ (Life Technologies) (Ludwig *et al* 2006). It has

been previously reported that the self-renewal, pluripotency and hepatocyte differentiation abilities of the hESCs are sustained on these defined media in a similar manner than on CM (Hannoun *et al*., 2010), providing a more defined culture system capable to sustain hESC self-renewal whilst maintaining pluripotency. Recently, the newly fully defined E8™ media has been shown to promote efficient self-renewal and differentiation of hESCs and induced pluripotent stem cells (iPSCs) (Chen *et al*., 2011).

3.1.2 Hepatocyte differentiation of hESCs

hESCs possess unlimited self-renewal and differentiation capacities, thereby represent a potentially unlimited source of hepatocytes with a known genetic background. The recent emergence of iPSCs supports the use of pluripotent stem cells in generating functional hepatocyte-like cells (HLCs). A better understanding of the development of the liver *in vivo* has allowed the generation of differentiation approaches to obtain HLCs from pluripotent stem cells in a step-wise manner, mimicking the stages observed during liver development: anterior definitive endoderm induction, hepatic endoderm specification, hepatocyte specification and hepatocyte maturation. The existing differentiation approaches of pluripotent stem cells to the hepatic lineage tend to replicate hepatocyte development in discrete stages, by using combinations of various soluble growth factors that mimic the dynamic cues observed during hepatogenesis *in vivo*. However, like any other tissue *in vivo*, the development of the liver is a continuous process. As a consequence, the duration and media composition of the stages varies between different approaches. However, most protocols share the use of certain growth factors and the duration of each of the stages.

Liver development requires the priming of the primitive streak towards the endoderm lineage in a process primarily driven by Activin/Nodal, BMPs, FGFs and Wnt signalling (D'Amour *et al*., 2005; Duboc *et al*., 2010). In most of the available hepatocyte differentiation protocols, definitive endoderm induction is mainly driven

by supplementing the media with Activin A alone or in combination with Wnt3a or different FGFs (D'Amour *et al*., 2005; Gadue *et al*., 2006; Hay *et al*., 2008a). Endodermal progenitor maintenance and expansion are controlled *in vivo* by the action of different FGFs and BMPs (Chen *et al*., 2012; Josephson *et al*., 2006; Jung, 1999; Zaret and Grompe, 2008). Therefore, these factors are commonly used in the hepatic specification from pluripotent stem cells to definitive endoderm *in vitro* (Basma *et al*., 2009; Brolén *et al*., 2009; Gai *et al*., 2010; Soldatow *et al*., 2013; Touboul *et al*., 2010). Specification of the primitive streak to endoderm depends on the duration and magnitude of nodal signalling (Lowe *et al*., 2001), triggered *in vivo* by BMPs (Zorn and Wells, 2009), which is replaced by activin A; Wnt3a maintains the nodal expression and mediates brachyury expression, critical in the specification of the anterior region of the primitive streak (PS) to definitive endoderm.

Hepatic endoderm specification results in the formation of the liver bud, which contains the bipotential progenitor cells called hepatoblasts. This process requires further activation of signalling pathways by FGF and BMP family molecules, specifically BMP4, FGF2, and FGF4. Commitment to the hepatic fate is induced by a treatment with a mixture of FGFs (Agarwal *et al*., 2008; Cai *et al*., 2007; Sekhon *et al*., 2004). Hepatic specification can also be induced by modifying the acetylation state of the histones by supplementing the media with DMSO (Duan *et al*., 2010; Hay *et al*., 2008a).

Following liver bud formation and expansion, the hepatoblasts are stimulated to differentiate towards hepatocyte fate by inductive signals, including hepatocyte growth factor (HGF) and oncostatin M (OSM). This process can be recapitulated *in vitro* by a treatment with cocktail of soluble factors including these cytokines in combination with insulin and glucocorticoids such as dexamethasone and hydrocortisone. OSM, an IL-6 related cytokine produced by hematopoietic cells present in mid-fetal livers, favours the hepatocyte differentiation over cholangiocytes, via STAT3 signalling (Kamiya *et al*., 2002). Upon binding of oncostatin M (OSM) to the gp130 membrane receptor, JAK/Stat3 signalling pathway

is activated (Ito *et al*., 2000; Kamiya *et al*., 1999), promoting morphological maturation into polarized epithelium via K-ras and E-Cadherin (Kamiya *et al*., 2001; Matsui, 2002; Michalopoulos *et al*., 2003), whereas HGF mimics the hepatic environment (Clotman, 2005; Kim and Rajagopalan, 2010) in a STAT3-independent manner (Kamiya *et al*., 2001), promoting hepatoblast migration and proliferation within the liver bud (Block *et al*., 1996; Medico *et al*., 2001; Michalopoulos and Bowen, 1993). HGF binding to the c-Met receptor activates both the SEK1/MKK4 and c-Jun signalling cascades resulting in glucose-6-phosphate, tyrosine amino transferase, carbamoyl-phosphate synthase and albumin expression, all of which are associated with mature liver phenotype (Duncan, 2003; Fiegel *et al*., 2008; Zaret, 2001). While insulin promotes hepatocyte attachment and morphology via PI3K-Akt and MAPK pathways (Kim *et al*., 2001), glucocorticoids upon binding to the glucocorticoids receptors, enhance the differentiation state of the cells through activation of liver specific transcriptional programs by either, increasing the DNA-binding activity of key transcription factors such as C/EBPα, -β, -γ, HNF1α,-1β and HNF4α (Elaut *et al*., 2006; Matsuno *et al*., 1996; Sinclair *et al*., 2008) or by binding to promoters found upstream of hepatic genes including albumin, thus increasing the secretion of this liver specific protein (Dich *et al*., 1988).

3.1.3 Characterization and functional evaluation of pluripotent stem cells derived definitive endoderm and hepatic lineages

Cell morphology, expression of stage specific mRNAs, protein markers and functional abilities are common techniques used to define the cells obtained at different stages during differentiation. Undifferentiated pluripotent stem cells express the well established pluripotency markers Octamer 4, Sox 2 and Nanog; Sox 17 and FoxA2 expression is characteristic of definitive endoderm (D'Amour *et al*., 2005; Snykers *et al*., 2009). Hepatoblasts display a characteristic cobblestone-like morphology. However, there is not a specific marker that defines hepatoblasts. Therefore, characterization of the hepatoblast stage can be determined using a panel of markers rather than individual markers. This panel includes transcription

factors such as Hhex, GATA 4, GATA 6, HNF6, Prox1 and Sox9 (Wells and Melton, 1999), and proteins including alpha-fetoprotein, albumin and cytokeratin 19 (Zaret, 2008). Finally, hepatocytes are defined by markers such as albumin, HNF4α and specific CYPs (Snykers *et al*., 2009). Assessment of functional abilities on the HLCs includes measurement of the liver specific protein production and secretion, measurement of the cytochrome P450 activity, drug induction by pleiotropic P450 inducers, assessment of the metabolism of toxic compounds, glycogen storage and uptake of indocyanine green and low density lipoproteins (Behbahan *et al*., 2011).

3.1.4 Phenotypic instability of the cells in culture

Currently, HLCs generated from pluripotent stem cells represent a reliable source of hepatocytes, making this technology a potential alternative to primary human hepatocytes tissues. However, improvements in cell fidelity are required (Godoy *et al*., 2015). A common problem in both stem cell derived HLCs and primary human hepatocytes are cell dedifferentiation (Beigel *et al*., 2008; Binda and Lasserre, 2003). Thus, the applications of HLCs, like primary human hepatocytes, are limited due to phenotypic instability in culture.

In primary human hepatocytes, the disruption of the liver tissue integrity occurred during isolation, which activates inflammatory and proliferative responses mediated by the nuclear factor κB (Nf-κβ) and mitogen-activated protein kinase (MAPK) respectively. These events initiate a transdifferentiation process from a epithelial to a mesenchymal phenotype, which leads to negative effects in the expression of liver specific genes, especially in genes encoding phase I and phase II biotransformation enzymes and liver-enriched transcription factors (LETFs) (Beigel *et al*., 2008; Boess *et al*., 2003). These alterations are at the most pronounced between 24 and 48 hours in both, the number of affected genes and the level of expression, which often parallel with a reduction in the expression of the corresponding protein and the enzymatic activity (Beigel *et al*., 2008; Boess *et al*., 2003; Rodriguez, 2002). Simultaneously, there is a cellular response to the stress suffered during isolation

and the time-dependent loss of hepatocellular morphology (Rowe *et al*., 2010), denoted by a lost in the cell polarity, an increase in the expression of acute-phase enzymes and proteins involved in the cytoskeletal remodelling ,including β-actin, α-tubulin and vimentin. These events affect the hepatocyte homeostasis leading to an apoptosis mediated cellular death, thus shortening survival and life span of the cells (Elaut *et al*., 2006; Paine and Andreakos, 2004; Vinken *et al*., 2006).

Reversion of the dedifferentiation process has been induced by modifying the culture media and/or the microenvironment surrounding the cells. Media supplementation with differentiation promoting factors, including insulin and glucocorticoids, have been extensively applied either alone or in combination with strategies that involve the modulation of the extracellular environment, using biological derived matrices and/or co-culture strategies (Fraczek *et al*., 2013).

The above section summarises the characteristics of hESCs, the culture conditions required to maintain the cells in an undifferentiated pluripotent state and the strategies used to generate hepatocytes from pluripotent stem cells. One of the main challenges associated with HLCs derived from pluripotent stem cells is the functional and phenotypical instability of the cells in culture. The next section of this chapter highlights the investigation carried out to overcome the above issues. The employment of a defined, serum- and xeno-free hepatocyte differentiation media will improve the reproducibility of the culture system, as it reduces batch-to-batch variations and allows for scalability. Furthermore, this system could be implemented as an accurate model for understanding the mechanisms underlying the hepatocyte differentiation from pluripotent stem cells.

3.2 Results

3.2.1 Characterization of the hESC population

Developing a culture system that supports the proliferation of undifferentiated and pluripotent hESCs requires a large amount of time and effort. The latest advances in developing successful defined culture approaches have allowed the possession of standardised, reproducible, scalable and efficient methods to culture hESCs, conferring the culture with suitable conditions for maintaining the self-renewal and the pluripotent abilities of the hESCs.

3.2.1.1 Culture and characterisation of hESCs maintained in mTeSR1™

hESC line H9 was thawed and cultured on conditioned media (CM) supplemented with bFGF on a monolayer of mitotically inactive mouse embryonic fibroblast feeder cells (MEFs) plated on matrigel coated surfaces, and gradually transitioned into mTeSR1™ (MT). At the first passage after thawing, hESCs cultured on MEFs were transferred into a feeder free matrigel surface containing 100% CM for 48 hours. Afterwards, cells were cultured in a mixture of CM:MT at the following ratios; 75:25, 50:50, 25:75 and finally 100% MT, 48 hours in each mixture. hESCs were then maintained in MT for a minimum of 5 passages before they were characterised for their ES cell identity and pluripotency capacity. For hepatocyte differentiation, cells were maintained for up to 30 passages in MT media. hESC identity was assessed by morphological analysis, examination of the expression of transcription factors ascribed to pluripotency; Oct 4 (Octamer 4) and Nanog, and their cell surface expression of SSEA-1, SSEA-4, TRA-1-60 and TRA-1-81. In addition, analysis of the pluripotency capacity of the cells was measured by studying their ability to spontaneously differentiate into all three germ layers, the ectoderm, mesoderm and endoderm, and directly differentiation into HLCs using a standardised protocol.

Morphological analysis of the hESCs in culture was used as a guide to assess culture homogeneity. hESCs H9 grown in mTeSR1™ formed tightly packed dome-like

colonies with well-defined edges and no observable spontaneous cellular differentiation. Cells displayed the characteristic hESC morphology, defined by the possession of a large nucleus to cytoplasm ratio with well-defined and pronounced nucleoli (Figure 6A). Further to morphological analysis, the 'stemness' nature of the hESCs cultured in MT was investigated by analysing the gene and protein expression of two well established transcription factors associated with 'stemness', Oct 4 (Octamer 4) and Nanog, employing quantitative PCR and immunofluorescence. Gene expression levels of these transcription factors in the hESC H9 were comparable to the expression observed in the hESC H7, a well described hESC line used as a control and cultured under the same conditions as H9 (Figure 6B). In addition, the protein expression, as depicted by the immunofluorescence, revealed that 97% and 98% of the cells stained positive for Oct 4 and Nanog, respectively (Figure 7). The high level of expression of Oct 4 and Nanog confirmed the undifferentiated state of the hESCs.

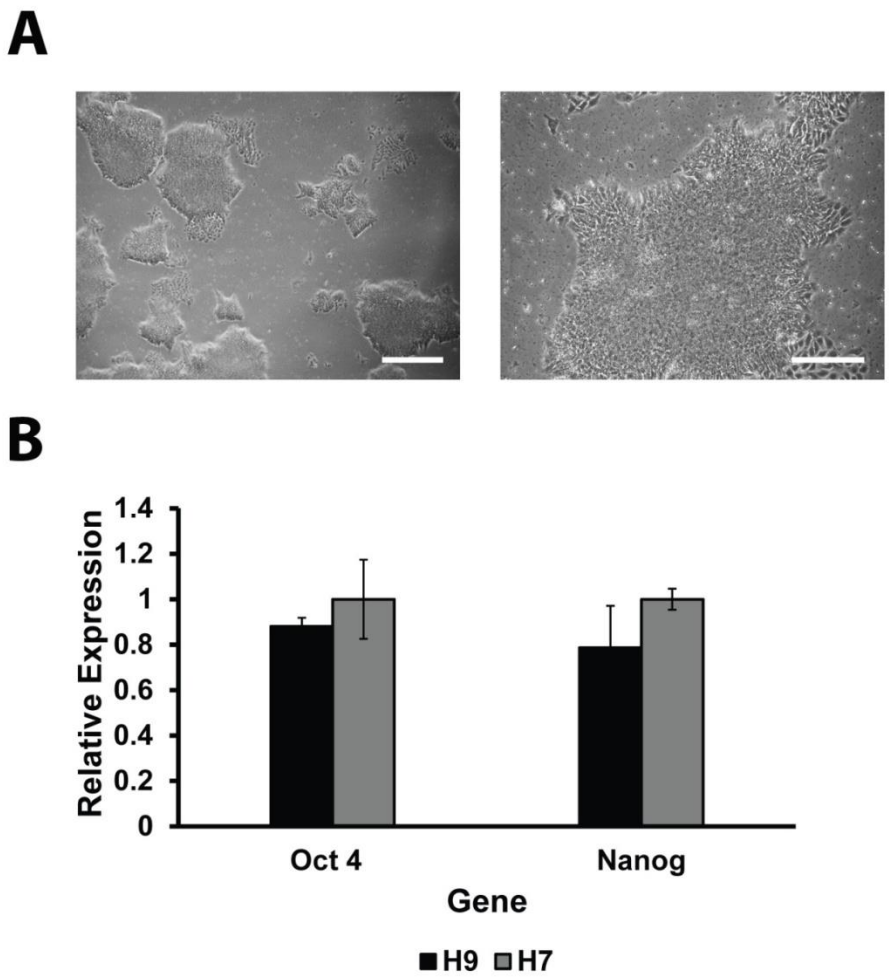

Figure 6. Analysis of hESCs in culture. A) hESC line H9 maintained in mTeSR1™ media displayed morphological features typical of hESCs, showing a large nucleus to cytoplasm ratio. hESCs formed colonies with well-defined edges and little to no differentiation observed between the colonies. Images were taken at 4x magnification (left) or 10x magnification (right), and scale bar represents 200 µm and 100 µm respectively. B) Gene expression analysis of the pluripotent markers Octamer 4 (Oct 4) and Nanog by quantitative PCR in hESCs H9 revealed comparable gene expression levels to hESC line H7, with no statistically significant difference between both cell lines. Relative expression refers to fold of induction normalised to the housekeeping gene GAPDH and to H7 cultured under the same conditions. The results represent the mean ± SD of three different samples, and each run in triplicate. Levels of significance were measured by student's *t-test* where $p<0.05$ represents non-significant difference. Abbreviations: Oct4-Octamer 4. GAPDH is not the best housekeeping gene to be used as its expression varies with the metabolic activity of the cells during the differentiation process.

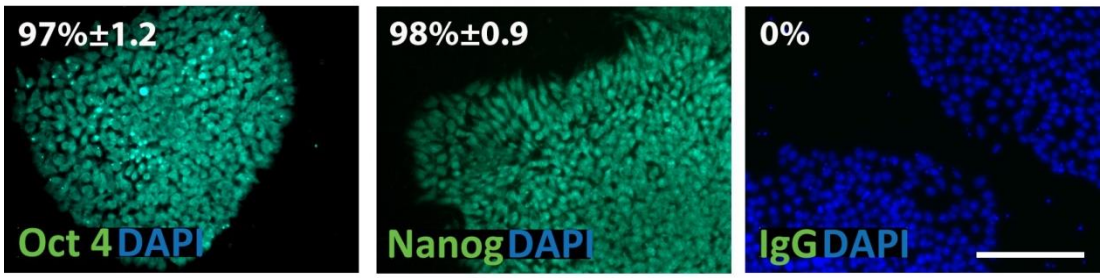

Figure 7. Immunofluorescence analysis of pluripotent markers in hESCs. Pluripotent marker expression in hESCs H9 was confirmed by immunofluorescence, with 97% and 98% of the cells expressing Oct 4 and Nanog respectively, further supporting the stem cell status of hESC maintained in mTeSR1™ media. The corresponding IgG control demonstrated the specificity of the staining. For each condition five random fields of view, containing at least 500 cells, were counted. Images were taken at 20x magnification and the scale bar represents 100 µm. Abbreviations: Oct4-Octamer 4, IgG-Immunoglobulin G.

Fluorescence activated cell sorting (FACS) is another technique employed to characterise the stem cell identity of hESCs. As such, the expression of cell surface antigens in hESCs at different passage ranges (p41 to 50, p51 to 60 and p61 to 70) was investigated by FACS. The surface markers used to identify hESCs within a population included SSEA-1 and -4 and the TRA surface antigens 1-60 and 1-81. Cells were gated according to their side scatter *vs.* forward scatter properties in order to eliminate dead, differentiated or cell aggregates. The results displayed in Figure 8 showed background level of SSEA-1 expression (a differentiation marker) in any of the cell passage range as expected. The percentage of cells expressing SSEA-4 (98% and 95%), TRA -1-60 (93% and 82%) and TRA-1-81 (95% and 90%) was confirmed in greater than 80% of the cells within cell passage range p41 to 50 and p51 to 60, respectively, supporting the undifferentiated state of the cells. Despite that cell passage range p51 to 60 expressed comparable levels of SSEA-4 to other cell passage range (95%), TRA-1-60 and TRA-1-81 expression levels were lower than expected (66% and 49% respectively). Therefore, based on these observations, cells at the passage range p41 to p60 were used for hepatocyte differentiation purpose.

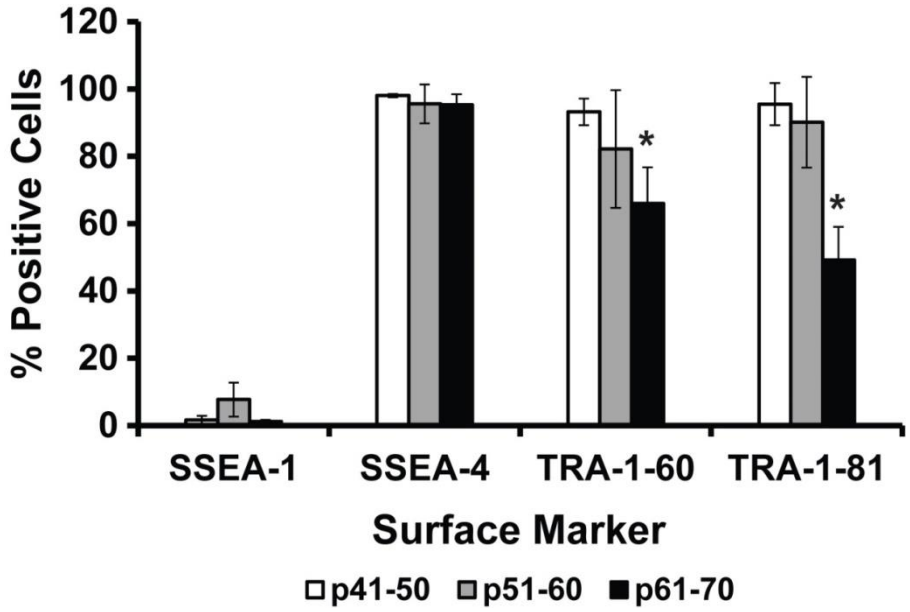

Figure 8. Expression of stem cell surface markers in hESCs. The graph shows the percentage of cells at different passage ranges expressing hESC surface markers, including SSEA-4, TRA-1-60 and TRA-1-81. Low percentages of cells expressed the differentiation marker SSEA-1 further supporting the stem cell nature of these hESCs. Unstained cells were used to define levels of background staining. The results represent the mean ± SD of six independent samples for cell passage range p41-50 and p51-60 and three independent samples for cell passage p61-70. Levels of significance were measured by student's t-test where $p<0.05$ is denoted as *.

3.2.1.2 Testing pluripotency of hESCs maintained in mTeSR1™

hESCs are able to spontaneously differentiate into cell types from all three germ layers; the endoderm, mesoderm and ectoderm. This pluripotency capacity can be tested by embryoid body (EB) formation assay, a widely accepted method (Xu *et al*., 2001). The cell types associated with the germ layers are frequently identified by detecting the expression of proteins associated to each of the three germ layers: alpha-fetoprotein (AFP) for endodermal lineage, alpha-smooth muscle actin (α-SMA) for mesodermal lineage and β-tubulin III for ectodermal lineage.

To perform the assay, hESCs at 80-90% confluency were lifted and placed into a suspension culture, suitable for promoting cell aggregation. After 7 days the EBs generated were well defined and vacuolated, suggesting efficient EB formation. Following this, the EBs were transferred to gelatin coated wells, where the aggregates attached to the surface and were allowed to spontaneously differentiate

over a 14-day period. The resulting cell cultures were then fixed in ice cold methanol and stained with antibodies that are specific for each lineage. Figure 9 displays the resulting cell types formed following EB spontaneous differentiation from hESCs cultured in MT. hESCs formed cell types that were positive for alpha-fetoprotein (endoderm), alpha-smooth muscle (mesoderm) and β-tubulin III (ectoderm). This data demonstrates that the culturing conditions used in this study maintained hESC pluripotency.

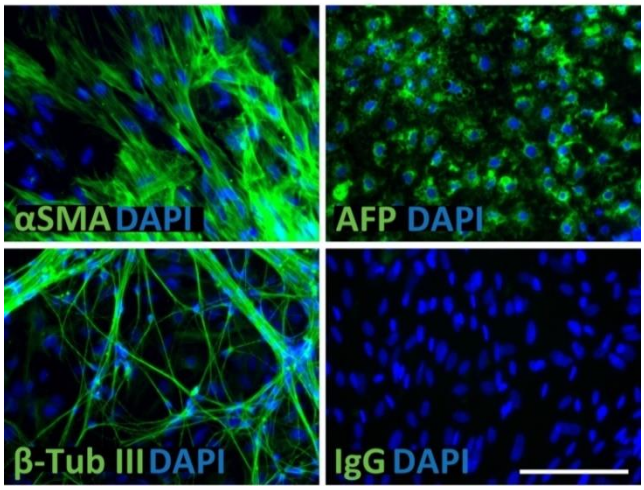

Figure 9. Analysing hESC spontaneous differentiation. Immunofluorescence analysis shows that hESCs were able to form cell types from all three germ layers, demonstrating their pluripotency. Smooth muscle actin positive cells represent cells from the mesoderm lineage, AFP represents endodermal cells and beta tubulin III defines cells from the ectodermal lineage. The IgG control demonstrated the specificity of the immunostaining. Images were taken at 20x magnification and the scale bar represents 100 μm. Abbreviations: α-SMA-alpha Smooth Muscle Actin, AFP-alpha-Fetoprotein, β-Tub III-beta Tubulin III and IgG-Immunoglobulin G.

In addition, I investigated the genetic stability of founding populations by SNP (single nucleotide polymorphism) ensuring that no major mutations compromising the results were detected (Supplementary Figure 1 and 2).

The data here presented shows that mTeSR1™ (MT) represents a suitable culture media to provide a stable environment for hESC culture as it supports hESC self-renewal and pluripotency. The next section will focus on the capacity of hESC line H9 to differentiate towards the hepatic endoderm lineage.

3.2.2 Direct differentiation and characterization of hESCs-derived hepatic endoderm

Delivery of pluripotent stem cell derived somatic cells requires the development of reliable and efficient differentiation procedures. Undifferentiated hESCs maintained in MT were scaled up to the desired quantity and the hepatic differentiation was performed using an efficient and well established differentiation procedure (Figure 10). hESCs were primed towards definitive endoderm in the presence of Wnt3a and Activin A prior to the hepatic specification, which was induced in a media containing Knock-Out Serum Replacement (KOSR) and DMSO (SR/DMSO media), resulting in liver progenitor cells, called hepatoblasts. Finally, hepatocyte differentiation and maturation was driven by culturing the cells in a media supplemented with oncostatin M (OSM) and hepatocyte growth factor (HGF). Morphological, transcriptional and functional analyses were performed at various time points to accurately define the end products obtained in each of the stages. Characterisation of the definitive endoderm and the hepatoblast stage of the cells will be described in more detail in the following sections.

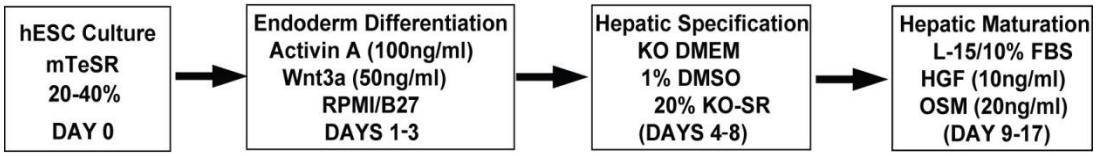

Figure 10. Flow diagram of the hepatocyte differentiation protocol in serum containing media. H9 hESCs were differentiated to hESCs-derived hepatocyte-like cells by using an efficient serum-free differentiation protocol for up to 17 days. Abbreviations hESC– human embryonic stem cells; KO DMEM – knock out Dulbecco's Modified Eagle Medium; DMSO – Dimethyl sulfoxide; KOSR-Knockout serum replacement; L-15-L-15 media; FBS-Foetal Bovine Serum; HGF – Hepatocyte growth factor; OSM – Oncostatin M. Protocol described in detail in Hay *et al*., 2008a

3.2.2.1 Characterisation of hESCs-derived definitive endoderm.

hESCs cultured in MT at 40-50% confluency were differentiated towards definitive endoderm by transferring the cells to a RPMI/B27 media supplemented with Wnt3a and Activin A. During the priming towards the endoderm fate, cells adopted a high

migratory and proliferative capacity, and 72 hours post-induction profound changes in the cell morphology were observed, with cells adopting the characteristic triangular endoderm shape (Figure 11A). In line with changes in cell morphology, quantitative PCR analysis showed a decrease in the expression of the pluripotent markers Oct 4 and Nanog (≈50 and 30% respectively) (Figure 11B), in parallel with an increase in the expression of the endodermal marker Sox 17 (≈14000-fold induction) (Figure 11C) when compared to undifferentiated hESCs ($p<0.001$). Analysis of the protein expression levels Sox 17 was performed by immunostaining, revealing that 93% of the cells stained positive for this marker (Figure 11D). All together the data presented demonstrates the commitment of the hESCs to definitive endoderm.

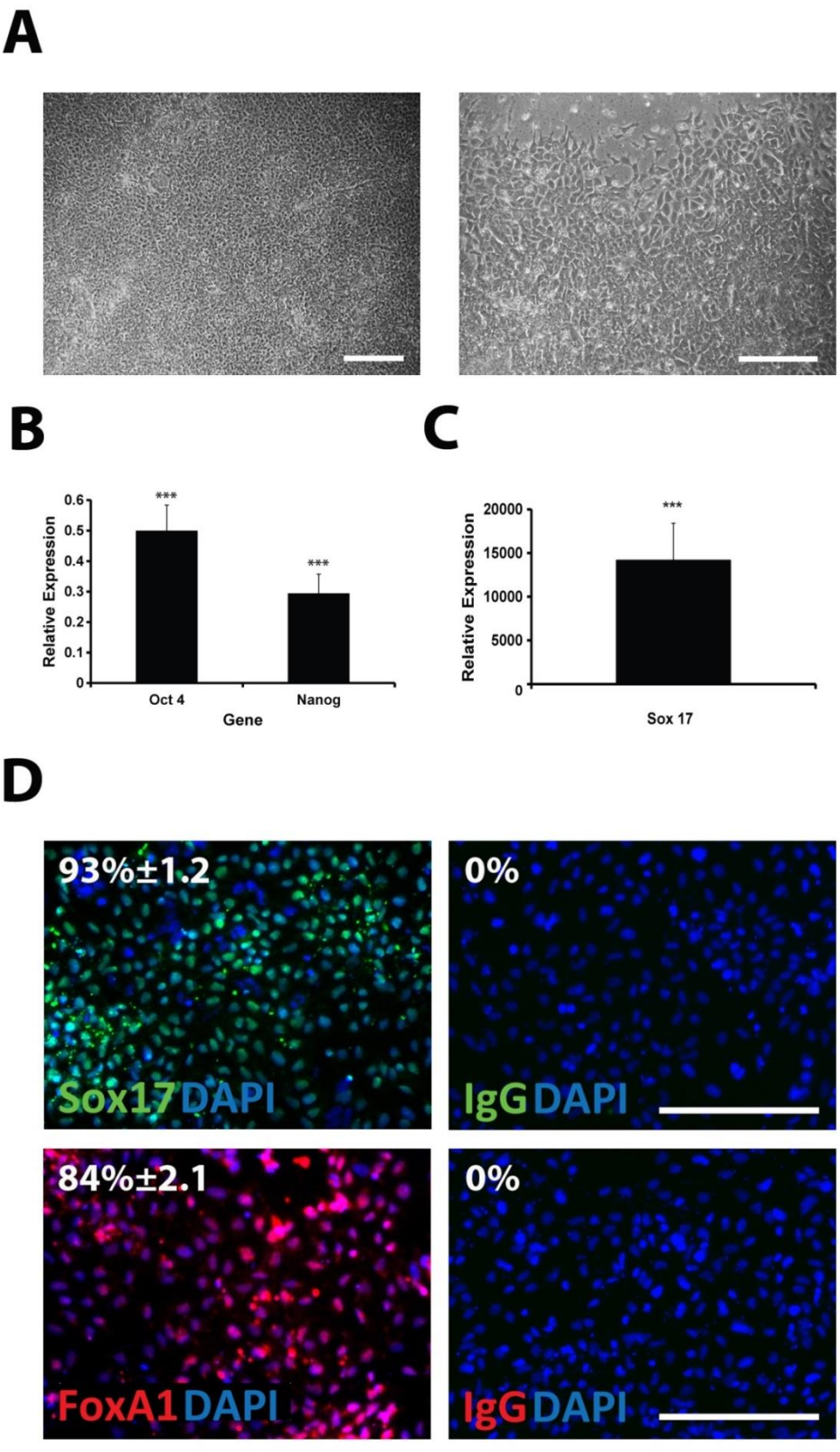

Figure 11.Characterisation of the hESCs-derived definitive endoderm. The hESCs H9 were stimulated to differentiate down the endodermal lineage using Wnt3a and Activin A. A) Phase

contrast images of the cells at Day 3 in the differentiation process showed cells adopting the characteristic definitive endoderm morphology, denoted by the possession of a triangular-shape. Images were taken at 4x magnification (left) or 10x magnification (right), and scale bar represents 200 µm and 100 µm respectively. B-C) Gene expression analysis of pluripotent and definitive endoderm markers in the cells at Day 3 in the differentiation. (B) Quantitative PCR analysis of the pluripotent makers Oct 4 and Nanog revealed a decrease in the expression of these makers as the differentiation progressed. C) Quantitative PCR analysis of the definitive endoderm marker Sox17 in the differentiating cells suggested the commitment of the cells to the endoderm lineage. Relative expression refers to fold of induction over hESCs and normalised to the housekeeping gene GAPDH. The results represent the mean ± SD of three different samples, each run in triplicate. Levels of significance were measured by student's t-test where $p<0.001$ is denoted as ***. D) Immunofluorescence analysis of Sox17. The commitment of the cells to definitive endoderm was confirmed by immunostaining, as 93% of the cells expressed Sox17, further supporting the definitive endoderm status of the cells. The corresponding IgG controls demonstrated the specificity of the immunostaining. For each condition five random fields of view containing at least 500 cells, were counted. Images were taken at 20x magnification and the scale bar represents 100 µm. Abbreviations: Oct 4-Octamer 4; IgG-Immunoglobulin G.

3.2.2.2 Defining the hepatoblast stage of the cells

Hepatic specification of hESCs-derived definitive endoderm cells was induced by transferring the cells to a media containing Knock-Out Serum Replacement (KOSR) and DMSO (KOSR/DMSO media) for 5 days. The resulting population of cells were then transferred to a hepatocyte maturation media supplemented with oncostatin M (OSM) and hepatocyte growth factor (HGF) for 24 or 48 hours. In order to define the stage at which the cells displayed the most hepatoblastic phenotype, morphological, transcriptional and protein analysis were performed in cells at Day 8 in the differentiation process (after 5 days on KOSR/DMSO), at Day 9 and Day 10 (24 or 48 hours on the maturation media, respectively).

Morphological analysis

The hepatic specification of the hESCs-derived definitive endoderm resulted in a compacted culture of hESCs-derived hepatoblasts (Figure 12), which displayed a greater morphological homogeneity at Day 8 and Day 9 (A-B) compared to cells at Day 10 (C). hESCs-derived hepatoblasts at Day 8 (D) adopted a cobblestone-like morphology, which was more distinct at Day 9 (E), with clearer cellular edges and well-defined cell-to-cell contacts observed on the cells. The progression of the

differentiation resulted in the display of a cellular heterogeneity regarding to cells length, width and size at Day 10 (F).

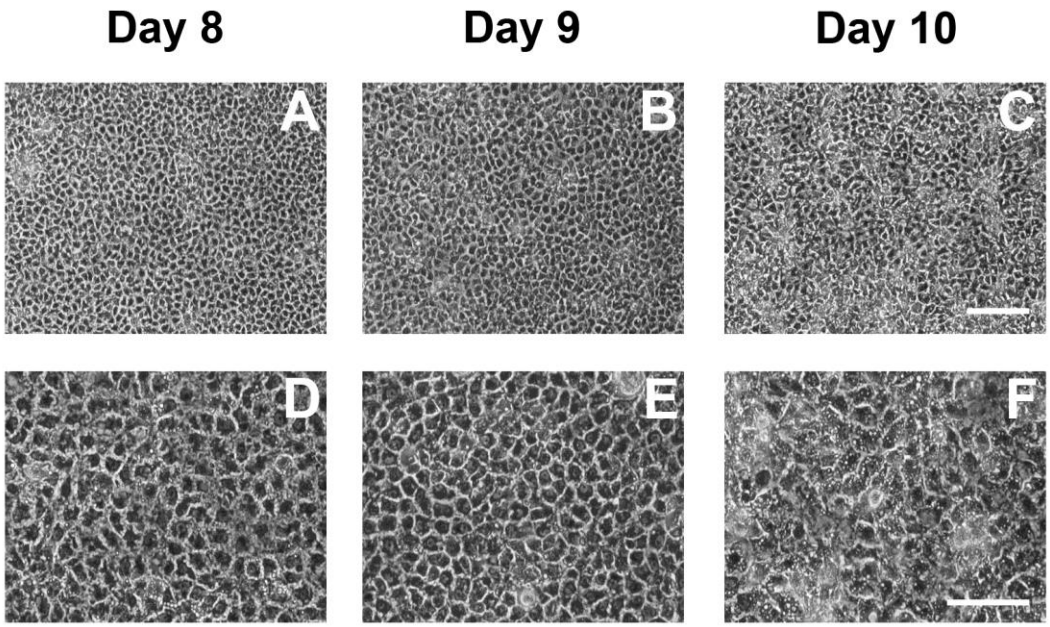

Figure 12.Morphological analysis of the hESCs-derived hepatoblast. The hESCs-derived definitive endoderm cells were stimulated to differentiate down the hepatic lineage in the presence of a media containing Knock-Out Serum Replacement (KOSR) and DMSO for 5 days (Day 8), prior to addition of the maturation media for 24 and 48 hours (Day 9 and Day 10, respectively). The resulting cell cultures displayed a homogeneous cell population consisting on cell adopting the typical hepatoblast morphology, denoted by the display of a cobblestone-like morphology with well-defined cell-to-cell contact. The images were taken at 4x magnification (A-C) or 10x magnification (D-F), and scale bar represents 200 µm and 100 µm respectively.

Gene expression profiling of hESCs-derived hepatoblasts.

To define hepatoblast gene expression stage of the cells, I analysed the expression of hepatoblast markers at Day 8, Day 9 and Day 10 using quantitative PCR. The gene expression profile is shown in Figure 13.

The peak in the gene expression of the foetal hepatic marker alpha-fetoprotein (panel A) was detected in hESCs-derived hepatoblasts at Day 10 in the differentiation approach with a 33 and 3.5-fold increase compared to Day 8 and Day

9, respectively ($p<0.001$), with statistically significant differences between these last two days ($p>0.05$).

Analysis in the gene expression of the hepatoblast marker Sox 9 (panel B) indicated that hESCs-derived hepatoblasts at Day 8 displayed the highest levels out of the analysed days , with 1.75 and 1.5-fold increase compared to Day 9 and Day 10, respectively ($p<0.05$), with statistically significant difference between these last two days ($p<0.05$).

hESCs-derived hepatoblasts at Day 8 in the differentiation approach displayed the highest gene expression levels of EpCAM (panel C) with a 1.85 and 1.25-fold increase compared to cells at Day 9 and Day 10, respectively ($p<0.05$), with statistically significant differences between these last two days ($p<0.001$).

Hepatocyte nuclear factor 1 β, HNF1β, gene expression (panel D) was detected at the highest in hESCs-derived hepatoblasts at Day 8 in the differentiation approach, with 2.7 and 3.4-fold increase compared to cells at Day 9 and Day 10, respectively ($p<0.001$), with a statistically significant difference between these last two days ($p<0.001$).

Analysis in the gene expression of the hepatoblast marker hepatocyte nuclear factor 3 β, HNF3β, (panel E) revealed that hESCs-derived hepatoblasts at Day 8 in the differentiation approach exhibited the highest level of expression, with 3 and 2.5-fold increase compared to cells at Day 9 and Day 10, respectively ($p<0.001$) and no statically significant difference between these two last days ($p>0.05$).

Comparable situation was observed when Cytokeratin 19 gene expression (panel F) was analysed. Cells at Day 8 displayed the highest level of expression, 1.5-fold increase compared to the rest of the days ($p<0.001$) and no statically significant difference between these two time points ($p>0.05$).

hESCs-derived hepatoblast at Day 8 in the differentiation approach showed higher levels of Prox-1 gene expression (panel G) than the rest of the analysed days, with 2

and 1.3-fold increase compared to Day 9 and Day 10 respectively ($p<0.001$), with a statistically significant difference between these last two days ($p<0.001$).

Analysis in albumin expression revealed that the peak in the gene expression in hESCs-derived hepatoblasts was reached at Day 10 (panel H), with 2-fold increase compared to cells at Day 8 ($p<0.05$) but no statically significant difference compared to cells at Day 9 (1.15-fold increase, $p>0.05$).

The hepatocyte lineage marker hepatocyte nuclear factor 4α, HNF4α, gene expression (panel I) was at the highest in cells at Day 8 in the differentiation approach, with 2.9 and 3.25-fold increase compared to Day 9 and Day 10, respectively ($p<0.001$), with a statistically significant difference between these last two days ($p>0.01$).

Cells at Day 10 in the differentiation approach displayed the highest epithelial marker E-Cadherin gene expression (panel J), with 1.85 and 2.85-fold increase compared to cells at Day 8 and Day 9, respectively ($p<0.001$), with a statistically significant difference between these last two days ($p<0.001$).

Analysis in the hepatoblast markers gene expression suggests that hESCs-derived hepatoblasts at Day 8 in the differentiation procedure display the most hepatoblastic phenotype out of all the analysed days.

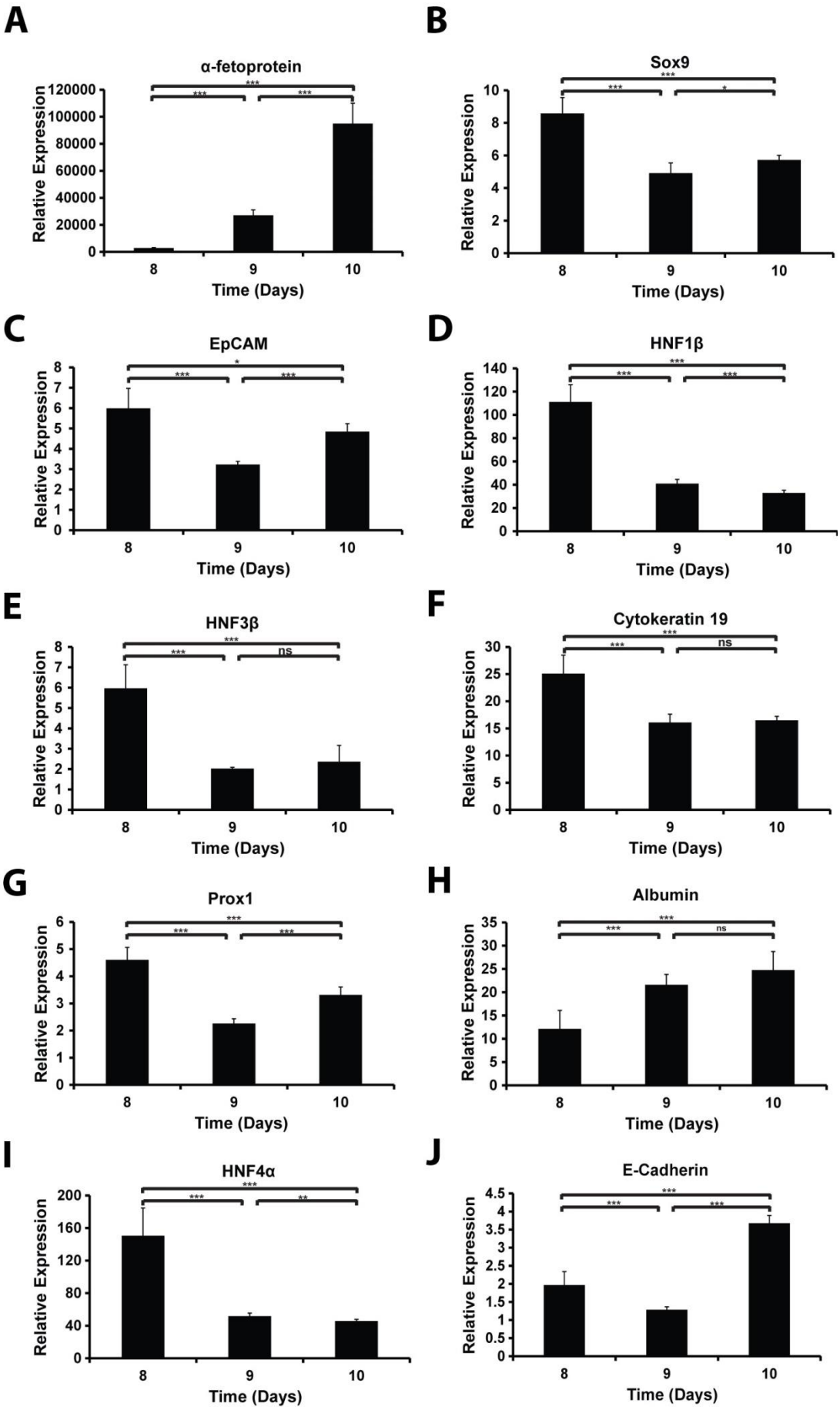
A
α-fetoprotein
Relative Expression
Time (Days)
B
Sox9
C
EpCAM
D
HNF1β
E
HNF3β
ns
F
Cytokeratin 19
G
Prox1
H
Albumin
I
HNF4α
J
E-Cadherin

Figure 13. Hepatoblast gene expression. Expression of the hepatoblast markers (α-fetoprotein, Sox9, EpCAM, HNF1β, HNF3β, Cytokeratin19, Prox1, Albumin and HNF4α) and the epithelial marker E-Cadherin in hESCs-derived hepatoblasts at Day 8, Day 9 and Day 10 in the differentiation approach were analysed by quantitative PCR. Relative expression refers to fold of induction over hESCs and normalised to the housekeeping gene GAPDH. The results represent the mean ± SD of three different samples, each run in triplicate. Levels of significance were measured by student's t-test where $p<0.05$ is denoted as *, $p<0.01$ is denoted as ** and $p<0.001$ is denoted as ***. Abbreviations: HNF4α- Hepatocyte nuclear factor 4α, HNF3β- Hepatocyte nuclear factor 3β, HNF1β- Hepatocyte nuclear factor 1β.

Protein expression profiling of hESCs-derived hepatoblast.

In addition to quantitative PCR, I also investigated the protein expression of hepatoblast and hepatocyte markers and the proliferative marker Ki67 in hESCs-derived hepatoblasts (Figure 14). Cells fixed at Day 8, Day 9 and Day 10 were stained with antibodies to hepatocyte nuclear factor 4α (HNF4α), α-fetoprotein (AFP), the transcription factors GATA4 and GATA6, cytokeratin 19 (CK19), albumin, and the proliferative marker Ki67.

Analysis of the percentage yield of hESCs-derived hepatoblasts expressing HNF4α (panels A-C) revealed that over 90% of the cells at Day 8, Day 9 and Day 10 expressed the transcription factor (94%, 94.1% and 92.8% respectively) with no statically significant differences ($p<0.05$) between the analysed days. Similar pattern of expression was found when alpha-fetoprotein expression was analysed (panels E-G) as 97%, 99% and 98% of hESCs-derived hepatoblasts at Day 8, Day 9 and Day 10, respectively stained positive, with no statically significant differences ($p<0.05$). Analysis of the protein expression of the hepatic endoderm transcription factor GATA4 (panels I-K) revealed no statistically significant differences between the days as ≈97%, 95% and 93% of the cells stained positive at Day 8, Day 9 and Day 10 respectively ($p<0.05$). In contrast, GATA6 expression (panels M-O) showed a decrease as the differentiation progressed as 99%, ≈76% and ≈50% of the cells stained positive for this transcription factor at Day 8, Day 9 and Day 10, respectively ($p>0.01$). Cytokeratin 19 (panels Q-S) was expressed in over 96% of the cells, reaching a peak at Day 10 when 99% of the cells stained positive for the hepatoblast

marker but with no statically significant differences between the analysed day ($p>0.05$). Analysis of the protein expression of the hepatic lineage marker albumin (panels U-W) revealed that the percentage of hESCs-derived hepatoblasts staining positive increased as the differentiation progressed, as ≈39% of cells at Day 10 ($p>0.01$) expressed albumin compared with ≈20% of cells at Day 9 and Day 8 .

In addition, I analysed the expression of the proliferative marker Ki67 (panels Y-AA) at the previously mentioned days. A decrease in the percentage yield of hESCs-derived hepatoblasts staining positive as the differentiation progresses was observed, as ≈86%, ≈82% and ≈73% of the cells expressed this protein at Day 8, Day 9 and Day 10, respectively but with not statically significant differences ($p<0.05$).

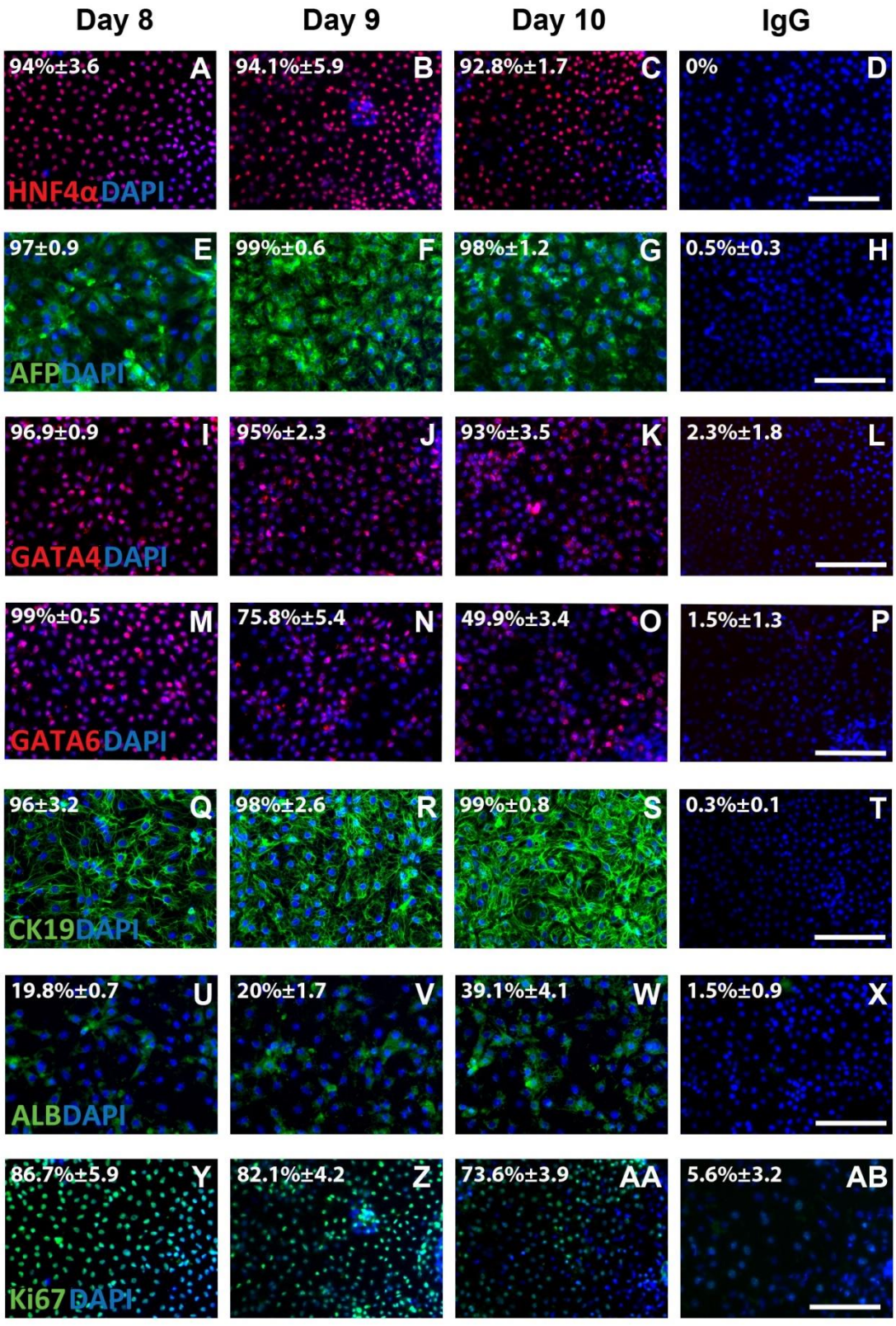

Figure 14. Immunofluorescence analysis of hESCs-derived hepatoblasts. At Day 8, 9 and 10, differentiated cells were stained for hepatoblast markers, including HNF4α (panels A-C), α-fetoprotein (panels E-G), GATA4 (panels I-K), GATA6 (panels M-O), Cytokeratin 19 (panels Q-S)

and Albumin (panels U-W). Ki67 staining (panels Y-AA) was used to assess the proliferative state of the cells. The corresponding IgG controls confirmed the specificity of the staining. For each condition five random fields of view, containing at least 400 cells, were counted. Images were taken at 20x magnification and the scale bar represents 100 µm. Abbreviations: HNF4α-Hepatocyte nuclear factor 4α, AFP-alpha-fetoprotein, CK19-Cytokeratin 19, ALB-Albumin, IgG-Immunoglobulin G.

As little differences were observed in the protein expression of hepatic markers between the analysed days, based on the gene expression and morphology features, I concluded that cells at Day 8 in the differentiation protocol displayed the most hepatoblastic phenotype out of all analysed days.

In conclusion, the hepatic endoderm generated from hESCs display markers resembling the development observed *in vivo*. The next section will focus in the generation of functional hepatocyte-like cells from human embryonic stem cells.

3.2.3 Hepatocyte maturation in a serum containing media.

Hepatocyte specification of hESCs-derived hepatoblasts was performed by transferring the cells to a foetal bovine serum (FBS) containing maturation media supplemented with oncostatin M (OSM) and hepatocyte growth factor (HGF), employing an efficient differentiation (Hay *et al*., 2008a). To accurately define the end product, morphological, transcriptional and functional analyses were performed on the hESCs-derived HLCs.

Morphological analysis of hESCs-derived HLCs at Day 17 in the differentiation protocol indicated that cell cultures underwent morphological changes, resulting in a homogeneous population of cells displaying morphological trails associated with cultures of mature hepatocytes. Cells adooted a hexagonal shape and clear and well defined large nuclei. These morphological changes indicated a successful hepatocyte maturation process (Figure 15A).

To further characterise the HLCs, I investigated the expression of different hepatocyte markers involved in the maintenance of the hepatocyte phenotype using immunostaining. Monolayers of HLCs were fixed at day 17 and stained with

antibodies to alpha-fetoprotein (AFP), albumin (ALB), cytochrome P450 3A (CYP3A) and the epithelial marker E-Cadherin (Figure 11B). Analysis of the expression revealed that 66%, 86%, 74% and 78% of the cells stained positive for alpha-fetoprotein, albumin, CYP3A and E-Cadherin respectively, demonstrating the high purity displayed by the cultures.

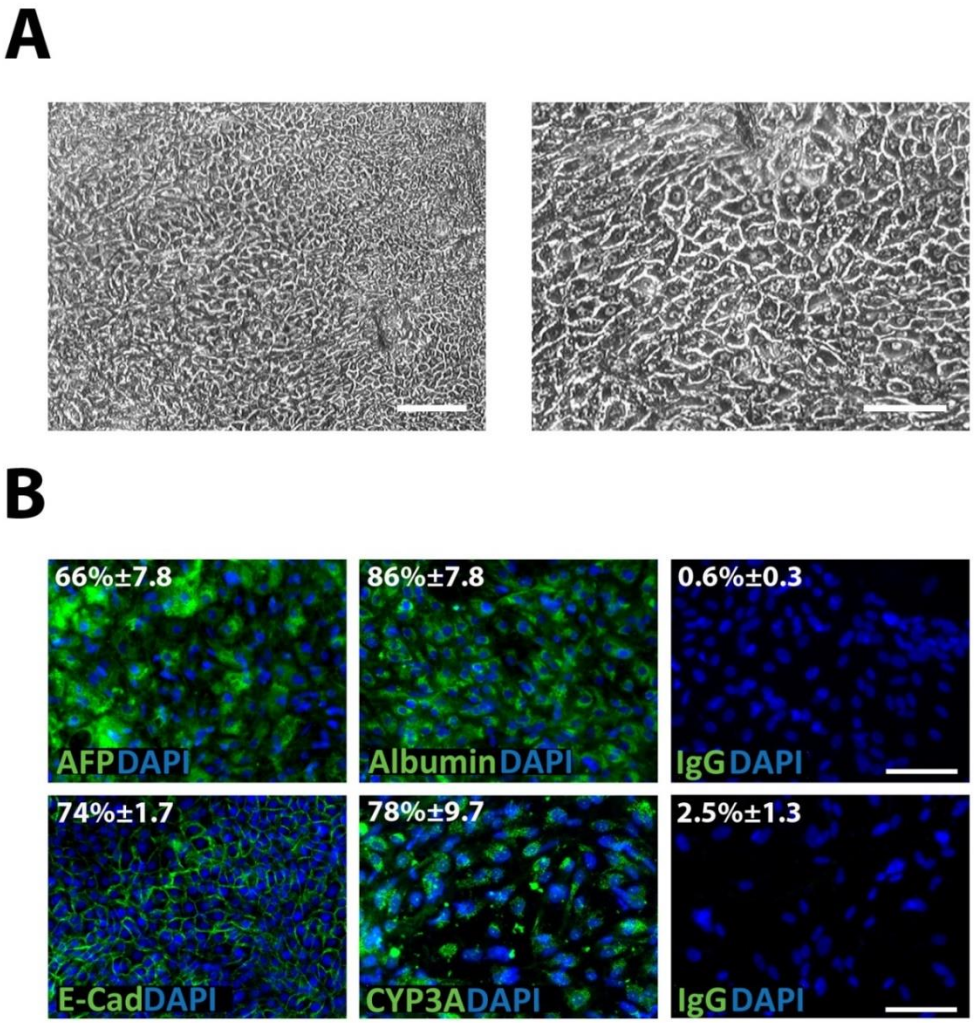

Figure 15. Characterisation of hESCs-derived HLCs on a serum containing media. hESCs-derived hepatoblasts were differentiated to HLCs using a serum containing media supplemented with OSM and HGF. A) Phase contrast images of the cells at Day 17 indicated the display of the hexagonal cellular shape characteristic of primary adult hepatocyte by the HLCs, suggesting successful differentiation into hepatocytes. The images were taken at 4x magnification (left) or 10x magnification (right) and scale bar represents 200 µm and 100 µm respectively. B) Immunofluorescence analysis of hepatocyte lineage markers. The expression of hepatocyte markers, including α-fetoprotein, albumin, CYP3A and the epithelial marker E-Cadherin were analysed by immunofluorescence in hESCs-derived HLC at Day 17 on the differentiation procedure, demonstrating the cell commitment to a hepatocyte fate. The corresponding IgG controls indicated the specificity of the staining. For each condition five random fields of view, containing at least 500 cells,

were counted. Images were taken at 20x magnification and the scales bar represents 100 µm. Abbreviations: AFP-Alpha-fetoprotein, ALB-Albumin, E-Cad-E-Cadherin, CYP3A-Cytochrome P450 3A, IgG-Immunoglobulin G.

3.2.4 Necessity of moving to a serum-free maturation media.

In addition to protein analysis, I measured the activity of the P450 cytochrome 3A (CYP3A), a member of the cytochrome P450 that is involved in the drug metabolism of xenobiotic compounds and accounts for up to 50% of the total cytochrome P450 activity *in vivo*. Therefore, measurement of the activity of this enzyme well reflects the functional capacity of the cells. Four parallel and individual differentiation experiments using a different batch of FBS in the maturation media were performed. CYP3A activity was measured in the resulting individual populations of HLCs, revealing differences between 1.5 and 2 fold activity depending on the batch of serum used (Figure 16). The values for CYP3A for the different FBS batches are follows; 34,068 RLU/ml/mg for batch 1, 39,367 RLU/ml/mg for batch 2, 25,900 RLU/ml/mg for batch 3 and 20,494 RLU/ml/mg for batch 4.

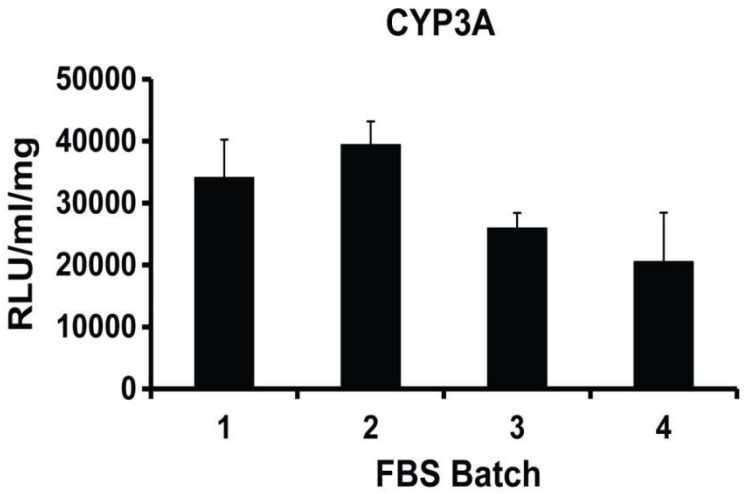

Figure 16. HLC functional characterisation. Cytochrome P450 function 3A in hESCs-derived HLCs was assessed using a commercially available system (pGLO®), revealing a high variability on the metabolic capacity of the cells depending on the batch of FBS serum used in the maturation media, with differences between 1.5 and 2 fold activity. The results represent the mean ± SD of three individual samples**.**

The data presented demonstrate that by applying the serum containing differentiation protocol to hESCs-derived hepatoblasts, I obtained homogeneous populations of cells committed to the hepatocyte lineage, but displayed variability which was associated to the use of serum in the maturation medium.

3.2.5 Hepatocyte differentiation using a serum-free approach.

The high level of variability associated with the use of serum containing media suggested the necessity of developing a serum-free differentiation protocol to obtain HLCs. Therefore, optimisation of the maturation step involved the replacement of the serum containing media for a defined serum-free media. The resulting population of cells were extensively characterised at different times during the differentiation procedure (Figure 17). Morphological analysis of the cells, RNA, protein expression pattern and functional analysis were performed.

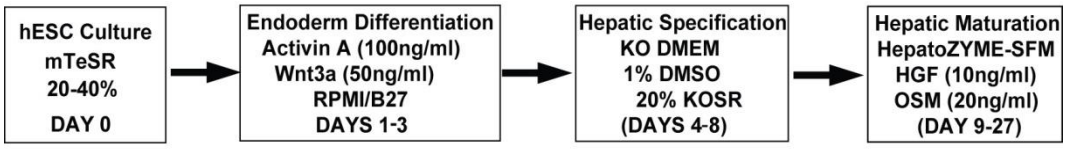

Figure 17. Flow diagram of the hepatocyte differentiation protocol in serum-free media. H9 hESCs are differentiated to HLCs by using an efficient serum-free differentiation protocol for up to 27 days. Abbreviations hESC– human embryonic stem cells; KO DMEM – knock out Dulbecco's Modified Eagle Medium; DMSO – Dimethyl sulfoxide; KOSR- Knockout serum replacement; HZM-HepatoZYME®-SFM; HGF – Hepatocyte growth factor; OSM – Oncostatin M.

3.2.5.1 Morphological analysis

Images of the HLCs were taken at different time points in the differentiation protocol (Figure 18). The resulting HLCs displayed morphological homogeneity (panels A-D) up to Day 21 in the differentiation process. By Day 15 (panel E), HLCs displayed morphological trails associated with mature hepatocytes, becoming clearer as the differentiation progressed. Cells adopted a hexagonal shape, the nuclei became larger and more defined, with clear cell-to-cell contact and the formation of canaliculi-like structures were observed (panels F-H, white and black

arrows), all morphological features characteristic of primary hepatocytes in culture. These observations supported the hepatocyte maturation in the defined serum-free maturation media with comparable morphology previously seen in the serum containing media.

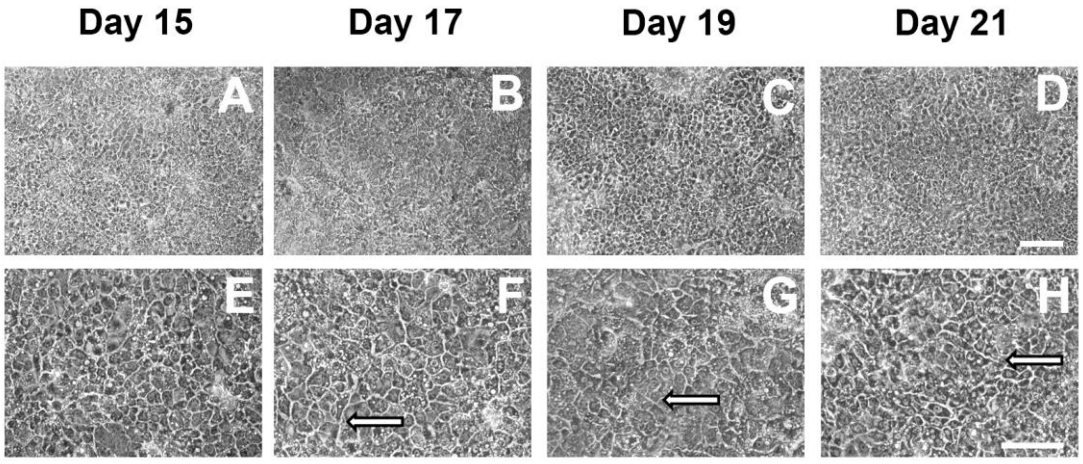

Figure 18. Morphological analysis of HLCs in a serum-free approach. The hESCs-derived hepatoblasts were differentiated to HLCs in the defined serum-free maturation media. During the maturation stage, cells underwent morphological changes mimicking processes observed *in vivo*. The nucleus became more defining and cells acquired a hexagonal morphology with an increase in the cell-to-cell contact resembling to cultures of human primary hepatocytes. Parallel to the acquisition of the typical primary hepatocyte morphology, the homogeneous cell cultures displayed canaliculi-like structures denoting the acquisition of mature hepatocyte morphology. The images were taken at 4x magnification (panels A-D) or 10x magnification (panels E-H) and scale bar represents 200 µm and 100 µm respectively.

3.2.5.2 Gene expression profiling of HLCs

To further characterise the *in vitro* HLCs obtained in the serum-free differentiation protocol, I explored the gene expression of hepatocyte markers at Day 15, 17, 19 and 21 in the differentiation approach by quantitative PCR. The gene expression profile is shown in Figure 19.

Albumin gene expression (panel A) significantly increase ($p<0.001$) as the differentiation progresses with a 50, 3.5 and 2 fold increase at Day 17, 19 and 21 respectively compared to the previous time point.

Analysis in the gene expression of the hepatocyte nuclear factor 4α, HNF4α (panel B) showed a stabilisation in the between Day 15 and 17, followed by a significant decreases of 1.25 and 2.6-fold ($p<0.05$) by Day 19 and 21, respectively.

CYP3A4 gene expression (panel C) reached a peak at Day 19, after an 18.5 and 4.75-fold increase compared to Day 15 and 17 respectively ($p<0.01$), followed by a decrease of 1.4-fold by Day 21 ($p=0.01$).

Alpha-fetoprotein gene expression (panel D) in HLCs showed a stabilisation in the expression between Day 17 and 19 after a 1.1-fold increase compared with Day 15 ($p<0.01$), and followed by a further 1.6-fold decrease by Day 21 ($p<0.001$).

HLCs at Day 15 and Day 17, displayed similar level of HNF1β gene expression (panel E) followed by a 1.25 ($p=0.01$) and 2.5-fold decrease ($p>0.0001$) observed at Day 19 and 21, respectively.

Analysis of the E-Cadherin gene expression (panel F) during the maturation approach indicated a maintenance in the expression ($p>0.05$) up to Day 19, after which gene expression decreased by 2-fold at Day 21 ($p<0.001$).

Analysis on the gene expression of hepatocyte markers suggested an efficient differentiation of hESCs-derived hepatoblasts to HLCs.

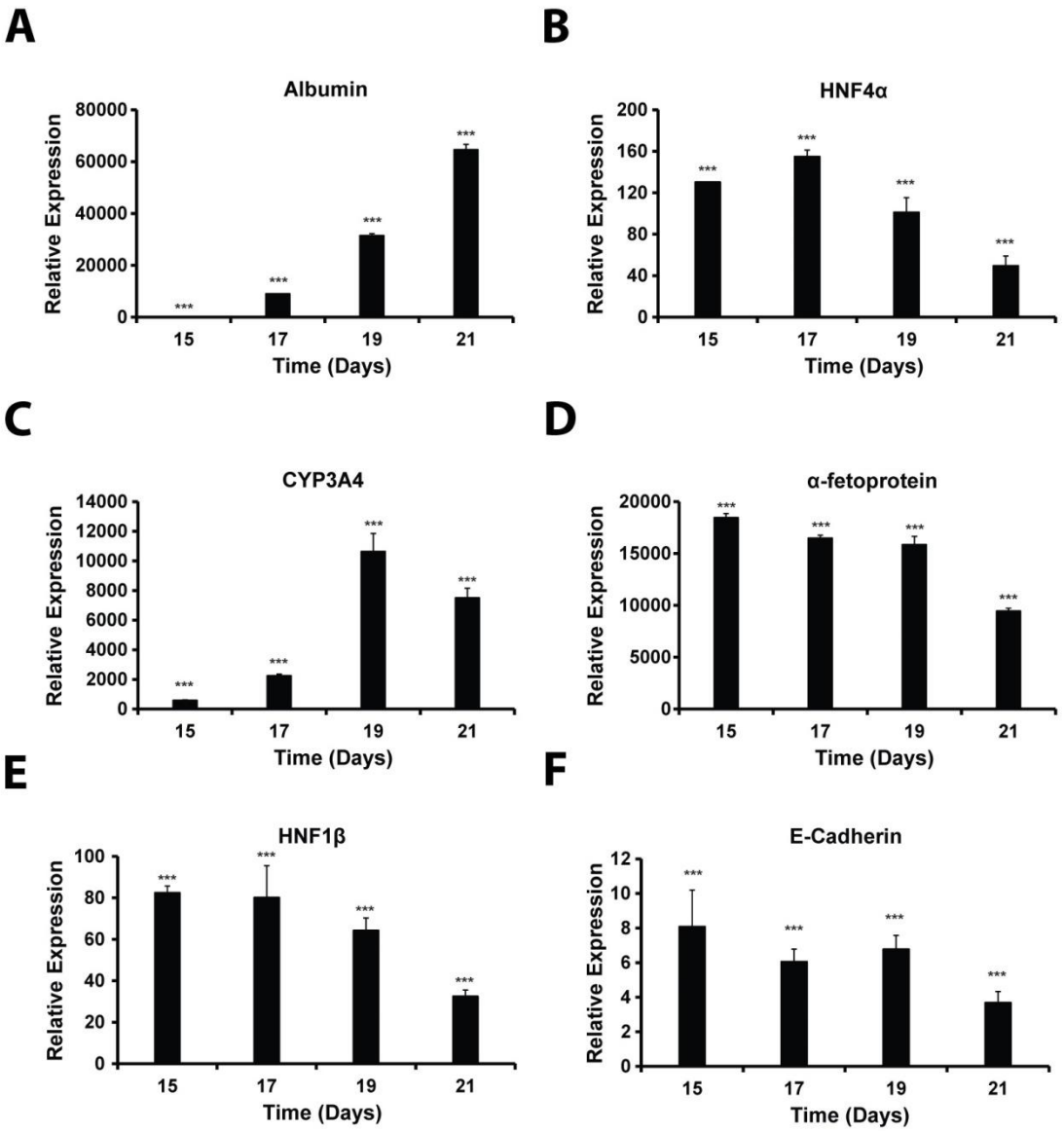

Figure 19. Serum-free derived hepatocytes gene expression. Graphs represent the gene expression analysed by quantitative PCR of different hepatocyte and hepatic endoderm markers (Albumin, HNF4α, CYP3A4, α-fetoprotein, HNF1β) and the epithelial marker E-Cadherin in the cells undergoing hepatocyte maturation at Day 15, 17, 19 and 21 in the differentiation protocol. The up-regulation in the expression of these hepatic genes suggests the commitment of the cells to the hepatocyte fate. Relative expression refers to fold of induction over hESCs and normalised to the housekeeping gene GAPDH. The results represent the mean ± SD of three different samples run, each run in triplicate. Levels of significance were measured by student's t-test where $p<0.001$ is denoted as *** versus hESC. Abbreviations: HNF4α-Hepatocyte nuclear factor 4α, CYP3A4-cytochrome P450 3A4, HNF1β- Hepatocyte nuclear factor 1β.

3.2.5.3 Protein expression profiling of HLC.

In addition to the gene expression analysis, to further characterised the HLCs, I investigated the expression of different hepatocyte markers involved in maintenance of the hepatocyte phenotype using immunostaining. Monolayers of HLCs were fixed at Day 21 and stained with antibodies to hepatocyte nuclear factor 4α (HNF4α), albumin (ALB), E-Cadherin (E-Cad), cytochrome P450 3A (CYP3A) and 2D6 (CYP2D6) (Figure 16). Analysis of the expression revealed that 86%, 95%, 97%, 94% and 98% of the cells stained positive for HNF4α, albumin, E-Cadherin, CYP3A and CYP2D6 respectively, demonstrating the high purity displayed by the cultures in the serum-free differentiation approach.

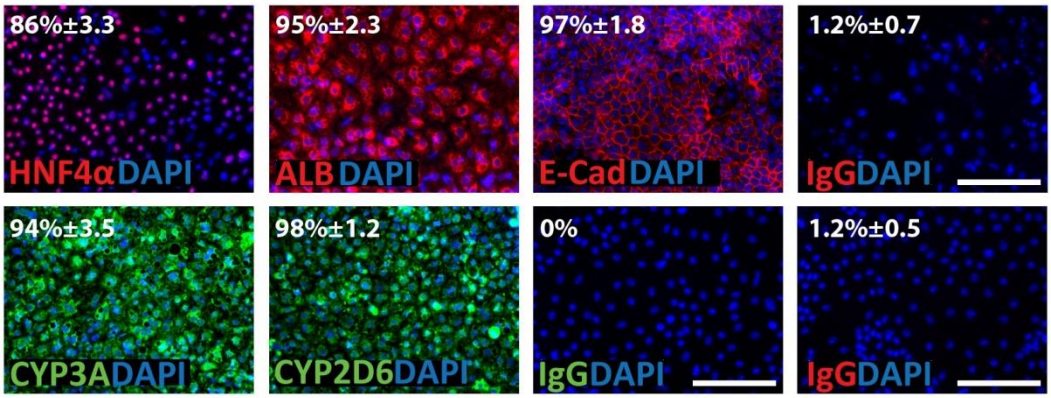

Figure 20. Immunofluorescence analysis for hepatocyte lineage markers. The expression of various hepatocyte markers including HNF4α, albumin, CYP3A, CYP2D6 and the epithelial marker E-Cadherin were analysed by immunofluorescence in HLCs at Day 21 on the serum-free maturation media, further supporting the presence of a homogeneous population of cells expressing hepatocyte specific markers. The corresponding IgG controls demonstrated the specificity of the staining. For each condition five random fields of view, containing at least 500 cells, were counted. Images were taken at 20x magnification and the scales bar represents 100 µm. Abbreviations: HNF4α-Hepatocyte nuclear factor 4α, E-Cad-E-Cadherin, ALB-Albumin, CYP3A-Cytochrome P450 3A4, CYP2D6-Cytochrome P450 2D6, IgG-Immunoglobulin G.

3.2.5.4 Functional characterisation of HLCs.

The possession of functional hepatocytes derived from hESCs is critical for a number of downstream applications ranging from *in vitro* models to the bio-artificial liver and cell based therapies. Therefore, I focused on characterising hepatocyte function

with direct implications in the generation of predictive toxicology tools and extra-corporal devices. As such, I measured important liver functions, including cytochrome P450 (CYP3A and CYP1A2) and albumin secretion.

The cytochrome P450 activity CYP3A and CYP1A2 in HLCs was measured at Day 15, 17, 19 and 21 in the differentiation procedure (Figure 21).

HLCs displayed CYP3A activity (Figure 21A) at Day 15, followed by a 3-fold increase by Day 17. A further 4-fold increase was observed at Day 19, when a stabilisation of the CYP3A activity was observed up to day 21,with not statically significant difference ($p>0.05$) between both days. The values for CYP3A at Day 15, 17, 19 and Day 21 are as follows: $1,3x10^4$ RLU/ml/mg, $4,6x10^4$ RLU/ml/mg, $18,1x10^4$ RLU/ml/mg and $19,5x10^4$ RLU/ml/mg, respectively.

CYP1A2 activity showed a similar trend than CYP3A (Figure 17B). Following a 6-fold increase in the activity observed at Day 17 compared to Day 15, the activity increased by 4-fold at day 19 and stabilised up to Day 21 with not statically significant difference ($p>0.05$) between both days. The values for CYP1A2 at Day 15, 17, 19 and Day 21 are as follows: $3,8x10^3$ RLU/ml/mg, $24,4x10^3$ RLU/ml/mg, $20,3x10^3$ RLU/ml/mg and $24x10^3$ RLU/ml/mg, respectively.

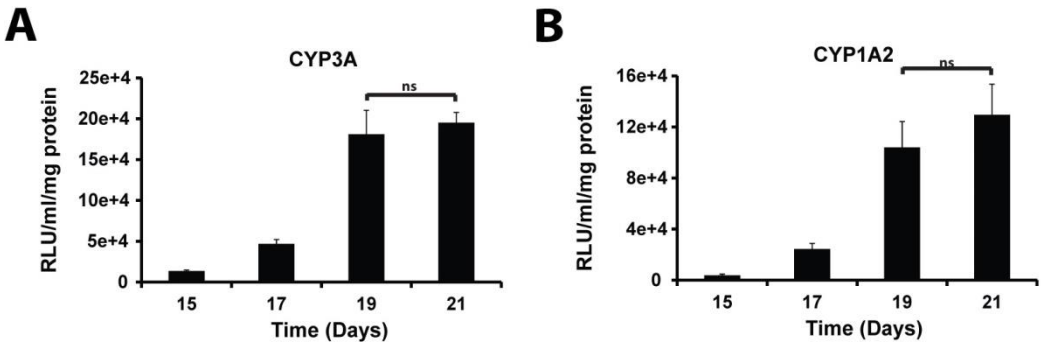

Figure 21. HLCs display stable stable cytochrome P450 activity in serum-free media. Cytochrome p450 function CYP3A (A) and CYP1A2 (B) were assessed using a commercially available system (pGLO®) in HLCs at Day 15, 17, 19 and 21 in the serum-free differentiation approach.. Analysis of the function of both CYPS in HLCs revealed an increase in the activity at Day 19 that was maintained at Day 21. The results represent the mean ± SD of six individual samples per time point per cytochrome P450 analysed. Levels of significance were measured by student's *t-test* where $p<0.05$ is denoted as ns.

Serum protein production is another vital function of mature hepatocytes required for healthy liver metabolism and homeostasis. As the HLCs exhibit mature hepatocyte morphological features and stable cytochrome P450 activity at Day 19 and 21 in the differentiation procedure, the secretion of albumin was analysed at these time points on collected supernatant using ELISA. Figure 22 demonstrates the production of albumin in HLCs. The levels of albumin maintained constant ($p>0.05$) between both days. The values of albumin produced at Day 19 and Day 21 are as follows; 637 ng/ml/24hours/mg and 637 ng/ml/24hours/mg, respectively.

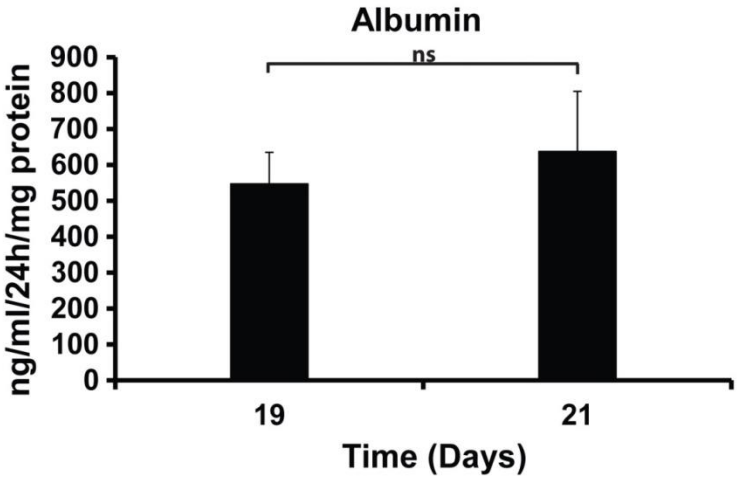

Figure 22. Albumin protein production revealed the maturity of the HLCs. The graph displayed shows the level of albumin secreted by HLCs at Day 19 and 21 when the cells displayed morphological features typical of mature hepatocytes. This protein is a good indicator of the hepatic maturity as it is uniquely produced by hepatocytes. As seen in the graph, there were not statistically significant differences between the analysed days. The results represent the mean ± SD of three individual samples per time point. Levels of significance were measured by student's *t-test* where $p<0.05$ is denoted as ns.

The function of the HLCs obtained in the defined serum-free maturation media was comparable between individual experiments, and it demonstrated an improvement in the function of the HLCs when compared to cells obtained in the serum containing protocol, indicating that the possession of a more defined differentiation approach is critical to obtain reliable, scalable and reproducible HLCs for downstream application.

3.2.6 Investigating the dedifferentiation process in HLCs

The window of activity of the HLCs was limited to Day 23, when a decrease in the cytochrome P450 function was observed. As the differentiation progressed, the mature hepatocyte morphological features displayed by the cells were gradually lost (Figure 23A). The homogeneous population of cells started to show a cellular heterogeneity in shape, size and length (panels A-E); intercellular spaces became larger and the cellular shape underwent to transition from the characteristic hepatocyte hexagonal shape to a large and more fusiform shape resembling to fibroblast morphology (panels F-I). Cellular detachment was observed (panels E, H-J, white and black arrows). The transition observed in the cellular morphology suggested the existence of a process of dedifferentiation from endoderm phenotype to mesoderm phenotype.

In order to study this deterioration process, I investigated the expression of the hepatocyte marker HNF4α, an important transcriptional factor in the hepatocyte biology, as it is estimated to bind to more than 50% of promoters of actively transcribed genes in hepatocytes, and the mesenchymal and dedifferentiation marker vimentin. Quantitative PCR was employed to study the gene expression of these markers in HLCs at late stages in the differentiation protocol. Analysis of the HNF4α gene expression (Figure 23B) showed a 2-fold decrease at Day 21 compared to Day 19 ($p<0.001$), but stabilised between Day 21 and 23 ($p>0.05$) prior to a further 1.35-fold decrease by Day 25 ($p=0.01$), and an 18-fold decrease by Day 27 ($p<0.001$). In parallel with the decrease in the HNF4α gene expression, an increased in vimentin gene expression (Figure 23C) of 1.8 and 2-fold from Day 21 to Day 23 and 25 respectively was detected ($p< 0.001$). A further 1.27-fold increase was observed at Day 27 compared with Day 25 ($p<0.05$).

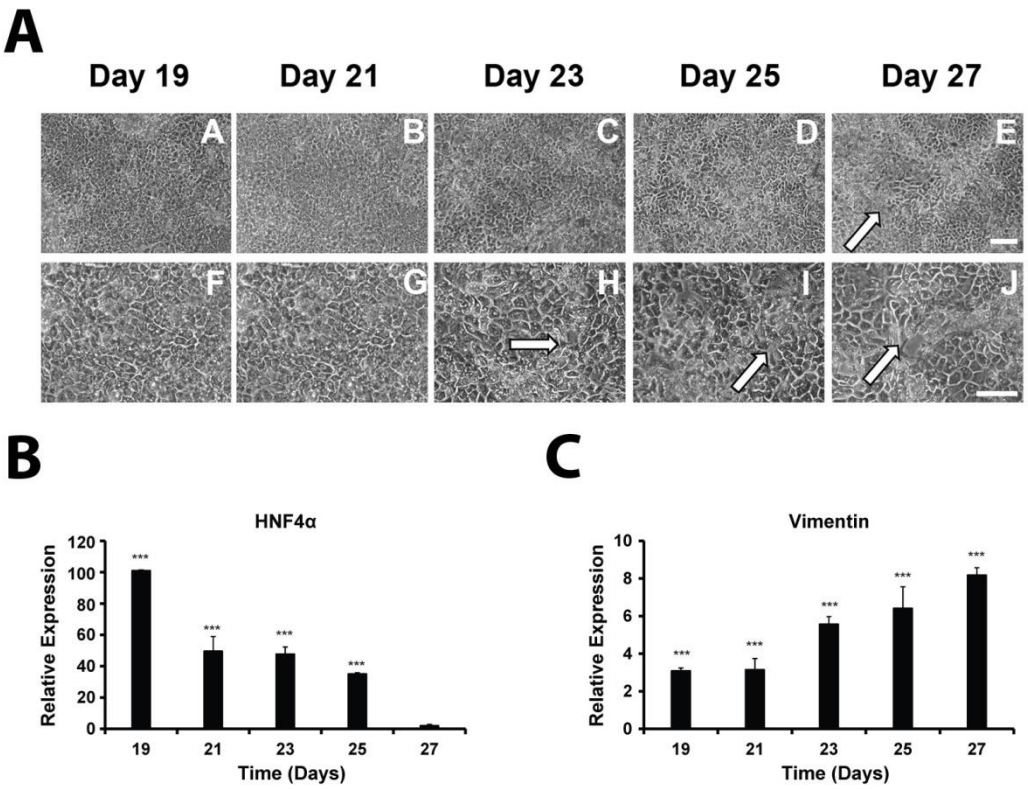

Figure 23. Analysing hESCs-derived HLCs at late stages on the differentiation process. A) Phase contrast images of HLCs during the serum- free differentiation process showed the display of morphological hepatocyte features, with a prominent nucleus, a hexagonal morphology and canaliculi-like structures (panels A-B and F-G). These features were gradually lost as the differentiation progressed, with cells suffering morphological deterioration, denoted by the acquisition of a fibroblast like morphology and increased cell detachment (white and black arrows). The images were taken at 4x magnification (panels A-E) or 10x magnification (panels F-J) and scale bar represents 200 µm and 100 µm respectively. B-C) Gene expression analysis of hepatocyte and mesenchymal phenotype markers. Graphs represent the gene expression analysed by quantitative PCR of the hepatocyte marker HNF4α (B) and the mesenchymal marker vimentin (C) in HLCs at late stage on the differentiation process. The down regulation in the expression of HNF4α was clearly observed from Day 21 onwards, and accompanied by an up regulation in the gene expression of vimentin, indicating the presence of a dedifferentiation process consisting in a loss of the endoderm phenotype on the cells in favour of a mesenchymal phenotype. Relative expression refers to fold of induction over hESCs and normalised to the housekeeping gene GAPDH. The results represent the mean ± SD of three different samples run, each run in triplicate. Levels of significance were measured by student's t-test where $p<0.001$ is denoted as ***. Abbreviations: HNF4α-Hepatocyte Nuclear Factor 4α.

The expression pattern of HNF4α and vimentin was confirmed by immunostaining on fixed HLCs (Figure 24). The yield percentage of HLCs staining positive for vimentin remained below 13% until day 19, when there was a significant and steady increase in the percentage of cell expressing the protein, reaching 37% by Day 21,

64% by Day 23, 85% by Day 25 and 97% by Day 27. In parallel to the increase in vimentin expression, a decrease in HNF4α expression was observed. The percentage of cells staining positive for HNF4α remained above 80% until Day 23 (95% and 86% at Day 19 and 21, respectively), when 79% of the cells stained positive for the hepatocyte marker. A rapidly decrease in the yield percentage of cells expressing HNF4α was observed by Day 25 and Day 27 when HNF4α was expressed by 56% and 38% of cells respectively.

3.2.7 Stability of the biological substrate used in the hepatocyte differentiation.

One of the main problems associated with the use of biological matrices as substrata to differentiate and culture hESCs derive cells is the degradation observed in the extracellular matrix components found in matrigel. To investigate if the functional deterioration observed in the cells at late stages in the differentiation was due to a process of degradation of the matrix at Day 9 in the differentiation procedure, cells primed towards hepatocyte fate were replated on matrigel surfaces coated on the same day (fresh MG) and on surfaces coated with matrigel plated at the start of the hepatocyte differentiation procedure (old MG). Cells were matured for 15 days and CYP3A activity was measured. Figure 21 shows the analysis of the activity in HLCs replated on fresh and old coated matrigel surfaces. A 2.5-fold increase in the CYP3A activity was observed in HLCs replated on fresh matrigel coated surfaces compared with old matrigel coated surfaces. The values for CYP3A in HLCs replated on freshly coated matrigel and old coated matrigel are as follows; $26{,}8x10^4$ RLU/ml/mg and $10{,}8\ x10^4$ RLU/ml/mg respectively ($p<0.01$).

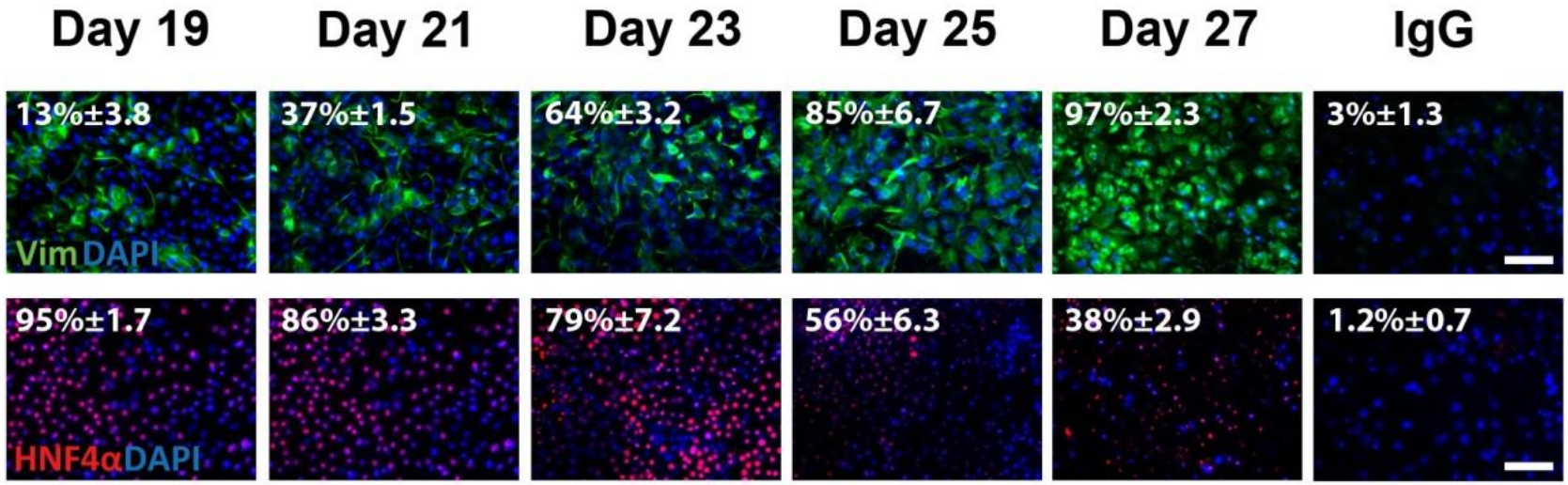

Figure 24. Immunofluorescence analysis of the dedifferentiation process. The expression of the hepatocyte marker HNF4α and the mesenchymal marker vimentin were analysed by immunofluorescence in HLCs at late stages on the differentiation procedure. The increase in the percentage of cells expressing vimentin was accompanied by a decrease in the number of cells expressing HNF4α, further supporting the acquisition of a mesenchymal phenotype previously observed on the morphology of the cells and indicated by the gene expression analysis. The corresponding IgG controls demonstrated the specificity of the staining. For each condition five random fields of view, containing at least 500 cells, were counted. Images were taken at 20x magnification and the scales bar represents 100 μm. Abbreviations: HNF4α-Hepatocyte nuclear factor 4α, Vim-Vimentin, IgG-Immunoglobulin G.

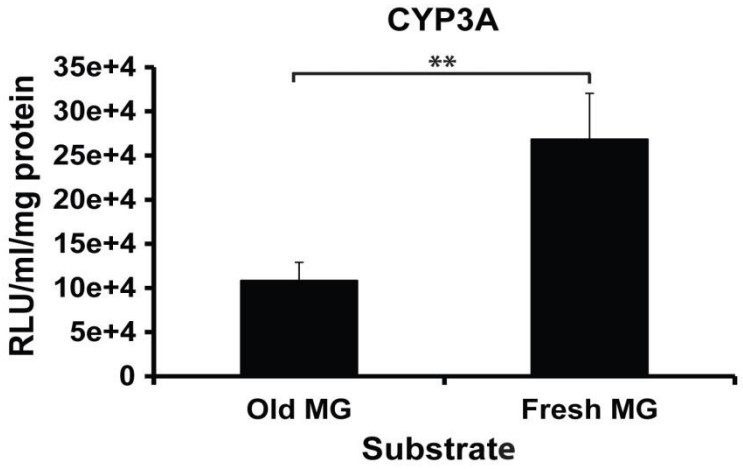

Figure 25. Influence of matrigel in the cytochrome P450 CYP3A activity. hESCs-derived hepatoblasts were replated on fresh or old plated matrigel and maintained for 15 days. Analysis of the CYP3A activity revealed a significant decrease in the activity of cells maintained on matrigel plated when hepatocyte differentiation of undifferentiated hESCs started (old plated matrigel) compared with the activity on cells maintained on surfaces coated with matrigel on the same day (fresh matrigel) . The results represent the mean ± SD of three individual samples per time point per cytochrome P450 analysed. Levels of significance were measured by student's t-test where $p>0.01$ is denoted as **. Abbreviations: MG-matrigel.

In conclusion, these data demonstrate that at late stages in the hepatocyte differentiation, there is a dedifferentiation process partially associated with the instability of the biological matrix matrigel.

3.3 Discussion

Freshly isolated human primary hepatocytes represent the current gold standard model to study human hepatocyte biology *in vitro* and to predict *in vivo* liver drug metabolism and clearance (Hewitt and Lechón, 2007; Lin, 2006; Obach, 2009). However, the scarcity, low proliferative capacity and high phenotypic and function variation of the available human tissues employed in research limit their use in therapeutic and clinical applications (Cheng *et al*., 2008; Fox and Strom, 2008). In

order to relieve the dependence on primary hepatocytes other sources of hepatocytes have been explored; unfortunately, each individual substitute has their disadvantages: the risk of xeno-contaminates and the low concordances between animal and clinical studies restrict the use of non-animal hepatocytes (Behnia *et al*., 2000; Guillouzo, 1998). Hepatocarcinoma and immortalised human hepatocyte derived cell lines display genetic characteristics and minimal metabolic activity that limit their use in therapeutic or clinical applications (Iyer *et al*., 2010); and the scarcity, highly inefficient isolation and sub-optimal purification of adult liver progenitor cells restrict their use as an alternative source of hepatocytes (Alison *et al*., 2007; Fiegel *et al*., 2006; Vessey and la M. Hall, 2001). As such there is an urgent need for reliable and predictable hepatocyte *in vitro* models.

Human embryonic stem cells (hESCs) have the potential to provide an inexhaustible supply of hepatocytes to be used for applications such as developmental biology studies, drug discovery, disease modelling and cell therapy (Greenhough *et al*., 2010; Rippon and Bishop, 2004; Sharma and Greenhough, 2010). hESCs possess two attributes that makes them an alternative source of hepatocytes: the unlimited self-renewal ability and the pluripotency capacity to differentiate into any cell of the human body (Cai *et al*., 2006; Hoffman and Carpenter, 2005; Vazin and Freed, 2010). As a consequence, a number of research groups, including ours, have invested large amount of time and resources in defining differentiation strategies to obtain functional and viable hepatocyte-like cells (HLCs) from pluripotent stem cells.

The development of the liver is a continuous process. However, the existing hepatocyte differentiation approaches from pluripotent stem cells replicate the hepatocyte development in discrete stages. In this study, I employed an efficient hepatocyte differentiation that recapitulates the development stages observed *in vivo*: definitive endoderm induction, hepatic endoderm specification and hepatocyte specification and maturation

The induction of definitive endoderm occurs during gastrulation in a process that requires coordinated signals secreted by the nascent cardiac mesoderm such as

FGF, a stimulator of hepatic gene expression and hepatocyte stability via RAS/MAPK pathway (Calmont *et al*., 2006); and BMP/Nodal signalling secreted by the septum transversum mesenchyme. BMP/Nodal signalling sustains the complete induction of hepatic endoderm, exerting its effect through a number of downstream transcription factors including Sox 17, Forkhead box (Fox) A1 and A2 (HNF3α and β) and GATA 4-6 (Clements *et al*., 2003; Kim *et al*., 2011). Wnt/β-catenin signalling is involved in both differentiation and proliferation of pre-hepatic endodermal cells (Burke *et al*., 2006; Fletcher *et al*., 2008; McLin *et al*., 2007); and cooperates with BMP signalling in the onset of the liver development (Zorn *et al*., 1999). The inductive role of BMP is mimicked in our system by a treatment with Activin A (D'Amour *et al*., 2005) and Wnt3a (Hay *et al*., 2008a), that induce the expression of the transcription factors Sox 17 demonstrating the generation of hESCs-derived definite endoderm cells (Cereghini, 1996; Cirillo and Zaret, 1999; Costa *et al*., 2003).

Hepatic specification from the definitive endoderm requires conformational changes in the chromatin; party induced by the expression of FoxA and GATA factors (Cirillo and Zaret, 1999; Cirillo *et al*., 2002), resulting in the expression in the nascent liver bud of hepatic genes including albumin, alpha-fetoprotein and HNF4α. This process can be recapitulated *in vitro* by either using a cocktail of growth factors including BMPs and/or FGFs (Agarwal *et al*., 2008; Brolén *et al*., 2009; Cai *et al*., 2007; Duan *et al*., 2010; Touboul *et al*., 2010), or like in this study, by supplementing the media with DMSO, either alone (Basma *et al*., 2009; Duan *et al*., 2010; Hay *et al*., 2008a) or in combination with other factors (Duan *et al*., 2010). Consistent with *in vivo* observations, I observed an increase in the expression of important transcription factors in the hepatic specification including HNF1β (Lokmane *et al*., 2008) and Prox1 (Papoutsi *et al*., 2007).

Hepatic specification results in hepatoblast, bipotential cells capable to differentiate into the liver parenchymal cells or hepatocytes (AFP+/albumin+) and cells of the biliary tract or cholangiocytes (cytokeratin 19+) (Jung, 1999). These cells exhibit many markers that can be used to isolate the population including the

epithelial cells adhesion molecules E-Cadherin and EpCAM, alpha-fetoprotein and cytokeratin 19 (Schmelzer *et al*., 2006). Still, hepatoblasts lack in the expression of specific markers. Therefore, identification of the hepatoblast stage of the cells was performed using a panel of markers. Analysis of the cell morphology, gene and protein expression profile revealed that hESCs-derived hepatoblasts displayed the most hepatoblastic phenotype at Day 8 in the differentiation procedure. Nevertheless, due to the bipotential nature of hepatoblasts, analysis of the differentiation ability into hepatocyte and cholangiocytes would represent an ideal functional assay to determine the hepatoblast phenotype (Dianat *et al*., 2014).

Hepatocyte specification requires the correct balance of a complex cell signalling network acting in a gradient manner and involving several reversible developmental stages, with oncostatin M (OSM) and hepatocyte growth factor (HGF) playing a key role. While OSM promotes hepatocyte maturation and polarisation, HGF promotes cell proliferation and induce organisation of hepatocytes into cord-like structures by regulating the expression of diphosphate-ribosylation factor 6 (ARF6), an enzyme involved in actin cytoskeleton remodelling. TNFα balance OSM and HGF signal activities by inhibiting maturation and maintaining the proliferative capacity of foetal hepatocytes, thus allowing the liver to grow to the appropriate size before differentiating (Kamiya and Gonzalez, 2004). TNFα repression after birth is necessary to obtain fully mature hepatocytes expressing cytochrome P450 genes (Hart *et al*., 2009).

Existent differentiation approaches use combinations these factors, in combination with glucocorticoids to induce hepatocyte differentiation and maturation from pluripotent stem cells derived hepatoblasts (Basma *et al*., 2009; Brolén *et al*., 2009; Cai *et al*., 2007; Duan *et al*., 2010; Hay *et al*., 2008a). The expression of the hepatocyte nuclear factor 4α (HNF4α) strongly correlates with hepatocyte phenotype and plays a key role in hepatocyte function by regulating the expression of essential transcription factors involved in the correct development of the foetal liver (Chen *et al*., 1994; Li *et al*., 2000) and in the function of mature hepatocytes

(Odom, 2004). Hepatocytes express genes involved in the metabolism of xenobiotic including several members of the cytochrome P450 enzymes. Consistently with previous observantions (Hay *et al*., 2008a; 2008b), analysis of the HLCs obtained in this study revealed the possession of a homogeneous population of cell expressing robust hepatocyte lineage markers and hepatocyte function.

Like in HLCs, dedifferentiation is a common process observed in primary hepatocytes in culture (Beigel *et al*., 2008; Binda and Lasserre, 2003). In order to tackle this issue, researchers have developed approaches involving modification of the media and/or the cellular environment.

Supplementation of the media with differentiation promoting factors, of both physiological and non-physiological origin, represents the simples approach to preserve the correct cell phenotype. Physiological factors such as insulin, glucocorticoids and foetal bovine serum (FBS) are commonly used in both primary hepatocytes and stem cells derived hepatocytes (Cai *et al*., 2007; Godoy *et al*., 2009; Szkolnicka *et al*., 2014; Touboul *et al*., 2010). It has been reported that supplementation of media with insulin or glucocorticoids, including dexamethasone and hydrocortisone, promotes cell attachment, display of hepatocyte morphological features and secretion of liver specific proteins (Dich *et al*., 1988; Kim *et al*., 2001). FBS has also been widely used in culturing hepatocyte as it favours epithelial identity, cell attachment and survival. However, long-term culture of hepatocyte in the presence of FBS compromise cellular polarisation, canaliculi-like network stability and the activity of phase I biotransformation enzymes. Moreover, batch-to-batch variability, fluctuating variability, cytotoxicity of uncharacterised factors contained in the serum, including growth factors and the presence of non-animal xeno-contaminants can interfere with the cellular function, growth and the phenotypic/genotypic stability of the cultures cells (Erickson *et al*., 1990). In this study cytochrome P450 3A (CYP3A) function was used as an indicator of hepatocyte function, as this enzyme is responsible of the metabolism of nearly half of the therapeutic drugs (Keshava and McCanlies, 2004). A high variability in CYP3A

function of the cells associated with the batch of FBS serum employed was observed, compromising reproducibility between experiments. Therefore, in order to tackle this issue I performed a screening to identify serum-free hepatocyte differentiation mediums that supported stable hepatic function *in vitro*. From this screening HepatoZYME®-SFM (HZ, Life Technologies) was identified as the most suitable media in promoting hepatocyte differentiation from pluripotent stem cells (Szkolnicka *et al*., 2014). HLCs obtained in the serum-free differentiation approach displayed increased life-span, mature hepatocyte morphological features, the expected gene and protein patterns expression observed during liver development and improved and stable metabolic functions. Furthermore, our group has previously reported that HLCs obtained using this defined differentiation approach can accurately predict human compounds toxicity in a comparable manner to cryo-preserve human hepatocytes (Szkolnicka *et al*., 2014). Other approaches have recently shown that supplementing the media with vitamin K2 and microbial derived licotid acid induces the expression of a mature hepatocyte phenotype with improved metabolic functions (Avior *et al*., 2015). DMSO represents one of the most common non-physiological additives used in preserving hepatocellular phenotype. DMSO like glucocorticoids, possesses an anti-dedifferentiation effect by promoting polarization of the cells, albumin secretion and an increase in the expression of key hepatic transcription factors including C/EBPα, -β, HNF3α, -β and HNF4α (Su and Waxman, 2004; Vinken *et al*., 2006). Shan and collegaues identified small molecules from a high-throughput screening platform that induced functional proliferation of primary human hepatocytes in culture and promoted the maturation of HLCs (Shan *et al*., 2013).

Equally important in the stabilization of the hepatocellular phenotype is the microenvironment surrounding the cells. Strategies in the modification of the extracellular environment include restoration of cell-to-ECM and cell-to-cell interactions. Biological matrices such as collagen I or matrigel have been extensively used in preserving primary hepatocytes in culture. While matrigel increases the expression of hepatocyte-specific transcription factors including C/EBPγ and –β

(Elaut *et al*., 2006), collagen I promotes the maintenance of the liver phenotype by enhancing hepatocyte attachment and survival (Skett and Bayliss, 1996). It has been shown that hepatocytes, via asialoglycoprotein (ASGR), bind to β-galactosidase residues (Wall *et al*., 1980). Based on this knowledge, Ghodsizadeh and colleagues developed a galactosylated collagen substrate that supported hepatocyte differentiation of hESCs, with cells displaying hepatocyte markers including albumin and alpha-fetoprotein, and hepatocyte functions such as albumin secretion, urea synthesis and increased cytochrome P450 activity (Ghodsizadeh *et al*., 2014).

These effects on the hepatocytes in culture are promoted when these biological matrices are used in three dimensional structures (Page *et al*., 2007; Rowe *et al*., 2010; Tuschl and Mueller, 2006). Still, the use of three dimensional matrigel structures have a negative impact on the cellular stress response signalling as evidenced by a decrease in the mRNA expression of interleukins, chemokines, stress related protein kinases and integrin pathways associated genes (Page *et al*., 2007) (Page *et al* 2007). Still, the biological nature of these matrices compromises the consistence and reproducibility of hepatocyte functions.

Restoration of cell-to-cell interactions represents another possibility to increase the stability of the cell cultures, either using a hepatic or non-hepatic partner. Liver sinusoidal endothelial cells (LSEC) are the most widespread hepatic partner for both, primary hepatocytes and pluripotent stem cell derived HLCs. LSEC secretes ECM components that influence the cytoskeleton organization, ultimately regulating the expression of liver-specific genes (Kasuya *et al*., 2010; Kim and Rajagopalan, 2010; McCuskey, 2008). Tabeke and colleagues generated vascularized and functional liver buds *in vitro* by combining iPSC-derived HLCs with human mesenchymal stem cells and human umbilical vein endothelial cells (HUVECs) (Takebe *et al*., 2013). Fibroblasts secrete ECM components and growth factors, including HGF (Hiramatsu *et al*., 2005), that affect the organization of the surrounding environment and the survival of the hepatocytes. Therefore, fibroblasts, in particular of mouse origin, represent the most common non-hepatic

partner used to restore cell-to-cell contact in cultures of hepatocytes (Leite *et al*., 2011; Sugimachi *et al*., 2004) and pluripotent stem cells derived hepatocytes. Berger and colleagues developed a culture system using mouse embryonic fibroblasts and PSCs derived HLCs embedded in a matrigel and collagen three dimensional matrix, observing an improvement in the hepatocyte phenotype and metabolic functions (Berger *et al*., 2015). Ware and colleagues employed a similar strategy to generate micropatterned co-cultures that were able to predict drug-induced liver injury (DILI) (Ware *et al*., 2015).

In this study matrigel, which is considered the gold-standard substrate for culturing pluripotent stem cells derived somatic cells, was employed as the culture substrate to maintain HLCs. The use of a defined hepatocyte maturation media allowed me to improve the life span of the cells while promoting hepatocyte phenotype and metabolic function. However, as the differentiation approach progressed, HLCs underwent a rapid deterioration, both morphological and phenotypic, losing the expression of HNF4α and increasing the expression of vimentin, displaying a limited life span and cell performance, all of which suggested the existence of a dedifferentiation process on the cells. Observations indicated that this rapid dedifferentiation process was partly induced by the instability of the biological matrix used, matrigel. Matrigel, like animal derived serums, suffers from batch-to-batch variations and degradation of the components presented in the mixture, thus influencing the cell performance. Despite all the recent advantages made in the field, the batch-to-batch variations and stability of the biological matrices and partner cell strategies compromise the reproducibility, functionality and purity of the cell cultures.

In conclusion, the use of biological matrices to maintain pluripotent stem cell derived HLCs in culture influences the reproducibility and phenotypic stability of cells. Therefore, it is necessary to identify stable and fully defined cellular supports to ensure the delivery of reliable, reproducible, stable and functional somatic cells for downstream applications. Next chapter will focus in the optimisation and

characterisation of a synthetic defined surface to maintain stem cells derived hepatocyte-like cells in culture.

CHAPTER FOUR

POLYMER SURFACE OPTIMIZATION AND COMBININATION WITH THE SERUM-FREE DIFFERENTIATION APPROACH

4.1 Introduction

The use of defined culture systems is important for the generation of reliable hepatocytes from pluripotent stem cells. In recent years, the use of the undefined and serum containing mouse embryonic fibroblast condition medium have been replaced by defined media such as StemPro®, mTeSR1™ and the xeno-free E8™. Still the biological derived matrix matrigel is the preferred culture substrate for the maintenance of undifferentiated pluripotent stem cells and stem cells derived somatic cells (Xu *et al*., 2001). However, this biological substrate suffers from batch-to-batch variations and contains xenogenic contaminants that influence cell function and phenotype, limiting the large scale manufacture of cells. In an attempt to overcome the limitations associated with the use of matrigel, researches have focused on developing more defined biological and synthetic substrates to culture and differentiate pluripotent stem cells.

4.1.1 Use of biological defining culture systems in stem cell technology

Extracellular matrix (ECM) plays crucial roles in the maintenance of cell phenotypes (Hazeltine *et al*., 2013; Noghero *et al*., 2010). Matrigel has been widely applied in the maintenance and differentiation of hPSC. However, its use limits the generation of faithful models of human 'in a dish' and cell based therapies. Therefore, it is necessary to identify more defined substrates for the maintenance and differentiation of pluripotent stem cells.

The replacement of matrigel with a humanised ECM represents the first approach developed to solve the animal origin of matrigel. Pakzad and colleagues recently described an extracellular matrix designated "RoGel", made of conditioned medium of human fibroblast under serum- and xeno-free culture conditions that supported long-term culture of human pluripotent stem cells (hPSC) in the presence of a serum containing media (Pakzad *et al*., 2013). Despite that this humanised ECM supported hepatocyte differentiation with HLCs performing in a comparable manner than on matrigel (Farzaneh *et al*., 2014), the use of this biological matrix is

still limited to the availability and variability of the human fibroblasts and the batch-to-batch variations of the resulting humanised extracellular matrix.

Other strategies to identify defined substrates to culture and differentiate hPSCs are based on the current knowledge of the existing relation between the structure and/or composition of the ECM *in vivo* and the expected biological response. Integrins represent the major cell surface receptors mediating ECM adhesion and signalling. As such, integrins play a key role in the interactions between cells and the surrounding microenvironment. Collagens, laminins, vitronectin and fibronectin represent some of the major proteins found in the ECM; therefore, their use represents an attractive alternative in the maintenance and differentiation of pluripotent stem cells.

Despite the fact that collagens interact with a wide range of extracellular and cell surface receptors linked to pluripotency (Heino, 2007), collagens have shown a limited capacity to support long-term cultures of PSCs (Brafman *et al*., 2010). Gelatin, a collagen derived matrix has been successfully applied in the maintenance of hPSCs in culture, but still, under the presence of a heavily supplemented serum-free medium emulating mouse PSC (mPSC) culture conditions. Consequently, PSCs display morphology and gene expression more similar to mPSC than their human counterparts (Xu *et al*., 2010).

Laminins are a group of extracellular matrix proteins that gained the attention of research. Laminins are considered the first extracellular proteins expressed in the stem cell niche of the early embryo (Cooper and MacQueen, 1983), interacting with hPSCs through α6β1 integrin, an important integrin expressed on stem cells (Nishiuchi *et al*., 2006), making laminins attractive substrates to culture hPSCs. As a result, Vouristo and colleagues employed the extracellular matrix secreted by the human choriocarcinoma cell line JAR, rich in laminins -111 and -511, as a substrate to successfully support hPSCs in culture while preserving the pluripotency capacity as revealed by the derivation into neuronal- and hepatocyte-like cells (Vuoristo *et al*., 2013). Still, the consistency of the extracellular matrix is compromised by the

availability and variability of the tumorigenic cell line employed. The production of recombinant proteins represents a solution to the use of cells as a source of extracellular matrix. Rodin and colleagues successfully employed recombinant laminin-511 in maintaining long-term cultures of hPSCs in xeno-free culture conditions, with cells displaying greater adhesive properties than on matrigel (Rodin *et al*., 2010). Further studies from the same group demonstrated that the combination of the recombinant laminin isoform 521 with E-Cadherin, both proteins widely expressed in the ICM, supported both, derivation and clonal survival of hESCs in defined and xeno-free conditions (Rodin *et al*., 2014), resulting in improved culture definition. Vitronectin is a protein expressed in both the ECM as well as in serum but not in matrigel. Vitronectin also contains integrin binding domains, making it an attractive substrate for the maintenance of pluripotent stem cells. Braam and colleagues successfully employed recombinant vitronectin matrices in the maintenance of three independent hESC lines (Braam *et al*., 2008). Despite the high cost associated to the use of recombinant proteins, these findings represent a significant milestone in the culture of hPSCs as they were one of the first examples of defined and xenogenic-free substrates

4.1.2 Use of synthetic substrates in stem cell technology

Combinatorial strategies involving biological derived substrates with synthetic and defined biomaterials represent an alternative strategy for the culture and differentiation of hPSCs. Biomaterials can be defined as a material or a combination of materials that can be used to repair, treat, or replace tissues or organs *in vitro* and *in vivo* and can be classified based on their performance and criteria such as polymers, metal, ceramics and composites.

Polymers are an attractive type of biomaterials with wide applications in stem cell biology. Polymers are physical networks composed of any polymer (long chains composed of monomers subunits) with high relevance in medical applications due to their inert nature, chemically diversity, easy process and malleability, as they can

be presented in different form including solids, fibers, films and gels. Polymers can be applied in various dimensions and can be combined or blended with other polymers or with biological derived culture substrates. All these characteristics make them an attractive alternative to biological substrates.

Combination of Poly (lactic-co-glycolic acid) (PLGA) with laminins isolated from Engelbreth-Holm Swarm (EHS) sarcoma represents an example of combinatorial approach. Gao and colleagues reported that this substrate supported hESC attachment in a more robust manner compared to mixtures of PGLA with rat collagen I, human collagen IV or human fibronectin. Moreover, this matrix efficiently maintained the differentiation capacity of the hESCs revealed by an efficient differentiation into definitive endoderm (Gao *et al*., 2010). Polymers with high acrylate content combined with vitronectin successfully maintained the pluripotency properties and colony formation of the hESCs for a prolonged period of time, revealing the structure–function relationships between the properties of the material and the biological performance (Mei *et al*., 2010). Combinations of biological derived and synthetic material have been also applied in the development of hepatic co-culture methods. Du and colleagues recently reported a culture system consisting on an alginate hydrogel containing fibres rich in galactose and collagen domains that successfully supported encapsulation of hPSCs-derived HLCs and endothelial cells. The authors observed enhanced albumin production and cell engraftment when injected in a recipient liver mouse (Du *et al*., 2014). Still, the biological derived components employed in these combinatorial approaches are expensive and the required post-translational modifications of these proteins may results in variability between batches, compromising the large scale manufacture of the cells (Villa-Diaz *et al*., 2013). Therefore, other strategies have explored the use of fully defined and synthetic substrates for stem cell culture.

4.1.3 Defined culture systems

The bioactive polymer on which hPSC cultures has been most heavily studied is the zwitterionic a sulfonil containing polymer poly [2-(methacryloyloxy) ethyl dimethyl-(3-sulfopropyl) ammonium hydroxide] (PMEDSAH). It is though that the sulfonic group mimics heparin sulphate proteoglycans, which are important extracellular proteins relevant in hPSC culture systems (Gasimli and Linhardt, 2012; Klim *et al*., 2010; Musah *et al*., 2012). PMEDSAH has been reported to support long-term culture of hPSCs (Nandivada and Villa, 2011; Villa-Diaz *et al*., 2010) and mesenchymal stem cells derived from hPSCs (Villa-Diaz *et al*., 2012) in a range of media but performing more consistently in serum containing media including CM and human cell conditioned medium.

Two-dimensional culture systems require fewer number of cells which can be enough in drug screening and diseases modelling. However, it has been shown that three-dimensional systems enhance cell proliferation and self-renewal while mimicking more accurately the *in vivo* environment, providing the required higher number of cells in large scale and cost effective manner (Postovit *et al*., 2006; Yim and Leong, 2005). Polymers can be also fine-tuned to satisfy the demand in three dimensional culture systems. Hydrogels represents an example of such applied on stem cell cultures. They are structures composed of cross-linked and hydrophilic polymer scaffolds, when exposed to water, they expand into an ECM-like gel state, making them to be easily applied in two or three-dimensional structures by varying the thickness of the hydrogel. Hyaluronic acid (Gerecht *et al*., 2007; Liu *et al*., 2012), polyacrylamide-based (Brafman *et al*., 2009; Zhang *et al*., 2013) and amino-propylmethacrylamide hydrogels (Irwin *et al*., 2011) have been reported to sustain long term cultures of hPSCs.

Li and colleagues described a hydrogel made by crosslinking acrylic acids and acrylate peptides as a suitable substrate to support hESC cultures. Due to their physical properties, including matrix stiffness and ligand density, the polymer can be easily fine-tuned to satisfy the culture requirements (Li *et al*., 2006). Synthetic

polymers can also be used to explore the biological cues of differentiation processes. As such, Yamazoe and colleagues employed a xeno-free three-dimensional synthetic polyamide nanofiber that promoted hepatocyte differentiation and function of hPSCs in a serum–free culture system to study the pattern activation of Rac 1 in undifferentiated and during hepatic differentiation of hECs. Rac 1 is a member of the Rho GTPase family protein involved in the remodelling of the cytoskeleton, which expression is critical for the self-renewal of hESCs (Nur, 2005). The findings suggested that continuous activation of Rac 1 throughout the hepatocyte differentiation stage is crucial for potentiating differentiation (Yamazoe *et al*., 2013).

Traditional approaches in identifying defined matrices compatible with maintenance of pluripotency and differentiation capacities of pluripotent stem cells have been traditionally notoriously slow and low throughput. However, in recent years high-throughput (HTP) approaches, such as microarraying, have allowed the rapid screening of chemically diverse substrates that modulate or control cell biology, thus representing an important tool for both novel material discovery and identification of correlations between cell performance and structure.

4.1.4 High-throughput approaches for biomaterials

Identification of suitable biomaterials for cell biology requires a deep understanding of the existing relation between the structure or composition of the desired material and the expected biological cell response. However, to date there are not enough theoretical basis for predicting cell performance from the physical and chemical parameters of a material. Combinatorial chemistry methodologies allow the identification of biomaterials for cell applications. These methodologies involve the synthesis, processing and screening of vast number of molecules in parallel in high throughput formats (Webster, 2008).

High throughput technologies allow the identification of polymer materials for biology applications, as these platforms offer the possibility of testing large

numbers of monomers and combinations of the monomers (Kohn, 2004). Microarray, extensively used for genomics by presenting DNA or protein based molecules (Heller, 2002; Venkatasubbarao, 2004), represents the preferred format for high throughput screening, as a high number of candidate polymers can be rapidly screened in parallel for a particular performance in an application of interest.

4.1.4.1 Polymer microarray fabrication

Microarrays can be formed using a variety of methods including the reproducible and versatile methods of contact printing and ink-jet printing.

Contact printing is the preferred approach in the fabrication of polymer microarrays. It involves the dispensing of pre-synthesised polymers using a metallic pin coupled to a robot, which dips the metallic pin into the polymer solution and then dispensing it onto the substrate surface by making contact. Parameters such as the solvent used, substrate, inking time, stamping time, number of stamps per spot and washing conditions affect the shape and uniformity of the printed polymers; therefore, influencing the quality and reproducibility of the final polymer microarray. Materials used as a surface to print the polymers include plastic surfaces, glass slides, gold-coated glass slides and aluminium slides. However, the 'non-stick' properties of agarose, known to supress cellular adhesion thus preventing nonspecific adhesions, make this substrate the preferred option (Tourniaire *et al*., 2006). Contact printing technology was firstly applied in monitoring gene expression of a large library of complementary DNA (Schena *et al*., 1995) and adapted to produce a microarray of polymers (Anderson *et al*., 2004). It has been extensively used in a variety of applications including; the maturation and phagocytosis of dendritic cells (Mant *et al*., 2006), identification of resistant materials to bacterial infection (Hook *et al*., 2013; 2012; Pernagallo *et al*., 2011), platelet activation (Hansen *et al*., 2013) and isolation of mesenchymal stem cells (Tare *et al*., 2009).

Inkjet printing represents an alternative technique to prepare polymer microarrays. Inkjet printing mainly differs with contact printing in the synthesis of the polymers. While contact printing requires pre-synthesised polymers, inkjet printing dispenses monomers and catalysts forming the final polymer on the same position of the microarray where the polymerisation reaction will occur. As such, inkjet printing possesses advantages in the properties of monomers to use, as non-water soluble monomers can be printed in agarose coated glass slides in the presence of organic solvents, with polymerisation triggered by UV radiation (Liberski *et al*., 2008). This technique was employed in the preparation of a polymer array from water soluble acrylamides and acrylate monomers, where three monomers were deposited sequentially in the same spot of the microarray along with a solution containing the catalyst, resulting in the creation of an array compromising thirty-six different polymer combinations (Zhang *et al*., 2009). This approach was further employed in the creation of an array compromising 609 polymers by printing mixtures of 18 monomers. From this array, Zhang and colleagues identified a synthetic thermoresponsive acrylate based hydrogel that supported long term hESC growth and pluripotency, involving reagent-free dissociation passaging in response to a reduction in ambient temperature (Zhang *et al*., 2013). However, despite hESCs maintained on this hydrogel displayed karyotypic abnormalities after 21 passages, these findings represent a hall mark in the development of xeno-free and fully defined hESC culture systems.

Independently of the technique employed for the preparation of the microarray, most of the detection and analysis systems used in the field of polymer microarray rely on the use of fluorescence. Scanning of microarrays consisting of a large number of polymer spots requires the use of high resolution high-content screening systems bases on fluorescence microscope able to analyse rapidly large number of spots within an array.

4.1.5 Identification of polyurethane 134

Microarray has been also employed in the identification of polymers compatible with hepatocyte differentiation of hPSCs. Hay and colleagues combined an efficient hepatocyte differentiation approach (Hay *et al*., 2008a) with high-throughput technologies to identify a synthetic and defined matrix that supported and promoted hepatocyte function and viability (Hay *et al*., 2011). For this purpose, by employing contact printing, the authors synthesised a microarray consisting of 380 polyacrylates and polyurethanes in an agarose coated aminoalkysilane microscope slide. hESCs differentiated towards hepatic endoderm on matrigel coated surfaces were replated onto the polymer microarray (Figure 26). Cells were culture for a further 9 days in the presence of a serum containing medium that supported hepatocyte identify and differentiation *in vitro*. Identification of polymer hits that supported cell attachment and albumin production was performed using phase contrast microscopy and immunofluorescence.

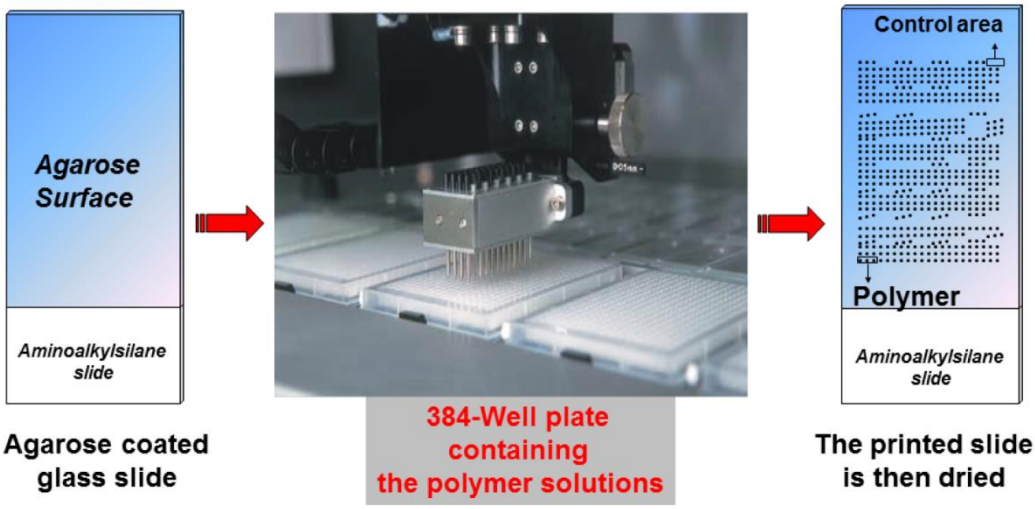

Figure 26. Polymer microarray fabrication.

From this screening 3 polyacrylates (2BG9, 9G7 and 3AA7) and 3 polyurethanes (134, 212, and 223) were identified as suitable substrates for hepatocyte differentiation. Analysis of the structure of the three identified polyacrylates

revealed little to none correlation. On the other hand, polyurethanes contained a chain extender that seemed essential in cell binding. In addition, polyurethane (PU) 134 and PU212 were made of the closely related (Poly[1,6-hexanodiol/neopentyl glycol/di(ethylene glycol)-alt-adipic acid]diol) (PHNGAD) and (Poly[1,6-hexanodiol/neopentyl glycol-alt-adipic acid]diol) (PHNAD) respectively, suggesting that this common feature is relevant in promoting hepatocyte binding and function. Moreover, physical parameters of the polymer such as elasticity and wettability are affected by the composition (Thaburet *et al*., 2003), which has an impact in the capacity of the polymer to absorb key extracellular matrix proteins involved in hepatocyte function (Hay *et al*., 2011).

Further functional characterisation of the HLCs replated on a scaled up version of these polymers was performed at Day 14 post-replating. Analysis in the secretion of fibrinogen, fibronectin and transthyretin (TTR) identified PU134 as an effective cellular matrix which supported superior hepatocyte function when compared to HLCs replated onto matrigel surfaces and freshly isolated human primary hepatocytes.

Studies of the signalling pathways activated in HLCs maintained on the PU134 surface revealed an increase focal adhesion kinase (FAK), Akt and ERK signalling pathways when compared to matrigel surfaces, indicating a strong cell attachment to the substrate. In addition, enhanced cytochrome P450 1A2 and 3A activity was observed in parallel to an increase in the protein levels of cell cycle inhibitors p15 and p21, suggesting that inhibition of cell proliferation is a requisite to obtain high functional HLCs. Moreover, HLCs replated on PU134 surfaces displayed increased expression of hepatocyte markers including albumin, hPXR and epithelial markers, such as E-Cadherin and N-Cadherin, compared to HLCs maintained on matrigel surfaces. This two-dimensional culture platform was successfully translated into a three-dimensional structure, by coating a bioartificial liver (BAL) device (Van de Kerkhove and Di Florio, 2002) with a solution of PU134. Scanning electron images revealed robust cell attachment and smooth tissue-like appearance of the HLCs in

the presence of PU134. This polymer technology was successfully translated to the iPSCs. Both, hESCs and iPSCs-derived HLCs generated on PU134 surfaces displayed stable cytochrome P450 activity and predicted cellular toxicity in response to specific pharmacological compounds in comparable levels than human primary material (Medine *et al*., 2013).

The identification of this synthetic polyurethane represents a hall mark in hepatocyte biology. It is cost-effective, easly scalable and manufacturable for clinical purpose, and has shown to be highlyt efficient in promoting hepatocyte function when compared with other polyurethanes (Fukuda *et al*., 2001). The possession of a xeno-free, defined and stable substrate that supports and enhances hepatocyte function compared with current biological matrices is a requirement if stable hPSCs-derived HLCs are going to be applied in drug toxicology process, disease modelling and the study of hepatocyte biology. In addition, no batch-to-batch variation has been observed between different PU134 batches (Medine *et al*., 2013), ensuring the delivery of reliable HLCs for downstream applications. Therefore, PU134 represents a novel substrate that can be applied in the hepatocyte biology field.

In this chapter, I will describe the optimization procedure performed on the polyurethane 134 surface and the combination with a serum- and xeno-free differentiation procedure to obtain long-term and functional cultures of HLCs, with implications in the stabilization of the hepatocyte phenotype In addition, a deep phenotypic and functional characterization of the HLCs obtained in the defined substrate will be described. The findings described in this chapter possess significant implications with regard to physical and nutritional parameters of defined culture systems

4.2 Results

The instability associated with the use of undefined biological additives in hepatocyte differentiation is a major limitation for downstream application. In

order to tackle this issue, Hay and colleagues performed an interdisciplinary approach to identify synthetic and defined polymers to be used as substrata for hepatocyte differentiation and maintenance. From a polymer microarray, the polyurethane 134 (PU134) was identified as a superior surface to animal derived substrates with regard to hepatocyte differentiation and function.

I subsequently optimised the polymer coated surface and media formulation to study the effect on the function and stability of the cells. The resulting population of hESCs-derived hepatocyte-like cells (HLCs) were extensively characterised and compared to their matrigel counterpart.

4.2.1 Optimization of the polymer PU134 coated surface

The optimisation of polymer surface involved the testing of different solvents to solubilise the polymer. The topography of the resulting coated surfaces was analysed employing atomic force microscopy (AFM) and scanning electron microscopy (SEM), and the effect of the surface topography on the cell function was measured by analysing the cytochrome P450 3A activity in HLCs

4.2.1.1 Polymer solvent influences the topography of the polymer coated surface

A correct solubilisation of the polyurethane 134 is essential in order to obtain a homogenous coating of the culture surface. For this purpose, I analyzed the topography of surfaces coated with solutions of PU134 dissolved in different solvents. I solubilized PU134 on chloroform, either alone or in combination with toluene and on tetrahydrofuran, either alone or in combination with dichloromethane. Following this, I span coated the culture surface. I employed SEM and AFM to characterize the topography of the polymer coated surfaces.

Scanning electron images of the resulting surfaces (Figure 27) showed that the coating obtained using toluene or chloroform was not homogeneous, displaying an uneven and uncompleted coated surface with the presence of PU134 precipitates

(black and white arrows), indicating a poor solubility of the polymer on these solvents. In contrast, the use of tetrahydrofuran as a solvent ensured the spin coating of completed and much more uniform surface.

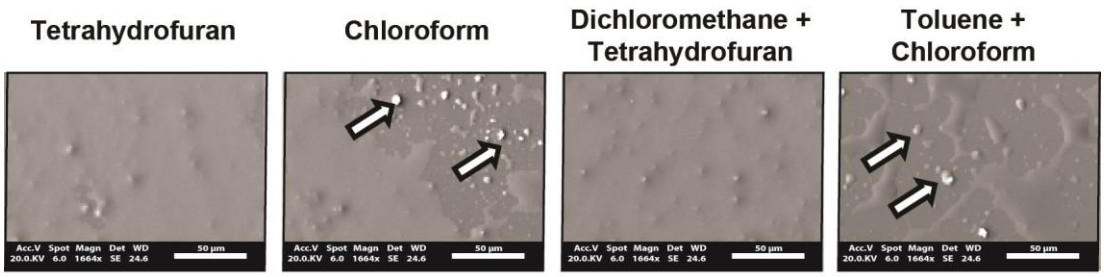

Figure 27. SEM images of different PU134 coated surface conditions. Culture surfaces were coated with a 2% solution of PU134 dissolved in different solvents. SEM was employed to study the PU134 coated surface obtained with each of the conditions. Representative images of each of the conditions show the presence of a homogeneous coated surface with absence of polymer precipitates when tetrahydrofuran was used as a solvent, in contrast chloroform alone or in combination with toluene (black and white arrows) which delivered unevenly coated surfaces. The images were taken at x1664 magnification and the scale bars represent 50 µm.

In addition to SEM, AFM was employed to study the topography of the coated surfaces. AFM three-dimensional images of the different coating conditions demonstrated that only PU134 solubilized in tetrahydrofuran delivered regular coated surfaces (Figure 27A).

The root mean square, RMS, and the mean roughness, Ra (peak to peak value) are two of the main parameters used in AFM to study the surface roughness. Analysis of these two parameters revealed that the polymer surface obtained by using tetrahydrofuran alone exhibited a 40% reduction in the roughness measurement comparing with the rest of the conditions (Figure 27B-C), confirming the previous observations indicating that out of the four solvents tested, tetrahydrofuran is the most suitable solvent to obtain homogeneous and evenly coated polymer surfaces.

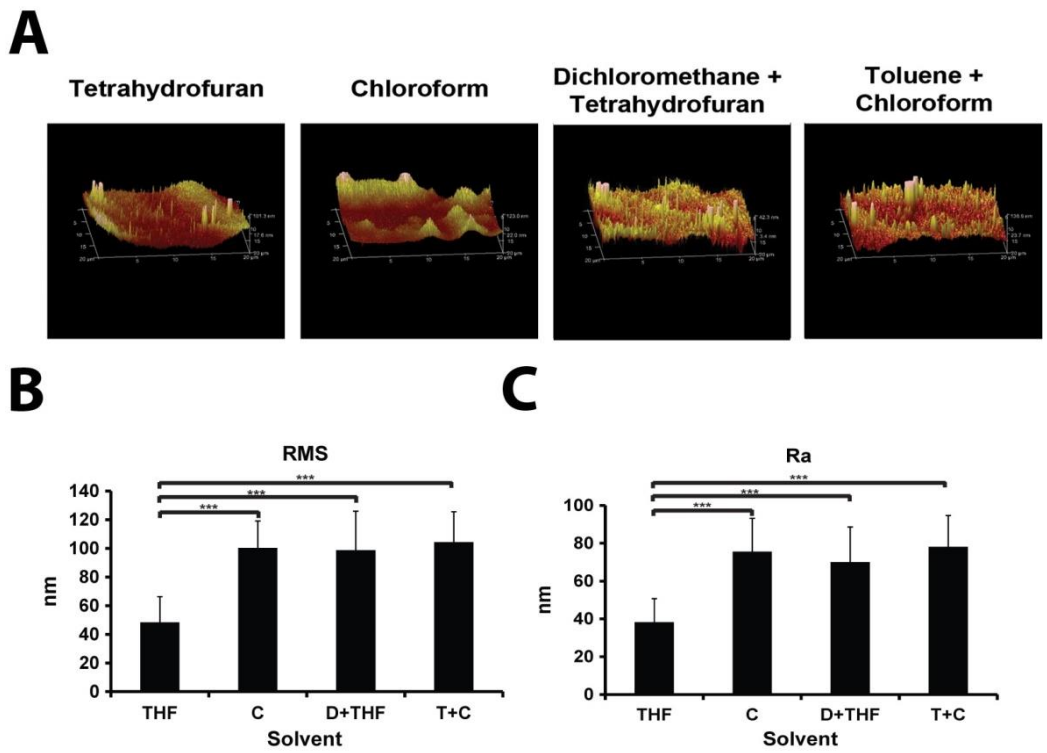

Figure 28. Topography of PU134 surfaces. A) Atomic force microscopy (AFM) images of different PU134 coated surfaces. AFM was employed to analyse the roughness of the PU134 coated surface using the selected solvents. High-magnification three-dimensional representative images of the different coating conditions show the topography of the surfaces, revealing that PU134 solubilised on the presence of tetrahydrofuran resulted in a more regular surface compared to the other solvents or combination of solvents. Images represent an area of 20 µm x 20 µm. B-C) Roughness measurements of different PU134 surface conditions. The roughness of the PU134 surfaces on selected solvents was measured using atomic force microscopy. Analysis of the roughness parameters Ra (the mean roughness) (B) and RMS (the root mean square) (C) of the different PU134 surfaces show that the coating obtained by using tetrahydrofuran as a solvent possessed the smoothest surface when compared with the rest of the conditions. The results represent the mean ± SD of seven individual samples per condition. Levels of significance were measured by student's t-test where $p < 0.001$ is denoted as *** in comparison to glass slides coated with PU134 solubilised in tetrahydrofuran. Abbreviations: THF-Tetrahydrofuran, C-Chloroform, D+THF: Dichloromethane and Tetrahydrofuran, T+C-Toluene and Chloroform.

4.2.1.2 HLC function in response to topographical changes

To assess the implications of the different coating conditions on the function of HLCs, hESCs-derived hepatoblasts were detached from matrigel surfaces and replated onto the different polymer surfaces. Cytochrome P450 3A function was tested at 4 days post-replating. A 2 fold increase in CYP3A activity was observed in HLCs replated on tetrahydrofuran/PU134 surfaces (Figure 29), demonstrating that

HLC metabolic activity is improved with a more uniform coating of PU134. Consequently, the optimised surface was used in all further experiments. The values for CYP3A for tetrahydrofuran, chloroform, dichloromethane/tetrahydrofuran and toluene/chloroform are as follows; 4,703 RLU/ml/cm^2, 1,737 RLU/ml/cm^2, 2,258 RLU/ml/cm^2 and 1,074 RLU/ml/cm^2, respectively.

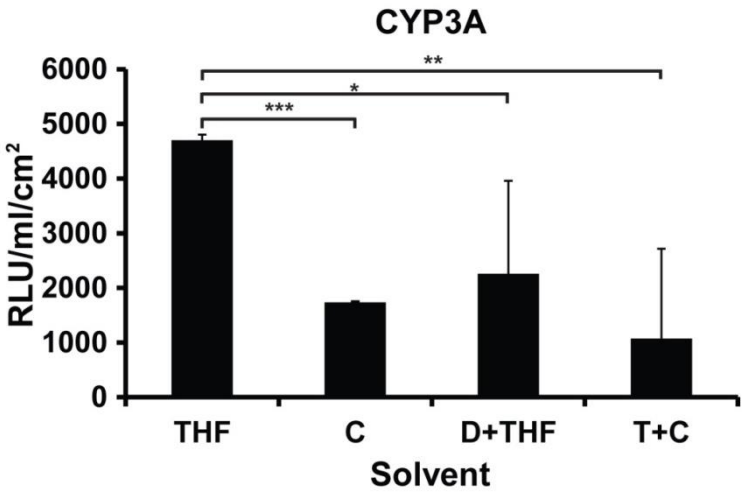

Figure 29. HLC function is topology dependent. Measurement of cytochrome P450 3A activity in HLCs maintained on the different surfaces 96 hours post-replating. Units of activity are expressed as relative light units (RLU) ml^{-1} cm^{-2} of culture surface. The results represent the mean ± SD of six individual samples per condition. Levels of significance were measured by student's t-test where $p<0.05$ is denoted as *, $p<0.01$ is denoted as ** and $p<0.001$ is denoted as *** in comparison to HLCs maintained on slides coated with PU134 solubilised on tetrahydrofuran. Abbreviations: THF-Tetrahydrofuran, C-Chloroform, D+THF: Dichloromethane and Tetrahydrofuran, T+C-Toluene and Chloroform.

4.2.1.3 Surface sterilisation impacts on the supportive properties of the polymer

Following the optimisation of the polymer coated surface, we analysed the effect of different polymer surface sterilisation procedures on the topography of the coated surfaces and measured their implications in cell function. For this purpose, PU134 surfaces were exposed to UV (UV-radiation) or gamma irradiation (γ-radiation) and the effect of these sterilisation treatments on the topography of the coated surfaces was analysed employing phase contrast images and SEM. The implications

on the cell function in HLCs was analysed by measuring the cytochrome P450 3A activity.

Phase contrast images of PU134 surfaces showed no gross differences in polymer coating post UV or gamma irradiation (Figure 30A). These observations were further confirmed by SEM analysis (Figure 30B). The biological performance of PU134 was examined by analysing cytochrome P450 3A activity in HLCs at Day 10 post-replating. Analysis of the function displayed a 3-fold increase in the activity in cells replated on γ-radiated polymer surfaces over cells replated on UV-radiated PU134 surfaces (Figure 31). These observations demonstrated that gamma-irradiation represents the optimal sterilisation technique. The values for CYP3A for γ-radiated or UV-radiated polymer coated surfaces are as follows; 6,590 RLU/ml/cm^2 and 2,042 RLU/ml/cm^2 respectively. The optimised surface was used in all subsequent experiments.

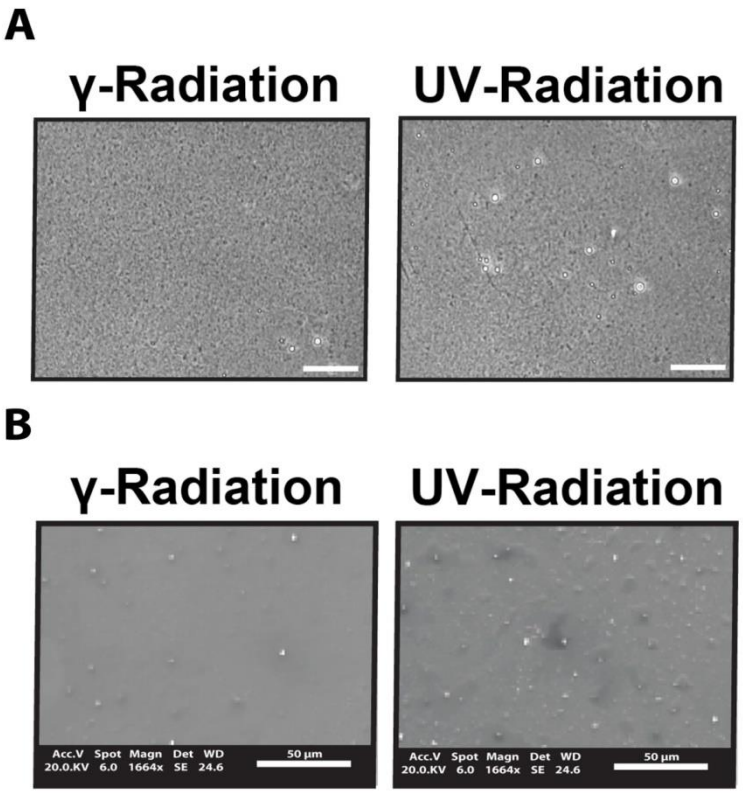

Figure 30. Polymer sterilisation. A) Phase contrast images of the PU134 surface after UV-radiation and γ-radiation show no gross differences on the PU134 surfaces between both treatments. Images were taken at 40x magnification and scale bar represents 20 µm. B) Scanning electron microscopy

(SEM) images of the polymer surface after UV-radiation and γ-radiation show no gross differences between both sterilisation treatments, confirming the previous observations. The images were taken at x1664 magnification and scale bar represents 50 µm.

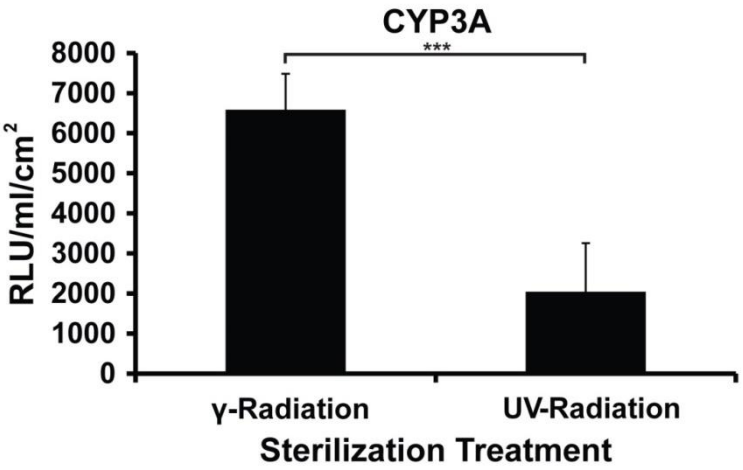

Figure 31. Functional changes in HLCs following polymer sterilization. Measurement of the cytochrome P450 3A activity in HLCs maintained for 10 days on PU134 surfaces sterilized by either using UV-radiation or γ-radiation shows a 3.3-fold increase in cytochrome activity in HLCs maintained on γ-radiated PU134 surfaces when compared with HLCs maintained on UV-radiated PU134 surfaces. Units of activity are expressed as relative light units (RLU) ml^{-1} cm^{-2} of culture surface. The results represent the mean ± SD of three individual samples per condition. Levels of significance were measured by student's t-test where $p<0.001$ is denoted as ***.

4.2.2 Optimization of the cellular replating onto polymer coated surface

Previously we have shown the inherent functional variability associated with the use of serum containing media in HLCs, making reproducibility between experiments difficult (Figure 16, chapter 3). As a result, I developed a serum-free differentiation approach to obtain highly functional, reproducible and reliable HLCs from pluripotent stem cells using matrigel surfaces as a culture substrate.

I translated this technology to PU134 surfaces, obtaining functional HLCs on a fully defined environment. However, cells were functional and viable on the PU134 surfaces for up 10 days post-replating; when cell detachment and death could be observed (Figure 32, panels A-C). These observations were not detected when we used matrigel surfaces, indicating the presence in matrigel of essential supporting factors and cytokines that promote cell survival. Therefore, in an attempt to

increase the life span of the cells while maintaining the serum-free environment, I added Knock-Out Serum Replacement (KOSR) to the replating media.

4.2.2.1 Morphological analysis of HLCs

Images of the HLCs were taken at Day 8, 12 and 16 post-replating. Phase contrast images of the cells (Figure 32) showed that in either condition, PU134 surfaces supported the attachment of the cells, displaying typical features of cultured hepatocytes *in vitro* (panels A and D). However, at Day 12 post-replating, the absence of KOSR in the medium compromised the viability of HLCs. Hepatic morphology began to disappear, with cellular detachment observed (panels B and C). Addition of KOSR preserved the integrity of the culture, enhancing hepatocyte morphological features, including canaliculi-like structures by Day 12 post-replating (panel E, white and black arrows) and the presence of binucleate cells by Day 16 post-replating (panel E, black arrows)

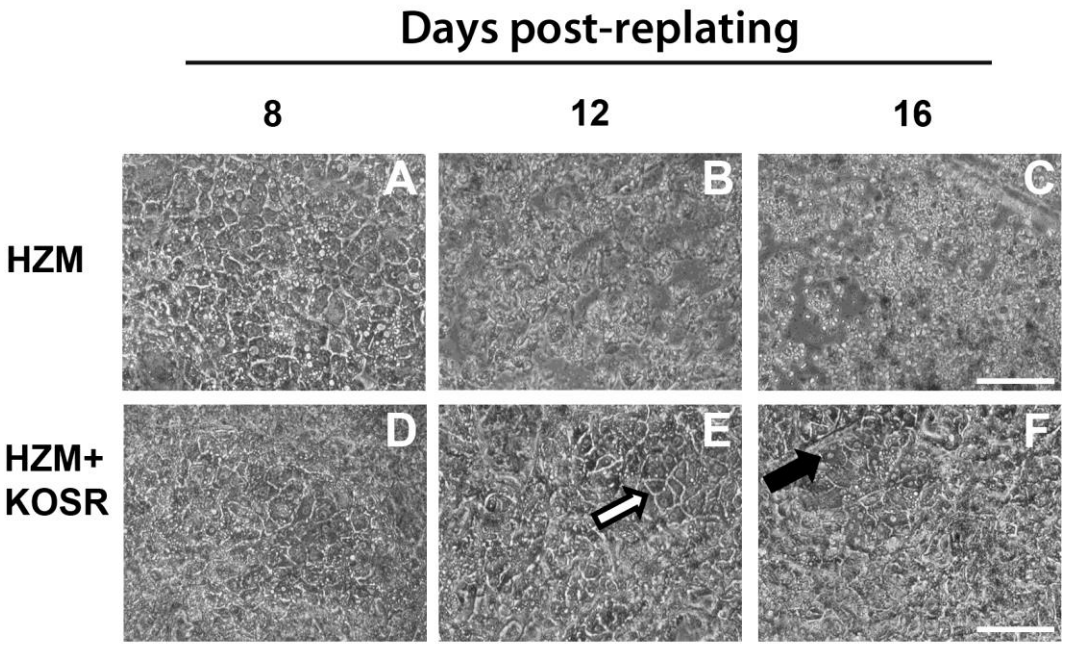

Figure 32. KOSR supports long term HLC culture on PU134 surfaces. hESCs-derived hepatoblast were replated onto PU134 surfaces in the presence of the defined maturation media with or without Knock-Out Serum Replacement (KOSR). Phase contrast images of the cells show that by Day 8 post replating, the HLCs were attached to the substrata in both conditions with cells displaying typical hepatocyte features. In the absence of KOSR and by Day 12 post-replating, HLCs rounded up and detached. In contrast, addition of KOSR in the maturation media supported cell attachment to PU134

surfaces with cells displaying typical hepatocyte features such as canaliculi-like structures (white and black arrows) and the presence of binucleate cells (black arrows) by Day 16 post-replating. The images were taken at 10x magnification and the scale bar represents 100 µm.

4.2.2.2 Functional characterisation of HLCs

In addition to morphological analysis, I investigated the metabolic function of the cells replated on PU134 surfaces under both conditions. Cytochrome P450 3A and 1A2 functions in HLCs were examined at Day 8, 12 and 16 post-replating (Figure 33). Analysis of the CYP3A activity (Figure 33A) revealed comparable levels of metabolic activity in HLCs at Day 8 post-replating independently of the addition of KOSR. However, as the differentiation progressed, I observed lower levels of CYP3A function without KOSR supplementation. In contrast, in the presence of KOSR CYP3A activity increased by 8.6-fold by Day 12 post-replating and maintained at least until Day 16 post-replating. The values for CYP3A in the absence or presence of KOSR are respectively as follows; 6,951 RLU/ml/cm^2 and 18,351 RLU/ml/cm^2 at Day 8 post-replating; 4,428 RLU/ml/cm^2 and 158,790 RLU/ml/cm^2 at Day 12 post-replating and; 0 RLU/ml/cm^2 and 158,351 RLU/ml/cm^2 at Day 16 post-replating.

Analysis of the CYP1A2 activity (Figure 33B) showed lower levels of CYP1A2 activity without KOSR supplementation at Day 8 post-replating and maintained until Day 12 post-replating. In contrast, in the presence of KOSR, CYP1A2 activity increase 2.4-fold at Day 12 post-replating and remained stable at least until Day 16 post-replating. The values for CYP1A2 in the absence or presence of KOSR are respectively as follows; 577 RLU/ml/cm^2 and 4,795 RLU/ml/cm^2 at Day 8 post-replating; 580 RLU/ml/cm^2 and 11,200 RLU/ml/cm^2 at Day 12 post-replating and; 0 RLU/ml/cm^2 and 12,536 RLU/ml/cm^2 at Day 16 post-replating.

These data demonstrate that the addition of Knock-Out Serum Replacement (KOSR) to the free serum maturation medium enhances cell attachment, cell morphology and possesses a clear effect on the cytochrome P450 function of HLCs. As a result, the serum-free maturation media was supplemented with KOSR in all subsequent experiments.

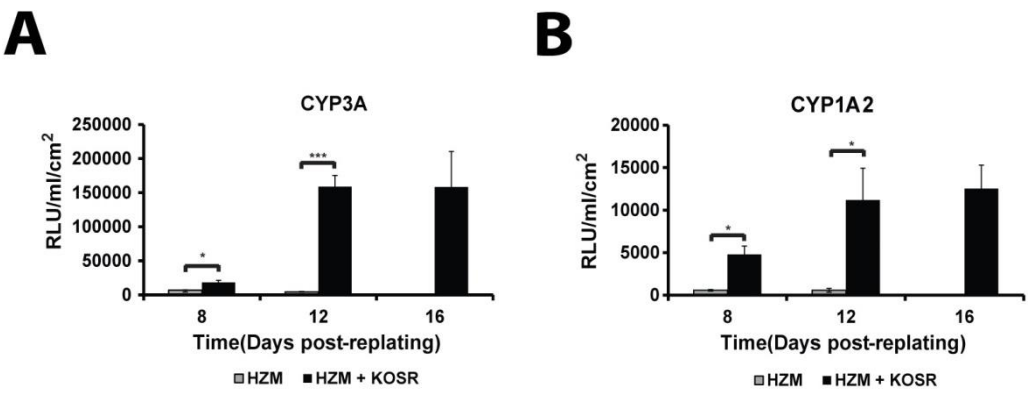

Figure 33. Addition of KOSR supports cytochrome P450 function in HLCs. Cytochrome P450 CYP3A (A) and CYP1A2 function (B) were assessed using the pGLO™ system on PU134 surfaces in the presence of the serum-free maturation media with or without Knock-Out Serum Replacement at Day 8, 12 and 16 post-replating. Analysis of the function of the cells revealed an increase in the activity of both CYP3A and CYP1A2 in media supplemented with KOSR, and this activity was maintained by Day 16 post-replating. Media without KOSR did not support the activity on the cells by Day 16 post-replating. Units of activity are expressed as relative light units (RLU) ml^{-1} cm^{-2} of culture surface. The results represent the mean ± SD of three individual samples per time point per cytochrome P450 analysed. Representative experiment is displayed. Levels of significance were measured by student's t-test where $p<0.001$ is denoted as *** and $p<0.05$ is denoted as *.

4.2.3 Cell performance is improved on PU134 surfaces compared with other biological substrates

Collagen, fibronectin and laminin are the main extracellular matrix (ECM) components found in the liver. I investigated HLCs on those matrices and compared with HLCs differentiated on matrigel and PU134 surfaces. For this purpose, hESCs-derived hepatoblasts were lifted and replated onto surfaces coated with collagen I, fibronectin and a mixture of the major types of laminins found in the human body. Following this, hepatocyte differentiation continued for 15 days.

Phase contrast images of the HLCs on each substrate revealed that cell attachment was supported in all substrata, but with differences in the cell morphology (Figure 34A). HLCs maintained on collagen I or laminin surfaces displayed a defined nucleus surrounded by a dense cytoplasm, resembling mature primary hepatocytes in culture (white and black arrows), with certain grade of cell morphological heterogeneity observed. HLCs on fibronectin surface exhibited a morphological heterogeneity in shape and size, and cells did not display typical hepatocyte

morphological features, suggesting that fibronectin did not support an efficient hepatocyte differentiation. HLCs on matrigel displayed typical hepatocyte morphology. Finally, HLCs obtained on PU134 surfaces displayed characteristic hepatocyte morphology features and high morphological homogeneity with the presence of canaliculi-like structures (black arrows).

In addition to morphological analysis, I investigated the metabolic function of the HLCs replated on the different surfaces. For this purpose I measured cytochrome P450 3A function at Day 15 post-replating (Figure 34B) as it represents the major P450 acitivity of the cells. No other functional measurements were performed. Analysis of the metabolic function revealed that HLCs maintained on PU134 surfaces displayed the highest CYP3A activity, with a 3.6 and 4.3-fold increase compared with HLCs maintained on fibronectin or laminin respectively; and 8 and 9.5-fold increase compared with HLCs replated on collagen I and matrigel respectively, indicating that morphology is not always a good indicator of the hepatic function. The values for CYP3A in HLCs maintained on collagen I, fibronectin, laminin, matrigel and PU134 surfaces are respectively as follows; $1{,}24x10^5$ RLU/ml/mg, $2{,}80x10^5$ RLU/ml/mg, $2{,}3x10^5$RLU/ml/mg, $1{,}05x10^5$ RLU/ml/mg and $1x10^6$ RLU/ml/mg.

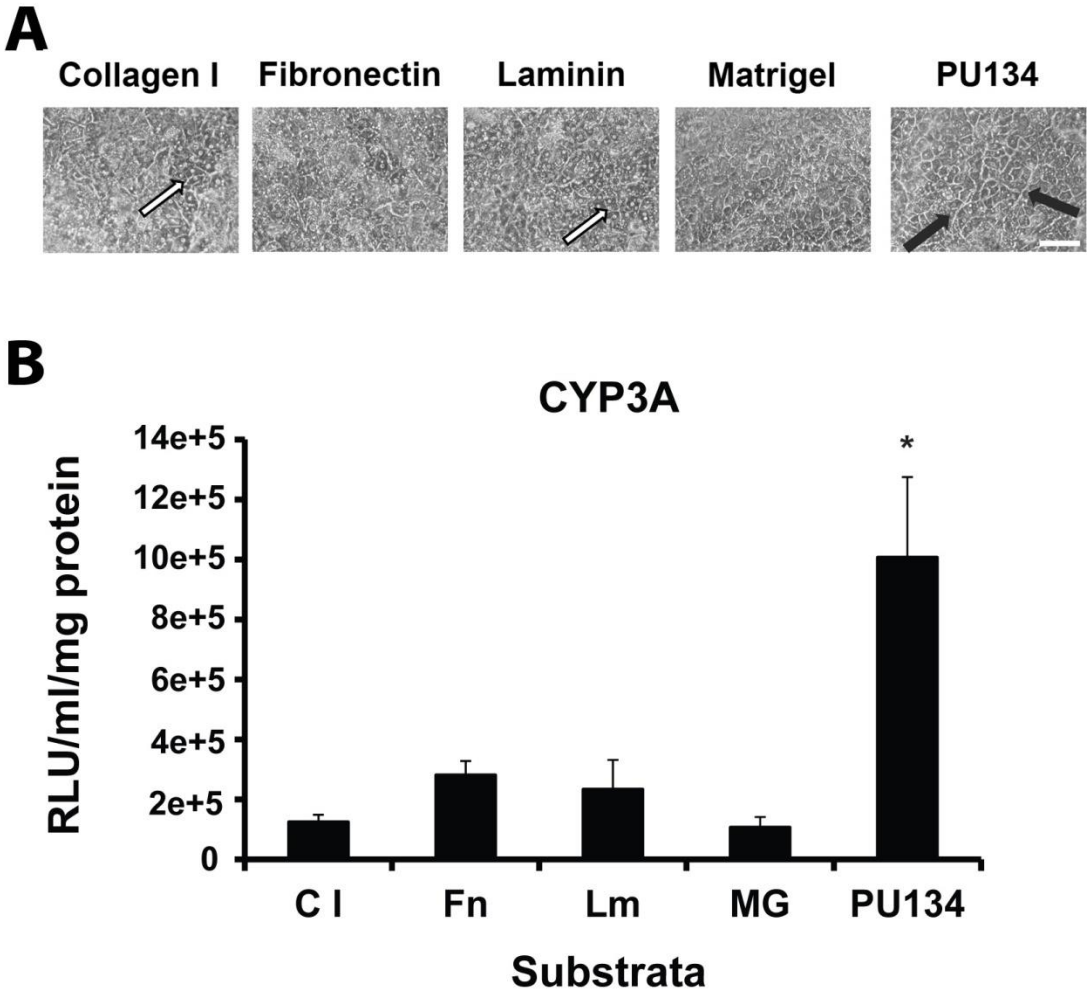

Figure 34. Improved cell performance on PU134 compared with other biological substrates. A) Phase contrast images of HLCs maintained on different biological matrices and PU134 surfaces. HLCs were replated in the serum-free maturation media supplemented with KOSR on biological matrices made out the major components of the extracellular matrix of the liver, on matrigel or on PU134 surfaces. Phase contrast images of HLCs at Day 15 post-replating revealed that all the tested substrates supported cell attachment but with cells displaying different morphology depending on the substrata. The acquisition of typical hepatocyte morphological features was displayed more notorious on collagen I, laminin and especially on PU134 surfaces. The images were taken at 10x magnification and scale bar represents 100 µm. B) CYP3A activity in HLCs is improved on PU134 surfaces comparing with biological substrates. The analysis of the hepatocyte cytochrome P450 function 3A in HLCs replated on different biological substrates and PU134 surfaces was assessed using the pGLO system, revealing an increase in the functional capacity of the cells when PU134 surfaces were used as substrate. An increase in the activity on PU134 surfaces between 3.6 and 9.5 fold compared with the rest of the substrates was observed. The results represent the mean ± SD of five individual samples per condition. The significance between differences in function of the cells replated on the different matrices was measured using ANOVA, and denoted on the graph by an asterisk (*). Abbreviations: C I-Collagen I, Fn-Fibronectin, Lm-Laminin, MG-Matrigel.

4.2.4 Detailed characterization of the hepatocyte differentiation on PU134 *versus* matrigel surfaces

As matrigel is considered the current 'gold standard' substrate to maintain PSCs-derived HLCs, I performed an extensive characterisation of HLCs obtained on PU134 surfaces and compared them with their matrigel counterparts. For this purpose, hESCs-derived hepatoblasts were replated onto matrigel or PU134 surfaces in the presence of the serum-free maturation media containing KOSR. The resulting population of cells were extensively characterised at different times during the differentiation procedure (Figure 35).

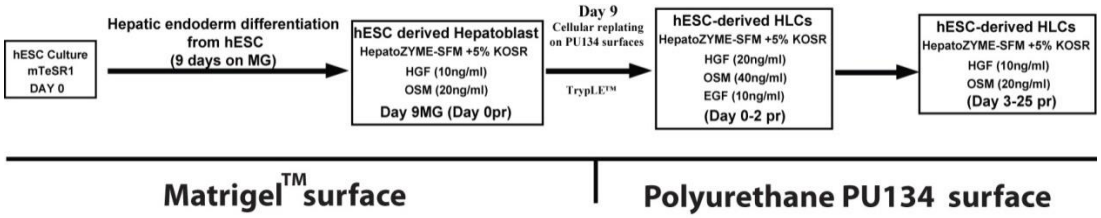

Figure 35. Flow diagram of the hepatocyte differentiation protocol on PU134 surface. H9 hESCs are primed towards the hepatic endoderm cells using an efficient differentiation protocol. hESCs-derived hepatoblasts at Day 9 on matrigel (MG) are replated on PU134 surfaces using a serum-free replating approach. Hepatocyte maturation on PU134 surface is induced using a serum-free maturation media supplemented with KOSR. Abbreviations hESC– human embryonic stem cells; KOSR- Knock-Out Serum Replacement; HZM-HepatoZYME-SFM; EGF-Epithelial Growth Factor; HGF – Hepatocyte growth factor; OSM – Oncostatin M.

4.2.4.1 Morphological analysis of HLCs on PU134 and matrigel surfaces

Morphological analysis of HLCs replated on matrigel or PU134 surfaces was performed at Day 5, 10, 15 ,20 and 25 post-replating in the differentiation approach (Figure 36). Phase contrast images of the resulting population of HLCs showed that both substrata supported cell attachment. At Day 5 and 10 post-replating there were no gross differences in the morphology of the cells replated on either substrate. The compacted and homogeneous resulting population of cells displayed a hexagonal morphology, with well-defined nucleus and clear cell-to-cell contacts, all features of primary hepatocytes in culture (panels A-B, F-G). As the differentiation progressed, cells maintained on matrigel surfaces started to lose

these hepatocyte characteristics, displaying a morphological heterogeneity, with cells rounding up and detaching (white arrows panels C-E). However, on PU134 surfaces, cell morphology was improved. Hepatocyte morphological features were preserved up to 25 days post-replating, with cells displaying canaliculi-like structures (black arrows, panels H-J).

4.2.4.2 Gene expression profile in HLCs on PU134 and matrigel surfaces

To further characterise HLCs obtained on PU134 and matrigel surfaces, I measured the gene expression of hepatocyte markers (albumin, HNF4α and alpha-fetoprotein), and the epithelial marker E-Cadherin at Day 5, 10, 15, 20 and 25 post-replating by quantitative PCR. The gene expression profile is shown in Figure 37.

No significant differences were observed in the albumin gene expression (panel A) between either substrate until Day 20 post-replating, when a 2-fold increase in HLCs maintained on PU134 surfaces compared with matrigel surfaces was observed ($p<0.001$). Following this, albumin gene expression could not be detected on matrigel surfaces at Day 25 post-replating, while it was still expressed on PU134 surfaces.

Hepatocyte nuclear factor 4α, HNF4α, gene expression (panel B) was stabilised in HLCs replated on PU134 surfaces in comparison with matrigel surfaces. By Day 20 post-replating, there was 2-fold increase in the gene expression on PU134 surfaces compared with matrigel surfaces ($p<0.001$). Following this, 2-fold decrease in the gene expression on PU134 surfaces at Day 25 post-replating was observed.

Day 10 post-replating represented the peak in the gene expression of alpha-fetoprotein for either substrate (panel C), with a 2.3-fold increase on matrigel surface compared with PU134 surfaces ($p<0.001$). Following this, independently on the substrate, there was a dramatic decrease in the gene expression (5-fold and 2-fold at Day 15 post-replating on matrigel or PU134 surface, respectively) with no significant differences between either substrate. However, by Day 20 post-

replating, a 1.6-fold increase was observed in HLCs maintained on matrigel surfaces compared with PU134 surfaces ($p<0.05$).

The pattern in the gene expression of E-Cadherin followed a similar trend independently of the substrate. As the differentiation progressed, a decrease in the gene expression was observed, but more denoted on matrigel surfaces (panel D). At Day 15 post-replating, a 1.7-fold increase in the gene expression on PU134 surfaces compared with matrigel surfaces was observed ($p<0.01$). The increased gene expression detected on PU134 surfaces compared with matrigel surfaces was maintained at late stages in the differentiation procedure, with 2 and 1.6-fold increase at Day 20 and 25 post-replating respectively ($p<0.001$).

In conclusion, analysis in the gene expression of hepatocyte and epithelial markers indicated that PU134 surfaces preserve the hepatocyte phenotype in HLCs for longer time, suggesting the existence of an anti-dedifferentiation strategy promoted by PU134 surface.

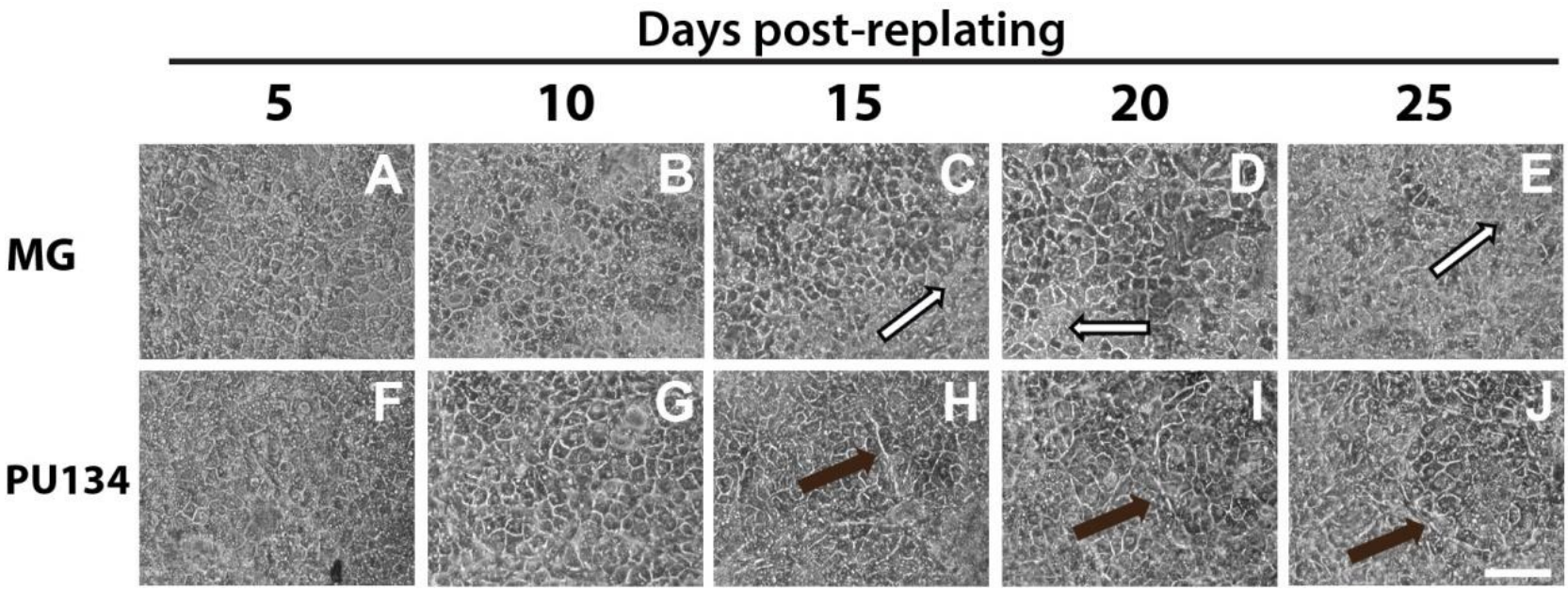

Figure 36. Combining serum-free differentiation with polymer surfaces. hESCs-derived hepatoblast at Day 9 in the differentiation protocol were removed from the culture substrate and replated onto matrigel (MG) or PU134 surfaces (PU134). Phase contrast images showed the morphology of HLCs at different days post-replating on either substrate. Independently of the substrate, the resulting homogeneous and compacted population of HLCs displayed by Day 10 post-replating typical hepatocyte morphological features, denoted by the acquisition of a more defined nucleus, with cells displaying a hexagonal morphology and an increase in the cell-to-cell contact, resembling to cultures of human primary hepatocytes. As differentiation progressed, cells maintained on matrigel surfaces underwent a morphological deterioration denoted by a gradual loss of these hepatocyte morphological features and the acquisition of a morphological heterogeneity. The life span of HLCs maintained on PU134 surfaces was improved, with enhanced expression of morphological features denoted by the presence of canaliculi-like structures, indicating the acquisition of mature hepatocyte morphology. The images were taken at 10x magnification and scale bar represents 100 µm.

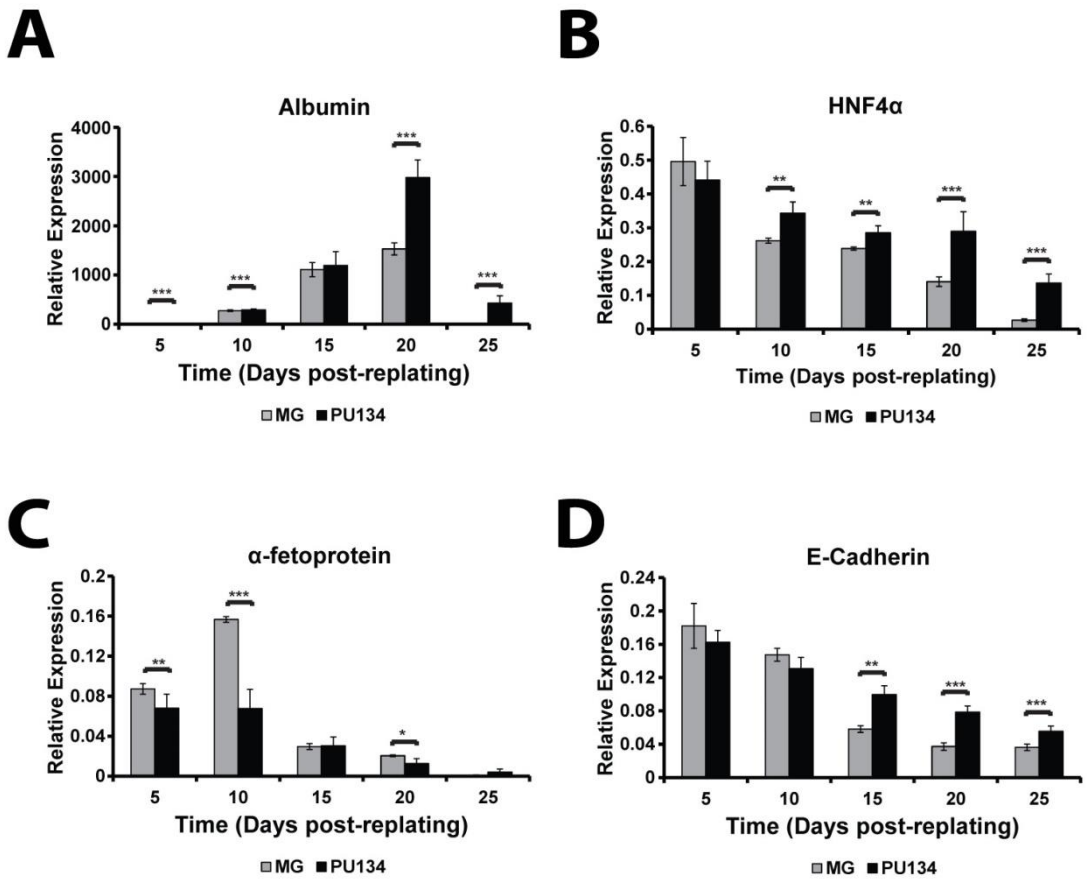

Figure 37. Hepatocyte gene expression. The gene expression of hepatocyte markers (Albumin, HNF4α, α-fetoprotein) and the epithelial marker E-Cadherin in HLCs maintained on matrigel (MG) or PU134 surfaces at Day 5, 10, 15, 20 and 25 post-replating were analysed by quantitative PCR. Relative expression refers to fold of induction over hESCs-derived hepatoblast at Day 9 and normalised to the housekeeping gene GAPDH. The results represent the mean ± SD of three different samples run, each run in triplicate. Levels of significance were measured by student's t-test where $p<0.05$ is denoted as *, $p<0.01$ is denoted as ** and $p<0.001$ is denoted as ***, compared with HLCs on MG at the same time points. Abbreviations: HNF4α-Hepatic Nuclear Factor 4α.

4.2.4.3 Investigating the dedifferentiation stage of HLCs

Long-term maintenance of stable HLCs in culture is essential if cells are going to be employed in research and clinical applications. For this purpose, I assessed the dedifferentiation state of the cells maintained on PU134 or matrigel surfaces by studying the expression of a well-established hepatocyte marker, HNF4α, and the mesenchymal marker vimentin.

The protein expression of the hepatocyte nuclear factor 4α, HNF4α, was analysed by immunofluorescence and Western Blot. Immunofluorescence analysis (Figure 38)

showed that independently of the culture substrate employed, at early stages in the differentiation protocol most of the HLCs stained positive for HNF4α, as 92% and 93% of the cells by Day 5 post-replating expressed the protein on matrigel or PU134 surfaces respectively, increasing to 94% and 95% respectively by Day 10 post-replating. The presence of PU134 stabilised the expression as the differentiation progressed, as 91% and 85% of the cells remained positive at Day 15 and Day 20 post-replating respectively. However, on matrigel surfaces the expression significantly declined and while 78% of the cells still expressed HNF4α by Day 15 post-replating, only 22% of the cells remained positive by Day 20 post-replating, representing 4-fold decrease compared with PU134 surfaces. By Day 25 post-replating, HNF4α expression was practically absent on matrigel (6% of the cells still expressed the protein), but was still maintained by 32% of the cells replated on PU134 surfaces.

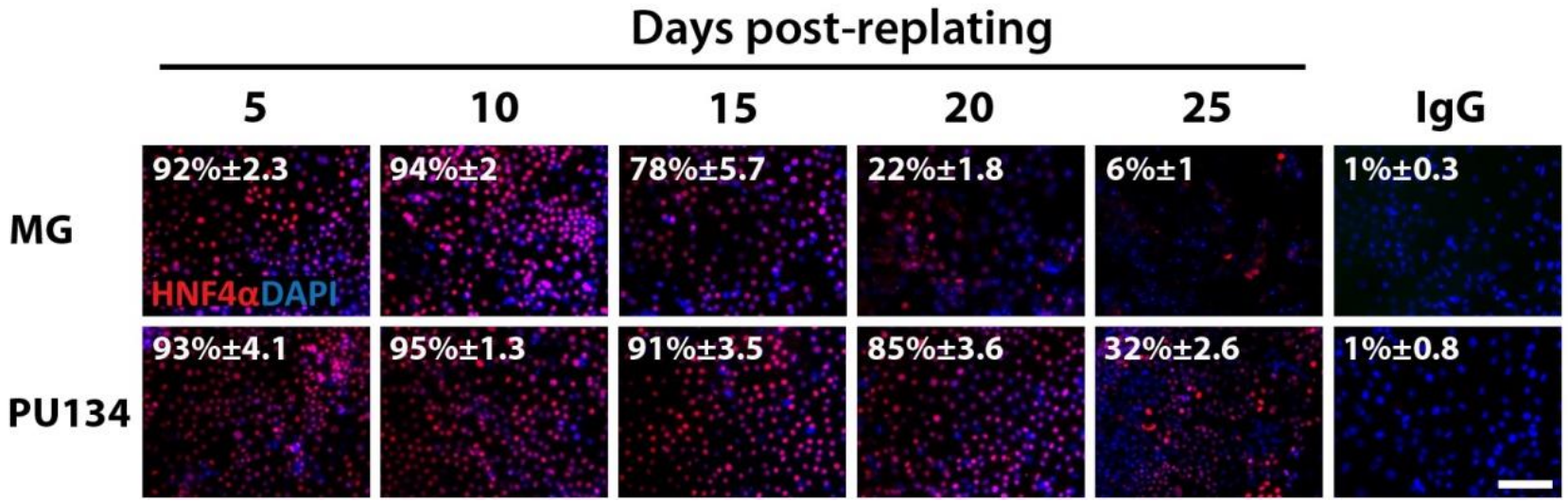

Figure 38. Immunofluorescence analysis of HNF4α in HLCs. HLCs maintained on matrigel (MG) or PU134 surfaces were collected and fixed throughout the differentiation protocol and the expression of the hepatocyte specific lineage transcription factor HNF4α was analysed by immunofluorescence. Results show the percentage yield of HLCs expressing HNF4α on either substrate. HNF4α expression was gradually lost in cell maintained on matrigel surfaces and by Day 20 post-replating 22% of cells still expressed the transcription factor. HNF4α expression remained constant in HLCs maintained on PU134 surfaces, with 4-fold increase in the percentage of cells still staining positive by Day 20 post-replating (85%). The corresponding IgG isotype controls demonstrated the specificity of the staining. For each condition five random fields of view, containing at least 500 cells, were counted. Images were taken at 20x magnification and the scales bar represents 100 µm. Abbreviations: HNF4α-Hepatocyte nuclear factor 4α, IgG-Immunoglobulin G.

These observations were further confirmed by Western Blot. The expression of HNF4α in HLCs replated on matrigel surfaces rapidly decreased after Day 10 post-replating, disappearing by Day 25 post-replating (Figure 39A), while in HLCs replated on PU134 surfaces, the expression was maintained up to Day 20 post-replating and could be detected by Day 25 post-replating (Figure 39B). Yet, despite Western Blot observations supported immunofluorescence analysis, the lower amount of HNF4α detected by Western blot compared with immunofluorescence suggested that the efficiency of the antibody employed varies with the protein conformation, being more efficient against the naïve conformation (immunofluorescence) than unfolded conformation (Western Blot).

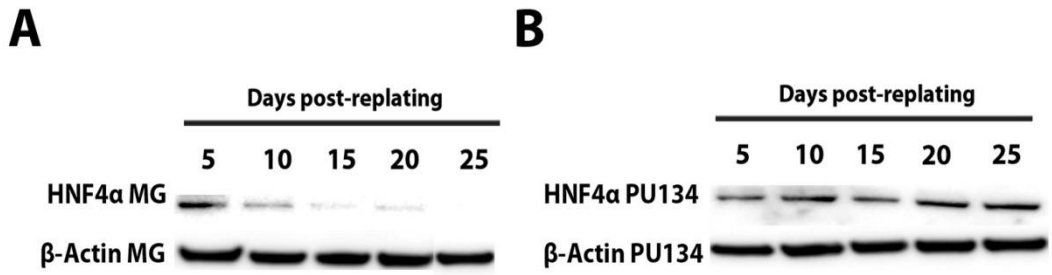

Figure 39. Analysing HNF4α expression by Western blotting. Cell extracts were collected throughout the differentiation protocol and probed with HNF4α antibody using standard western blotting. Panel A displays HLCs maintained on matrigel surfaces and panel B displays HLCs maintained on PU134 surfaces. As previously observed by immunofluorescence, there was a decrease in the expression of HNF4α in cell maintained on matrigel coated surfaces as the differentiation progressed, while the expression was maintained constant throughout the differentiation process on the presence of PU134 surfaces. β-actin was used as a loading control. Abbreviations: HNF4α-Hepatocyte nuclear factor 4α.

The expression of the mesenchymal marker vimentin was analysed by immunofluorescence (Figure 40), revealing that at Day 5 post-replating, 36% and 20% of the cells expressed vimentin on matrigel and PU134 surfaces respectively. The percentage of cells replated on matrigel surfaces expressing the mesenchymal marker rapidly increased as the differentiation progressed, and by Day 10 post-replating, there was a ≈2-fold increase in the percentage yield of positive cells, reaching 63% and 78% by Day 15 and 20 post-replating respectively. By Day 25 post-replating most of HLCs displayed the mesenchymal marker. On PU134 surfaces the

expression of vimentin was delayed. By Day 10 post-replating 23% of HLCs stained positive for the protein, reaching 27% and 35% at Day 15 and 20 post-replating. However, at late stages in the differentiation approach, 80% of HLCs replated on PU134 surfaces expressed vimentin. Analysis in the expression of HNF4α and vimentin indicate that PU134 surfaces promote the maintenance of the hepatocyte phenotype and delay the dedifferentiation process in HLCs.

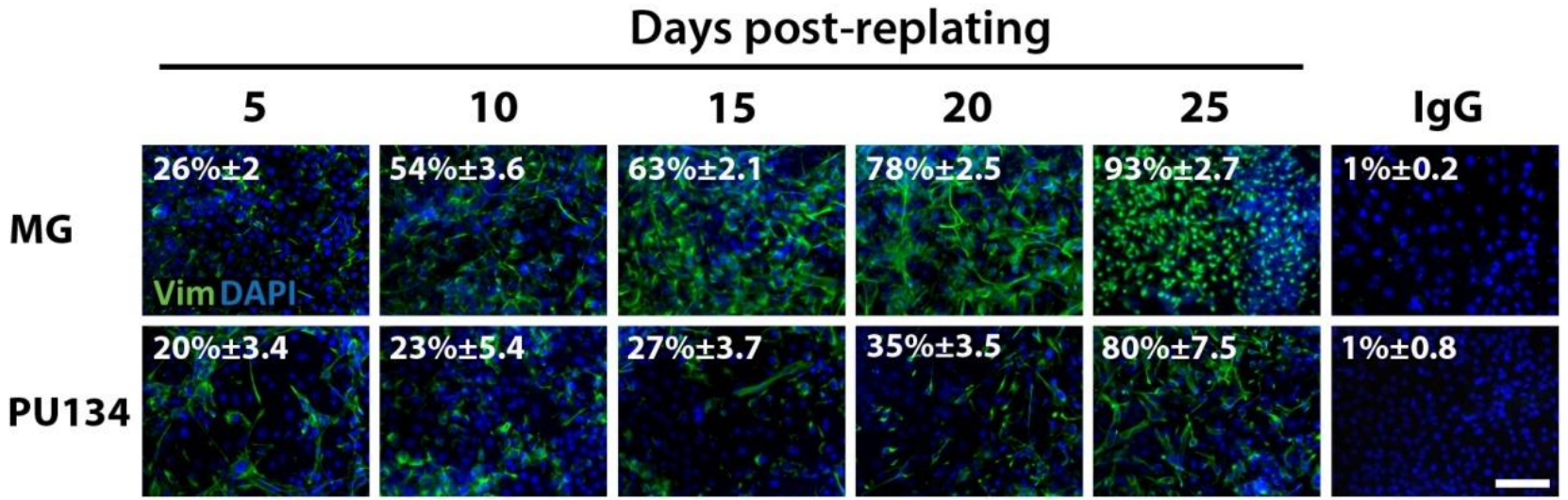

Figure 40. Immunofluorescence analysis of vimentin expression. The expression of the mesenchymal marker vimentin in HLCs maintained on either substrate at different time points on the differentiation procedure was analysed by immunofluorescence. Results showed a gradual increase in the percentage of cells maintained on matrigel surfaces expressing vimentin as the differentiation progressed, with most of the cells staining positive for the mesenchymal marker by Day 20 post-replating. Vimentin expression remained constant throughout the differentiation protocol in HLCs maintained on PU134 surfaces, with a 2-fold decrease in the percentage of cells staining positive by Day 20 post-replating compared with cells maintained on matrigel surfaces. The corresponding IgG isotype controls demonstrated the specificity of the staining. For each condition five random fields of view, containing at least 500 cells, were counted. Images were taken at 20x magnification and the scales bar represents 100 µm. Abbreviations: Vim-Vimentin, IgG-Immunoglobulin G.

4.2.4.4 Protein expression of hepatocyte markers in HLCs on PU134 and matrigel surfaces

To further characterised the HLCs obtained in the defined polymer surfaces, in addition to gene expression analysis, I investigated the protein expression of hepatocyte markers including albumin, alpha-fetoprotein, cytochrome P450 3A (CYP3A) and 2D6 (CYP2D6) by immunofluorescence and Western blotting. HLCs replated on matrigel or PU134 surfaces were fixed and stained at Day 5, 10, 15, 20 and 25 post-replating.

Analysis in the percentage yield of HLCs staining positive for the hepatocyte marker albumin (Figure 41), showed that at Day 5 post-replating, 17% and 28% of the cells maintained on matrigel or PU134 surfaces respectively expressed albumin. This percentage increased at Day 10 post-replating as 44% and 89% of the cells stained positive on matrigel or PU134 surfaces respectively. The expression stabilised on PU134 surfaces as 91% and 86% of cells stained positive at Day 15 and 20 post-replating respectively. The peak in the expression of albumin on matrigel surfaces was reached at Day 15 post-replating as 82% of the cells stained positive, before a 2-fold decrease by Day 20 post-replating as 43% of the cells expressed albumin. At Day 25 post-replating only 12% of HLCs remained positive on matrigel surfaces compared with 62% of the cells maintained on PU134 surfaces.

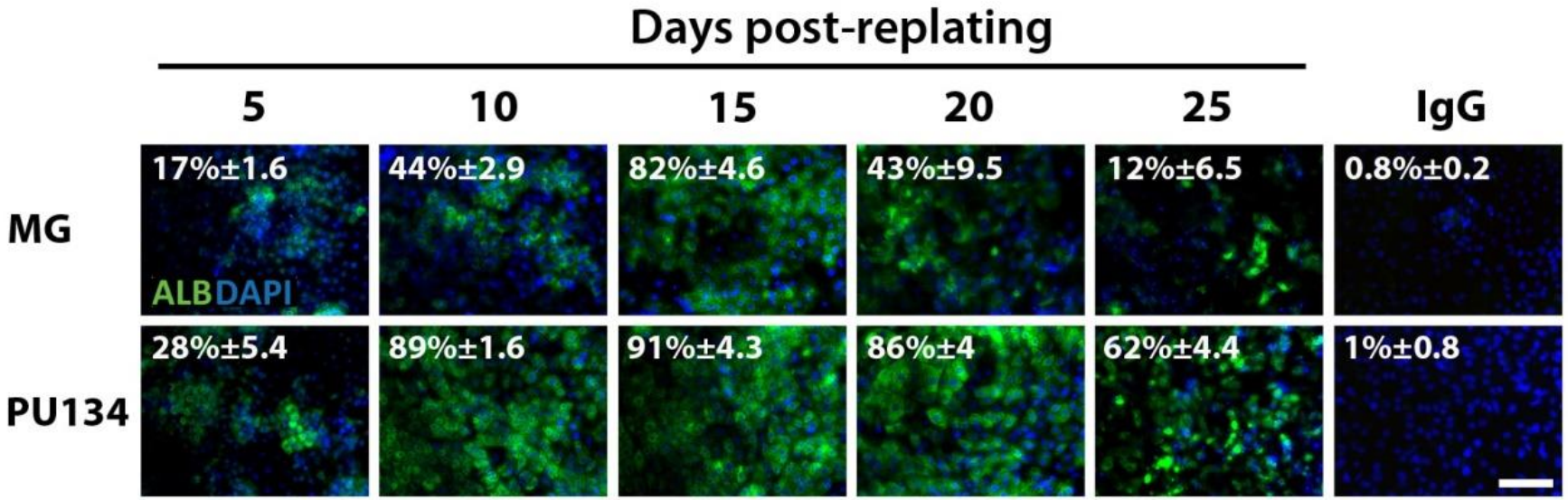

Figure 41. Immunofluorescence analysis of albumin expression in HLCs. HLCs maintained on matrigel (MG) or PU134 surfaces were fixed throughout the differentiation protocol and the expression of the hepatocyte marker albumin was analysed by immunofluorescence. Results show the percentage yield of HLCs expressing albumin on either surface. While the percentage of cells staining positive for albumin decreased at late stages of the differentiation on matrigel surface, on PU134 surfaces the percentage of positive cells remained constant for most of the differentiation process with a 2-fold increase at Day 20 post-replating (86%) compared with cells maintained on matrigel surfaces (43%). The corresponding IgG isotype controls demonstrated the specificity of the staining. For each condition five random fields of view, containing at least 500 cells, were counted. Images were taken at 20x magnification and the scales bar represents 100 µm. Abbreviations: ALB-Albumin, IgG-Immunoglobulin G.

The immunofluorescence observations were further confirmed by Western Blot (Figure 42). On matrigel surface (Figure 42A) the peak in the albumin expression was reached at Day 15 post-replating, followed to a reduction by Day 20 and Day 25 post-replating. However, in HLCs replated on PU134 surfaces (Figure 42B) there was a stabilisation in the expression of albumin up to Day 25 post-replating.

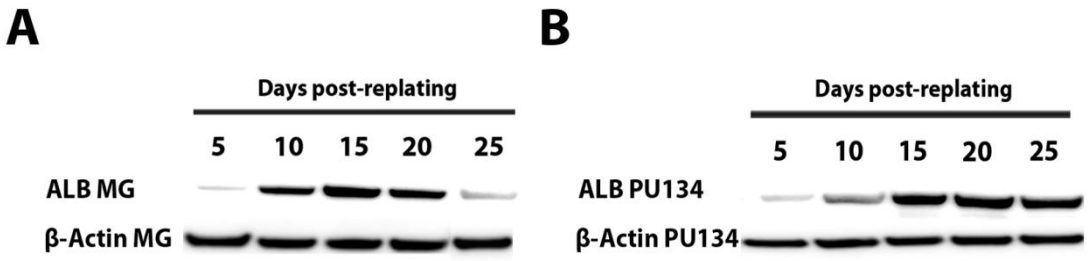

Figure 42. Assessing albumin expression by Western blotting. Cell extracts were collected throughout the differentiation protocol and probed with albumin antibody using standard western blotting. Panel A displays HLCs maintained on matrigel surfaces and panel B displays HLCs maintained on PU134 surfaces. As previously observed by immunofluorescence, there was a decrease in the expression of albumin on matrigel surfaces as the differentiation progressed, while the expression was maintained constant throughout the differentiation process on PU134 surfaces. β-actin was used as a loading control. Abbreviations: ALB-Albumin.

The expression of the foetal hepatocyte marker alpha-fetoprotein (AFP) was investigated by immunofluorescence (Figure 43). Results showed that on either substrate, by Day 5 post-replating, 72% of the cells stained positive for this protein. The percentage yield of HLCs further increased to 83% at Day 10 post-replating on matrigel surfaces while it began to decrease on PU134 surfaces (69%). As the differentiation progressed, there was a decrease in the percentage of cells staining positive, in a steadier manner on PU134 surfaces as 47%, 22% and 9% of the cells stained positive at Day 15, 20 and 25 post-replating respectively, while on matrigel surfaces, the percentage of cells expressing alpha-fetoprotein was reduced to 32%, 15% and 5% respectively

.

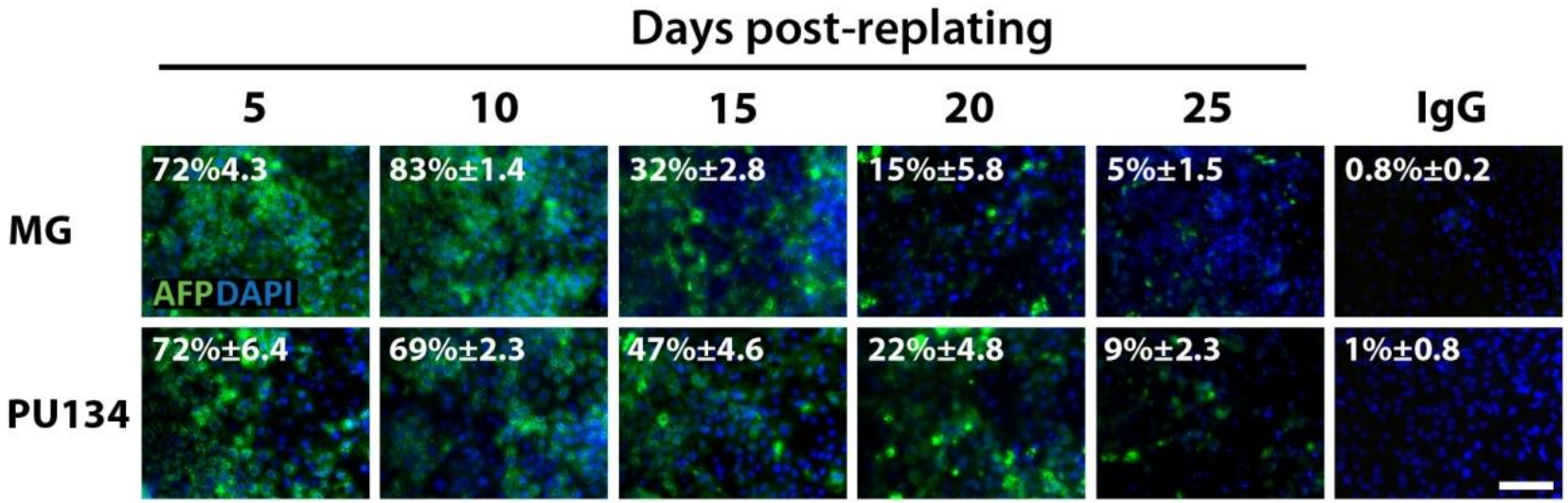

Figure 43. Analysing α-fetoprotein expression. The expression of the foetal hepatocyte marker alpha-fetoprotein in HLCs maintained on matrigel (MG) or PU134 surfaces was investigated by immunofluorescence. Results showed that each condition generated similar levels of HLCs expressing alpha-fetoprotein, and the presence of this protein decreased as the differentiation progressed. The corresponding IgG isotype controls demonstrated the specificity of the staining. For each condition five random fields of view, containing at least 500 cells, were counted. Images were taken at 20x magnification and the scales bar represents 100 µm. Abbreviations: AFP-Alpha-fetoprotein, IgG-Immunoglobulin G.

In addition to analysing the expression of these hepatocyte markers, the expression of the hepatocyte specific cytochrome P450s, CYP3A and CYP2D6 in HLCs replated on matrigel or PU134 surfaces were investigated in at different times during the cell differentiation by immunofluorescence.

Analysis of the percentage yield of cells expressing CYP3A (Figure 44) revealed that as the differentiation progressed, the percentage of HLCs replated on matrigel surfaces expressing CYP3A decreased. The initial 85% of the cells expressing CYP3A at Day 5 post-replating, decreased to 80%, 68% and 44% by Day 10, 15 and 20 post-replating, respectively. However, in cells maintained on PU134 surfaces, at Day 5 post-replating 65% of the cells stained positive. This percentage rapidly increased and by Day 10 post-replating 86% of the cells expressed the protein. The expression was maintained up to Day 20 post-replating, when 88% of the cells stained positive (2-fold increase compared with matrigel surfaces). By Day 25 post-replating, the expression of the protein dramatically decreased on matrigel surfaces, as 9% of the cells stained positive in contrast to 45% of the cells still expressing CYP3A on PU134 surfaces.

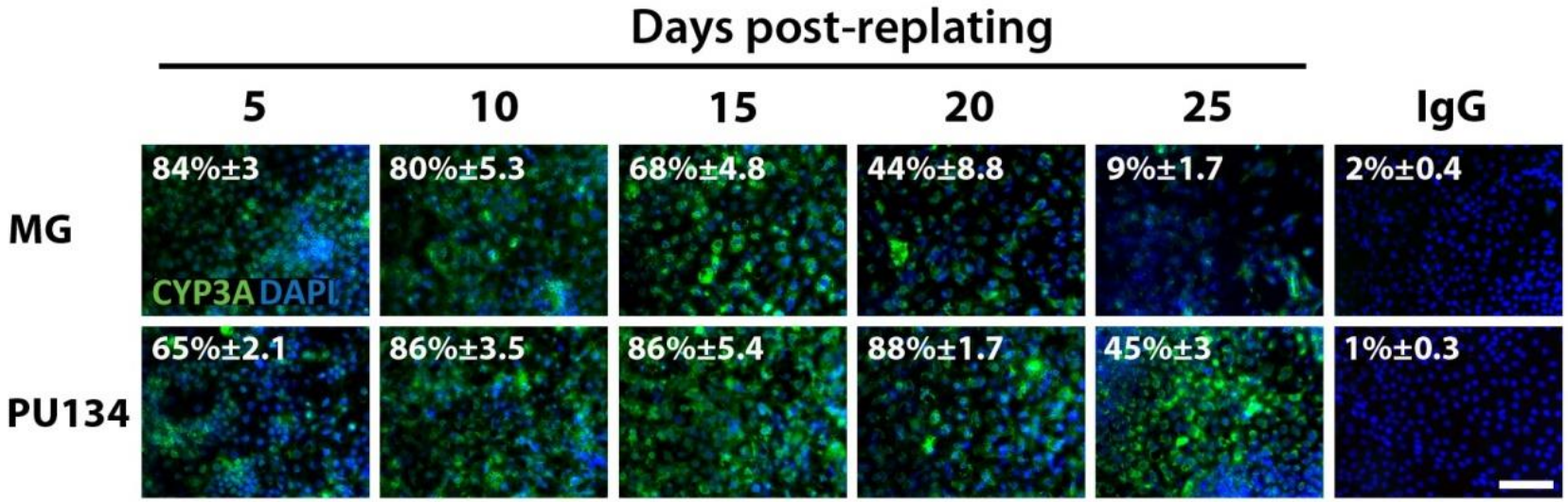

Figure 44. Monitoring the expression of CYP3A. Immunofluorescence was used to study the percentage yield of HLCs expressing the functional hepatocyte marker CYP3A throughout the differentiation protocol on either surface. While CYP3A expression in HLCs maintained on matrigel surfaces was gradually lost as the differentiation progressed, disappearing after Day 20 post-replating; in HLCs maintained on PU134 surfaces there was a stabilisation in the expression as its presence remained constant throughout the differentiation process, with a 2-fold increase in the percentage of cells expressing CYP3A by Day 20 post-replating compared with matrigel coated surfaces. The corresponding IgG isotype controls demonstrated the specificity of the staining. For each condition five random fields of view, containing at least 500 cells, were counted. Images were taken at 20x magnification and the scales bar represents 100 µm. Abbreviations: CYP3A-Cytochrome P450 3A, IgG-Immunoglobulin G.

The pattern of the expression was similar for CYP2D6 (Figure 45). From an initial 67% and 60% of the cells expressing CYP2D6 at Day 5 post-replating on matrigel and PU134 surfaces respectively, the percentage increased, reaching a peak of 96% and 94% by Day 10 post-replating, respectively. The expression stabilised by Day 15 post-replating before a further decrease at Day 20 post-replating when 82% and 85% of the cells replated on matrigel or PU134 surfaces respectively stained positive. However, by Day 25 post-replating only 16% of HLCs replated on matrigel surfaces still expressed the protein in contrast to 55% of the cells on PU134 surfaces.

The analysis in the expression of hepatocyte markers indicated that, in line with the reduced dedifferentiation process observed, PU134 surfaces promote the stabilisation of hepatocyte markers, including functional markers in HLCs.

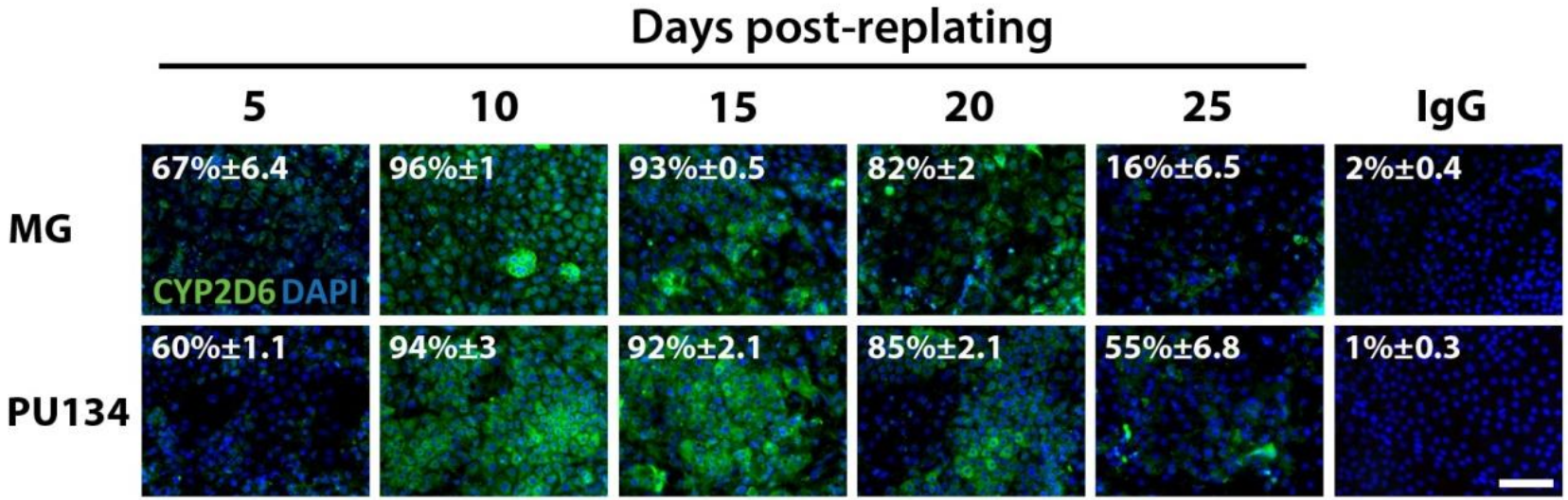

Figure 45. Analysis of CYP2D6. The expression of the functional hepatocyte marker CYP2D6 in HLCs throughout the differentiation protocol on either substrate was analysed by immunofluorescence. Results showed that each condition generated similar levels of HLCs expressing CYP2D6, and the presence of this protein dramatically decreased on matrigel surfaces by Day 25 post-replating (16%), while more than half of the cells maintained on PU134 surfaces still expressed CYP2D6 (55%). The corresponding IgG isotype controls demonstrated the specificity of the staining. For each condition five random fields of view, containing at least 500 cells, were counted. Images were taken at 20x magnification and the scales bar represents 100 µm. Abbreviations: CYP2D6-Cytochrome P450 2D6, IgG-Immunoglobulin G.

4.2.4.5 Analysis of cell proliferation in HLCs on PU134 and matrigel surfaces

To define the cell proliferation in the cultures, I studied the expression of Ki67, a robust proliferative marker in cell biology (Scholzen *et al* 2000). Protein expression was examined by immunofluorescence (Figure 46). Analysis of the percentage yield of HLCs expressing Ki67 revealed that at Day 5 post-replating 40% and 28% of cells stained positive on matrigel and PU134 surfaces respectively. Independent of the substrate, there was a 2-fold decrease by Day 10 post-replating, followed by further ≈2-fold decrease (6%) on PU134 surfaces, while the yield percentage remained still on matrigel surfaces. By Day 20 post-replating, 5% and 6% of the HLC on matrigel and PU134 surfaces respectively still expressed the proliferative marker. Cell proliferation was not detected by Day 25 post-replating.

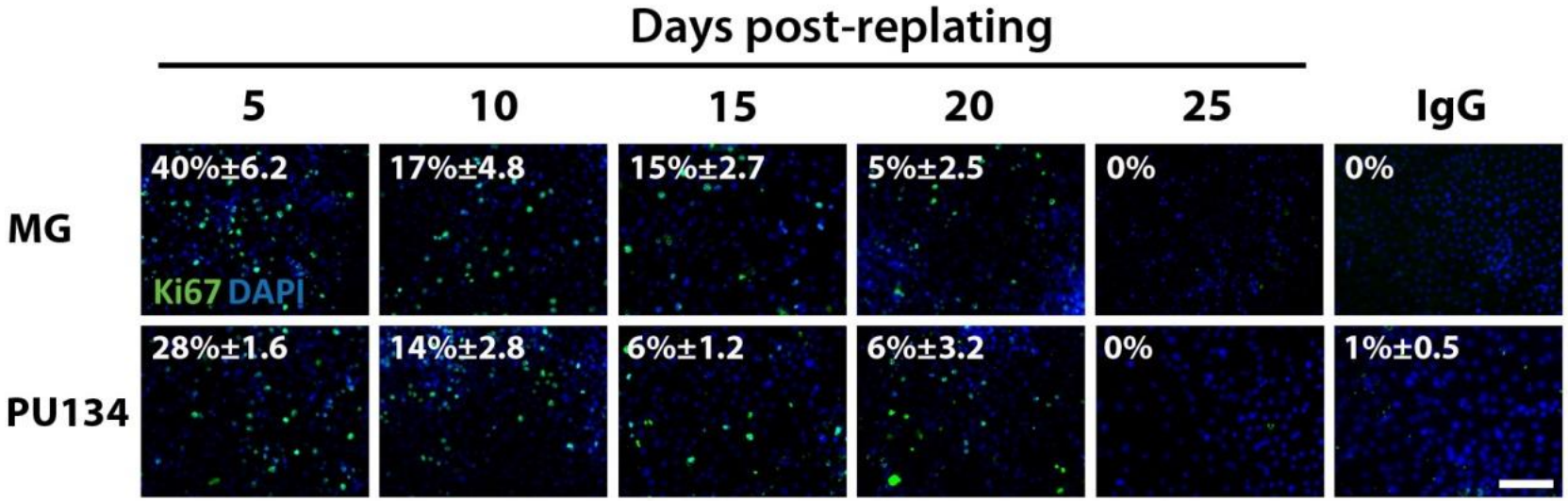

Figure 46. Analysis of cell proliferation. The expression of the proliferative marker Ki67 in HLCs maintained on either substrate was analysed by immunofluorescence. Results showed that on PU134 surfaces the percentage of cells expressing Ki67 dramatically reduced at early stages on the differentiation process when compared with matrigel surfaces (28% by Day 5 post-replating on PU134 surfaces *vs* 40% on matrigel surfaces). At late stages in the differentiation process, there were not significant differences in the percentage yield of HLCs expressing Ki67 on either substrate. The corresponding IgG isotype controls demonstrated the specificity of the staining. For each condition five random fields of view, containing at least 500 cells, were counted. Images were taken at 20x magnification and the scales bar represents 100 µm. Abbreviations: IgG-Immunoglobulin G.

4.2.4.6 Characterization of the polarisation markers in HLCs on PU134 and matrigel surfaces

The maintenance of the epithelial hepatocyte phenotype and function requires a correct cell-to-cell contact (Treyer *et al*, 2013). Previous observations by immunofluorescence indicated that PU134 surfaces stabilised the expression of the hepatocyte phenotype, suggesting the maintenance of cell-to-cell contacts. Therefore, I aimed to explore the expression of different proteins involved in the maintenance of the epithelial phenotype.

The expression of the epithelial marker E-Cadherin at different times in the differentiation approach in HLCs replated on either surface was studied by immunofluorescence (Figure 47). Analysis of the percentage yield of cells staining positive for E-Cadherin revealed that on matrigel surfaces, the expression decreased as the differentiation progressed. At Day 5 post-replating 77% of the cells stained positive for the epithelial marker; and the percentage decreased to 67%, 61% and 46% at Day 10, 15 and 20 post-replating, respectively. Residual expression was observed at Day 25 post-replating. However, on PU134 surfaces, the expression of the protein was maintained through the differentiation. At Day 5 post-replating 84% of HLCs expressed the protein. This percentage was maintained at Day 10 and 15 post-replating when 82% and 84% of the cells stained positive. By Day 20 post-replating 71% of the cells still expressed E-Cadherin, which was maintained at Day 25 post-replating as it was still presented in 68% of the cells.

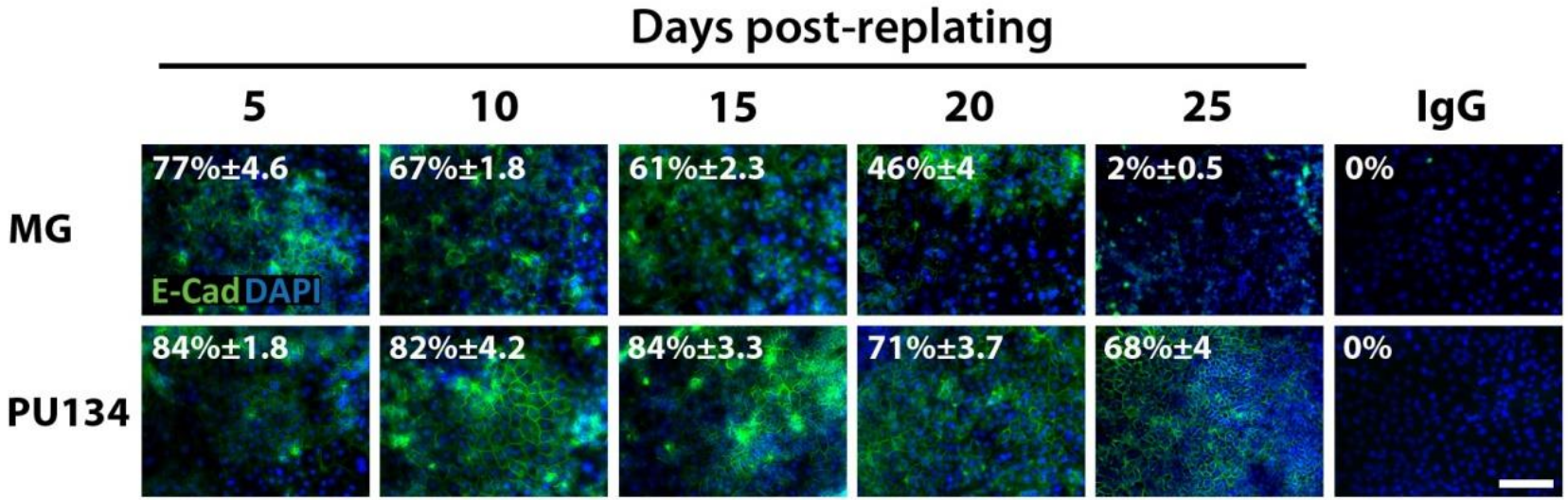

Figure 47. Immunofluorescence analysis of E-Cadherin. Cells maintained on matrigel (MG) or PU134 surfaces were fixed throughout the differentiation protocol and the expression of the epithelial marker E-Cadherin was analysed by immunofluorescence. Results showed the percentage yield of HLCs expressing E-Cadherin on either substrate. The expression of E-Cadherin was gradually lost in HLCs maintained on matrigel surfaces as the differentiation progressed and by Day 20 post-replating, 46% of the cells still stained positive for E-Cadherin. On PU134 surfaces there was a stabilisation in the E-Cadherin expression with 71% of the cells staining positive by Day 20 post-replating. The corresponding IgG isotype controls demonstrated the specificity of the staining. For each condition five random fields of view, containing at least 500 cells, were counted. Images were taken at 20x magnification and the scales bar represents 100 µm. Abbreviations: E-Cad-E-Cadherin, IgG-Immunoglobulin G.

In addition to analysing the epithelial marker E-Cadherin, I studied by immunofluorescence the expression of zonula occudens-1 (ZO-1), a key component of the tight junctions protein complexes involved in establishing cell-to-cell interactions. Analysis in the expression of ZO-1 (Figure 48) revealed that, independently of the substrate, the majority of HLCs expressed the protein up to Day 20 post-replating, as 88% and 92% of the cells replated on matrigel or PU134 surfaces, respectively stained positive for the marker. The values for the percentage yield of cells replated on matrigel surfaces expressing ZO-1 at Day 5, 10 and 15 post-replating were as follows: 96%, 88% and 87%, respectively; and on PU134 surface were 99%, 93% and 85%, respectively. However, no expression was detected on cells replated on matrigel surface at Day 25 post-replating. On the contrary, 77% of the cells maintained on PU134 surface still expressed the protein, suggesting that ZO-1 stability was improved in the presence of PU134 surface.

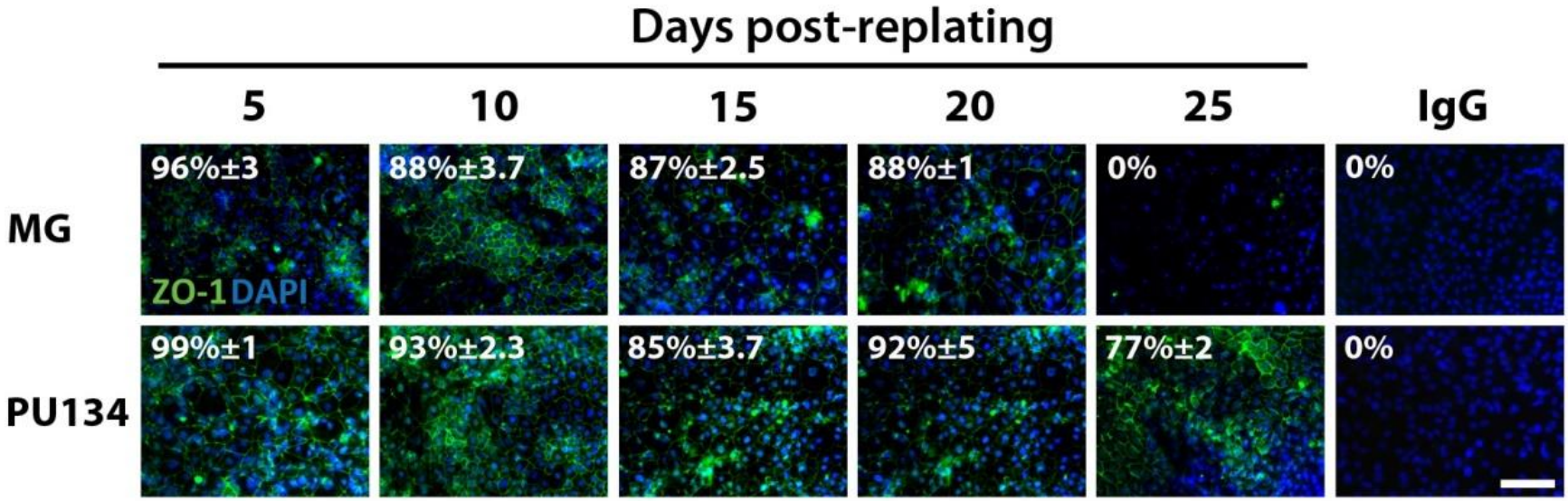

Figure 48. Analysing the expression of zonula occludens-1. HLCs maintained on matrigel (MG) or PU134 surfaces were fixed throughout the differentiation protocol and the expression of the tight junction protein zonula occludens-1 (ZO-1) was analysed by immunofluorescence. Results showed that either condition generated similar levels of HLCs expressing ZO-1. The presence of this protein disappeared in HLCs maintained on matrigel surfaces by Day 25 post-replating, while in HLCs on PU134 surfaces the expression remained high, supporting the stabilisation of the epithelial phenotype on the cells induced by PU134. The corresponding IgG isotype controls demonstrated the specificity of the staining. For each condition five random fields of view, containing at least 500 cells, were counted. Images were taken at 20x magnification and the scales bar represents 100 µm. Abbreviations: ZO-1- Zona Ocludens-1, IgG-Immunoglobulin G**.**

All together, these observations suggest that PU134 surfaces promote the maintenance of an epithelial phenotype and the establishment of cell-to-cell contact required for the maintenance of cell polarity in a better manner than matrigel surfaces.

4.2.4.7 Functional characterisation of HLCs on PU134 and matrigel surfaces

To observe the functional consequences of the promotion and stabilisation of the hepatocyte phenotype induced by PU134 surfaces, I measured the metabolic and synthetic capabilities of HLC on PU134 surfaces and compared them with HLCs on matrigel surfaces.

Measuring cytochrome P450 activity in HLCs on PU134 and matrigel surfaces

Cytochrome P450 activity CYP3A and CYP1A2 in HLCs replated on matrigel or PU134 surfaces was measured at Day 10, 15 and 20 post-replating (Figure 49). HLCs displayed comparable levels of CYP3A activity at Day 10 post-replating on either surface (Figure 49A). However, we observed a 6-fold increase at Day 15 post-replating in HLCs replated on PU134 surfaces compared with matrigel surfaces ($p>0.05$). A further 3-fold increase in the activity of HLCs on PU134 surfaces was observed at Day 20 post-replating, with a 30-fold increase comparing with cells replated on matrigel surfaces ($p<0.001$). The values for CYP3A at Day 10, 15 and 20 post-replating in HLCs replated on matrigel or PU134 surfaces are as follows; $4{,}69 \times 10^5$ RLU/ml/mg, $3{,}55 \times 10^5$ RLU/ml/mg, $7{,}28 \times 10^5$ RLU/ml/mg, $4{,}34 \times 10^6$ RLU/ml/mg, $4{,}44 \times 10^5$ RLU/ml/mg and $13{,}59 \times 10^6$ RLU/ml/mg, respectively.

CYP1A2 activity showed a similar trend to CYP3A (Figure 49B). No significant differences in the activity of the cells on either surface at Day10 post-replating were observed. By Day 15 post-replating, there was a 9-fold increase in the activity on PU134 surfaces compared with matrigel surfaces ($p<0.001$) and 24-fold increase when compared with PU134 surfaces at the previous time point. CYP1A2 activity stabilised on cells replated on PU134 surfaces at Day 20 post-replating (0.91 fold

difference, p>0.05), but only displaying a ≈2.2-fold increase when compared with cells maintained on matrigel surfaces at the same time in the differentiation approach (p<0.05). The values for CYP1A2 at Day 10, 15 and 20 post-replating in HLCs replated on matrigel or PU134 surfaces are as follows; 5,38x10^{4}RLU/ml/mg, 6,18x10^4 RLU/ml/mg, 1,65x10^5 RLU/ml/mg, 1,5 x10^6 RLU/ml/mg, 6,24x10^5 RLU/ml/mg and 1,37x10^6 RLU/ml/mg, respectively.

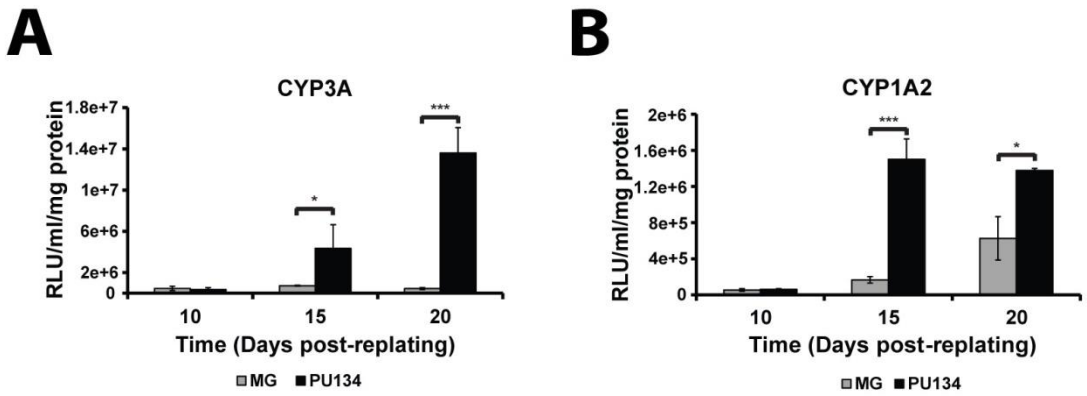

Figure 49. HLCs on PU134 surfaces displayed superior cytochrome P450 activity. Cytochrome P450 function 3A (A) and 1A2 (B) were assessed using a commercially available system (pGLO®) in HLCs maintained on either substrate at Day 10, 15 and 20 post-replating. Analysis of the function revealed similar CYP3A and CYP1A2 activity by Day 10 post-replating independently of the substrate used. As the differentiation progressed, a greater increase in CYP3A and CYP1A2 activity were observed when PU134 was used as culture substrate, reaching a peak in the activity by Day 20 post-replating, with a 30-fold and 2-fold increase in CYP3A and in CYP1A2 activity respectively compared with matrigel surfaces (MG), which displayed their peak in the activity by Day 15 post-replating. The results represent the mean ± SD of four individual samples per time point per cytochrome p450 analysed. Levels of significance were measured by student's t-test where p>0.05 is denoted as * and p>0.001 is denoted as ***.

Albumin secretion in HLCs on PU134 and matrigel surfaces

Albumin protein production and secretion is a critical function of the liver. I investigated the secretion of albumin using ELISA in HLCs replated on matrigel or PU134 surfaces at Day 10, 15 and 20 post-replating. Figure 50 demonstrates the production of albumin in HLCs on both substrates. At Day 10 post-replating, consistent with the measure of the basal CYP activity, there were no differences in the production of albumin (p>0.05). By Day 15 post-replating, a 2 fold increase in the albumin production on PU134 surfaces compared with matrigel surfaces was

observed (p>0.05); and by Day 20 post-replating, the difference in the production of albumin increased to 3.2-fold (p<0.001). The levels of albumin production were maintained constant on PU134 surfaces between Day 15 and Day 20 post-replating (p>0.05). The values of albumin produced at Day 10, 15 and 20 post-replating on matrigel or PU134 surfaces are as follows; 0.539 µg/ml/24hours/mg, 0.858 µg/ml/24hours/mg, 2.038 µg/ml/24hours/mg, 1.021 µg/ml/24hours/mg, 0.955 µg/ml/24hours/mg and 3.037 µg/ml/24hours/mg, respectively.

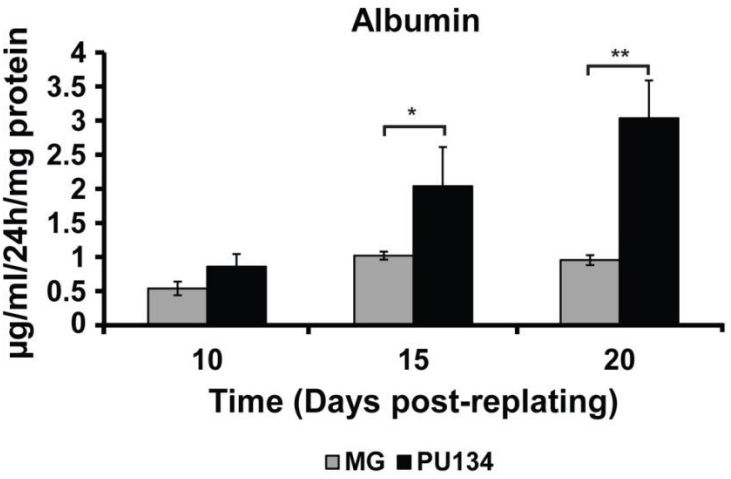

Figure 50. Improvement in the albumin protein secretion on PU134 surfaces. The graph displayed shows the level of albumin secreted by HLCs maintained on matrigel (MG) or PU134 surfaces (PU134) at Day 10, 15 and 20 post-replating. Results revealed a 2-fold increase by Day 20 post-replating in the secretion of albumin on PU134 surfaces compared with matrigel surfaces. The results represent the mean ± SD of three individual samples per time point. Levels of significance were measured by student's t-test where p>0.05 is denoted as * and p>0.01 is denoted as **.

Drug induction of HLCs on PU134 and matrigel surfaces

Basal cytochrome P450 activity provides important background information about the functionality of the cells. However, the capacity of drugs inducing the cytochrome activity represents a hallmark of mature hepatocytes. For this purpose 48 hours prior to the assessment of the P450 activity, HLCs replated on either substrate were cultures on the presence of different drugs, including phenobarbital and rifampicin combined with dexamethasone. Induction of cytochrome P450

activity was compared with the appropriated vehicle control for each of the conditions, PBS for phenobarbital and DMSO/H_2O for rifampicin/dexamethasone.

Cytochrome P450 activity induction with 10 µM of rifampicin combined with 2 µM of dexamethasone was analysed at Day 20 post-replating (Figure 51). Analysis of the function revealed no CYP3A activity induction in HLCs replated on matrigel surfaces. However, on PU134 surfaces, CYP3A activity displayed a 1.8-fold increase compared with the vehicle control upon incubation with rifampicin and dexamethasone ($p<0.05$). The values for CYP3A in HLCs replated on matrigel or PU134 surfaces induced with 10 µM of rifampicin and 2 µM of dexamethasone are as follows; $9{,}9x10^4$ RLU/ml/mg and $6{,}35x10^5$ RLU/ml/mg, respectively.

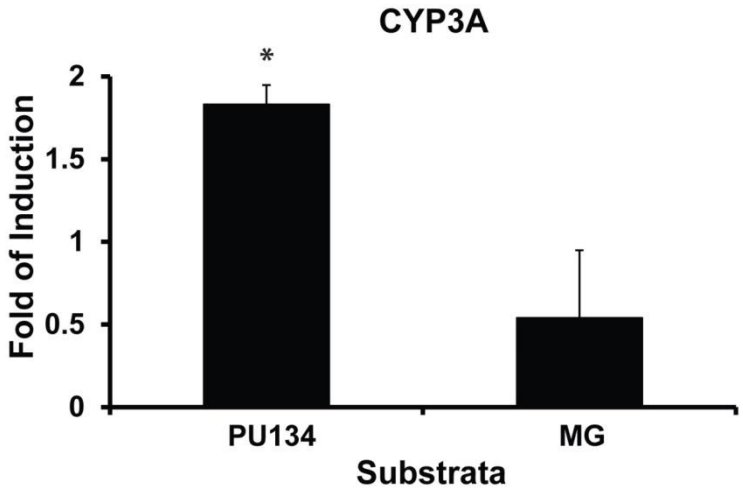

Figure 51. CYP3A induction by rifampicin and dexamethasone. Cytochrome P450 3A activity was induced in HLCs at Day 20 post-replating using 10 µM of rifampicin and 2µM of dexamethasone for 48 hours, changing the medium and the drug inducers on a daily basis. CYP3A activity was measured using a commercially available system (pGLO®). Analysis of the function revealed that HLCs maintained on matrigel surfaces (MG) were not susceptible to drug induction. CYP3A activity showed a 1.8-fold increase on PU134 surfaces (PU134) in the presence of 10 µM of rifampicin and 2µM of dexamethasone compared to the appropriate vehicle control. The results represent the mean ± SD of three individual samples per time point. Levels of significance were measured by student's t-test where $p>0.05$ is denoted as * in comparison to HLCs supplemented with the vehicle control. Abbreviations: Rif-rifampicin, Dex-dexamethasone.

Cytochrome activity inductor phenobarbital was used at 1 mM, and CYP3A and 1A2 activity were measured at Day 20 post-replating. Analysis of CYP3A activity (Figure 52A) revealed that CYP3A activity in HLCs replated on matrigel surfaces was not

susceptible, while on PU134 surfaces, HLCs displayed a 1.6-fold increase in CYP3A activity compared to the vehicle control ($p<0.05$). Similar trend was observed when CYP1A2 activity was analysed (Figure 52B), with no cytochrome activity induction observed in HLCs replated on matrigel surfaces. However, CYP1A2 activity in HLCs replated on PU134 surfaces displayed a 2.3-fold increase to the phenobarbital concentration employed compared to the vehicle control ($p<0.05$). The values for CYP3A in HLCs replated on matrigel or PU134 surfaces induced with 1 mM of phenobarbital are as follows; $1{,}85 \times 10^5$ RLU/ml/mg and $8{,}49 \times 10^5$ RLU/ml/mg, respectively; and the values for CYP1A2 on matrigel or PU134 surfaces induced with 1 mM of phenobarbital are as follows; $3{,}1 \times 10^4$ RLU/ml/mg and $1{,}44 \times 10^5$ RLU/ml/mg, respectively.

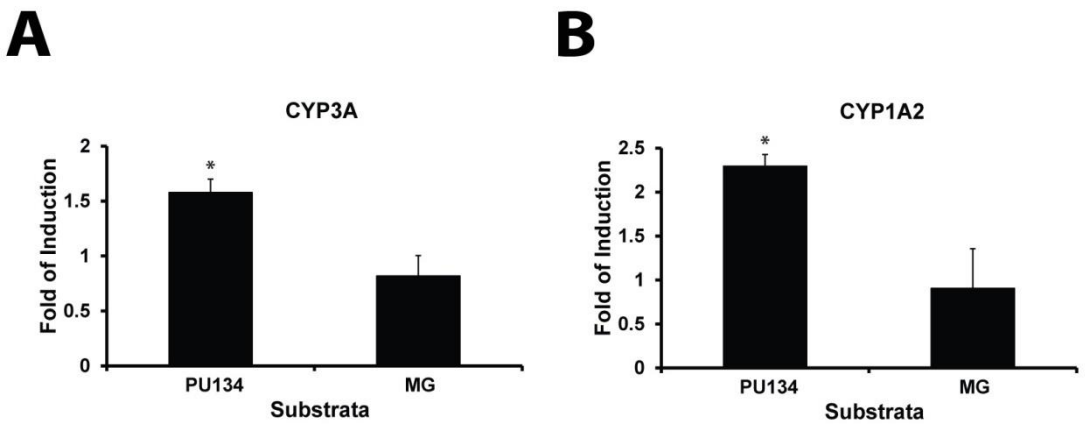

Figure 52. Cytochrome P450 3A4 and 1A2 induction by phenobarbital. Cytochrome P450 3A and 1A2 activity were induced in HLCs at Day 20 post-replating using 1 mM of phenobarbital, changing the medium and the drug inducers on a daily basis. CYP3A (A) and CYP1A2 activity (B) were measured using a commercially available system (pGLO®). Analysis of the function revealed that HLCs maintained on matrigel surfaces (MG) were not susceptible to drug induction to phenobarbital. In HLCs maintained on PU134 surfaces (PU134), there were a 1.5-and 2.3-fold increase in CYP3A and CYP1A2 activity respectively when 1mM of phenobarbital was used compared with the appropriate vehicle control. The results represent the mean ± SD of three individual samples per time point. Levels of significance were measured by student's t-test where $p>0.05$ is denoted as * in comparison to HLCs supplemented with the vehicle control. Abbreviations: PhB-Phenobarbital.

Measuring cell toxicity in response to pharmaceutical grade compounds

To further characterise HLCs on PU134 or matrigel surfaces I investigated whether the cells were able to process pharmaceutical grade compounds to toxic endpoints. For this purpose I used two compounds, BMS-827278 and BMS-835981, both metabolised by CYP2D6. HLCs replated on either substrate were incubated with the compounds for 72 hours prior to the assessment of cell viability, measured at Day 20 post-replating. Cell viability was compared with the vehicle control, DMSO.

Analysis of the cells viability (Figure 53) showed that HLCs were sensitive to BMS-835981 on either substrate as HLCs viability decreased to 2% and 1.5% on matrigel or PU134 surfaces respectively. The compound BMS-827278 also induced toxicity in HLCs, but it was greater in HLCs replated on PU134 surfaces. On PU134 surfaces, cell viability decreased ≈5-fold (Figure 53B) in response to this compound, compared with cells replated on matrigel surface, which viability was reduced 0.7-fold (Figure 53A).

Analysis of the functional data reveals a stable and greater metabolic function in HLCs in the presence of PU134 surfaces. Moreover, HLCs on PU134 surfaces display drug inducible CYP activity and toxicity to pharmacological compounds, indicating the possession of more intact drug metabolism in the presence of the defined substrate PU134.

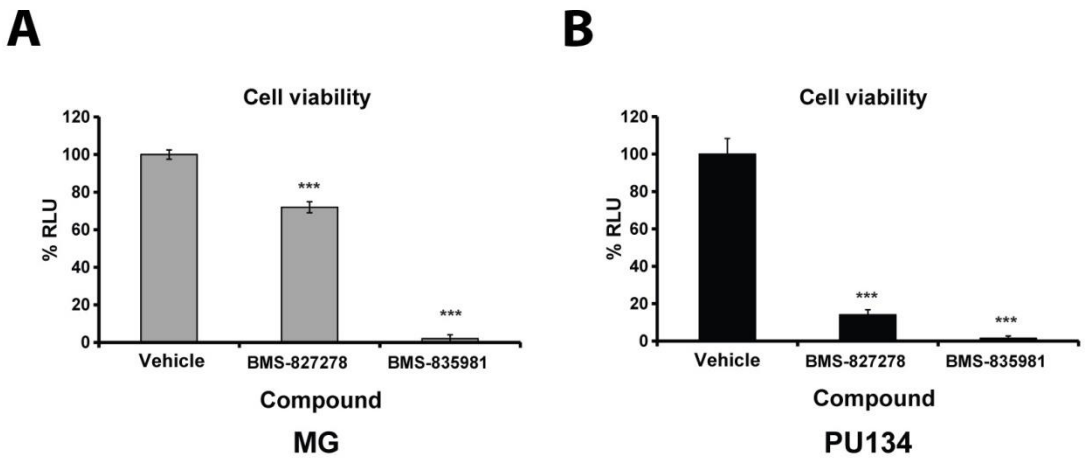

Figure 53. Cell viability in response to pharmaceutical grade compounds. Functional metabolism of HLCs maintained on matrigel (A) or PU134 surfaces (B) at Day 20 post-replating was established by incubation with compunds which requiered CYP metabolic activation and toxic intermediate formation. HLCs were cultured for 72 hours with 50 µM of BMS-827278 or BMS-835981. Control cultures did not receive the BMS compunds but had their medium supplemented with the appropriated vehicle, DMSO. Cell viability was assessed using a commercially available system (pGLO®). Results showed a significant reduction in cell viability compared with the appropriate vehicle control, to both compounds on the HLCs independently of the culture substratum used, but more pronounced for BMS-827278 when PU134 was used as a substrate. The results represent the mean ± SD of six individual samples per time point. Levels of significance were measured by student's t-test where $p>0.001$ is denoted as *** in comparison to HLCs supplemented with the vehicle control.

4.3 Discussion

Most of the current methods to generate hepatocytes from stem cells rely on the use of undefined matrices of animal origin. These substrates can be costly and highly variable, affecting cell function and stability, representing a significant barrier to applications. Handling of existing biological matrices, commonly used in culturing and differentiating stem cells such as matrigel or more defined biological matrices including the recombinant proteins vitronectin (Braam *et al*., 2008) and laminin 521(Rodin *et al*., 2014), is effective for short term maintenance, but not for long term enough to promote the maturation of HLCs. Therefore, the development of defined cell based systems is required if the true potential of stem cells derived HLCs is to be realised. Such systems should be simple to use, scalable and highly defined, and capable of delivering cells with predictable and reliable performance.

In an effort to reduce the dependency on biological derived matrices, different approaches have relied on the use of polymers, a type of biomaterials with chemical and physical properties that make them ideal candidates for medical and biological applications. Combinatorial strategies involving biological derived substrates with synthetic and defined polymers have been used in the maintenance and differentiation of pluripotent stem cells including laminin (Gao *et al*., 2010),

vitronectin (Mei *et al*., 2010) and collagen (Du *et al*., 2014; Ng *et al*., 2005). While these matrices have shown certain success in supporting hepatocyte differentiation of hPSCs still, the presence of undefined components and/or the variable composition contribute to variable cell performance, resulting in models of short duration, which makes difficult to unravel the complexity behind hepatocyte differentiation and dedifferentiation.

In an attempt to overcome the limitations associated to the use of undefined cell culture substrates, interdisciplinary collaborations between chemistry and biology have identified synthetic substrates with defined composition and reliable performance. Synthetic substrates are scalable, cost effective, and can be manufactured into complex three dimensional structures, mimicking the *in vivo* environment. Due to these properties synthetic substrates have been widely used to support and drive differentiation of many cell types (Cameron *et al*., 2013; Li *et al*., 2011; Pernagallo *et al*., 2008).

Traditional approaches in the screening, identification and testing of new polymers have relied on slow and low throughput approaches, limiting the discovery of novel synthetic substrates compatible with biological systems. However, in recent years automated and parallel screening systems for polymers have grown enormously. High throughput approaches (HTP) such as microarraying has allowed the screening of chemical diverse polymers, representing a valuable tool for both, novel material discovery and the identification of correlation performance and structure (Hook *et al*., 2010; Meier and Hoogenboom, 2004).

These HTP approaches allow the synthesis and testing of multiple combinations of polymers in short period of time (Zhang *et al*., 2009), facilitating the identification of compatible substrates with multiple applications including bone and cartilage regeneration (Khan *et al*., 2010; Tare *et al*., 2009), endothelial vascularisation (Pernagallo *et al*., 2012) and culture of pancreatic islet cells (Mei *et al*., 2010). Hay and colleagues employed this microarray technology to perform an unbiased screening of a polymer library to identified polymers that supported and enhanced

hepatocyte differentiation of PSCs. From this screening they identified a a simple polyurethane, PU134, formed by polymerizing PHNGAD, MDI and an chain extender, that in combination with a robust hepatocyte differentiation approach, stabilized hepatocyte phenotype and improved cell function when compared with matrigel (Hay *et al*., 2011).

The possession of an optimized polymer coating surface that promotes hepatocyte function is essential if the true potential of stem cells derived HLCs is to be realized. For this purpose, I significantly altered the coating conditions, topography and sterilization process to access effects on polymer performance in stabilising hepatocyte function and lifespan (Lucendo-Villarin *et al*., 2014). From this optimisation process I observed that the topography of the coated surface is highly dependent on the nature of the solvent employed, which had direct implications in the function of the cells (Biggs *et al*., 2008; Dang and Leong, 2007; Engler *et al*., 2006; Hamilton and Brunette, 2007; Lim and Donahue, 2007; Teixeira *et al*., 2003). Previously, Sharma and colleagues showed that hepatocyte biology is affected by the roughness of the culture substrate, with improved cell spreading in rough surfaces when compared with smooth surfaces. However, no significant differences were found on the function of the cells between surfaces displaying different roughness (Sharma *et al*., 2009). In this study I have shown an improvement in the cell function when a smooth surface of polymer PU134 is employed. Physical parameters of the solvent such as the solubility rate, diffusion rate, boiling temperature and density can influence the topography of the polymer coated which may partly explain the improved polymer surface observed. Whether it is a specific characteristic of PU134 or it is share between polyurethanes has still to be resolved. In addition to analyze the influence of the polymer surface topography in the cell function, the polymer surface optimization procedure revealed that cell performance is influenced by the sterilization procedure employed. This may be due to the presence of sensitive area(s) within the structure of the polymer to different sterilization procedures (Azevedo *et al*., 2013; Rosu *et al*., 2005; Yang *et al*., 2002). Still, despite the improved cell performance observed in the optimized polymer

surfaces, cells displayed a limited life span which was not observed on matrigel surfaces. This could be due to the cell attachment supporting factors and cytokines presented on matrigel that are absented on the polymer surface. This limited life span was resolved by supplementing the maturation media with Knock-Out Serum Replacement, KOSR, a defined good manufactured practices (GMP) grade serum-free formulation that is more stable and consistent in quality than foetal bovine serum (Tekkatte *et al*., 2011).

The resulting population of HLCs obtained in the optimised polymer surfaces in the supplemented maturation media displayed improved life span and hepatocyte morphological features, such as canaliculi-like structures and binucleate cells. Moreover, polymer surfaces prevented the dedifferentiation of the cells observed on matrigel surfaces as denoted by a delay in the expression of the mesenchymal marker vimentin (Godoy *et al*., 2010), accompanied by a stabilisation in the expression of the hepatocyte marker HNF4α. Moreover, the maintenance in the expression of hepatocyte markers including albumin, HNF4α and cytochrome P450 3A and 2D6 in the presence of polymer surfaces further supported the anti-dedifferentiation effect of the polymer surfaces. In parallel, the reduced expression of the foetal hepatocyte marker alpha-fetoprotein and the cell proliferative marker Ki67 observed on polymer surfaces suggest the possession of a more mature hepatocyte phenotype than their matrigel counterparts.

These observations were supported by analysing hepatocyte functions including cytochrome P450 activity and albumin secretion. The improved differentiation status of HLCs generated under defined conditions was further confirmed by their response to inducers of cytochrome P450 activities and to compounds which measure hepatocyte metabolic capacity. Cytochrome P450 3A and 1A2 activity in HLCs maintained on polymer surfaces responded to different drug inducers, a hallmark of a mature hepatocyte. Consistently with previous observations (Medine *et al*., 2013), I observed that HLCs replated on polymer surfaces displayed consistent performance in response two compounds, BMS-827278 and BMS-

835981, which require metabolic activation, via CYP2D6, to hepatic toxic endpoints. Clearly drug metabolism is a key need of any hepatocyte model and this was in contrast to HLCs differentiated using matrigel surfaces which exhibited poorer performance, presumably due to incomplete differentiation of the CYP2D6 metabolic pathway.

The improved hepatocyte phenotype and cell performance observed on the polymer surfaces suggested the maintenance of the cell-to-cell interactions on HLCs. Hepatocytes tightly connect with each other by intercellular protein complexes including tight and adherens junctions (Kojima *et al*., 2003). In hepatocytes, tight junctions are localised to the apical end of the basolateral membrane surrounding the bile canaliculi, playing key roles in the establishment on the epithelial polarityand hepatocyte functions. Tight junctions bind to the cell membrane of adjacent cells via homophilic recognition, sealing paracellular spaces between hepatocytes thus, keeping bile within the bile canaliculi and away from the blood (Anderson *et al*., 2001; Tsukita *et al*., 2001), therefore, enforcing transport of macromolecules across epithelial cells. The cytoplasmic domain of the transmembrane proteins conforming tight junctions such as claudins and occludin (Furuse *et al*., 1998), binds to adaptor proteins such as zona occludent-1 (ZO-1), a member of the membrane associated guanalate kinase that binds to actin filaments, which suggest a role of tight junctions in the organization of the actin cytoskeleton (Tsukita *et al*., 2001).

Adherent junctions represent another protein complex involved in the cell-to-cell contact. Adherent junctions are Ca^{2+} dependent homophilic cell adhesion protein complexes involve in the maintenance of cell-to-cell contact and epithelial polarity in hepatocytes, providing mechanical integrity to tissues (Gumbiner, 1996). They form continuous adhesion belts localised near the apical end of the cells, just below tight junctions. E-Cadherin, a transmembrane protein primarily expressed on epithelial cells, represents the best characterised cadherin member of adherent junctions. The cytoplasmic tail of E-Cadherin is linked to the actin cytoskeleton and

other signalling elements through several peripheral membrane proteins, including catenins, vinculin and α-actinin (Gumbiner, 1996; Takeichi, 1995; Tsukita *et al*., 2001; Yonemura *et al*., 1995) , thus providing a role for E-cadherin in the establishment of hepatocyte polarity.

Therefore, I analysed the expression of key proteins involved in cell-to-cell interactions: zonula occludens-1 and E-Cadherin. The maintenance and stabilisation in the expression of these proteins in HLCs maintained on the polymer surface suggested an improved hepatocyte polarity in the cells, which is essential in the maintenance of hepatocyte function (Müsch, 2013). This could partly explain the improved metabolic function observed in the presence of polymer surface. Additionally, it has been reported that tight junctions play a key role in the in the hepatitis C virus (HCV) entry (Ploss *et al*., 2010), and it has been shown that HLCs obtained on the serum-free differentiation approach employing matrigel surfaces (Szkolnicka *et al*., 2014) efficiently supports HCV entry and replication (Zhou *et al*., 2014). Therefore, the improved cell-to-cell interactions observed in the presence of polymer surfaces suggest that these HLCs would support HCV infection in a better manner than their matrigel counterpart. However, this has to be addressed in the future.

In conclusion, data presented here demonstrate the influence of optimised polymer surfaces possess on the cell function, highlighting the nutritional requirements needed when working with defined media and synthetic substrates. In addition, extensive characterisation of HLCs on the PU134 surface reveals the differentiation properties that the polymer surface possesses in promoting hepatocyte function whilst preserving the phenotype. The mechanism behind this improved cell phenotype and performance induced by PU134 surfaces will be discussed in the next chapter.

CHAPTER FIVE

IDENTIFYING THE MECHANISM OF ACTION OF PU134 AND TRANSLATION OF THE TECHNOLOGY TO CLINICAL GRADE hESC LINES

5.1 Introduction

The liver is a highly organised tissue. Liver cell function requires right structural support and contact with neighbouring cells and extracellular matrix (ECM). The acinus represents the basic functional unit of the liver and it is form by cords of hepatocytes radiating from the central vein and lined by sinusoidal capillaries. While hepatocytes represent the parenchymal cells of the liver, bile duct epithelial cells, liver sinusoidal endothelial cells, hepatic stellate cells and Kupffer cells compose the non-parenchymal fraction. The ECM of the liver is produced by epithelial and stroma cells found within the tissue itself. It is located in the Space of Disee, between the hepatocytes and the liver sinusoidal endothelial cells. The composition of ECM in the liver varies in a gradient manner, paralleled by those of soluble factors; and it consists mostly of fibronectin, proteoglycans and collagens, mainly type I and minor quantities of types III, IV, V, and VI (Bissell *et al*., 1987; 1990; Martinez, 1995). Laminin is mainly found in the niche of the hepatic progenitor cells (Lorenzini *et al*., 2010). Liver development, like any another organ, requires an extensive network of signals from the ECM and nearby mesoderm acting in a time- and/or dose-dependent manner. These factors interact with protein membrane receptors including the integrin family of proteins (Hynes, 1992; Ruoslahti, 1991; Schwartz and Schaller, 1995), activating signalling pathways that drive liver development. The liver microenvironment changes with the development, especially after birth, when the nutritional supplies change from placental to enteral nutrition, activating mature hepatocyte functions (Morelli, 2008).

5.1.1 Extracellular signalling and transcription factors involved in liver development

The liver specifies form the anterior portion of the definitive endoderm. These cells are separated from the surrounding septum transversum mesenchyme by a basement membrane (Medlock and Haar, 1983), and lie adjacent to the nascent heart. Hepatic induction from the endodermal cells requires coordinate signalling of

fibroblast growth factors (FGFs) from the cardiac mesoderm, and bone morphogenetic proteins (BMPs) from the septum transversum mesenchyme (Calmont *et al*., 2006; Jung, 1999; Rossi *et al*., 2001). While FGF signalling activates MAPK and phosphoinositide 3-kinase, PI3K/AKT pathways (Bottcher, 2005; Schlessinger, 2004), which are involved in hepatic specification and hepatic growth respectively (Calmont *et al*., 2006); BMPs binding to serine/threonine kinase receptors (Heldin *et al*., 1997; Shi and Massagué, 2003) activates Smad signalling pathway by inducing the phosphorylation of Smad1, Smad5 and Smad8, which is then able to complex with Smad4 thus, regulating gene transcription in the nucleus.

In response to the inductive cues from the heart and mesenchyme, junctional complexes between the pre-hepatic cells are lost. Cells forming the hepatic endoderm transits from a simple cuboidal to a pseudostratified columnar epithelium forming the liver bud that is composed of hepatoblasts (Bort *et al*., 2006). During this process, the base membrane separating the pre-hepatic cells and the STM, which is rich in laminin, nidogen, collagen IV, fibronectin and sulphate proteoglycans (Shiojiri and Sugiyama, 2004), is progressively disrupted (Baker *et al*., 2007; Zaret, 2002) inducing the delamination and migration of the pre-hepatic cells from the foregut into the surrounding STM, as cords, to form the nascent liver bud (Bort *et al*., 2006; Margagliotti *et al*., 2008; Medlock and Haar, 1983; Shiojiri and Sugiyama, 2004). During this process, the homeodomain protein Hhex plays an important role in the hepatic proliferation and migration into the STM (Bort *et al*., 2006).

These processes of delamination and migration are characterised by modification and remodelling of the surrounding ECM. Transcription factors including Prox1 and Oncecut regulate the expression of extracellular matrix (ECM) proteins and ECM remodelling enzymes such as the matrix metalloproteinase (MMPs) -14, expressed in hepatic progenitors, and MMP-2, expressed predominantly in the surrounding mesenchyme (Margagliotti *et al*., 2007; Medico *et al*., 2001; Papoutsi *et al*., 2007). Cell proliferation and liver bud growth observed during these processes result as a

response to an extensive network of signals, including coordinate paracrine signalling from the surrounding hepatic mesenchyme such as FGF8 and BMP4 (Berg *et al*., 2007; Calmont *et al*., 2006; Jung, 1999; Rossi, 2001; Sekhon *et al*., 2004; Shin *et al*., 2007; Yanai *et al*., 2008), in conjunction with Wnt/β-catenin signalling (Behbahan *et al*., 2011; Monga *et al*., 2003; Tan *et al*., 2008). Hepatocyte growth factor (HGF) is also involved in hepatoblast migration and proliferation (Birchmeier *et al*., 2003; Bladt *et al*., 1995; Block *et al*., 1996; Medico *et al*., 2001; Michalopoulos and Bowen, 1993; Moumen *et al*., 2007; Sachs *et al*., 2000; Schmidt *et al*., 1995), via activation of the small GTPase Arf6 (Suzuki *et al*., 2006) and binding to its tyrosine kinase receptor c-Met, respectively (Iida *et al*., 2003; Ishikawa *et al*., 2001).

Specification of the hepatoblasts into the hepatocyte lineage is a process regulated by an extended network of transcription factors and cytokines, favoured by the presence of a gradient of TGFβ signalling, that is negatively modulated by the transcription factors Onecut-1 (OC-1) and Onecut-2 (OC-2) (Clotman, 2005), that act in coordination with Jagged-Notch signalling pathway in supporting biliary differentiation (McCright *et al*., 2002; Tanimizu, 2004).

Hepatocyte growth and maturation extended beyond birth. During this process, the liver switches its functional role as the main hematopoietic system in the body to a metabolic organ at around birth (Nagao *et al*., 1986; Noda *et al*., 1994). Important factors involved in this hepatocyte maturation include oncostatin M (OSM), glucocorticoid (Kamiya *et al*., 1999) and hepatocyte growth factor (HGF). Stimulation of foetal hepatocytes with glucocorticoids alone revealed that HGF triggers hepatocyte maturation, while OSM enhances the effect of glucocorticoid in promoting cell differentiation towards hepatocyte lineage. Binging of OSM to the oncostatin M receptor complex, OSMR, composed of a OSMR β chain and a common signal transducer gp130, induces the activation of two main signalling pathways: STAT-3 and Ras pathways, which are involved in the expression of hepatocyte differentiation markers induced by OSM (Ito *et al*., 2000) and the formation of adherent junctions (Matsui *et al*., 2002), respectively. On the other

hand, HGF has been proposed to promote hepatocyte specification, proliferation and maturation by stimulating the expression of important transcription factors in the hepatocyte biology including C/EBPα (Suzuki, 2003). TNFα signalling ensures a correct balance between HGF and OSM signalling, allowing the liver to grow to the appropriate size before differentiating (Kamiya and Gonzalez, 2004). In addition, during the postpartum transition from placenta to enteral nutrition, as a result of the gut colonisation by intestinal flora, the neonatal liver is exposed to bacterial-derived secondary metabolites such as lithocholic acid (LCA) and manaquinones (vitamin K_2) (Avior *et al*., 2015), which activates the pregnane X receptor (PXR), a nuclear receptor controlling expression of cytochrome P450 enzymes such as 2C9 and 3A4 (Ichikawa and Horie, 2006; Staudinger *et al*., 2001).

In addition to cytokines, extracellular matrix receptors are also involved in the hepatocyte development. Integrins represent one of the major receptors for components of the extracellular matrix. It has been reported that integrin α3β1 is important for the attachment of hepatocytes to laminins, which are present in both, the early foetal liver (Baloch *et al*., 1992; Couvelard *et al*., 1998) and around the perisinusoidal spaces in the adult liver (Bissell *et al*., 1987; Maher *et al*., 1988). In addition, hepatocyte binding to fibronectin, one of the major components of the ECM in the liver, occurs via α5β1 integrin (Gullberg *et al*., 1990). The importance of cell-to-ECM interactions is illustrated by the fact that hepatoblasts deficient for β1-integrin are unable to colonize the liver bud (Fässler and Meyer, 1995). Moreover, it has been shown that during liver bud growth HGF and TGFβ signalling act in parallel converging on β1-integrin regulating and controlling hepatic architecture (Weinstein *et al*., 1994). In addition, α1β1 integrin plays an essential role during regeneration after toxic liver injury, as revealed in mice deficient for this heterodimeric integrin which shows defects in cell survival (Duncan *et al*., 2013). Together, this data demonstrate the importance of a correct cell-to-ECM interactions in liver development and homeostasis

5.1.2 Liver enriched factors and extracellular microenvironment regulate hepatic phenotype

In mature hepatocytes, the expression of characteristic genes of the hepatocyte phenotype is controlled by a complex inter-regulatory network of liver-enriched transcription factors, (LEFs), including C/EBPα, and the hepatocyte nuclear factors (HNFs) 1α, 3α-γ, 4α and 6 (Kuo *et al*., 1992; Qu *et al*., 2007; Zaret, 2001; 2002), which can act individually or forming multi-input motifs by collectively binding to set of genes in hepatocytes. The expression of a broad range of genes associated with the hepatocyte biology including metabolism, urea cycle, serum plasma proteins and drug processing genes, are controlled by these transcription factors (Cereghini, 1996; Gonzalez, 2007; Johnson, 1990). Previous studies indicate that HNF1α, -4α and -6 strongly correlate with the hepatocyte performance. These factors are at the centre of a network of transcription factors that regulates developmental and metabolic functions in hepatocytes, by binding to promoters of genes encoding a large population of transcription factors and cofactors (Kuo *et al*., 1992; Zaret, 2002). This includes genes encoding for cell adhesion and functional proteins, important in hepatocyte epithelial structure, ensuring the correct development of the foetal liver architecture and maintenance of the phenotype in the adult (Chen *et al*., 1994; Li *et al*., 2000). HNF1α and HNF4α binding to one another's promoters form a multicomponent loop that induces the expression of the other factor (Boj *et al*., 2001; Ferrer, 2002; Thomas, 2001). In addition, HNF6 acts as a master regulator for feed-forward motifs in hepatocytes, including induction of the expression of phosphoenolpyruvate, a key enzyme in gluconeogenesis, by binding together with HNF4α to the gene promoter (Odom, 2004). C/EBPα and HNF1α expression are essential to ensure complete hepatocyte maturation and metabolic hepatic functions including regulation of glucose and glycogen metabolism (Pontoglio *et al*., 1996; Wang *et al*., 1995). C/EBPα, which expression is induced by HGF (Rastegar *et al*., 2000; Soriano *et al*., 1995; Suzuki *et al*., 2003; Tomizawa *et al*., 1998; Yamasaki *et al*., 2006), inhibits hepatoblast proliferation by stabilizing the cycling dependent inhibitor kinase p21 and the S-

phase-specific E2F-p107 complex (Harris, 2001; Timchenko *et al*., 1997). Finally, FoxA factors -1, -2 and -3 (HNF3α-γ) possess overlapping DNA binding properties regulating numerous hepatic functions (Friedman and Kaestner, 2006).

The microenvironment surrounding the hepatocytes also plays an important role in the cell biology. The extracellular matrix within the healthy liver is composed of a series of macromolecules including collagens (types I-VI) and non-collagenous glycoproteins such as laminins, fibronectin and proteoglycans. The dynamic of the ECM in the liver depends upon ECM synthesis and the proteolytic degradation activity performed by metalloproteinases (MMP), which have emerged as essential mediators in defining how cells interact with their surrounding microenvironment. The regulation of MMPs activity is a tightly controlled process and it takes place at transcriptional, post-transcriptional, and at protein levels (Kessenbrock *et al*., 2010), being the tissue inhibitors of metalloproteinases (TIMPs) the main regulators of MMP activity (Kessenbrock *et al*., 2010; Visse and Nagase, 2003). The role of MMPs and TIMPs in the extracellular matrix remodelling reveals the importance of equilibrium in maintaining liver homeostasis.

The expression of ECM and extracellular matrix receptors varies during liver diseases. This is manifested in the deposition of matrix and scarring with a progressive loss of liver functions. Recent data indicate a pivotal for integrins in the progression of fibrosis and cirrhosis. Upon injury of hepatocytes or bile duct epithelial cells, there is an activation of stellate cells by pro-inflammatory and pro-fibrogenic cytokines including; transforming growth factor beta 1 (TGFβ-1), platelet-derived growth factor (PDGF), fibroblast growth factor (FGF), and connective tissue growth factor (CTGF). This results in increased production and secretion of interstitial collagens and other ECM components (basement membrane collagens, non-collagenous glycoproteins, proteoglycans, and growth factors), leading to an impaired balance between fibrogenesis and fibrolysis, which eventually results in distorted liver architecture and a loss of function (Bataller and Brenner, 2005; Popov and Schuppan, 2009; Rockey, 2005). In experimental liver fibrosis, an

upregulation of laminin-binding integrins α6β1, α2β1, and αvβ8 (Levine *et al*., 2000) and fibronectin-binding α5β1 (Znoyko *et al*., 2006) have been reported. The importance of integrins in liver homeostasis is revealed by studies suggesting that changes in particular integrin expression levels on the cell surface may indicate cellular abnormalities or malignant transformation (Rathinam and Alahari, 2010). As such, several studies have revealed the correlation between an abnormal expression of integrins with pathologies such as viral hepatitis, cholestatic liver disease and alcoholic and non-alcoholic liver diseases. Reports have linked integrin activity with the impaired balance of fibrogenesis and fibrolysis. For example, αvβ6 and αvβ8 integrin activities activate the latent form of TGFβ-1, which is a potent regulator of ECM expression by hepatic stellate cells (HSC) (Munger *et al*., 1999). Conversely, enhanced ECM-degrading proteases MMP-2, -3 and -9 activity have been shown to be associated with an engagement of αvβ3 and αvβ5 (Bendeck *et al*., 2000; Jackson, 2002). An increased expression of β1 integrin on hepatocyte membranes has been observed in human alcoholic liver diseases (Chedid *et al*., 1993), and in patients with advanced alcoholic liver fibrosis or cirrhosis, the serum level of β3 integrin was increased (Yamauchi *et al*., 1993).

These observations demonstrate the importance of the extracellular environment and extracellular matrix and their receptors in hepatocyte biology. Identification of key extracellular factors, including extracellular matrix proteins, matrix associated receptors, involved in the stabilisation of the hepatocyte phenotype represents an important target in hepatocyte biology.

5.1.3 Translating stable hepatocyte phenotype to the clinic.

Human pluripotent stem cells (hPSCs) represent an unlimited source of somatic cells. As such, they hold great promise for disease modelling, basic scientific research, drug development and cell based therapy. However, the use of animal derived research grade reagents during the isolation, establishment and maintenance of current research grade PSCs limit their use in clinical applications.

Therefore, the establishment of PSCs lines using Good Manufacture Practices (GMP) is essential if stem cell derived somatic cells are to be scale and used clinically.

Traditional successful methods in the isolation of ICM from blastocyst such as immunosurgery (Kim *et al*., 2005) require the use of animal derived reagents, which are not desirable when developing defined culture systems. As such, alternative animal free and clinical grade isolation techniques including mechanical (Amit and Itskovitz-Eldor, 2002; Hovatta, 2006; Liu *et al*., 2009b; Touboul *et al*., 2010), laser-assisted-dissection and isolation of hESCs from plated blastocyst outgrowth have been reported (Cortes *et al*., 2008). Culture definition is also required for the establishment and maintenance of clinical grade hESC lines. The use of MEFs has been progressively replaced by human fibroblasts (Fong and Bongso, 2006; Richards *et al*., 2002); or hESCs-derived feeder cells (Ellerström *et al*., 2006). However, these feeder systems are not defined neither scalable. Therefore, feeder-free defined culture systems have been developed, which may involve the use of recombinant (Rodin *et al*., 2010) or synthetic (Villa-Diaz *et al*., 2010; Zhang *et al*., 2009) ECM. Animal and human derived serum containing media have proved to be successful in the derivation and maintenance of several hESCs (Ellerström *et al*., 2006; Reubinoff *et al*., 2000; Richards *et al*., 2002b; Thomson, 1998). Still, the fact that serum is a complex mixture containing unknown compounds with variable composition between batches is reflected in their capability of maintaining undifferentiated hESCs. Therefore, development of defined and xeno-free sera is required for GMP production of hPSCs. As such, companies have released new defined clinical grade sera and media, including Knock-Out Serum Replacement and E8™ medium.

In the next section I investigate the stabilisation of the HLCs maintained on the defined polyurethane PU134 surface under serum-free conditions, identifying key genes and their effect in the cell performance. In addition, these findings are translated to GMP grade cell lines.

5.2 Results

5.2.1 Identifying target genes involved in the stabilization promoted by PU134

hESCs-derived hepatocyte-like cells (HLCs) maintained on PU134 surfaces display a robust, stable and superior hepatocyte phenotype and function than their matrigel counterparts. As such, I aimed to identify the mechanism behind this process. I therefore employed PCR array technology to screen for candidate genes involved in the stabilisation of the hepatocyte phenotype. The RT² Profiler PCR array employed analysed the expression of 84 genes important for extracellular matrix components, cell-to-cell and cell-to-matrix interactions. For this purpose, gene profile expression was compared between HLCs differentiated on matrigel and PU134 surfaces at Day 20 post-replating, when the greatest difference in HLC cell performance was displayed.

PCR array analysis (Figure 54) revealed increased expression (>3-fold) of 6 genes on PU134 surfaces compared to matrigel surfaces: a disintegrin-like and metalloprotease with thrombospondin type 1 motif no. 13, ADAMTS13, neural cell adhesion molecule 1, NCAM1, catenin (cadherin associated protein) delta 2, CTNND2, thrombospondin-2, THBS2, metalloproteinase 10, MMP10 and metalloproteinase 13, MMP13 (Figure 54 and Table 7, Supplementary Information). The fold of increase in the expression for each of the identified genes were as follows; 3.85-fold in ADMTS13, 3.52-fold in NCAM1, 4.1-fold in CTNND2, 3.3-fold in THBS2, 3.38 and 5.7-fold increase in MMP10 and MMP13 respectively (Figure 55). A 3-fold increase was set as a threshold in order to discard stochastic differences and differences in genes with high Ct values (>30 cycles) (Supplementary Table 1).

The output of the array was validated by quantitative PCR, whereby one of the candidate genes, ADAMTS13, was not amplified as expected (1.6-fold) and therefore, was excluded from further studies. The fold of increase in the gene expression of the remaining identified genes were as follows; 4.1-fold in NCAM1,

4.6-fold in CTNND2, 4.8-fold in THBS2, 3.6 and 3.8-fold increase in MMP10 and MMP13 respectively (Figure 56). These results highlighted the importance of confirming the outputs of the PCR array as the expression of one of the identified genes, ADAMTS13, was not amplified as indicated in the PCR array.

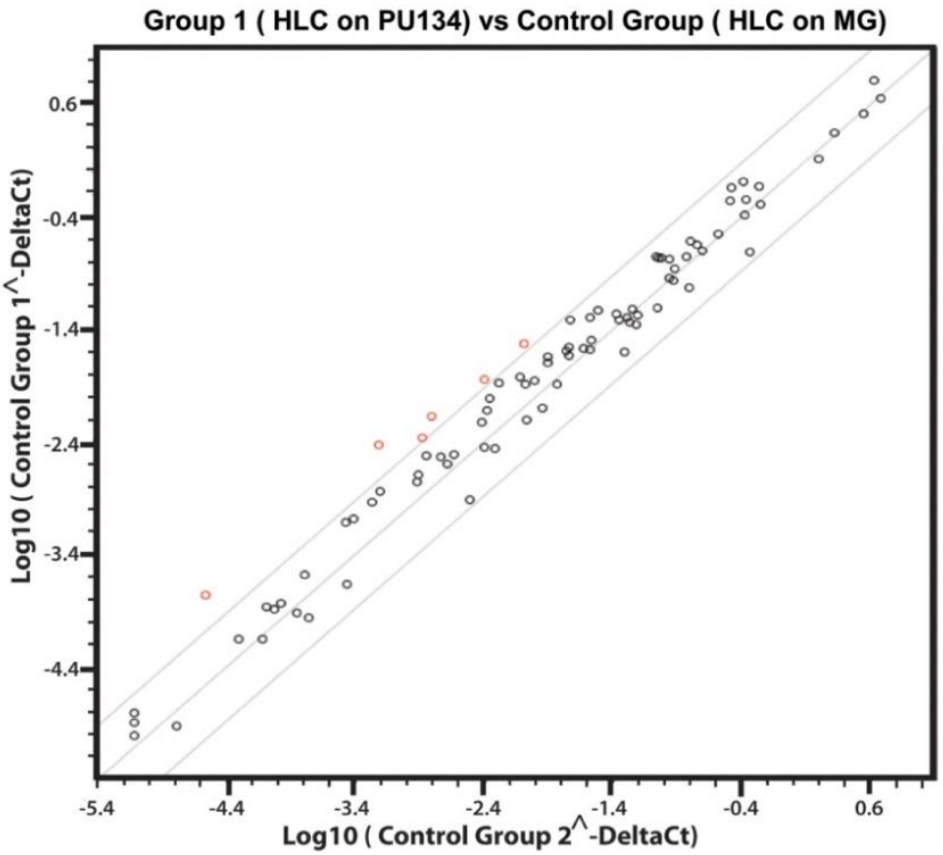

Figure 54. Gene expression in HLCs on PU134 and matrigel surfaces. A PCR array for the major extracellular matrix components and matrix associated receptors expressed on human cells was performed in HLCs maintained on matrigel and PU134 surfaces at Day 20 post-replating. Gene expression was performed using RT^2 Profiler PCR array (Qiagen) according to the manufacturer's instructions. The gene expression was analysed by RT^2 Profiler PCR array Data Analysis version 5.0 (Qiagen). The scatter plot represents 3-fold change in gene expression. The graph plots the log10 of normalized gene expression levels in a control condition (x-axis) versus and experimental condition (y-axis). Symbols outside the boundary area indicate fold-differences larger than a threshold (3 fold). The red symbols identify up-regulated genes.

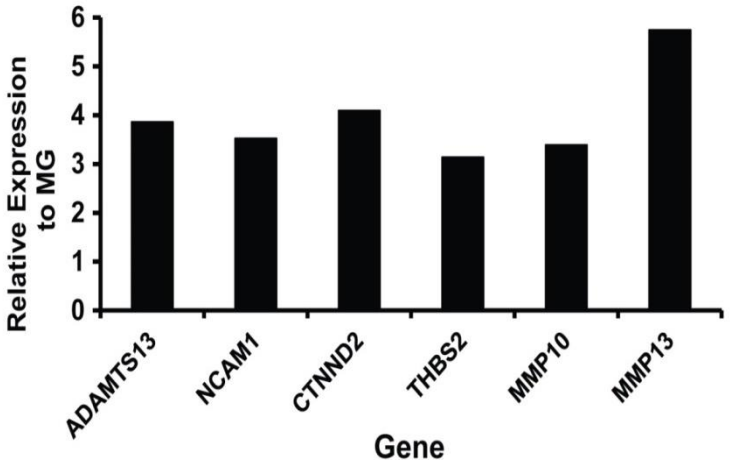

Figure 55. Up-regulated genes identified on the PCR array. The graph represents the identified genes which expression was upregulated more than 3-fold change in HLCs maintained on PU134 surfaces compared to HLCs maintained on matrigel surfaces.

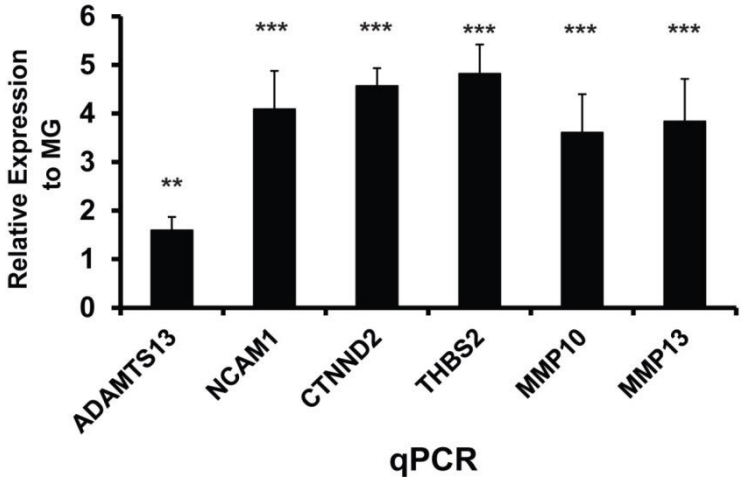

Figure 56. qPCR confirmation of the PCR array. Confirmation of the up-regulated genes previously identified on the PCR array was performed by quantitative PCR in HLCs maintained on matrigel or PU134 surfaces at Day 20 post-replating. Relative expression refers to fold of induction over HLCs maintained on matrigel surfaces at Day 20 post-replating and normalised to the housekeeping gene GAPDH. The results represent the mean ± SD of three different samples run, each run in triplicate. Levels of significance were measured by student's t-test where $p<0.01$ is denoted as ** and $p<0.001$ is denoted as ***.

5.2.2 Testing gene function by gene knockdown

In order to understand the importance of each gene in hepatocyte function, I employed siRNA-mediated loss of function. HLCs maintained on PU134 were

transfected at Day 13 and 14 post-replating with specific siRNAs against the target genes at an optimised concentration. At Day 15 post-replating, gene knockdown was assessed by quantitative PCR (Figure 57), revealing that the efficiency in the gene knockdown was dependent on the siRNA employed. NCAM1 and CTNND2 gene expression levels were decreased by ≈25% ($p<0.05$), THBS2 levels fell by ≈75%, MMP10 was decreased by ≈40%, and MMP13 levels fell by ≈60% ($p<0.001$) compared to the scrambled siRNA control.

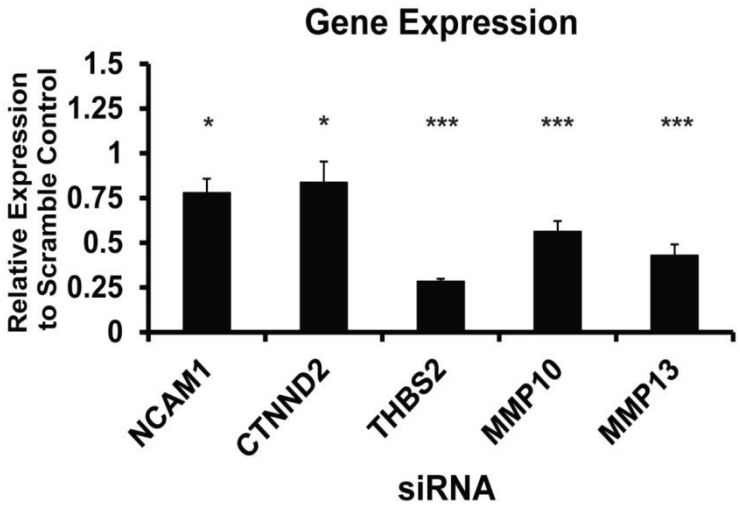

Figure 57. Knock-down optimisation of the candidate genes expression. HLCs maintained on PU134 surfaces were transfected at Day 13 and 14 post-replating with 80 µM of specific small interference RNA (siRNA) against the candidate genes identified on the PCR array. The transfection was performed using Lipofectamin 2000® (Invitrogen) at 1 in 10 ratio (µg RNA), following manufacturer's instructions. Cells were harvested at Day 15 post-replating for further analysis. Relative expression refers to fold of induction over transfected scrambled siRNA control (random sequences that are not complementary with any gene in the genome) and normalised to the housekeeping gene GAPDH. The results represent the mean ± SD of three different samples run, each run in triplicate. Levels of significance were measured by student's t-test where $p<0.05$ is denoted as *, $p<0.01$ is denoted as ** and $p<0.001$ is denoted as ***.

5.2.2.1 Phenotype implies metabolic function

Next I assessed the effect that gene knockdown had on the hepatocyte phenotype. For this purpose, I analysed the gene expression of two well established hepatocyte genes and hepatocyte functions.

The effect gene knockdown was assessed by measuring two key hepatocyte genes, hepatocyte nuclear factor 4α, HNF4α and albumin (Figure 55). Analysis of HNF4α

gene expression (Figure 58A) revealed that in response to the gene knockdown of CTNND2 and MMP13, HNF4α expression decreased ≈25% and ≈65%, respectively ($p<0.001$) compared with gene expression levels observed upon transfection of a scrambled siRNA control. In contrast, MMP10 gene knockdown resulted in a 1.68-fold increase in HNF4α gene expression ($p<0.001$). Transfections with siRNAs to NCAM1 or THBS2, demonstrated little effect on HNF4α gene expression, in comparison to the scrambled siRNA control ($p>0.05$).

Albumin gene expression (Figure 58B) was significantly decreased in response to the gene knockdown of CTNND2, THBS2 and MMP13 by ≈60%, ≈50% and ≈65% ($p<0.001$). No significant differences were observed in response to the gene knockdown of NCAM1 and MMP10.

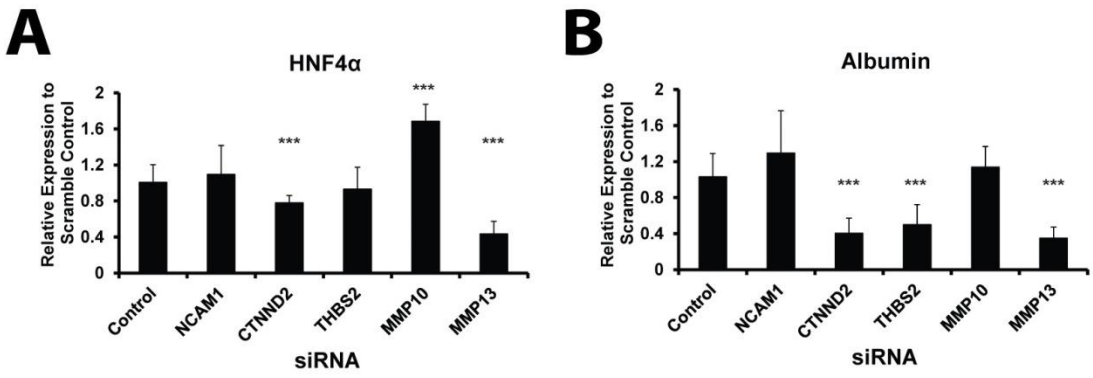

Figure 58. Effect in the expression of hepatocyte markers upon target gene expression knockdown. Graph represents the gene expression of the hepatocyte markers HNF4α and albumin analysed by quantitative PCR in hESCs-derived HLCs at Day 15 post-replating on PU134 surfaces upon transfection with siRNAs to the target genes. Results revealed that HNF4α gene expression significantly decreased upon knocking down CTNND2 and MMP13 gene expression (A) and albumin gene expression significantly reduced when CTNND2, THBS2 or MMP13 gene expression was knocked down (B). Relative expression refers to fold of induction over cells transfected with scrambled siRNA control and normalised to the housekeeping gene GAPDH. The results represent the mean ± SD of three different samples run, each run in triplicate. Levels of significance were measured by student's *t-test* where $p<0.001$ is denoted as ***. Abbreviations: HNF4α-Hepatic Nuclear Factor 4α.

5.2.2.2 Influence of the knockdown in the expression of targeted gene products in the function of HLCs maintained on PU134.

In addition to studying gene expression, I also studied the effect that gene knockdown had in HLC function. Analysis of the cytochrome P450 3A function (Figure 59) revealed a statistically significant decrease in CYP3A activity in response to THBS2 and MMP13 knockdown. CYP3A function was reduced by ≈25% and ≈30%, respectively ($p<0.01$). No significant differences were observed in the CYP3A function in cells transfected with siRNAs to NCAM1, CTNND2 and MMP10 ($p>0.05$).

Measurement in the secretion of albumin upon knocking down gene expression was performed using ELISA (Figure 60). In response to CTNND2 and MMP13 knockdown, albumin secretion decreased by ≈30% and ≈50%, respectively ($p<0.05$). No statistically significant differences were observed in response to NCAM1, THBS2 and MMP10 knockdown ($p>0.05$).

These results demonstrated that THBS2, MMP13 and CTNND2 influence the hepatocyte function in HLCs maintained on PU134 surfaces, serving as a gene signature associated with stable HLC phenotype

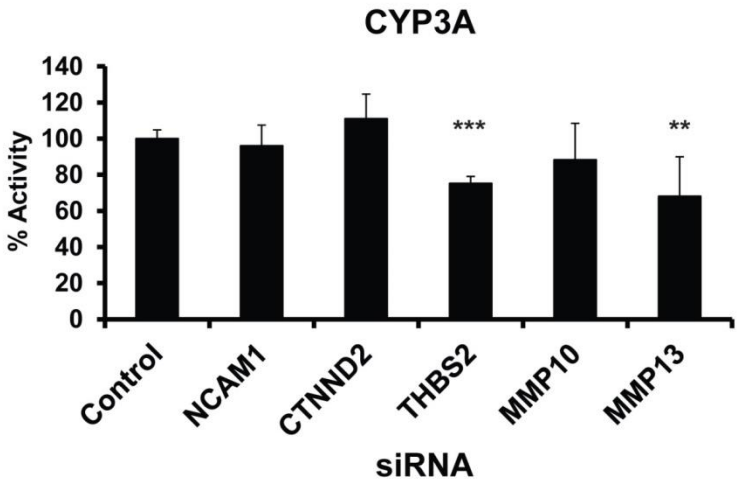

Figure 59. Cytochrome P450 3A activity was influenced upon knockdown in the expression of target gene products. CYP3A activity was assessed using a commercially available system (pGLO®) in HLCs maintained on PU134 surfaces at Day 15 post-replating upon transfection with siRNAs to the target genes. Analysis of the function of the cells revealed that, knocking-down the expression of THBS2 or MMP13 decreased CYP3A activity of the cells. Relative expression refers to fold of

induction over the activity displayed by cells transfected with a scrambled siRNA control. The results represent the mean ± SD of three individual samples per condition. Levels of significance were measured by student's *t-test* where $p>0.01$ is denoted as ** and $p>0.001$ is denoted as ***.

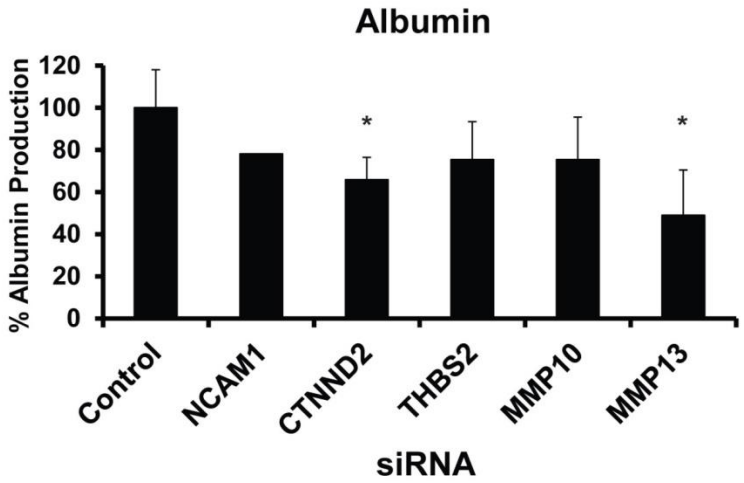

Figure 60. Albumin secretion was influenced upon target gene expression knockdown. The secretion of albumin in HLCs maintained on PU134 surfaces at Day 15 post-replating upon transfection with siRNAs to the target genes was analysed using a commercial available ELISA kit for human albumin. Analysis of the results revealed that knocking-down the expression of CTNND2 or MMP13 significantly decreased the secretion of albumin. Relative expression refers to fold of induction over the albumin secreted by cells transfected with a scrambled siRNA control. The results represent the mean ± SD of three individual samples per condition. Levels of significance were measured by student's t-test where $p>0.05$ is denoted as *.

5.2.3 Translating PU134 technology to GMP grade hESC lines

The manufacture of stem cell derived somatic cells is likely to play an important part in developing cell based therapies in the future. To be able to deliver clinical grade materials, highly defined biological processes are required. In this vein, I employed two hESC lines which were derived under GMP conditions, Man 11 and Man 12.

5.2.3.1 Pluripotency characterisation of GMP hESC lines Man 11 and Man 12

Prior to Man hESCs hepatocyte differentiation on PU134 surfaces, I performed a detailed characterisation of the undifferentiated and pluripotent state of both GMP cell lines. Morphological analysis, examination of transcription factors ascribed to pluripotency expression, and expression of stem cell surface markers were

examined. In addition, the pluripotency capacity of the cells was measured by studying their ability to spontaneously differentiate into the three germ layers, and their ability to differentiate into hepatocytes using direct differentiation (Szkolnicka *et al*, 2014).

Both cell lines were cultured in feeder free in mTeSR1™ media (MT), and hESC identity was assessed. Morphological analysis of Man 11 and Man12 grown in MT demonstrated tightly packed dome-like colonies with well-defined edges and little spontaneous cellular differentiation. Both cell lines displayed the characteristic hESC morphology defined by the possession of a large nucleus to cytoplasm ratio with a well-defined and pronounced nucleoli (Figure 61A). Further to morphological analysis, the stem cell nature of the hESCs cultured in MT was investigated by analysing protein expression of two transcription factor associated with 'stemness', Oct 4 (Octamer 4) and Nanog, using immunofluorescence (Figure 8B). Analysis of the yield percentage of hESC displaying pluripotent markers revealed that while 99% of Man 11 cells expressed Oct 4 and Nanog, in Man 12 cells these proteins were presented in 98% and 99% of the cells respectively (Figure 61B). The high level of expression of Oct 4 and Nanog confirmed the undifferentiated state of the hESCs.

hESC identity was further confirmed by analysing the expression of stem cell surface markers by flow cytometry (Figure 61C). Both cell lines expressed background levels of the differentiation marker SSEA-1 with 1.3% and 0.9% of Man 11 and Man 12 cells stained positive. SSEA-4 was expressed by 97% and 98% of Man 11 and Man 12 cells. While 97% and 92% of Man 11 hESC line expressed TRA-1-60 and TRA-1-81 respectively, the expression of these markers was detected in 95% and 98% of the Man 12 hESC line, respectively.

In addition, both cell lines were able to spontaneously form three germ layers (Figure 61D). hESCs from both cell lines formed cell types that were positive for alpha-fetoprotein (endoderm), alpha-smooth muscle (mesoderm) and β-tubulin III (ectoderm), and showed no karyotypic abnormalities (supplementary Figure 3 and 4).

The ability to directly differentiate to HLCs on matrigel surfaces was confirmed in both cell lines using a serum-free differentiation approach previously described (Figure 17). Monolayers of HLCs were fixed at day 18 in the differentiation procedure and stained with antibodies to HNF4α and albumin by immunofluorescence. Analysis of the percentage yield of HLCs expressing the hepatocyte markers revealed that 87% and 95% of Man 11 HLCs stained positive for HNF4α and albumin respectively, while the expression of these markers were present in 84% and 99% of Man 12 HLCs, respectively (Figure 62).

All together, the data here presented demonstrate the undifferentiated and pluripotent nature of both GMP grade hESC lines.

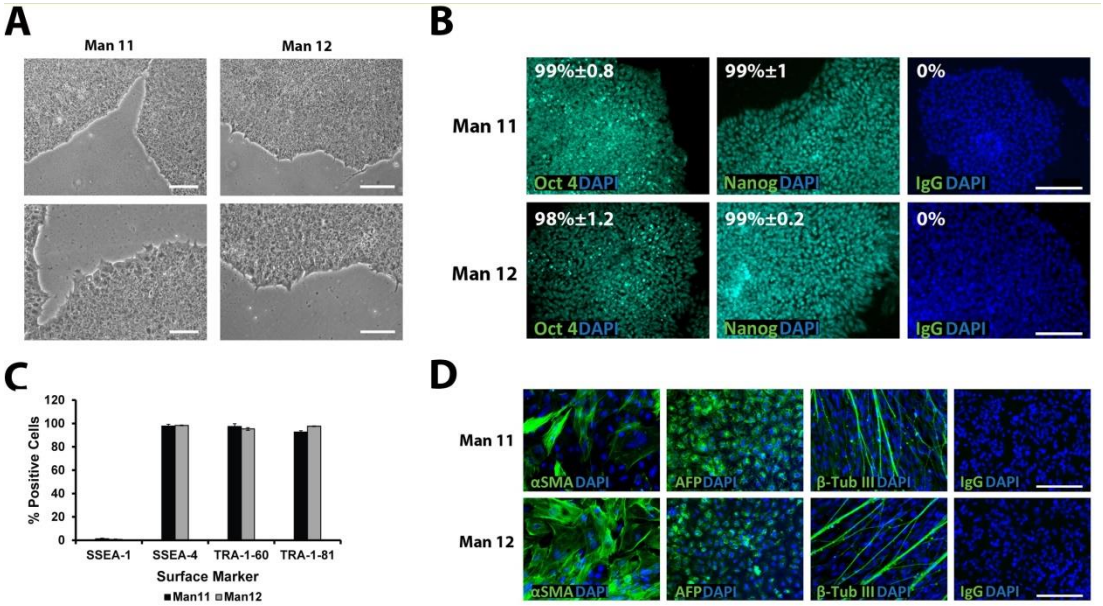

Figure 61. Analysis of GMP hESC lines Man 11 and Man 12. A) hESC lines Man11 and Man12 maintained in mTeSR1™ medium displayed morphological features typical of hESC, maintaining a large nucleus to cytoplasm ratio. hESCs formed colonies with well-defined edges and little to no differentiation observed between the colonies. Images were taken at 4x magnification (top) or 10x magnification (bottom), and scale bar represents 200 µm and 100 µm respectively. B) Pluripotent marker expression in both hESC lines was analysed by immunofluorescence, with 99% and 98% of the Man11 and Man12 expressing Oct 4 respectively, and 99% of both cell lines expressing Nanog. IgG controls demonstrated the specificity of immunostaining. For each condition five random fields of view, containing at least 500 cells, were counted. Images were taken at 20x magnification and the scale bar represents 100 µm. C) Cell surface marker expression of SSEA1, SSEA-3, SEEA-4, TRA-1-60 and TRA-1-81, but not SSEA1, was assessed by flow cytometry. The results represent the mean ± SD of three independent samples per cell line. E) hESC pluripotency was measured by spontaneous differentiation. Following EB formation, α-smooth muscle (αSMA), α-fetoprotein (AFP) and β-

tubulin III (β-tub III) (green) were detected by immunostaining. IgG control demonstrated the specificity of immunostaining. Images were taken at 20x magnification and the scale bar represents 100 µm.

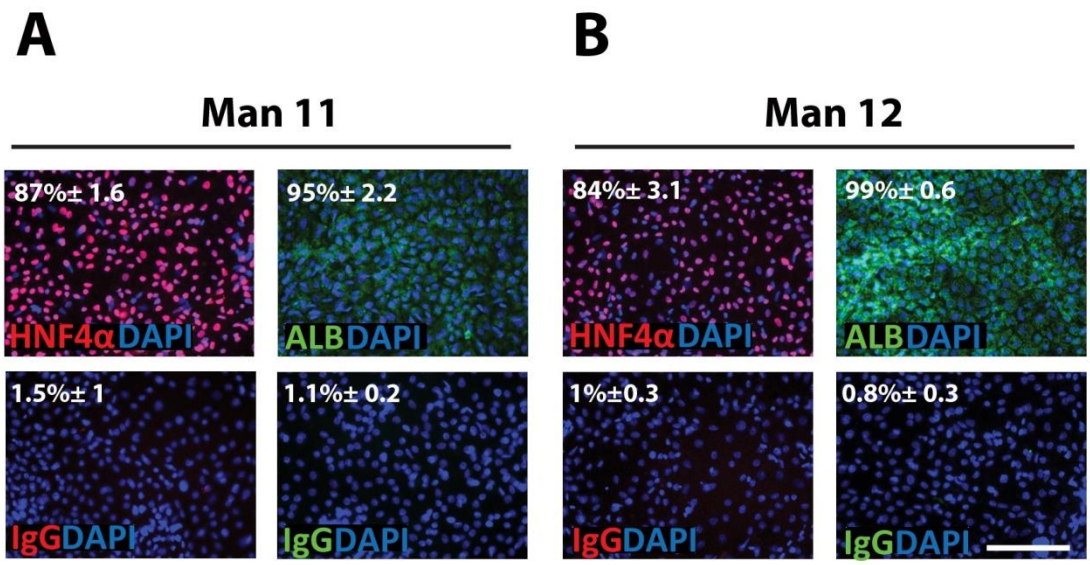

Figure 62. Man 11 and Man 12 directed differentiation to HLCs. Immunofluorescence analysis of hepatocyte lineage markers on A) Man 11 and B) Man 12 HLCs on matrigel at Day 18 on the differentiation approach, demonstrating an efficient differentiation to a hepatocyte fate. The corresponding IgG controls indicated the specificity of the staining. For each condition five random fields of view, containing at least 500 cells, were counted. Images were taken at 20x magnification and the scales bar represents 100 µm. Abbreviations: HNF4α-Hepatocyte nuclear factor 4α, ALB-Albumin, IgG-Immunoglobulin G.

5.2.3.2 HLCs derived from GMP hESC lines Man 11 and Man 12 are supported on PU134 surface.

Next, I tested whether hepatocyte differentiation of both GMP hESC lines was supported on PU134 surfaces. For this purpose Man 11 and Man 12 hESCs-derived hepatoblasts were replated onto matrigel or PU134 surfaces in the presence of the serum-free maturation media containing KOSR. The resulting population of cells were characterised at different times during the differentiation procedure. Morphological analysis of the resulting population of HLCs and functional analysis were performed.

5.2.3.3 Hepatocyte differentiation on PU134 surface of Man 11 HLCs

Characterisation of the Man 11 HLCs maintained on matrigel or PU134 surfaces were firstly performed by analysing the morphology of the cells at Day 5, 10 and 15 post-replating (Figure 63A). Phase contrast images of the resulting population of HLCs demonstrated that either substrate supported cell attachment. At Day 5 and 10 post-replating there were no gross differences in the morphology of the cells replated on either substrate. The compacted and homogeneous resulting population of cells displayed typical primary hepatocyte morphological features, with hexagonal morphology, well-defined nucleus and clear cell-to-cell contacts (panels A, B, D and E). As the differentiation progressed, these features were preserved on matrigel surfaces, but improved on PU134 surfaces, with cells displaying canaliculi like structures (black arrows, panel F).

In addition to cell morphology, functional analysis of the cells, including CYP3A activity, albumin and alpha-fetoprotein (AFP) secretion were performed to further characterise the resulting cells.

Cytochrome P450 3A function was measured at Day 5, 10 and 15 post-replating (Figure 63B). Man 11 HLCs maintained on matrigel surfaces displayed the peak in the CYP3A function at Day 10 post-replating after a 1.5-fold increase compared to Day 5 post-replating and prior to a 3-fold decreased by Day 15 post-replating. CYP3A function in HLCs replated on PU134 surfaces displayed comparable CYP3A function at Day 5 and 10 post-replating, prior to a 1.6-fold increase by Day 15 post-replating, with a 2.7-fold increase compared with HLCs replated on matrigel surfaces ($p<0.01$), representing the peak in the activity on PU134 surfaces. The values for CYP3A at Day 5, 10 and 15 post-replating in HLC replated on matrigel or PU134 surfaces are as follows; $5{,}1x10^4$ RLU/ml/mg, $4{,}6x10^4$ RLU/ml/mg, $8x10^4$ RLU/ml/mg, $3{,}8x10^4$ RLU/ml/mg, $2{,}4x10^4$ RLU/ml/mg and $6{,}2x10^4$ RLU/ml/mg, respectively.

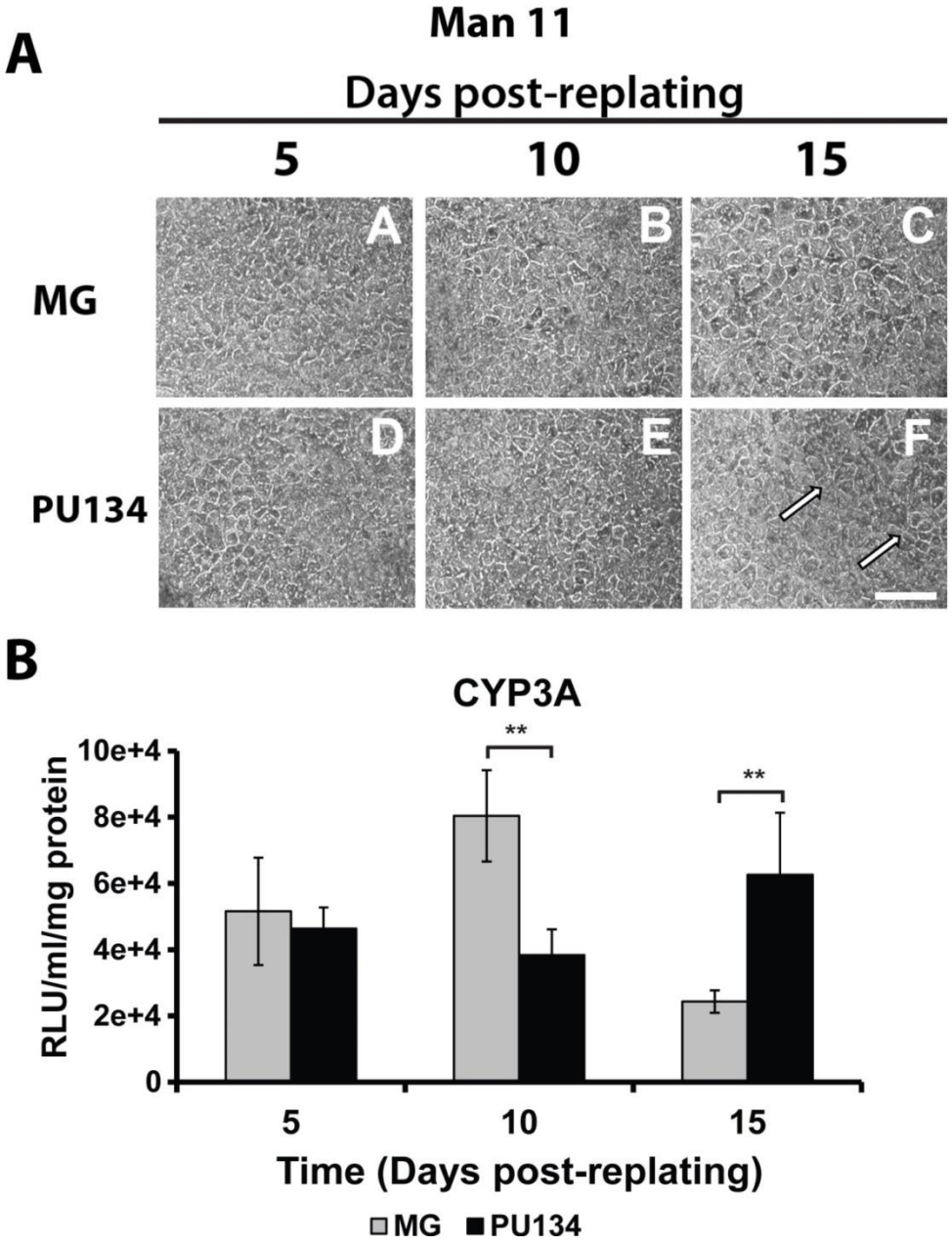

Figure 63. Man 11 hepatocyte differentiation compatible with PU134. The serum-free hepatocyte differentiation protocol compatible with PU134 surfaces was successfully applied on the GMP hESC line Man 11. At Day 9, hESCs-derived hepatoblast were removed from the culture substrates and replated onto matrigel (MG) or PU134 surfaces (PU134). (A) Phase contrast images show the morphology of HLCs at different days post-replating on either substrate. Independently of the substrate, compacted populations of Man 11 HLCs were maintained for at least 15 days post replating, exhibiting typical hepatocyte morphological features, denoted by the acquisition of a more defined nucleus, with cells displaying a hexagonal morphology and an increase in the cell-to-cell contact resembling to cultures of human primary hepatocytes. These features were clearer in HLCs maintained on PU134 surface (white and black arrows). The images were taken at 10x magnification and scale bar represents 100 µm. B) Man 11 HLCs maintained on PU134 surfaces displayed a superior cytochrome P450 3A function at late stages of the differentiation procedure. CYP3A activity

was assessed using a commercially available system (pGLO®) in HLCs maintained on either surface at Day 5, 10 and 15 post-replating. Analysis of the function revealed that cells on matrigel surfaces displayed a better activity at early stages in the differentiation process, with a peak in the activity by Day 10 post-replating. On PU134 surfaces (PU134), the activity increased at Day 15 post-replating, with a 3-fold increase compared with matrigel surfaces (MG). The results represent the mean ± SD of three individual samples per time point per cytochrome p450 analysed. Levels of significance were measured by student's *t-test*, where p>0.01 is denoted as **.

Albumin and alpha-fetoprotein (AFP) are two important secreted proteins in the hepatocyte biology. While albumin is expressed on both mature and immature hepatocytes, AFP secretion is characteristic of immature hepatocyte phenotype. Therefore, measurement of the secretion of both proteins represents a good indicator of the function and the mature stage of the cells.

Analysis in the secretion of both proteins in Man 11 HLCs replated on matrigel or PU134 surfaces was performed using ELISA at Day 15 post-replating, when improved CYP3A activity was observed on PU134 surfaces compared to matrigel surfaces (Figure 64). Analysis in albumin secretion revealed a ≈39-fold increase in Man 11 HLCs maintained on PU134 surfaces compared to HLCs on matrigel surfaces (Figure 64A). Measurement of secreted AFP did not display any statistically significant differences between both substrates. The values of albumin secreted at Day 15 post-replating on matrigel or PU134 surfaces are as follows; 1.74 ng/ml/24hours/mg and 68.38 ng/ml/24hours/mg respectively; and the values of alpha-fetoprotein secreted at Day 15 post-replating on matrigel or PU134 surfaces are as follows; 23.3 ng/ml/24hours/mg and 271.9 ng/ml/24hours/mg, respectively.

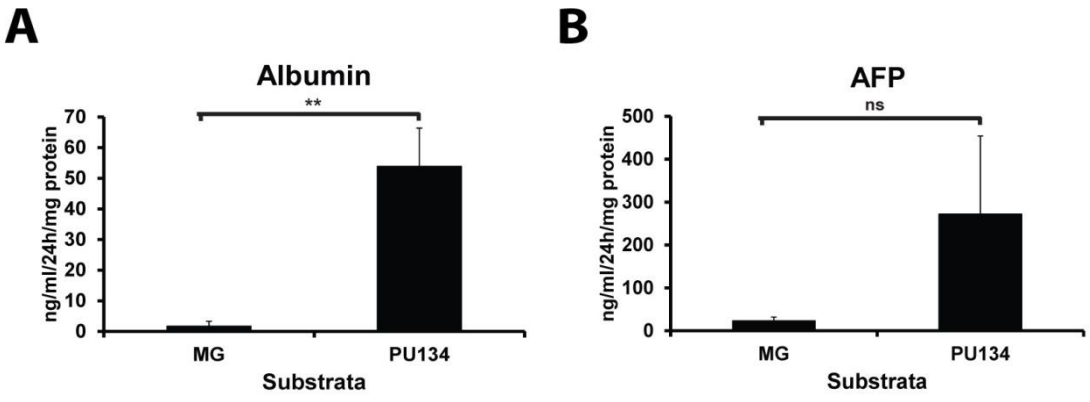

Figure 64. Improvement in the serum protein secretion in Man 11 HLCs on PU134. The graphs displayed show the levels of albumin (A) and alpha-fetoprotein (B) secreted by Man 11 HLC maintained on matrigel (MG) or PU134 surfaces at Day 15 post-replating, revealing an improvement in the albumin secretion in the presence of PU134 surfaces while cells secreting comparable levels between both surfaces of the foetal hepatocyte marker AFP. The results represent the mean ± SD of three individual samples per time point. Levels of significance were measured by student's *t-test* where $p<0.05$ is denoted as ns and $p>0.01$ is denoted as **.

5.2.3.4 Hepatocyte differentiation on PU134 surface of Man 12 hESCs-derived HLCs

Analysis of the morphology of Man 12 HLCs replated on either surface was used as a first step to characterise the HLCs at Day 5, 10, 15 and 20 post-replating (Figure 65A). Phase contrast images of the resulting population of HLCs demonstrated that either substrate supported cell attachment. Up to Day 10 post-replating cells did not show gross morphological differences between either substrate, with the resulting populations of HLCs displaying typical primary hepatocyte morphological features, with a high homogeneity with hexagonal cellular shape, well-defined nucleus and clear cell-to-cell contacts (panels A, B, E and F). As the differentiation progressed, HLCs maintained on matrigel surfaces lost hepatocyte morphological features, displaying morphological heterogeneity, with cells rounding up and detaching (panels C-D). On PU134 surfaces, HLCs morphology was improved up to 20 days post-replating, with cells displaying canaliculi-like structures (black arrows, panels G-H).

In addition to cell morphology, cytochrome P450 3A activity in Man 12 HLCs was measured at different times during the differentiation procedure (Figure 65B). HLCs maintained on matrigel surfaces displayed the peak in the CYP3A function at Day 10 post-replating after a 2.9-fold increase compared to Day 5 post-replating. Following this, CYP3A function decreased ≈1.3-fold at Day 15 post-replating prior to a further ≈2.4-fold decrease by Day 20 post-replating. On the other hand, HLCs maintained on PU134 surfaces displayed increased levels of CYP3A function as the differentiation progressed. At Day 10 post-replating, a 2.1-fold increase compared with Day 5 post-replating was observed, prior to a further ≈1.6-fold increase at Day

15 post-replating. Following this, CYP3A activity increased 1.2-fold at Day 20 post-replating, with a 3.3-fold difference compared with matrigel surfaces at Day 20 post-replating ($p<0.01$), representing the peak in the activity on PU134 surfaces. The values for CYP3A at Day 5, 10, 15 and 20 post-replating in HLC replated on matrigel or PU134 surfaces are as follows; $2,6x10^4$ RLU/ml/mg, $2,1x10^4$ RLU/ml/mg, $7,6x10^4$ RLU/ml/mg, $4,6x10^4$ RLU/ml/mg, $5,9x10^4$ RLU/ml/mg, $7,3x10^4$ RLU/ml/mg, $2,5x10^4$ RLU/ml/mg and $8,2x10^4$ RLU/ml/, respectively.

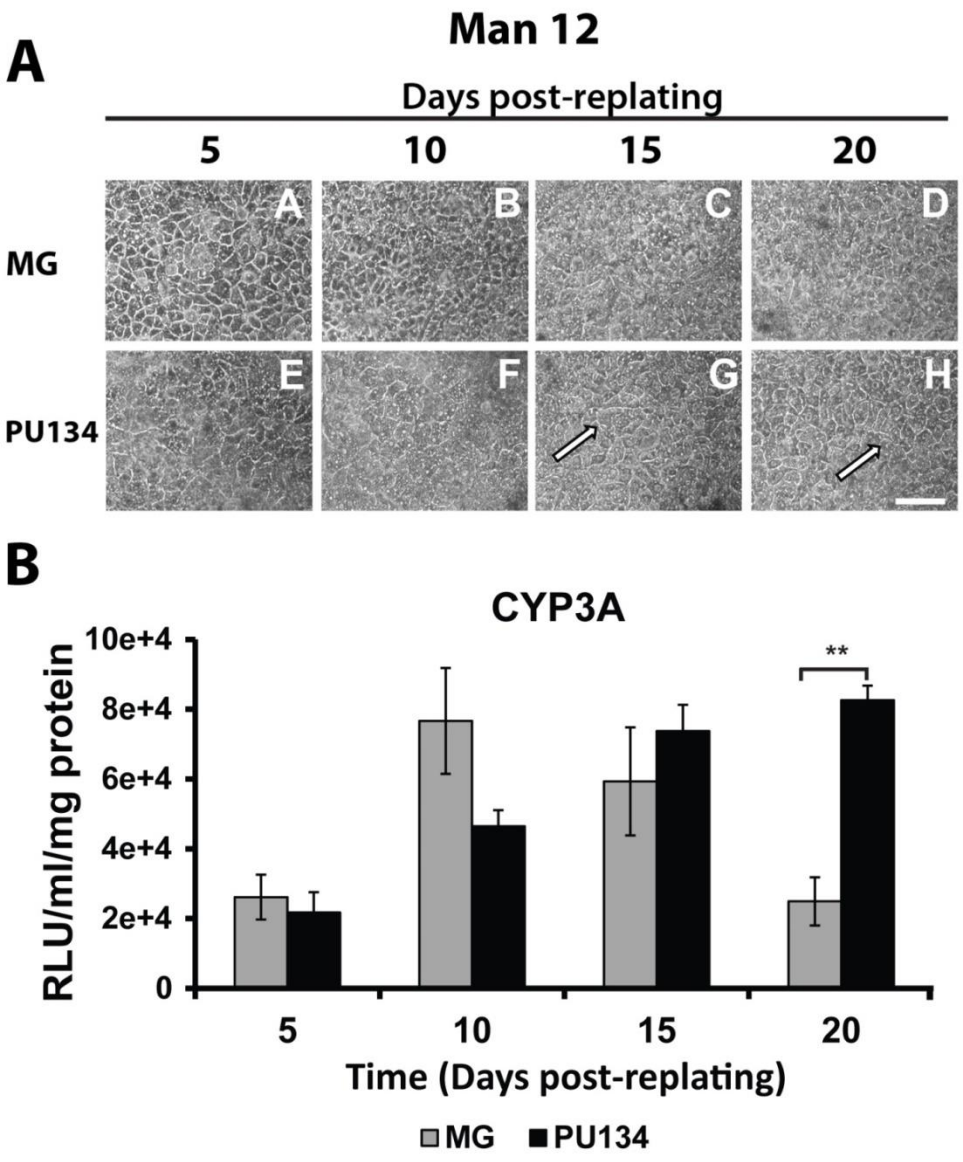

Figure 65. Man 12 hepatocyte differentiation compatible with PU134. The serum-free hepatocyte differentiation protocol compatible with PU134 surfaces was successfully applied on the GMP hESC line Man 11. At Day 9, hESCs-derived hepatoblast were removed from the culture substrates and replated onto matrigel (MG) or PU134 surfaces (PU134). (A) Phase contrast images showed the

morphology of HLCs at different days post-replating on either substrate. Independently of the substrate a compacted population of HLCs was maintained for at least 20 days post replating, exhibiting typical hepatocyte morphological features, denoted by the acquisition of a more defined nucleus, with cells displaying a hexagonal morphology and an increase in the cell-to-cell contact resembling to cultures of human primary hepatocytes. These features were clearer in HLCs maintained on PU134 surface (white and black arrows).The images were taken at 10x magnification and scale bar represents 100 µm. B) Man 12 HLCs maintained on PU134 surfaces displayed a superior cytochrome p450 3A function. CYP3A activity was assessed using a commercially available system (pGLO®) in HLCs maintained on either surface at Day 5, 10, 15 and 20 post-replating. Analysis of the function revealed that cells on Matrigel surfaces (MG) displayed a better activity at early stages in the differentiation process, but decreasing as the differentiation progressed. The converse was true on PU134 surfaces (PU134), reaching a peak in the activity by Day 20 post-replating with a 4-fold increase compared with matrigel surfaces, which display their peak in the activity by Day 10 post-replating. The results represent the mean ± SD of three individual samples per time point per cytochrome p450 analysed. The results represent the mean ± SD of three individual samples per time point per substrate. Levels of significance were measured by student's t-test where $p>0.01$ is denoted as **.

The function and mature stage of the cells was investigated by measuring albumin and AFP secretion using ELISA (Figure 66). For this purpose, secretion of both proteins were analysed in Man 12 HLCs replated on either substrate at Day 15 and 20 post-replating, when improved CYP3A function was observed on PU134 surfaces. Analysis in albumin secretion (Figure 66A) revealed a stabilisation in its secretion on PU134, with no statistically significant difference between both analysed days ($p<0.05$). In addition, improved albumin secretion was detected when compared to matrigel surfaces, with ≈1.8 ($p>0.05$) and ≈5.4-fold increase ($p>0.001$) at Day 15 and 20 post-replating respectively. The values of albumin secreted at Day 15 and Day 20 post-replating on matrigel or PU134 surfaces are as follows; 109.4 ng/ml/24hours/mg, 49.67 ng/ml/24hours/mg, 195.46 ng/ml/24hours/mg and 267.34 ng/ml/24hours/mg, respectively.

The maturity stage of the cells was studied by analysing AFP secretion in either substrate at both days in the differentiation approach. Analysis in the secretion of AFP (Figure 66B) on matrigel surfaces revealed a ≈3.4-fold decrease by Day 20 post-replating compared to Day 15 post-replating; and a ≈4.9-fold decrease on PU134 surfaces by Day 20 post-replating compared to Day 15 post-replating, with no statistically significant difference between both substrates ($p<0.05$), indicating the

possession of a mature phenotype when PU134 surface was used as a culture substrate. The values of alpha-fetoprotein secreted at Day 15 and Day 20 post-replating on matrigel or PU134 surfaces are as follows; 127.4 ng/ml/24hours/mg, 36.9 ng/ml/24hours/mg, 171.9 ng/ml/24hours/mg and 35.2 ng/ml/24hours/mg, respectively.

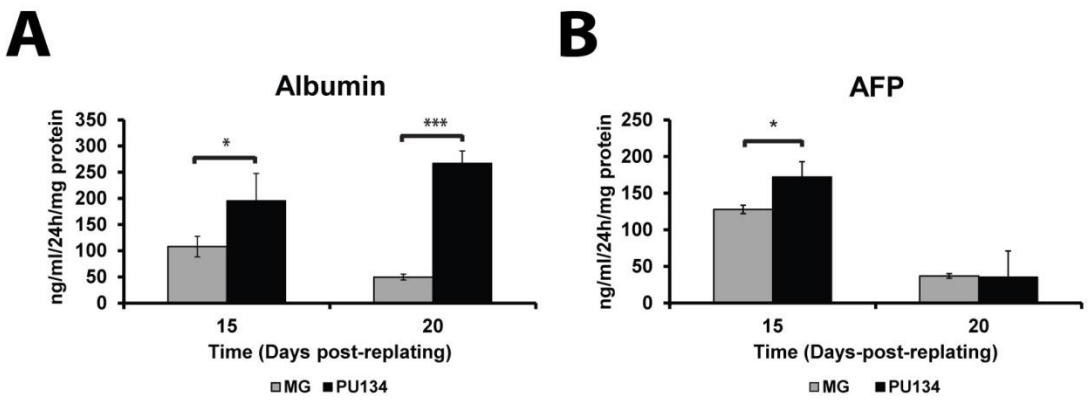

Figure 66. Improvement in the serum protein secretion in Man 12 HLCs on PU134 surfaces. The graphs displayed show the levels of albumin (A) and alpha-fetoprotein (B) secreted by Man 11 HLC maintained on matrigel (MG) or PU134 surfaces at Day 15 and 20 post-replating, revealing an improved albumin secretion in the presence of PU134 surfaces while a reduced AFP secretion as the differentiation progressed. The results represent the mean ± SD of three individual samples per time point. Levels of significance were measured by student's t-test where $p>0.05$ is denoted as *, $p>0.01$ is denoted as ** and $p>0.001$ is denoted as ***.

In conclusion, this data demonstrate that PU134 surface supports functional hepatocyte differentiation of the GMP hESC lines Man 11 and Man 12 in a greater manner than matrigel surfaces, with differences in the life span between both GPM hESC lines. Man 12 HLCs performed best in culture, demonstrating stable albumin production and a reduction in AFP secretion over a five day period compared to matrigel cultures, indicating a greater maturity state of the cells induced by PU134 surfaces.

5.2.4 Gene expression profile of target genes on GMP grade HLCs on PU134 surface

In order to study whether up-regulation in the expression of the target genes previously identified in the PCR array was also observed in GMP grade HLCs on PU134 surface, I analysed using quantitative PCR the expression of the target genes at Day 15 post-replating on Man 11 and Man 12 HLCs (Figure 67).

Analysis of the gene expression revealed that in Man 11 HLCs on PU134 surfaces (Figure 67A), the expression of CTNND2, THBS2 and MMP13 were upregulated by 1.57, 3 and 1.8-fold, respectively compared with matrigel surfaces ($p<0.01$). No statistically significant differences in the gene expression of NCAM1 and MMP10 were observed ($p>0.05$).

In Man 12 HLCs (Figure 67B), analysis of the gene expression revealed a statistically significant increase in THBS2 and MMP13 of 2.4 and 5.9-fold, respectively on PU134 surfaces compared with matrigel surfaces ($p<0.001$). NCAM1 expression decreased 2-fold on PU134 surface ($p<0.001$). No statistically significant differences in the gene expression of CTNND2 and MMP10 were observed ($p>0.05$).

Altogether, this data suggest a role for MMP13, CTNND2 and THBS2 in the stabilisation of the GMP grade HLCs function.

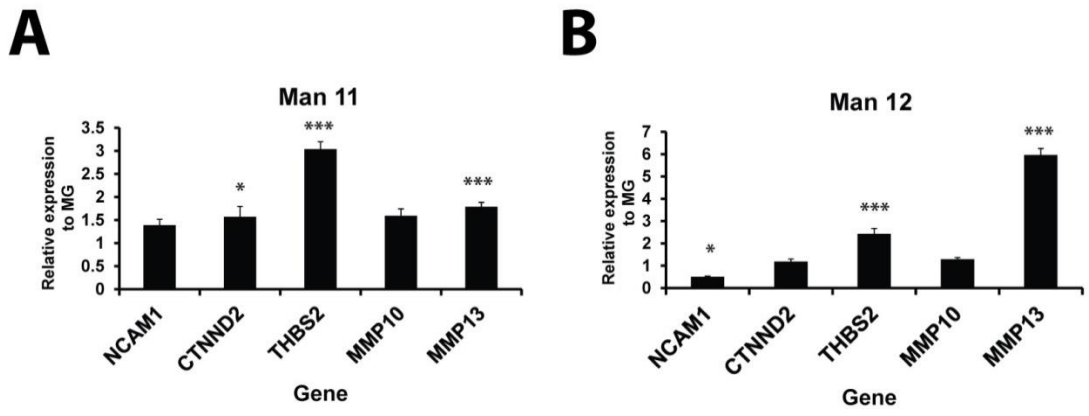

Figure 67. Gene signature of the GMP grade hESC lines derived HLCs. Graphs representing the gene expression analysed by quantitative PCR of candidate genes previously identified on the PCR array at Day 15 post-replating in A) Man 11 HLCs and B) Man 12 HLCs. Analysis in the expression

of candidate gene revealed an increased expression of THBS2 and MMP13 in both cell populations and CTNND2 in Man 11 HLCs compared with matrigel surface. Relative expression refers to fold of induction over HLCs replated on matrigel surfaces and normalised to the housekeeping gene GAPDH. The results represent the mean ± SD of three different samples run, each run in triplicate. Levels of significance were measured by student's *t-test* where $p>0.05$ is denoted as * and $p>0.001$ is denoted as ***.

5.3 Discussion

Differentiation and maintenance of stem cell derived somatic cells represents a cutting-edge technology with revolutionary potential applications in the study of human biology, drug screening and regenerative medicine. However, the delivery of reliable and stable human models is a major barrier, limiting current endeavours as most of the current approach use non-defined and biological derived media and/or substrates to differentiate and maintain hPSCs-derived somatic cells. As such, the development of defined differentiation systems free of xenobiotic materials or undefined additives is required to achieve this objective. Previously, Hay and colleagues (Hay *et al*., 2011) employed an inter-disciplinary approach, blending polymer chemistry with an efficient hepatocyte differentiation approach (Hay *et al*., 2008a) to identify defined synthetic matrices that supported cultures of PSCs-derived hepatocytes. They identified a simple polyurethane 134, PU134, as a suitable extracellular matrix support to obtain reliable, stable and functional stem cells derived HLCs.

Identification of the PU134 surface was performed in a serum containing media, which compromised the reliability of the resulting HLCs. In an attempt to reduce the functional variability associated with the use of serum in the differentiation approach, which compromised reproducibility between experiments, and in collaboration with other members of the group, I developed a serum-free differentiation approach to obtain functional and stable HLCs from pluripotent stem

cells (Szkolnicka *et al*., 2014). In addition to develop a serum-free differentiation approach, I fine-tuned the polymer surface to obtain functional and stable HLCs in the serum-free hepatocyte maturation media (Lucendo-Villarin *et al*., 2014). However, the resulting cells displayed limited life span, which was solved by supplementing the serum-free maturation media with defined components that preserve cell viability and function.

The improved tissue integrity displayed by HLCs maintained on this synthetic and defined substrate suggested the existence of a mechanism(s) induced by the PU134 surfaces in promoting and stabilising cell polarity, which is essential in the maintenance of hepatocyte function (Müsch, 2013). Therefore, in order to identify the mechanism behind this stabilisation process promoted by PU134 surfaces, I employed a focused survey of human extracellular matrix proteins, cell membrane components and receptors, using PCR array technology in HLCs maintained on either substrate at Day 20 post-replating, when the biggest phenotypic and functional differences were observed between HLCs maintained on either substrate. From this screening I identified five genes which expression was enhanced in cells differentiated in the defined culture environment. Those genes, which appear to be new markers of hepatocyte differentiation, could be broadly divided in to 2 categories, as extracellular matrix remodellers (MMP10 and 13) or cell-cell and cell-matrix interactors (THBS2, CTNND2 and NCAM1).

Matrix metalloproteinases (MMPs) are a family of proteins known to display substrate specificity for particular extracellular matrices (ECMs), emerging as essential mediators in defining how cells interact with their surrounding microenvironment (Kessenbrock *et al*., 2010). MMPs are essential for normal remodelling of the extracellular matrix, tissue morphogenesis, and wound healing (Iredale, 2007), and their activity is regulated by post translational modifications and by the tissue inhibitor of matrix metalloproteinases (TIMPs) (Iredale, 2007; Kessenbrock *et al*., 2010; Visse and Nagase, 2003). MMP13, the main interstitial collagenase, has highly specific ability to degrade insoluble fibrillary type I collagen

(Knäuper and López, 1996; Quinn *et al*., 1990) and it has been reported to promote recovery from liver cirrhosis by converting the secretion of precursor HGF to the mature HGF form, thus, activating a signalling cascade involved in liver regeneration (Endo *et al*., 2011). Our analysis indicated that both MMP13 and -10 gene expression was increased over cultures differentiated in an undefined manner. It is possible that differences in gene expression may reflected the capacity of the cell to remodel the ECM, which is known to be important in the maintenance of hepatocyte phenotype (Freije and Diez, 1994; Garcia-Irigoyen *et al*., 2014; Muller *et al*., 1988).

The second group of identified genes that were expressed at greater levels in cell populations differentiated under defined conditions includes genes which code for proteins involved in cell-to-cell and cell-to-matrix interactions: THBS2, CTNND2 and NCAM1.

THBS2 and CTNND2 are known to regulate cell adhesion, organisation and migration, in response to growth factor stimulation (Ezaki *et al*., 2007; Fujiyoshi and Ozaki, 2010; Liu *et al*., 2009). THBS2, an extracellular matrix protein involved in the organogenesis of branches organs, affects the metalloproteinase 2 (MMP2) activity by inhibiting conversion of the MMP zymogen to the activated form (Bein and Simons, 2000), which expression is increased during the resolution of liver injury at the end stages of cirrhosis (Han, 2006; Roeb *et al*., 2005; Takayama *et al*., 2013). CTNND2, an adhesive junction associated protein of the armadillo/beta catenin superfamily, possesses a role in cell adhesion and cell movement (Kosik *et al*., 2005). In addition, it is also involved in the formation of stable junctional structures, thereby establishing cell polarity in epithelial cells by mediating localisation of zonula occludens-1 (ZO-1) in the lateral membrane, which is required for E-Cadherin-mediated formation of proper cell junctions (Fujiyoshi and Ozaki, 2010). Along similar lines, NCAM1, an integral membrane glycoprotein that can promote cell-to-cell adhesion thorough a homophilic binding mechanism (Doherty *et al*.,

1990; Hall *et al*., 1990), has been identified as important factor in cell motility, essential to normal liver development and regeneration (Tsuchiya *et al*., 2014).

In order to study the role that these genes had in the hepatocyte biology under defined conditions, I modulated their expression by employing siRNA technology. From this study, besides its role in collagen remodelling, MMP13 was identified as a potential regulator of hepatocyte phenotype influencing cytochrome P450 activity and human albumin secretion. In addition to MMP13, I reported a novel finding: a decreased expression of THBS2 and CTNND2, two genes with proposed roles in cell attachment, organisation and migration, led to reduced cytochrome P450 function and albumin secretion, respectively, proposing a new role for these genes in the hepatocyte biology (Lucendo-Villarin *et al*., 2015).

As a result of these findings, further experiments focused on the functional gene signature for MMP13, THBS2, and CTNND2. For these studies, I employed two hESC lines which had been derived under GMP conditions and maintained serum-free, displaying an undifferentiated and pluripotent state as demonstrated by the expression of stem cell morphological features and markers and their ability to differentiate into cells of the three germ layers.

Prior to study the gene signature of the target genes in the GMP grade derived HLCs, I studied the hepatocyte differentiation efficiency of these cells on polymer surfaces. The defined conditions efficiently supported hepatocyte differentiation of both GMP grade cell lines in a greater manner than the biological derived surface, with differences in the life span between the cell lines, which can be due to genotypic differences. Of note the Man 12 HLCs performed best in culture, demonstrating stable albumin production and a reduction in AFP secretion over a five day period, indicating a greater grade of maturity in the cells in the presence of the PU134 surface.

For comparison studies, I analysed the expression of the targeted genes in GMP grade derived HLCs at Day 15 post-replating and notably, defined and directed

differentiation of both GMP lines yielded cell populations which expressed increased levels of MMP13, THBS2 and CTNND2 and thereby, supporting data derived from the research grade hESC line.

In addition to the roles previously described, it has been reported that the protein encoded by CTNND2 promotes the disruption of E-cadherin to favour cell spreading upon stimulation by HGF (Lu *et al*., 1999). In rats, THBS2 has been implicated in the cell surface properties of mesenchymal cells with regards to cell adhesion and migration (Zou *et al*., 2013). Finally, it has been shown a role for the protein encoded by MMP13 in the degradation of newly-formed matrix in the early phases of rat liver fibrosis (Yan *et al*., 2005). Interestingly, this *in vitro* study has revealed new roles for the targeted genes in hepatocyte biology. Whether these findings can be translated to an *in vivo* system has yet to be elucidated.

Numerous hepatocyte differentiation protocols have been established using synthetic substrates in two and three-dimensional cultures, and encouragingly, the stem cell derived HLCs exhibited typical hepatocyte characteristics. Takayama and colleagues employed a Nanopillar plate technology (Takahashi *et al*., 2010) to obtain spheroids of HLCs displaying hepatocyte functions, including albumin production and urea secretion with cells displaying metabolism against hepatotoxic drugs. Despite the promising results observed, the assembly of spheroids required overlays of matrigel (Takayama *et al*., 2013). Ware and colleagues combined iPSC technology with a previously developed micropatterned co-culture platform (Khetani and Bhatia, 2008) to obtain functional HLCs capable of DILI prediction. However, the use of research cell lines and rat collagen coated culture platforms limited their use in therapeutic and clinical application (Ware *et al*., 2015). Sivertsson and colleagues employed a perfused three-dimensional bioreactor in the hepatocyte differentiation and maturation of hESCs, demonstrating an enhancement in the display of hepatocyte markers and hepatocyte signalling pathways when compared to two-dimensional systems. Still, the technical difficulties of this technology represent a limitation for their use in research

(Sivertsson *et al*., 2012). On the other hand, the polymer technology here employed possesses advantages compared with other methods as the simple polymer chemistry employed is cost-effective, ensuring low variability between polymer batches and can be efficiently employed in three-dimensional systems (Medine *et al*., 2013). In addition, HLCs obtained on the PU134 surface display an extended life span with improved hepatocyte phenotype and function than their matrigel counterparts.

In conclusion, dependable differentiation from pluripotent stem cells requires defined culture parameters as the conditions offered by the differentiation approach compatible with the use of the defined polymer PU134 surface employed in this study. Such systems will permit informative and mechanistic analysis of human biology. The novel gene signature identified in these studies is one example, which may also serve as important gold standard parameters for quality control and manufacture of GMP grade products at scale.

CHAPTER SIX

CONCLUSIONS AND FUTURE PERSPECTIVES

6.1 Conclusions

Current sources of hepatocytes including; primary human hepatocytes, hepatoblast, hepatic cell lines and animal derived hepatocytes possess significant limitations meaning that they are not able to satisfy demand. The aim of my thesis was to produce hepatocyte-like cells (HLCs) from a renewable and scalable source, human embryonic stem cells.

Human embryonic stem cells (hESCs) are able to self-renew indefinitely whilst remaining pluripotency (Thomson, 1998). As a result, they can differentiate into cells types from all three germ layers. Therefore hESCs represent a promising source of somatic cells to study human hepatocyte biology. Despite encouraging outcomes, most of the current hepatocyte differentiation approaches are performed in undefined microenvironments which influence the function and stability of the derivative cells.

During my project I have tackled culture definition and stability by establishing a serum-free differentiation process on defined polymer matrix, permitting long-term culture of functional HLCs. To elucidate the mechanism of action of the polyurethane 134, I employed PCR array and loss of function analysis. From these experiments I identified a novel genetic signature, MMP13, CTNND2 and THBS2, which predicted stable hepatocyte phenotype from research and GMP grade hESC-HLCs. While the results are promising further refinements are necessary to permit technology translation to industry and the clinic.

6.2 Future perspectives

As discussed above the production of hESC-HLCs in a defined environment represents a good starting point to improve the technology. The key areas where the current state of the art would benefit from are:

1. Improved HLC biochemical characterisation

Although current differentiation approaches from pluripotent stem cells generate HLCs displaying hepatocyte markers and function, they still express features remaining foetal hepatocytes. The HLC population generated in this study expressed mature liver markers, cytochrome P450 activity 3A and D6 and albumin. However, a recent study performed by Baxter and collegaues showed that the activity of these enzymes are already displayed in foetal hepatocytes (Baxter *et al*., 2015). As such, in order to identify reliable markers of hepatocyte maturity, Rowe and colleagues performed a comparative proteomic and functional analysis between foetal hepatocytes isolated at different times during the gestation period, and commercially available fresh human hepatocytes. From this study, the authors recommended a simple set of proteins, including cytochrome P450 2A6, glutathione S transferase P, and alcohol dehydrogenases as specialized indicators of hepatocyte differentiation (Rowe *et al*., 2013). Additionally, a recent from Godoy and colleagues employed bioinformatics to perform a comparative gene regulatory network analysis between different pluripotent stem cell derived HLC populations, identifying groups of genes associated with mature hepatocyte functions. In comparison, HLCs expressed the majority of those genes. However, there were many genes which did not approach the levels of primary hepatocytes. In these studies we identified three problematic clusters including colon, fibroblast and stem cell-associated transcription factors. Moreover, increased expression of genes controlling proliferation and dedifferentiation (e.g. FoxQ1 and YBX3) may be responsible for not obtaining fully differentiated phenotype (Godoy *et al*., 2015). These studies suggest that the culture conditions may be responsible for the HLCs not reaching mature hepatocytes. As shown, HLCs, like cultures of primary human hepatocytes, display a loss in the expression of key ‘liver‘ genes and the transcription factors controlling liver functions. This study provides a ‘blue-print’ to eliminate non-desired cell traits; however, care must be taken when selecting genes to over express or suppress. For example, depletion of the colon-associated transcription factor CDX2, which is important in hindgut specification and cell

biology, may also disrupt HNF4α DNA occupancy, and HNF4α driven gene expression (Verzi *et al*., 2013).

2. The influence of the microbiome on cell maturity

Liver development is a process that extends beyond birth, when there is a switch from placental to enteral nutrition. Fatty acids from the breastfeeding become the main energy source, and those are further metabolised by the gut microbiome to secondary metabolites which instruct liver development in the neonate (Morelli, 2008). In line with this, Avior and colleagues recently demonstrated that a secondary metabolite, lithocholic acid (LCA), or the use of Vitamin K may drive maturation of HLCs. They demonstrated that these additives synergise, regulating the activity of a key nuclear factor, PXR, improving cytochrome P450 enzymes 2C9 and 3A4 expression and function (Avior *et al*., 2015). These studies demonstrated that microbial-derived cues are essential for maturing HLCs, and therefore future work should focus on secondary metabolites generated by the gut microbiome.

3. Tissue engineering to deliver three dimensional and better organised organoids

Correct hepatocyte development and homeostasis requires signals from the neighbouring cells and extracellular matrix. Most of the current differentiation approaches, while promising, lack the appropriate niche and three dimensional structural. Therefore the development of co-culture strategies employing relevant cell types, and three dimensional structures are required. In this vein, Takebe and colleagues developed an innovative approach. In the presence of endothelial and mesenchymal cells, PSC-HLCs self-organised into three dimensional liver-like tissue structures. These liver buds were injected into a mouse liver and successfully engrafted by establishing host-vessel connections. Moreover, the authors

demonstrated liver function outside the relevant organ as PSC-liver buds were also injected and successfully engrafted in a mice cranial window model and into the mesentery, being the latest a more realistic target site for future transplantations. As such, these findings represent an example of successful generation of vascularised PSC- derived organoids (Takebe *et al*., 2013). This study represents a proof-of-concept of how cell-to-cell interactions are important in hepatocyte differentiation. Additionally, a recent paper by Celiz and colleagues demonstrates that polymer screening technology could be used to identify polymer(s) that support stem cell self-renewal and stem cell differentiation to cells representative of the three germ layers. They identified a polymer (HPhMA-*co*-HEMA) compatible with the use of defined media which potentially can fulfil culture requirements for stem cell scale up, differentiation and application (Celiz *et al*., 2015).

4. The role of matrix remodelling on cell phenotype

The defined differentiation approach described in this study identifies a novel gene signature associated with stable hepatocyte function, revealing the matrix remodelling capacity and the establishment of cell-to-cell interactions of the cells under defined conditions. Interestingly, MMP13 and THBS2 play important roles in hepatocyte biology. MMP13 represents the main interstitial metalloproteinase degrading collagen II during recovery of liver fibrosis (Endo *et al*., 2011). THBS2 is known to regulate cell adhesion, organisation and migration (Liu *et al*., 2009). Moreover, THBS2 inhibits the conversion of MMP2 zymogen to the activated form (Bein and Simons, 2000). As such, the action of both proteins regulates the liver homeostasis by modulating extracellular matrix deposition. Further description of their mechanism of action, with regards to long-term stabilization of the hepatocellular phenotype and function, represent an interesting area for future studies with clear implications in clinical and toxicological applications.

5. Use of microfluidics to scale up the production

Microfluidics allows constant perfusion of cells under low levels of fluid shear stress. As such, these systems represent a suitable format to study cell differentiation and tissue formation. Recently, Giobbe and colleagues reported a microfluidic system on a chip to differentiated PSC into HLCs displaying drug response to toxicological compounds (Giobbe *et al*., 2015). Berger and colleagues have described successful microfluidic systems employing co-cultures of PSC derived HLCs and stroma cell, reporting enhanced maturity and polarity (Berger *et al*., 2015). Moreover, these systems are compatible with synthetic polymers, which prove opportunities to develop cost effective and scalable culture systems.

6. The use of bioprinting to scale up the production

Bioprinting represents an attractive technology to produce PSC derived HLCs in isolation or in combination with non-parenchymal cells. Of note, the recently reported Organovo's exVive3D liver tissue (Organovo®; USA) has been shown to secrete fibrinogen, albumin and transferrin in proportion to levels observed in in whole liver (Visk, 2015). With regard to PSCs, valve-based cell printers have been already employed to deliver viable hESC populations in programmable patterns, and offer promise in the quest to deliver *in vitro* derived organoids for clinical and research applications (Faulkner, 2013).

In conclusion, my study demonstrates that differentiation from pluripotent stem cells requires defined culture parameters. This system has permitted me to study in more detail HLC differentiation and has yielded a better understanding of the basic biology. In future, and in combination with the above disciplines, PSC HLCs represent a promising resource for research and the clinic.

BIBLIOGRAPHY

Agarwal, S., Holton, K.L., and Lanza, R. (2008). Efficient Differentiation of Functional Hepatocytes from Human Embryonic Stem Cells. Stem Cells 26, 1117-1127.

Alison, M.R., Choong, C., and Lim, S. (2007). Application of liver stem cells for cell therapy. Semin. Cell Dev. Biol 18, 819-26.

Allen, J.W., Hassanein, T., and Bhatia, S.N. (2001). Advances in bioartificial liver devices. Hepatology 34, 447-55.

Amit, M., and Itskovitz-Eldor, J. (2002). Derivation and spontaneous differentiation of human embryonic stem cells. J. Anat 200, 225-32

Amit, M., Chebath, J., Margulets, V., and Laevsky, I. (2010). Suspension culture of undifferentiated human embryonic and induced pluripotent stem cells. Stem Cell Reviews 6, 248-59.

Amit, M., Shariki, C., and Margulets, V. (2004). Feeder layer-and serum-free culture of human embryonic stem cells. Biology Reprod 70, 837-45.

Anderson, D.G., Levenberg, S., and Langer, R. (2004). Nanoliter-scale synthesis of arrayed biomaterials and application to human embryonic stem cells. Nature Biotechnology 22, 863-6.

Anderson, J.M., Van Italllie, C. (2009). Introduction: evolution of ideas on the tight junction.Col Spring Harb Persperct Biol 1:a002584

Andrews, P.W., Banting, G., and Damjanov, I. (1984). Three monoclonal antibodies defining distinct differentiation antigens associated with different high molecular weight polypeptides on the surface of human embryonal carcinoma cells 3, 347-61.

Avilion, A.A., Nicolis, S.K., Pevny, L.H., and Perez, L. (2003). Multipotent cell lineages in early mouse development depend on SOX2 function. Genes Dev 17, 126-40.

Avior, Y., Levy, G., Zimerman, M., and Kitsberg, D. (2015). Microbial-derived lithocholic acid and vitamin K2 drive the metabolic maturation of pluripotent stem cells–derived and fetal hepatocytes 62, 265-78.

Azevedo, E.C., Nascimento, E.M., and Chierice, G.O. (2013). UV and gamma irradiation effects on surface properties of polyurethane derivate from castor oil. Polímeros 23, 305-11.

Bader, A., Rinkes, I., Closs, E.I., and Ryan, C.M. (1992). A stable long-term hepatocyte culture system for studies of physiologic processes: cytokine stimulation of the acute phase response in rat and human hepatocytes. Biotechnology Prog 8, 219-25.

Baharvand, H., Hashemi, S.M., and Ashtiani, S.K. (2006). Differentiation of human embryonic stem cells into hepatocytes in 2D and 3D culture systems in vitro. International J Dev Bio 50, 645-52.

Baker, D.E.C., Harrison, N.J., Maltby, E., Smith, K., Moore, H.D., Shaw, P.J., Heath, P.R., Holden, H., and ANDREWS, P.W. (2007). Adaptation to culture of human embryonic stem cells and oncogenesis in vivo. Nature Biotechnology 25, 207-15.

Baloch, Z., Klapper, J., Buchanan, L., and Schwartz, M. (1992). Ontogenesis of the murine hepatic extracellular matrix: an immunohistochemical study. Differentiation 51, 209.

Basma, H., Gutiérrez, A.S., Yannam, G.R., Liu, L., Ito, R., Yamamoto, T., Ellis, E., Carson, S.D., Sato, S., Chen, Y., *et al*. (2009). Differentiation and Transplantation of Human Embryonic Stem Cell–Derived Hepatocytes. YGAST 136, 990-999.e4.

Bataller, R., and Brenner, D.A. (2005). Liver fibrosis. J. Clin. Invest. 115, 209-218.

Baxter, M., Withey, S., Harrison, S., and Segeritz, C.P. (2015). Phenotypic and functional analyses show stem cell-derived hepatocyte-like cells better mimic fetal rather than adult hepatocytes. Journal Hepatol 62, 581-9.

Behbahan, I.S., Duan, Y., Lam, A., Khoobyari, S., Ma, X., Ahuja, T.P., and Zern, M.A. (2011). New approaches in the differentiation of human embryonic stem cells and induced pluripotent stem cells toward hepatocytes. Stem Cell Rev And Rep 7, 748-59-759.

Behnia, K., Bhatia, S., Jastromb, N., and Balis, U. (2000). Xenobiotic metabolism by cultured primary porcine hepatocytes. Tissue Eng 6, 467-79.

Beigel, J., Fella, K., Kramer, P.J., Kroeger, M., and Hewitt, P. (2008). Genomics and proteomics analysis of cultured primary rat hepatocytes. Toxicology In Vitro 22, 171-81.

Bein, K., and Simons, M. (2000). Thrombospondin Type 1 Repeats Interact with Matrix Metalloproteinase 2. Regulation of metalloproteinase activity. J Bio Chem. 13, 32167-73.

Bendeck, M.P., Irvin, C., Reidy, M., and Smith, L. (2000). Smooth muscle cell matrix metalloproteinase production is stimulated via αvβ3 integrin. Arterioscler CThrom Vasc Biol 20, 1467-72.

Benhamouche, S., Decaens, T., Godard, C., and Chambrey, R. (2006). Apc tumor suppressor gene is the “zonation-keeper” of mouse liver. Dev Cell 10, 759-70.

Berg, T., Rountree, C.B., Lee, L., Estrada, J., Sala, F.G., Choe, A., Veltmaat, J.M., De Langhe, S., Lee, R., Tsukamoto, H., *et al*. (2007). Fibroblast growth factor 10 is

critical for liver growth during embryogenesis and controls hepatoblast survival via β-catenin activation. Hepatology 46, 1187-1197.

Berger, D.R., Ware, B.R., Davidson, M.D., and Allsup, S.R. (2015). Enhancing the functional maturity of induced pluripotent stem cell–derived human hepatocytes by controlled presentation of cell–cell interactions in vitro. Hepatology 61, 1370.

Biggs, M.J.P., Richards, R.G., Wilkinson, C.D.W., and Dalby, M.J. (2008). Focal adhesion interactions with topographical structures: a novel method for immuno-SEM labelling of focal adhesions in S-phase cells. J Microsc 231, 28-37.

Binda, D., and Lasserre, D. (2003). Time course of cytochromes P450 decline during rat hepatocyte isolation and culture: effect of L-NAME. Toxicol In Vitro 17, 59-67.

Birchmeier, C., Birchmeier, W., Gherardi, E., and Vande Woude, G.F. (2003). Met, metastasis, motility and more. Nat Rev Mol Cell Biol 4, 915-925.

Bissell, DM; Caron, JM; Babiss and Friedman, JM. (1990). Transcriptional regulation of the albumin gene in cultured rat hepatocytes. Role of basement-membrane matrix. Mol Bio Med 7, 187-97.

Biswas, A., and Hutchins, R. (2007). Embryonic stem cells. Stem Cells Dev. 16, 213.

Bladt, F., Riethmacher, D., Isenmann, S., and Aguzzi, A. (1995). Essential role for the c-met receptor in the migration of myogenic precursor cells into the limb bud. Nature 376, 768.

Block, G.D., Locker, J., and Bowen, W.C. (1996). Population expansion, clonal growth, and specific differentiation patterns in primary cultures of hepatocytes induced by HGF/SF, EGF and TGF alpha in a chemically defined (HGM) medium. J Cell Biol 132, 1133-49.

Boess, F., Kamber, M., Romer, S., and Gasser, R. (2003). Gene expression in two hepatic cell lines, cultured primary hepatocytes, and liver slices compared to the in vivo liver gene expression in rats: possible implications for toxicogenomics use of in vitro systems. Toxicol Sci 73, 386-402.

Boj, S.F., Párrizas, M., and Maestro, M.A. (2001). A transcription factor regulatory circuit in differentiated pancreatic cells. Proc Natl Acad Sci USA 98, 14481-6.

Bort, R. (2004). Hex homeobox gene-dependent tissue positioning is required for organogenesis of the ventral pancreas. Development 131, 797-806.

Bort, R., Signore, M., Tremblay, K., Barbera, J.P.M., and Zaret, K.S. (2006). Hex homeobox gene controls the transition of the endoderm to a pseudostratified, cell emergent epithelium for liver bud development. Developmental Biology 290, 44-56.

Bossard, P., and Zaret, K.S. (1998). GATA transcription factors as potentiators of gut endoderm differentiation. Development 225, 4909-17.

Bottcher, R.T. (2005). Fibroblast Growth Factor Signaling during Early Vertebrate Development. Endocrine Reviews 26, 63-77.

Boussie, T.R., and Devenney, M. (2004). Polymer libraries on a substrate, method of forming polymer libraries on a substrate and characterization methods with same. US Patent EP1160262A1.

Braam, S.R., Denning, C., Matsa, E., Young, L.E., and Passier, R. (2008). Feeder-free culture of human embryonic stem cells in conditioned medium for efficient genetic modification. Nat Protoc 3, 1435-43.

Braam, S.R., Zeinstra, L., Litjens, S., Ward-van Oostwaard, D., van den Brink, S., van Laake, L., Lebrin, F., Kats, P., Hochstenbach, R., Passier, R., *et al*. (2008). Recombinant Vitronectin Is a Functionally Defined Substrate That Supports Human Embryonic Stem Cell Self-Renewal via αVβ5 Integrin. Stem Cells 26, 2257-2265.

Brafman, D.A., Chang, C.W., Fernandez, A., and Willert, K. (2010). Long-term human pluripotent stem cell self-renewal on synthetic polymer surfaces. Biomaterials 31, 9135-44.

Brafman, D.A., Shah, K.D., and Fellner, T. (2009). Defining long-term maintenance conditions of human embryonic stem cells with arrayed cellular microenvironment technology. Stem Cells Dev 18, 1141-54.

Brambrink, T., Foreman, R., Welstead, G.G., and Lengner, C.J. (2008). Sequential expression of pluripotency markers during direct reprogramming of mouse somatic cells. Cell Stem Cell 7, 151-9.

Brandenberger, R., Khrebtukova, I., Thies, R.S., Miura, T., Jingli, C., Puri, R., Vasicek, T., Lebkowski, J., and Rao, M. (2004). MPSS profiling of human embryonic stem cells. BMC Dev Biol 4, 10.

Brandon, E.F.A., Raap, C.D., Meijerman, I., Beijnen, J.H., and Schellens, J.H.M. (2003). An update on in vitro test methods in human hepatic drug biotransformation research: pros and cons. Toxicology And Applied Pharmacology 189, 233-246.

Brimble, S.N., Zeng, X., Weiler, D.A., Luo, Y., Liu, Y., Lyons, I.G., Freed, W.J., Robins, A.J., Rao, M.S., and Schulz, T.C. (2005). Karyotypic stability, genotyping, differentiation, feeder-free maintenance, and gene expression sampling in three human embryonic stem cell lines derived prior to August 9, 2001. Stem Cells Dev. 13, 585-97.

Brolén, G., Sivertsson, L., Björquist, P., Eriksson, G., Ek, M., Semb, H., Johansson, I., Andersson, T.B., Ingelman-Sundberg, M., and Heins, N. (2009). Hepatocyte-like cells

derived from human embryonic stem cells specifically via definitive endoderm and a progenitor stage. J. Biotechnol. 145, 284-94.

Bulla, G.A. (1997). Hepatocyte nuclear factor-4 prevents silencing of hepatocyte nuclear factor-1 expression in hepatoma × fibroblast cell hybrids. Nucleic Acids Res 25, 2051-8.

Burke, Z.D., Thowfeequ, S., and Tosh, D. (2006). Liver specification: a new role for Wnts in liver development. Curr Biol 5, R688-90.

Cai, J., Chen, J., Liu, Y., Miura, T., Luo, Y., Loring, J.F., Freed, W.J., Rao, M.S., and Zeng, X. (2006). Assessing self-renewal and differentiation in human embryonic stem cell lines. Stem Cells 24, 516-30-530.

Cai, J., Zhao, Y., Liu, Y., Ye, F., Song, Z., Qin, H., Meng, S., Chen, Y., Zhou, R., Song, X., *et al*. (2007). Directed differentiation of human embryonic stem cells into functional hepatic cells. Hepatology 45, 1229-39-1239.

Calmont, A., Wandzioch, E., Tremblay, K.D., Minowada, G., Kaestner, K.H., Martin, G.R., and Zaret, K.S. (2006). An FGF Response Pathway that Mediates Hepatic Gene Induction in Embryonic Endoderm Cells. Developmental Cell 11, 339-348.

Cameron, K., Travers, P., Chander, C., Buckland, T., Campion, C., and Noble, B. (2013). Directed osteogenic differentiation of human mesenchymal stem/precursor cells on silicate substituted calcium phosphate. J. Biomed. Mater. Res. 101, 13-22.

Campos, P.B., Sartore, R.C., and Abdalla, S.N. (2009). Chromosomal spread preparation of human embryonic stem cells for karyotyping. J Vis Exp 4, 1512.

Celiz, A.D., Smith, J., Patel, A.K., and Hook, A.L. (2015). Discovery of a Novel Polymer for Human Pluripotent Stem Cell Expansion and Multilineage Differentiation. Adv Mater 27, 4006-12.

Cereghini, S. (1996). Liver-enriched transcription factors and hepatocyte differentiation. FASEB J 10, 267-82.

Chakraborty, C., Shah, K.D., and Caob, W.G. (2010). Potentialities of induced pluripotent stem (iPS) cells for treatment of diseases. Curr Mol Med 10, 756-62.

Chambers, I., Colby, D., Robertson, M., Nichols, J., Lee, S., Tweedie, S., and Smith, A. (2003). Functional expression cloning of Nanog, a pluripotency sustaining factor in embryonic stem cells. Cell 113, 643-55.

Chapman, L.M., and Eddy, E.M. (1989). A protein associated with the mouse and rat hepatocyte junctional complex. Cell Tissue Res 257, 333-41.

Chedid, A., Mendenhall, C.L., and Moritz, T.E. (1993). Expression of the beta 1 chain (CD29) of integrins and CD45 in alcoholic liver disease. The VA Cooperative Study Group No. 275. Am J Gastroenterol 88, 1920-7.

Chen, D., Lepar, G., and Kemper, B. (1994). A transcriptional regulatory element common to a large family of hepatic cytochrome P450 genes is a functional binding site of the orphan receptor HNF-4. J Biol Chem 269, 5420-7

Chen, G., Gulbranson, D.R., Hou, Z., Bolin, J.M., and Ruotti, V. (2011). Chemically defined conditions for human iPSC derivation and culture. Nat Methods 8, 424-9.

Chen, Y., Tseng, C., Wang, H., Kuo, H., Yang, V.W., and Lee, O.K. (2012). Rapid generation of mature hepatocyte-like cells from human induced pluripotent stem cells by an efficient three-step protocol. Hepatology 55, 1193-1203.

Cheng, L., Hammond, H., Ye, Z., Zhan, X., and Dravid, G. (2003). Human adult marrow cells support prolonged expansion of human embryonic stem cells in culture. Stem Cells 21, 131-42.

Cheng, N., Wauthier, E., and Reid, L.M. (2008). Mature human hepatocytes from ex vivo differentiation of alginate-encapsulated hepatoblasts. Tissue Eng Part A 14, 1-7.

Cheng, W., Guo, L., Zhang, Z., Soo, H.M., Wen, C., and Wu, W. (2006). HNF factors form a network to regulate liver-enriched genes in zebrafish. Dev Biol 294, 482-96.

Cirillo, L.A., and Zaret, K.S. (1999). An early developmental transcription factor complex that is more stable on nucleosome core particles than on free DNA. Mol Cell 4, 961-9.

Cirillo, L.A., Lin, F.R., Cuesta, I., Friedman, D., and Jarnik, M. (2002). Opening of compacted chromatin by early developmental transcription factors HNF3 (FoxA) and GATA-4. Mol Cellecula 9, 279-89.

Clements, D., Cameleyre, I., and Woodland, H.R. (2003). Redundant early and overlapping larval roles of Xsox17 subgroup genes in Xenopus endoderm development. Mech Dev 120, 337-48.

Clotman, F. (2005). Control of liver cell fate decision by a gradient of TGF signaling modulated by Onecut transcription factors. Genes &Amp; Development 19, 1849-1854.

Cogger, V.C., McNerney, G.P., Nyunt, T., and DeLeve, L.D. (2010). Three-dimensional structured illumination microscopy of liver sinusoidal endothelial cell fenestrations. J Struct Biol 171, 382-8.

Cooper, A.R., and MacQueen, H.A. (1983). Subunits of laminin are differentially synthesized in mouse eggs and early embryos. Dev Biol 96, 467-71.

Corson, L.B. (2003). Spatial and temporal patterns of ERK signaling during mouse embryogenesis. Development 130, 4527-4537.

Cortes, J.L., Sanchez, L., and Catalina, P. (2008). Whole-blastocyst culture followed by laser drilling technology enhances the efficiency of ICM isolation and ESC derivation from good-and poor-quality mouse embryos: new insights for derivation of human embryonic stem cells lines. Stem Cells Dev 17, 255-67.

Costa, R.H., Kalinichenko, V.V., and Holterman, A. (2003). Transcription factors in liver development, differentiation, and regeneration. Hepatology 38, 1331-47.

Couvelard, A., Bringuier, A.F., Dauge, M.C., Nejjari, M., Darai, E., Benifla, J.L., Feldmann, G., Henin, D., and Scoazec, J.Y. (1998). Expression of integrins during liver organogenesis in humans. Hepatology 27, 839-847.

D'Amour, K.A., Agulnick, A.D., Eliazer, S., Kelly, O.G., Kroon, E., and Baetge, E.E. (2005). Efficient differentiation of human embryonic stem cells to definitive endoderm. Nature Biotechnology 23, 1534.

Dang, J.M., and Leong, K.W. (2007). Myogenic Induction of Aligned Mesenchymal Stem Cell Sheets by Culture on Thermally Responsive Electrospun Nanofibers. Adv. Mater. 19, 2775-2779.

Davis, R.L., Weintraub, H., and Lassar, A.B. (1987). Expression of a single transfected cDNA converts fibroblasts to myoblasts. Cell 51, 987-1000.

Decaens, C., Durand, M., Grosse, B., and Cassio, D. (2008). Which in vitro models could be best used to study hepatocyte polarity? Biol. Cell 100, 387-98.

Deutsch, G., Jung, J., Zheng, M., Lóra, J., and Zaret, K.S. (2001). A bipotential precursor population for pancreas and liver within the embryonic endoderm. Development.

Dianat, N., Dubois-Pot-Schneider, H., Steichen, C., Desterke, C., Leclerc, P., Raveux, A., Combettes, L., Weber, A., Corlu, A., and Dubart-Kupperschmitt, A. (2014). Generation of functional cholangiocyte-like cells from human pluripotent stem cells and HepaRG cells. Hepatology 60, 700-714.

Diaz, JJ., Tourniare, G., and Bardely, M. (2007). Microarray platforms for enzymatic and cell-based assays. Chem Soc Rev 36, 449-57.

Dich, J., Vind, C., and Grunnet, N. (1988). Long-term culture of hepatocytes: Effect of hormones on enzyme activities and metabolic capacity. Hepatology 8, 39-45.

Doherty, P., Fruns, M., Seaton, P., Dickson, G., and Barton, C.H. (1990). A threshold effect of the major isoforms of NCAM on neurite outgrowth. Nature 343, 464-6.

Draper, J.S., Smith, K., Gokhale, P., Moore, H.D., Maltby, E., Johnson, J., Meisner, L., Zwaka, T.P., Thomson, J.A., and ANDREWS, P.W. (2003). Recurrent gain of chromosomes 17q and 12 in cultured human embryonic stem cells. Nature Biotechnology 22, 53-4.

Du, C., Narayanan, K., Leong, M.F., and Wan, A. (2014). Induced pluripotent stem cell-derived hepatocytes and endothelial cells in multi-component hydrogel fibers for liver tissue engineering. Biomaterials 35, 6006-14.

Duan, Y., Ma, X., Ma, X., Zou, W., Wang, C., Bahbahan, I.S., Ahuja, T.P., Tolstikov, V., and Zern, M.A. (2010). Differentiation and characterization of metabolically functioning hepatocytes from human embryonic stem cells. Stem Cells 28, 674-86-686.

Duboc, V., Lapraz, F., Saudemont, A., and Bessodes, N. (2010). Nodal and BMP2/4 pattern the mesoderm and endoderm during development of the sea urchin embryo. Development 137, 223-35.

Duncan, M.B., Yang, C., and Tanjore, H. (2013). Type XVIII collagen is essential for survival during acute liver injury in mice. Dis Model Mech 6, 942-51.

Duncan, S.A. (2003). Mechanisms controlling early development of the liver. Mech Dev 120, 19-33.

Dunn, J.C., Yarmush, M.L., Koebe, H.G., and Tompkins, R.G. (1989). Hepatocyte function and extracellular matrix geometry: long-term culture in a sandwich configuration. FASEB J 3, 174-7.

Efe, J.A., Hilcove, S., Kim, J., Zhou, H., and Ouyang, K. (2011). Conversion of mouse fibroblasts into cardiomyocytes using a direct reprogramming strategy. Nat Cell Biol 13, 215-22.

Elaut, G., Henkens, T., Papeleu, P., Snykers, S., Vinken, M., Vanhaecke, T., and Rogiers, V. (2006). Molecular mechanisms underlying the dedifferentiation process of isolated hepatocytes and their cultures. Curr. Drug Metab. 7, 629-60.

Ellerström, C., Strehl, R., Moya, K., and Andersson, K. (2006). Derivation of a xeno-free human embryonic stem cell line. Stem Cells 24, 2170-6.

Endo, H., Niioka, M., Sugioka, Y., Itoh, J., and Kameyama, K. (2011). Matrix metalloproteinase-13 promotes recovery from experimental liver cirrhosis in rats. Pathobiology 78, 239-52.

Engler, A.J., Sen, S., Sweeney, H.L., and Discher, D.E. (2006). Matrix elasticity directs stem cell lineage specification. Cell 126, 677-689.

Erickson, G.A., Bolin, S.R., and Landgraf, J.G. (1990). Viral contamination of fetal bovine serum used for tissue culture: risks and concerns. Dev Biol Stand 75, 173-5.

Evans, M.J., Hahn, von, T., Tscherne, D.M., and Syder, A.J. (2007). Claudin-1 is a hepatitis C virus co-receptor required for a late step in entry. Nature 443, 801-5.

Ezaki, T., Guo, R.J., Li, H., and Reynolds, A.B. (2007). The homeodomain transcription factors Cdx1 and Cdx2 induce E-cadherin adhesion activity by reducing β-and p120-catenin tyrosine phosphorylation. Am J Physiol Gastrointest Liver Physiol 293, 54-65.

Farzaneh, Z., Pakzad, M., Vosough, M., and Pournasr, B. (2014). Differentiation of human embryonic stem cells to hepatocyte-like cells on a new developed xeno-free extracellular matrix. Histochemistry Cell Biol 142, 217-26.

Fassler, R. and Meyer, M. (2008). Consequences of lack of beta 1 integrin gene expression in mice. Genes Dev 9, 1896-1908

Faulkner, A. (2013). Development of a valve-based cell printer for the formation of human embryonic stem cell spheroid aggregates. Biofabrication 5, 015013.

Ferrer, J. (2002). A Genetic Switch in Pancreatic β-Cells Implications for Differentiation and Haploinsufficiency. Diabetes 51, 2355-62.

Fiegel, H.C., Kaufmann, P.M., and Bruns, H. (2008). Hepatic tissue engineering: From transplantation to customized cell-based liver directed therapies from the laboratory. J Cell Mol Med 12, 56-66.

Fiegel, H.C., Lange, C., and Kneser, U. (2006). Fetal and adult liver stem cells for liver regeneration and tissue engineering. J Cell Mol Med 10, 577-87.

Fletcher, J., Cui, W., Samuel, K., Black, J.R., Hannoun, Z., Currie, I.S., Terrace, J.D., Payne, C., Filippi, C., Newsome, P., *et al*. (2008). The Inhibitory Role of Stromal Cell Mesenchyme on Human Embryonic Stem Cell Hepatocyte Differentiation is Overcome by Wnt3a Treatment. Cloning And Stem Cells 10, 331-340.

Fong, C.Y., and Bongso, A. (2006). Derivation of human feeders for prolonged support of human embryonic stem cells. Methods Mol Biol 331, 129-35.

Forbes, S., Vig, P., Poulsom, R., and Thomas, H. (2002). Hepatic stem cells. J. Pathol 197, 510.

Fox, I.J., and Strom, S.C. (2008). To Be or Not to Be: Generation of Hepatocytes From Cells Outside the Liver. Gastroenterology 134, 878-881.

Fraczek, J., Bolleyn, J., Vanhaecke, T., and Rogiers, V. (2013). Primary hepatocyte cultures for pharmaco-toxicological studies: at the busy crossroad of various anti-dedifferentiation strategies. Arch Toxicol 87, 577-610.

Freije, J.M., Diez, I., Balbin, M., Sanchez, LM., Blasco, R., Tolivia, J., and Lopez-Otin, C. (1994). Molecular cloning and expression of collagenase-3, a novel human matrix metalloproteinase produced by breast carcinomas. J Biol Chem 269, 16766-73.

Friedman, J.R., and Kaestner, K.H. (2006). The Foxa family of transcription factors in development and metabolism. Cell Mol Life Sci 63, 2317-28.

Friedman, S.L. (2008). Hepatic stellate cells: protean, multifunctional, and enigmatic cells of the liver. Physiol Rev 88, 125-72.

Fukuda, J., Sakiyama, R., and Nakazawa, K. (2001). Mass preparation of primary porcine hepatocytes and the design of a hybrid artificial liver module using spheroid culture for a clinical trial. Int J of Art Organs 4, 799–806.

Fujiyoshi, M., and Ozaki, M. (2010). Molecular mechanisms of liver regeneration and protection for treatment of liver dysfunction and diseases. J Hepatobiliary Pancreat Sci 18, 13-22.

Furuse, M., Fujita, K., Hiiragi, T., and Fujimoto, K. (1998). Claudin-1 and-2: novel integral membrane proteins localizing at tight junctions with no sequence similarity to occludin. J Cell Biol 141, 1539-50.

Fusaki, N., Ban, H., Nishiyama, A., and Saeki, K. (2009). Efficient induction of transgene-free human pluripotent stem cells using a vector based on Sendai virus, an RNA virus that does not integrate into the host genome. Proc Jpn Acad Ser B Phys Biol Sci 85, 348-62.

Gadue, P., Huber, T.L., and Paddison, P.J. (2006). Wnt and TGF-β signaling are required for the induction of an in vitro model of primitive streak formation using embryonic stem cells. Proc Natl Acad Sci USA 103, 16806-11

Gai, H., Nguyen, D.M., Moon, Y.J., Aguila, J.R., Fink, L.M., Ward, D.C., and Ma, Y. (2010). Generation of murine hepatic lineage cells from induced pluripotent stem cells. Differentiation 79, 171-81.

Gao, S.Y., Lees, J.G., Wong, J.C.Y., Croll, T.I., George, P., Cooper-White, J.J., and Tuch, B.E. (2009). Modeling the adhesion of human embryonic stem cells to poly(lactic- co-glycolic acid) surfaces in a 3D environment. J. Biomed. Mater. Res. 92, 683-92.

Garcia-Irigoyen, O., Carotti, S., and Latasa, M.U. (2014). Matrix metalloproteinase-10 expression is induced during hepatic injury and plays a fundamental role in liver tissue repair. Liver Int 34, 257-70.

Gardner, R.L., and Rossant, J. (1979). Investigation of the fate of 4· 5 day post-coitum mouse inner cell mass cells by blastocyst injection. J Embryol Exp Morphol 52, 141-52.

Gasimli, L., and Linhardt, R.J. (2012). Proteoglycans in stem cells. Biotechnol Appl Biochem 59, 65-76.

Gaudio, E., Carpino, G., Cardinale, V., and Franchitto, A. (2009). New insights into liver stem cells. Dig Livr Dis 41, 455-62.

Gerecht, S., Burdick, J.A., and Ferreira, L.S. (2007). Hyaluronic acid hydrogel for controlled self-renewal and differentiation of human embryonic stem cells. Pro Natl Acad Sci USA 104, 11298-303.

Ghodsizadeh, A., Hosseinkhani, H., and Piryaei, A. (2014). Galactosylated collagen matrix enhanced in vitro maturation of human embryonic stem cell-derived hepatocyte-like cells. Biotechnol Lett 36, 1095-106.

Giobbe, G.G., Michielin, F., Luni, C., Giulitti, S., and Martewicz, S. (2015). Functional differentiation of human pluripotent stem cells on a chip. Nat. Methods 12, 637.

Godoy, P., Lakkapamu, S., Schug, M., and Bauer, A. (2010). Dexamethasone-dependent versus-independent markers of epithelial to mesenchymal transition in primary hepatocytes. Biological Chemistry 391, 73-83.

Godoy, P., Lakkapamu, S., Schug, M., Bauer, A., Stewart, J.D., Bedawi, E., Hammad, S., Amin, J., Marchan, R., Schormann, W., *et al*. (2009). Dexamethasone-dependent versus -independent markers of epithelial to mesenchymal transition in primary hepatocytes. Biological Chemistry 391, 1-11.

Godoy, P., Schmidt-Heck, W., Natarajan, K., Lucendo-Villarin, B., *et al* (2015). Gene networks and transcription factor motifs defining the differentiation of stem cells into hepatocyte-like cells. J Hepatol pii: S0168-8278(15)00340-2

Goessling, W., North, T.E., Lord, A.M., Ceol, C., and Lee, S. (2008). APC mutant zebrafish uncover a changing temporal requirement for wnt signaling in liver development. Dev Biol 320, 161-74.

Gómez-Lechón, M.J., Castell, J.V., and Donato, M.T. (2010). The Use of Hepatocytes to Investigate Drug Toxicity. In Hepatocytes, (Totowa, NJ: Humana Press), pp. 389-415.

Gonzalez, F.J. (2007). Regulation of hepatocyte nuclear factor 4 alpha-mediated transcription. Drug Metabolism And Pharmacokinetics 23, 2-7.

Green, J.B., and Smith, J.C. (1990). Graded changes in dose of a Xenopus activin A homologue elicit stepwise transitions in embryonic cell fate. Nature 347, 391-4.

Greenhough, S., Medine, C.N., and Hay, D.C. (2010). Pluripotent stem cell derived hepatocyte like cells and their potential in toxicity screening. Toxicology 278, 250-5.

Griffith, L.G., and Swartz, M.A. (2006). Capturing complex 3D tissue physiology in vitro. Nat Rev Mol Cell Biol 7, 211-24.

Gualdi, R., Bossard, P., Zheng, M., Hamada, Y., Coleman, J.R., and Zaret, K.S. (1996). Hepatic specification of the gut endoderm in vitro: cell signaling and transcriptional control. Genes &Amp; Development 10, 1670-1682.

Guillouzo, A. (1998). Liver cell models in in vitro toxico... [Environ Health Perspect. 1998] - PubMed - NCBI. Environ. Health Perspect. 106 Suppl 2, 511-532.

Guillouzo, A., Corlu, A., Aninat, C., Glaise, D., and Morel, F. (2007). The human hepatoma HepaRG cells: a highly differentiated model for studies of liver metabolism and toxicity of xenobiotics. Chem Biol Interact 168, 66-73.

Gullberg, D., Turner, D.C., Borg, T.K., and Terracio, L. (1990). Different β 1-integrin collagen receptors on rat hepatocytes and cardiac fibroblasts. Exp Cell Res 190, 254-64.

Gumbiner, B.M. (1996). Cell adhesion: the molecular basis of tissue architecture and morphogenesis. Cell 84, 345-57-357.

Gurdon, J.B., and Wilmut, I. (2011). Nuclear transfer to eggs and oocytes. Cold Spring Harbor Perspectives Biol 3, pii:a002659.

Hall, A.K., Nelson, R., and Rutishauser, U. (1990). Binding properties of detergent-solubilized NCAM. J Cell Biol 110, 817-24.

Hamilton, D.W., and Brunette, D.M. (2007). The effect of substratum topography on osteoblast adhesion mediated signal transduction and phosphorylation. Biomaterials 28, 1806-1819.

Han, S., Dziedzic, N., Gadue, P., Keller, G.M., and Gouon-Evans, V. (2011). An Endothelial Cell Niche Induces Hepatic Specification Through Dual Repression of Wnt and Notch Signaling. Stem Cells 29, 217-228.

Han, Y.P. (2006). Matrix metalloproteinases, the pros and cons, in liver fibrosis. J Gastroenterol Hepatol 21, Suppl 3: S88-91

Hannoun, Z., Fletcher, J., Greenhough, S., Medine, C., Samuel, K., Sharma, R., Pryde, A., Black, J.R., Ross, J.A., Wilmut, I., *et al*. (2010). The comparison between conditioned media and serum-free media in human embryonic stem cell culture and differentiation. Cell Reprogram 12, 133-40.

Hansen, A., Corless, S., Cleland, A., Petrik, J., Gilbert, N., and Bradley, M. (2013). Polymers for the cell-specific immobilisation of megakaryocytic cell lines. Macromol. Biosci. 13, 437-443.

Hardy, K., and Spanos, S. (2002). Growth factor expression and function in the human and mouse preimplantation embryo. J Endocrinol 172, 221-36.

Hardy, K., Handyside, A.H., and Winston, R.M. (1989). The human blastocyst: cell number, death and allocation during late preimplantation development in vitro. Development 107, 597-604.

Harris, T.E. (2001). CCAAT/Enhancer-binding Protein-alpha Cooperates with p21 to Inhibit Cyclin-dependent Kinase-2 Activity and Induces Growth Arrest Independent of DNA Binding. Journal Of Biological Chemistry 276, 29200-29209.

Hart, S.N., Cui, Y., Klaassen, C.D., and Zhong, X. (2009). Three patterns of cytochrome P450 gene expression during liver maturation in mice. Drug Metabolism Dispos 37, 116-21.

Hay, D.C., Fletcher, J., Payne, C., Terrace, J.D., Gallagher, R.C.J., Snoeys, J., Black, J.R., Wojtacha, D., Samuel, K., and Hannoun, Z. (2008a). Highly efficient differentiation of hESCs to functional hepatic endoderm requires ActivinA and Wnt3a signaling. Proc. Natl. Acad. Sci. U.S.A. 105, 12301-12306.

Hay, D.C., Pernagallo, S., Diaz-Mochon, J.J., Medine, C.N., Greenhough, S., Hannoun, Z., Schrader, J., Black, J.R., Fletcher, J., Dalgetty, D., *et al*. (2011). Unbiased screening of polymer libraries to define novel substrates for functional hepatocytes with inducible drug metabolism. Stem Cell Research 6, 92-102.

Hay, D.C., Zhao, D., Fletcher, J., Hewitt, Z.A., McLean, D., Urruticoechea-Uriguen, A., Black, J.R., Elcombe, C., Ross, J.A., Wolf, R., *et al*. (2008b). Efficient Differentiation of Hepatocytes from Human Embryonic Stem Cells Exhibiting Markers Recapitulating Liver Development In Vivo. Stem Cells 26, 894-902.

Hazeltine, L.B., Selekman, J.A., and Palecek, S.P. (2013). Engineering the human pluripotent stem cell microenvironment to direct cell fate. Biotechnol. Adv.

Heino, J. (2007). The collagen family members as cell adhesion proteins. Bioessays 29, 1001.

Heldin, C.H., Miyazono, K., and Dijke, Ten, P. (1997). TGF-β signalling from cell membrane to nucleus through SMAD proteins. Nature.

Heller, M.J. (2002). DNA microarray technology: devices, systems, and applications. Annu. Rev. Biomed. Eng. 4, 129-53.

Herrera, M.B., Bruno, S., Buttiglieri, S., Tetta, C., and Gatti, S. (2006). Isolation and characterization of a stem cell population from adult human liver. Stem Cells 24, 2840-50.

Hewitt, N.J., and Lechón, M.G. (2007). Primary hepatocytes: current understanding of the regulation of metabolic enzymes and transporter proteins, and

pharmaceutical practice for the use of hepatocytes in metabolism, enzyme induction, transporter, clearance and hepatotoxicity studies. Drug Metab Rev 39, 159-234.

Hewitt, N.J., LeCluyse, E.L., and Ferguson, S.S. (2007). Induction of hepatic cytochrome P450 enzymes: methods, mechanisms, recommendations, and in vitro-in vivo correlations. Xenobiotica 37, 1196-224.

Hiramatsu, K., Matsumoto, Y., Miyazaki, M., Tsubouchi, H., Yamamoto, I., and Gohda, E. (2005). Inhibition of hepatocyte growth factor production in human fibroblasts by ursodeoxycholic acid. Biol. Pharm. Bull. 28, 619-24.

Hoffman, L.M., and Carpenter, M.K. (2005). Characterization and culture of human embryonic stem cells. Nature Biotechnology 23, 699-708.

Hook *et al*., (2012). Combinatorial discovery of polymers resistant to bacterial attachment. Nat Biotechnol 30, 868-75.

Hook, A.L., Anderson, D.G., Langer, R., and Williams, P. (2010). High throughput methods applied in biomaterial development and discovery. Biomaterials 31, 187-98.

Hook, A.L., Chang, C.Y., Yang, J., and Atkinson, S. (2013). Discovery of novel materials with broad resistance to bacterial attachment using combinatorial polymer microarrays. Adv Mater 25, 2524-7.

Hovatta, O. (2006). Derivation of human embryonic stem cell lines, towards clinical quality. Reprod Fertil Dev 18, 823-8.

How, S.E., Yingyongnarongkul, B., Fara, M.A. and Diaz-Monchon, JJ. (2004). Polyplexes and lipoplexes for mammalian gene delivery: from traditional to microarray screening. Comb Chem High Throughput Screen 7, 423-30.

Huang, H., Ruan, H., Aw, M.Y., Hussain, A., Guo, L., Gao, C., Qian, F., Leung, T., Song, H., Kimelman, D., *et al*. (2008). Mypt1-mediated spatial positioning of Bmp2-producing cells is essential for liver organogenesis. Development 135, 3209-18-3218.

Huang, P., He, Z., Ji, S., Sun, H., Xiang, D., Liu, C., and Hu, Y. (2011). Induction of functional hepatocyte-like cells from mouse fibroblasts by defined factors. Nature 475, 286-9.

Huang, P., Zhang, L., Gao, Y., He, Z., Yao, D., Wu, Z., Cen, J., Chen, X., Liu, C., Hu, Y., *et al*. (2014). Direct Reprogramming of Human Fibroblasts to Functional and Expandable Hepatocytes. Cell Stem Cell 14, 370-384.

Hynes, R.O. (1992). Integrins: versatility, modulation, and signaling in cell adhesion. Cell 69, 11-25.

Ichikawa, T., and Horie, K. (2006). Steroid and xenobiotic receptor SXR mediates vitamin K2-activated transcription of extracellular matrix-related genes and collagen accumulation in osteoblastic cells. J Biol Chem 281, 16927-34.

Ieda, M., Fu, J.D., and Delgado, P. (2010). Direct reprogramming of fibroblasts into functional cardiomyocytes by defined factors. Cell 42, 375-86.

Iida, I., Johkura, K., Teng, R., Kubota, S., Cui, L., Zhao, X., Ogiwara, N., Okouchi, Y., Asanuma, K., Nakayama, J., *et al*. (2003). Immunohistochemical Localization of Hepatocyte Growth Factor Activator (HGFA) in Developing Mouse Liver Tissues: Heterogeneous Distribution of HGFA Protein. Journal Of Histochemistry &Amp; Cytochemistry 51, 1139-1149.

Ilic, D. (2006). Culture of human embryonic stem cells and the extracellular matrix microenvironment. Regen Med 1, 95-101.

Iredale, J.P. (2007). Models of liver fibrosis: exploring the dynamic nature of inflammation and repair in a solid organ. J. Clin. Invest 117, 539-48.

Irwin, E.F., Gupta, R., Dashti, D.C., and Healy, K.E. (2011). Engineered polymer-media interfaces for the long-term self-renewal of human embryonic stem cells. Biomaterials 32, 6912-9.

Ishii, T., Fukumitsu, K., Yasuchika, K., Adachi, K., Kawase, E., Suemori, H., Nakatsuji, N., Ikai, I., and Uemoto, S. (2008). Effects of extracellular matrixes and growth factors on the hepatic differentiation of human embryonic stem cells. Am. J. Physiol. Gastrointest. Liver Physiol. 295, G313-21.

Ishikawa, K., Masui, T., Ishikawa, K., and Shiojiri, N. (2001). Immunolocalization of hepatocyte growth factor and its receptor (c-Met) during mouse liver development. Histochemistry And Cell Biology 116, 453-462.

Ito, Y., Matsui, T., Kamiya, A., Kinoshita, T., and Miyajima, A. (2000). Retroviral gene transfer of signaling molecules into murine fetal hepatocytes defines distinct roles for the STAT3 and ras pathways during hepatic development. Hepatology 32, 1370-6.

Iyer, V.V., Yang, H., and Ierapetritou, M.G. (2010). Effects of glucose and insulin on HepG2-C3A cell metabolism. Biotechnol Bioeng 107, 347-56.

Jackson, C. (2002). Matrix metalloproteinases and angiogenesis. Curr Opin Nephro Hypertens 11, 295-9

Jaeschke, H. (2007). Kupffer cells. Textbook Of Hepatology: From Basic Science To Clinical Practice, 3er edition.

Jochems, C., and van der Valk, J. (2002). The use of fetal bovine serum: ethical or scientific problem? Altern Lab Anim 30, 219-27.

Joddar, B., Hoshiba, T., Chen, G., and Ito, Y. (2014). Stem cell culture using cell-derived substrates. Biomaterials Science 2, 1595-1603.

Johnson, M.H., Chisholm, J.C., and Fleming, T.P. (1986). A role for cytoplasmic determinants in the development of the mouse early embryo? J Embryol Exp Morphol 97, Suppl 97-121.

Johnson, P.F. (1990). Transcriptional activators in hepatocytes. Cell Growth Differ 1, 47-52.

Josephson, R., Sykes, G., Liu, Y., Ording, C., Xu, W., Zeng, X., Shin, S., Loring, J., Maitra, A., Rao, M.S., *et al*. (2006). A molecular scheme for improved characterization of human embryonic stem cell lines. BMC Biol. 4, 28.

Jung, J. (1999). Initiation of Mammalian Liver Development from Endoderm by Fibroblast Growth Factors. Science 284, 1998-2003.

Jungermann,R., Katz, N. (1989). Functional specialization of different hepatocyte populations. Physiological Reviews 69, 708-764.

Kamiya, A., and Gonzalez, F.J. (2004). TNF-α regulates mouse fetal hepatic maturation induced by oncostatin M and extracellular matrices. Hepatology 40, 527-536.

Kamiya, A., Kinoshita, T., and Miyajima, A. (2001). Oncostatin M and hepatocyte growth factor induce hepatic maturation via distinct signaling pathways. FEBS Lett. 492, 90-94.

Kamiya, A., Kinoshita, T., Ito, Y., and Matsui, T. (1999). Fetal liver development requires a paracrine action of oncostatin M through the gp130 signal transducer. EMBO J 18, 2127-36.

Kamiya, A., Kojima, N., Kinoshita, T., Sakai, Y., and Miyaijma, A. (2002). Maturation of fetal hepatocytes in vitro by extracellular matrices and oncostatin M: induction of tryptophan oxygenase. Hepatology 35, 1351-9-1359.

Kang, H., Shih, Y., Hwang, Y., Wen, C., Rao, V., and Seo, T. (2014). Mineralized gelatin methacrylate-based matrices induce osteogenic differentiation of human induced pluripotent stem cells. Acta Biomaterialia.

Kannagi, R., Cochran, N.A., Ishigami, F., Hakomori, S., Andrews, P.W., Knowles, B.B., and Solter, D. (1983). Stage-specific embryonic antigens (SSEA-3 and -4) are epitopes of a unique globo-series ganglioside isolated from human teratocarcinoma cells. The EMBO Journal 2, 2355-61.

Kasuya, J., Sudo, R., Mitaka, T., Ikeda, M., and Tanishita, K. (2010). Hepatic stellate cell-mediated three-dimensional hepatocyte and endothelial cell triculture model. Tissue Eng Part A 17, 361-70.

Kaufman, D.S., and Thomson, J.A. (2002). Human ES cells--haematopoiesis and transplantation strategies. J. Anat. 200, 243-8-248.

Kehat, I., Kenyagin-Karsenti, D., Snir, M., Segev, H., Amit, M., Gepstein, A., Livne, E., Binah, O., Itskovitz-Eldor, J., and Gepstein, L. (2001). Human embryonic stem cells can differentiate into myocytes with structural and functional properties of cardiomyocytes. The Journal Of Clinical Investigation 108, 407-14.

Keshava, C., McCanlies, E.C. and Weston, A. (2004). CYP3A4 polymorphisms—potential risk factors for breast and prostate cancer: a HuGE review. Am J Epidemiol 160, 825-41

Kessenbrock, K., Plaks, V., and Werb, Z. (2010). Matrix metalloproteinases: regulators of the tumor microenvironment. Cell 141, 52-67.

Khan, F., Tare, R.S., Kanczler, J.M., Oreffo, R.O.C., and Bradley, M. (2010). Strategies for cell manipulation and skeletal tissue engineering using high-throughput polymer blend formulation and microarray techniques. Biomaterials 31, 2216-2228.

Khetani, S.R., and Bhatia, S.N. (2008). Microscale culture of human liver cells for drug development. Nat Biotechnol 26, 120-6.

Kim, H.S., Oh, S.K., Park, Y.B., Ahn, H.J., and Sung, K.C. (2005). Methods for derivation of human embryonic stem cells. Stem Cells 23, 1228-33.

Kim, J.B., Greber, B., and Araúzo, M.J. (2009). Direct reprogramming of human neural stem cells by OCT4. Nature 461, 649-3.

Kim, J.J., Park, B.C., Kido, Y., and Accili, D. (2001). Mitogenic and metabolic effects of type I IGF receptor overexpression in insulin receptor-deficient hepatocytes. Endocrinology 142, 3354-60.

Kim, S.W., Yoon, S.J., Chuong, E., Oyolu, C., and Wills, A.E. (2011). Chromatin and transcriptional signatures for Nodal signaling during endoderm formation in hESCs. Dev Biol 357, 492-504.

Kim, Y., and Rajagopalan, P. (2010). 3D hepatic cultures simultaneously maintain primary hepatocyte and liver sinusoidal endothelial cell phenotypes. Plos ONE 5, e15456.

Klim, J.R., Li, L., Wrighton, P.J., and Piekarczyk, M.S. (2010). A defined glycosaminoglycan-binding substratum for human pluripotent stem cells. Nature 7, 989-94.

Knäuper, V., and López, C. (1996). Biochemical characterization of human collagenase-3. Journal Of Biological Chemistry 271, 1544.

Kobayashi, N., Okitsu, T., and Tanaka, N. (2003). Cell choice for bioartificial livers. Keio J Med 52, 151-7.

Kohn, J. (2004). New approaches to biomaterials design. Nat Materials 3, 745-7.

Kojima, T., Yamamoto, T., Murata, M., and Chiba, H. (2003). Regulation of the blood–biliary barrier: interaction between gap and tight junctions in hepatocytes. Med Electron Microsc 36, 157-64.

Konopka, G., Tekiela, J., Iverson, M., Wells, C., and Duncan, S.A. (2007). Junctional adhesion molecule-A is critical for the formation of pseudocanaliculi and modulates E-cadherin expression in hepatic cells. Journal Of Biological Chemistry 282, 28137-28148.

Kosik, K.S., Donahue, C.P., Israely, I., Liu, X., and Ochiishi, T. (2005). δ-Catenin at the synaptic–adherens junction. Trends Cell Biol 15, 172-8.

Kuo, C.J., Conley, P.B., Chen, L., Sladek, F.M., and Darnell, J.E. (1992). A transcriptional hierarchy involved in mammalian cell-type specification. Nature 355, 457.

Lavon, N., Yanuka, O., and Benvenisty, N. (2004). Differentiation and isolation of hepatic-like cells from human embryonic stem cells. Differentiation 72, 230-238.

Lawson, K.A., and Pedersen, R.A. (1987). Cell fate, morphogenetic movement and population kinetics of embryonic endoderm at the time of germ layer formation in the mouse. Development 101, 627-652.

Lawson, K.A., Meneses, J.J., and Pedersen, R.A. (1991). Clonal analysis of epiblast fate during germ layer formation in the mouse embryo. Development.

LeCluyse, E.L. (2001). Human hepatocyte culture systems for the in vitro evaluation of cytochrome P450 expression and regulation. European Journal Of Pharmaceutical Sciences.

LeCluyse, E.L., Alexandre, E., and Hamilton, G.A. (2005). Isolation and culture of primary human hepatocytes. Methods Mol Biol 290, 207-29.

LeCluyse, E.L., Bullock, P.L., and Parkinson, A. (1996). Cultured rat hepatocytes. Pharm Biotechnol 8, 121-59.

Leite, S.B., Teixeira, A.P., Miranda, J.P., and Tostões, R.M. (2011). Merging bioreactor technology with 3D hepatocyte-fibroblast culturing approaches: improved in vitro models for toxicological applications. Toxicology In Vitro.

Lemaigre, F., and Zaret, K.S. (2004). Liver development update: new embryo models, cell lineage control, and morphogenesis. Current Opinion In Genetics &Amp; Development.

Levine, A.J., Besser, D., and Hemmati, A. (2005). TGFβ/activin/nodal signaling is necessary for the maintenance of pluripotency in human embryonic stem cells.

Li, D., Zhou, J., Chowdhury, F., and Cheng, J. (2011). Role of mechanical factors in fate decisions of stem cells. Regen Med 6, 229-40.

Li, J., Li, L.J., Cao, H.C., Sheng, G.P., Yu, H.Y., and Xu, W. (2005). Establishment of highly differentiated immortalized human hepatocyte line with simian virus 40 large tumor antigen for liver based cell therapy. A 51, 262-8.

Li, J., Ning, G., and Duncan, S.A. (2000). Mammalian hepatocyte differentiation requires the transcription factor HNF-4α. Genes Dev 14, 464-74.

Li, L., Bennett, S., and Wang, L. (2012). Role of E-cadherin and other cell adhesion molecules in survival and differentiation of human pluripotent stem cells. Cell Adh Migr 6, 59-73

Li, Y.J., Chung, E.H., and Rodriguez, R.T. (2006). Hydrogels as artificial matrices for human embryonic stem cell self-renewal. J. Biomed. Mater. Res. 79A, 1-5.

Li, Z., Guo, X., Matsushita, S., and Guan, J. (2011). Differentiation of cardiosphere-derived cells into a mature cardiac lineage using biodegradable poly (N-isopropylacrylamide) hydrogels. Biomaterials.

Liberski, A.R., Tizzard, G.J., and Diaz, J.J. (2008). Screening for polymorphs on polymer microarrays. J Comb Chem 10, 24-7.

Lim, J.Y., and Donahue, H.J. (2007). Cell Sensing and Response to Micro- and Nanostructured Surfaces Produced by Chemical and Topographic Patterning. Tissue Engineering 13, 1879-1891.

Lin, J.H. (2006). CYP induction-mediated drug interactions: in vitro assessment and clinical implications. Pharm Res 23, 1089-116.

Liu, A., Garg, P., Yang, S., Gong, P., and Pallero, M.A. (2009). Epidermal growth factor-like repeats of thrombospondins activate phospholipase Cγ and increase epithelial cell migration through indirect epidermal growth factor receptor activation. J boil Chem 284, 6389-402.

Liu, H., Ye, Z., Kim, Y., Sharkis, S., and Jang, Y.Y. (2010). Generation of endoderm-derived human induced pluripotent stem cells from primary hepatocytes. Hepatology 51, 1810-9.

Liu, S., Jin, M., Quan, Y., Kamiyama, F., and Katsumi, H. (2012). The development and characteristics of novel microneedle arrays fabricated from hyaluronic acid, and their application in the transdermal delivery of insulin. J Control Release 161, 933-41.

Liu, W., Yin, Y., Long, X., Luo, Y., Jiang, Y., and Zhang, W. (2009b). Derivation and characterization of human embryonic stem cell lines from poor quality embryos. J Genet Genomics 36, 229-39.

Lokmane, L., Haumaitre, C., Garcia-Villalba, P., Anselme, I., Schneider-Maunoury, S., and Cereghini, S. (2008). Crucial role of vHNF1 in vertebrate hepatic specification. Development 135, 2777-2786.

Lorenzini, S., Bird, T.G., Boulter, L., Bellamy, C., Samuel, K., Aucott, R., Clayton, E., Andreone, P., Bernardi, M., Golding, M., *et al*. (2010). Characterisation of a stereotypical cellular and extracellular adult liver progenitor cell niche in rodents and diseased human liver. Gut 59, 645-654.

Lowe, L.A., Yamada, S., and Kuehn, M.R. (2001). Genetic dissection of nodal function in patterning the mouse embryo. Development 128, 1831-43-1843.

Lu, Q., Paredes, M., Medina, M., and Zhou, J., *et al*. (1999). Δ-Catenin, an adhesive junction–associated protein which promotes cell scattering. J Cell Bio 144, 519-532.

Lucendo-Villarin, B., Cameron, K., Szkolnicka, D., Rashidi H., and Hay, DC. (2015). Polymer supported direct differentiation reveals a unique gene signature predicting stable hepatocyte performance. Adv Healthc Mater 4(12): 1820-1825.

Lucendo-Villarin, B., Cameron, K., Szkolnicka, D., Travers, P., Khan, F., Walton, J.G., Iredale, J., Bradley, M., and Hay, D.C. (2014). Stabilizing hepatocellular phenotype using optimized synthetic surfaces. J Vis Exp e51723-e51723.

Ludwig, T.E., Levenstein, M.E., Jones, J.M., Berggren, W.T., Mitchen, E.R., Frane, J.L., Crandall, L.J., Daigh, C.A., Conard, K.R., Piekarczyk, M.S., *et al*. (2006). Derivation of human embryonic stem cells in defined conditions. Nature Biotechnology 24, 185-187.

Maher, JJ; Friednman, SL; Roll, FJ and Bissell, DM. (1988). Immunolocalization of laminin in normal rat liver and biosynthesis of laminin by hepatic lipocytes in primary culture. Gastroenterology 94, 1053-62.

Malinen, M.M., Kanninen, L.K., Corlu, A., and Isoniemi, H.M. (2014). Differentiation of liver progenitor cell line to functional organotypic cultures in 3D nanofibrillar cellulose and hyaluronan-gelatin hydrogels. Biomaterials 3, 5110-21.

Mallon, B.S., Park, K.Y., Chen, K.G., and Hamilton, R.S. (2006). Toward xeno-free culture of human embryonic stem cells. Int J Biochem Cell Biol 38, 1063-75.

Mant, A., Tourniaire, G., and Diaz, J.J. (2006). Polymer microarrays: identification of substrates for phagocytosis assays. Biomaterials 27, 5299-306.

Margagliotti, S., Clotman, F., and Pierreux, C.E. (2008). Role of metalloproteinases at the onset of liver development. Dev Growth Differ 50, 331-8.

Margagliotti, S., Clotman, F., Pierreux, C.E., Beaudry, J., Jacquemin, P., Rousseau, G.G., and Lemaigre, F.P. (2007). The Onecut transcription factors HNF-6/OC-1 and OC-2 regulate early liver expansion by controlling hepatoblast migration. Developmental Biology 311, 579-589.

Martinez (1995). The extracellular matrix in hepatic regeneration. FASEB J 9, 1401-10.

Matsui, T. (2002). STAT3 Down-regulates the Expression of Cyclin D during Liver Development. Journal Of Biological Chemistry 277, 36167-36173.

Matsui, T., Kinoshita, T., Morikawa, Y., and Tohya, K. (2002). K-Ras mediates cytokine-induced formation of E-cadherin-based adherens junctions during liver development. EMBO J 21, 1021-30.

Matsumoto, K. (2001). Liver Organogenesis Promoted by Endothelial Cells Prior to Vascular Function. Science 294, 559-563.

Matsuno, F., Chowdhury, S., and Gotoh, T. (1996). Induction of the C/EBPβ gene by dexamethasone and glucagon in primary-cultured rat hepatocytes. J Biochem 119, 524-32.

McCright, B., Lozier, J., and Gridley, T. (2002). A mouse model of Alagille syndrome: Notch2 as a genetic modifier of Jag1 haploinsufficiency. Development 129, 1075-82.

McCuskey, R.S. (2008). The hepatic microvascular system in health and its response to toxicants. Anat Rec (Hoboken) 291, 661-71-671.

McLin, V.A., Rankin, S.A., and Zorn, A.M. (2007). Repression of Wnt/ β-catenin signaling in the anterior endoderm is essential for liver and pancreas development. Development 134, 2207-2217.

Medico, E., Gentile, A., Celso, Lo, C., Williams, T.A., Gambarotta, G., Trusolino, L., and Comoglio, P.M. (2001). Osteopontin is an autocrine mediator of hepatocyte growth factor-induced invasive growth. Cancer Research 61, 5861-5868.

Medine, C.N., Lucendo-Villarin, B., Storck, C., Wang, F., Szkolnicka, D., Khan, F., Pernagallo, S., Black, J.R., Marriage, H.M., Ross, J.A., *et al*. (2013). Developing high-fidelity hepatotoxicity models from pluripotent stem cells. Stem Cells Transl Med 2, 505-509.

Medlock, E.S., and Haar, J.L. (1983). The liver hemopoietic environment: I. Developing hepatocytes and their role in fetal hemopoiesis. Anat Rec (Hoboken) 207, 31-41.

Mees, C., Nemunaitis, J., and Senzer, N. (2009). Transcription factors: their potential as targets for an individualized therapeutic approach to cancer. Cancer Gene Therapy 16, 103-12.

Mei, Y., Saha, K., Bogatyrev, S.R., Yang, J., and Hook, A.L. (2010). Combinatorial development of biomaterials for clonal growth of human pluripotent stem cells. Nat Materials 9, 768-78.

Meier, M., and Hoogenboom, R. (2004). Combinatorial methods, automated synthesis and high-throughput screening in polymer research: The evolution continues. Macromol Rapid Comm 25, 21-23.

Melkoumian, Z., Weber, J.L., Weber, D.M., and Fadeev, A.G. (2010). Synthetic peptide-acrylate surfaces for long-term self-renewal and cardiomyocyte differentiation of human embryonic stem cells. Nat Biotechnol 28, 606-10.

Meng, Y., Eshghi, S., Li, Y.J., Schmidt, R., Schaffer, D.V., and Healy, K.E. (2010). Characterization of integrin engagement during defined human embryonic stem cell culture. The FASEB Journal 24, 1056-1065.

Menger, F.M., Eliseev, A.V., and Migulin, V.A. (1995). Phosphatase catalysis developed via combinatorial organic chemistry. J Org Chem 60, 6666-7.

Michalopoulos, G.K., and Bowen, W. (1993). Comparative analysis of mitogenic and morphogenic effects of HGF and EGF on rat and human hepatocytes maintained in collagen gels. J. Cell. Physiol. 156, 443-452.

Michalopoulos, G.K., Bowen, W.C., Mulé, K., and Luo, J. (2003). HGF, EGF and Dexamethasone induced gene expression patterns during formation of tissue in hepatic organoid cultures. Gene Expr 11,55-75.

Mitalipova, M.M., Rao, R.R., Hoyer, D.M., Johnson, J.A., Meisner, L.F., Jones, K.L., Dalton, S., and Stice, S.L. (2005). Preserving the genetic integrity of human embryonic stem cells. Nature Biotechnology 23, 19-20.

Mitsui, K., Tokuzawa, Y., Itoh, H., Segawa, K., Murakami, M., Takahashi, K., Maruyama, M., Maeda, M., and Yamanaka, S. (2003). The homeoprotein Nanog is required for maintenance of pluripotency in mouse epiblast and ES cells. Cell 113, 631-42.

Monga, S.P.S., Monga, H.K., Tan, X., Mulé, K., Pediaditakis, P., and Michalopoulos, G.K. (2003). β-catenin antisense studies in embryonic liver cultures: Role in proliferation, apoptosis, and lineage specification. Gastroenterology 124, 202-216.

Morelli, L. (2008). Postnatal development of intestinal microflora as influenced by infant nutrition. J Nutr 138, 1791S-1795S.

Moumen, A., Ieraci, A., Patané, S., Solé, C., Comella, J.X., Dono, R., and Maina, F. (2007). Met signals hepatocyte survival by preventing Fas-triggered FLIP degradation in a PI3k-Akt-dependent manner. Hepatology 45, 1210-1217.

Muller, D., Quantin, B., Gesnel, M.C., and Millon, R. (1988). The collagenase gene family in humans consists of at least four members. Biochem J 253, 187-92.

Munger, J.S., Huang, X., Kawakatsu, H., and Griffiths, M. (1999). A mechanism for regulating pulmonary inflammation and fibrosis: the integrin αvβ6 binds and activates latent TGF β1. Cell 96, 319-28

Musah, S., Morin, S.A., Wrighton, P.J., Zwick, D.B., and Jin, S. (2012). Glycosaminoglycan-binding hydrogels enable mechanical control of human pluripotent stem cell self-renewal. ACS Nano 27, 10168-77.

Müsch, A. (2013). Hepatocyte polarity. Compr Physiol 3, 243-287.

Nagao, M., Nakamura, T., and Ichihara, A. (1986). Developmental control of gene expression of tryptophan 2, 3-dioxygenase in neonatal rat liver. Biochim Biophys Acta 867, 179-86.

Nandivada, H., and Villa, L.G. (2011). Fabrication of synthetic polymer coatings and their use in feeder-free culture of human embryonic stem cells. Nat Protoc 6, 1037-43.

Nelson, K.F., Acosta, D., and Bruckner, J.V. (1982). Long-term maintenance and induction of cytochrome P-450 in primary cultures of rat hepatocytes. Biochemical Pharmacology 31, 2211.

Ng, S., Wu, Y.N., Zhou, Y., Toh, Y.E., Ho, Z.Z., Chia, S.M., and Zhu, J.H. (2005). Optimization of 3-D hepatocyte culture by controlling the physical and chemical properties of the extra-cellular matrices. Biomaterials 26, 3153-63.

Niebruegge, S., Bauwens, C.L., Peerani, R., Thavandiran, N., Masse, S., Sevaptisidis, E., Nanthakumar, K., Woodhouse, K., Husain, M., Kumacheva, E., *et al*. (2008). Generation of human embryonic stem cell-derived mesoderm and cardiac cells using size-specified aggregates in an oxygen-controlled bioreactor. Biotechnol. Bioeng. 102, 493-507-507.

Nishiuchi, R., Takagi, J., Hayashi, M., Ido, H., and Yagi, Y. (2006). Ligand-binding specificities of laminin-binding integrins: a comprehensive survey of laminin–integrin interactions using recombinant α3β1, α6β1, α7β1 and α6β4 integrins. Matrix Biol 25, 189-97.

Noda, C., Fukushima, C., Fujiwara, T., and Matsuda, K. (1994). Developmental regulation of rat serine dehydratase gene expression: evidence for the presence of a repressor in fetal hepatocytes. Biochim Biophys Acta 121, 163-73.

Noghero, A., Bussolino, F., and Gualandris, A. (2010). Role of the microenvironment in the specification of endothelial progenitors derived from embryonic stem cells. Microvasc Res 79, 178-83.

Nur, A. (2005). Three dimensional nanofibrillar surfaces induce activation of Rac. Biochem Biophys Res commun 331, 428-34.

Obach, R.S. (2009). Predicting drug-drug interactions from in vitro drug metabolism data: challenges and recent advances. Current Opinion In Drug Discovery &Amp; Development 12, 81-89.

Odom, D.T. (2004). Control of Pancreas and Liver Gene Expression by HNF Transcription Factors. Science 303, 1378-1381.

Okita, K., and Yamanaka, S. (2010). Induction of pluripotency by defined factors. Exp Cell Res 316, 2526-70.

Okita, K., Ichisaka, T., and Yamanaka, S. (2007). Generation of germline-competent induced pluripotent stem cells. Nature 449, 313-7.

Page, J.L., Johnson, M.C., and Olsavsky, K.M. (2007). Gene expression profiling of extracellular matrix as an effector of human hepatocyte phenotype in primary cell culture. Toxicol Sci 97, 384-97.

Paine, A.J., and Andreakos, E. (2004). Activation of signalling pathways during hepatocyte isolation: relevance to toxicology in vitro. Toxicol In Vitro 18, 187-93.

Pakzad, M., Ashtiani, M.K., and Mousavi, S.L. (2013). Development of a simple, repeatable, and cost-effective extracellular matrix for long-term xeno-free and feeder-free self-renewal of human pluripotent stem cells. Histochem Cell Biol 140, 635-48.

Pang, Z.P., Yang, N., Vierbuchen, T., and Ostermeier, A. (2011). Induction of human neuronal cells by defined transcription factors. Nature 476, 220-3.

Papoutsi, M., Dudas, J., Becker, J., Tripodi, M., Opitz, L., Ramadori, G., and Wilting, J. (2007). Gene regulation by homeobox transcription factor Prox1 in murine hepatoblasts. Cell Tissue Res 330, 209-220.

Payne, C.M., Samuel, K., Pryde, A., King, J., Brownstein, D., Schrader, J., Medine, C.N., Forbes, S.J., Iredale, J.P., Newsome, P.N., *et al*. (2010). Persistence of functional hepatocyte-like cells in immune-compromised mice. Liver International 31, 254-262.

Pera, M.F., Reubinoff, B., and Trounson, A. (1999). Human embryonic stem cells. Journal Of Cell Science 113 (Pt 1), 5-10-10.

Pernagallo, S., Tura, O., Wu, M., Samuel, K., Diaz-Mochon, J.J., Hansen, A., Zhang, R., Jackson, M., Padfield, G.J., Hadoke, P.W.F., *et al*. (2012). Novel Biopolymers to Enhance Endothelialisation of Intra-vascular Devices. J. Biomed. Mater. Res. 1, 646-656.

Pernagallo, S., Unciti-Broceta, A., Diaz-Mochon, J.J., and Bradley, M. (2008). Deciphering cellular morphology and biocompatibility using polymer microarrays. Biomed. Mater. 3, 034112.

Pernagallo, S., Wu, M., and Gallagher, M.P. (2011). Colonising new frontiers—microarrays reveal biofilm modulating polymers. J Mater Chem 1, 96-101.

Pesce, M., Anastassiadis, K., and Schöler, H.R. (1999). Oct-4: lessons of totipotency from embryonic stem cells. Cells Tissues Organs (Print) 165, 144-52-152.

Peura, T.T., Bosman, A., and Stojanov, T. (2006). Derivation of human embryonic stem cell lines. Theriogenology 67, 32-42.

Ploss, A., Khetani, S.R., and Jones, C.T. (2010). Persistent hepatitis C virus infection in microscale primary human hepatocyte cultures. Proc Natl Acad Sci USA 107, 3141-5

Pontoglio, M., Barra, J., Hadchouel, M., Doyen, A., and Kress, C. (1996). Hepatocyte nuclear factor 1 inactivation results in hepatic dysfunction, phenylketonuria, and renal Fanconi syndrome. Cell 84, 575-85.

Popov, Y., and Schuppan, D. (2009). Targeting liver fibrosis: strategies for development and validation of antifibrotic therapies. Hepatology 50, 1294-306.

Postovit, L.M., Seftor, E.A., Seftor, R., and Hendrix, M. (2006). A three-dimensional model to study the epigenetic effects induced by the microenvironment of human embryonic stem cells. Stem Cells 24, 501-5.

Qu, X., Lam, E., Doughman, Y., Chen, Y., Chou, Y., Lam, M., Turakhia, M., Dunwoodie, S.L., Watanabe, M., Xu, B., *et al*. (2007). Cited2, a coactivator of HNF4α, is essential for liver development. The EMBO Journal 26, 4445-4456.

Quinn, C.O., Scott, D.K., and Brinckerhoff, C.E. (1990). Rat collagenase. Cloning, amino acid sequence comparison, and parathyroid hormone regulation in osteoblastic cells. J boil Chem 25, 22342-7.

Rastegar, M., Rousseau, G.G., and Lemaigre, F.P. (2000). CCAAT/Enhancer-Binding Protein-α Is a Component of the Growth Hormone-Regulated Network of Liver Transcription Factors 1. Endocrinology 141, 1686-92.

Rathinam, R., and Alahari, S.K. (2010). Important role of integrins in the cancer biology. Cancer Metastasis Rev 29, 223-37.

Reubinoff, B.E., Pera, M.F., Fong, C.Y., Trounson, A., and Bongso, A. (2000). Embryonic stem cell lines from human blastocysts: somatic differentiation in vitro. Nature Biotechnology 18, 399-404.

Richards, M., Fong, C.Y., Chan, W.K., and Wong, P.C. (2002). Human feeders support prolonged undifferentiated growth of human inner cell masses and embryonic stem cells. Nature 20, 933-6.

Richert, L. (2006). Gene expression in human heptocyres in suspension after isolation is similar to the liver of origin, is not affected by hepatocyte cold storage and cryopreservation, but it is strongly changed after hepatocyte plating. Drug Metab Dispos 34, 870-9.

Rippon, H.J., and Bishop, A.E. (2004). Embryonic stem cells. Cell Prolif. 37, 23-34.

Rockey, D.C. (2005). Antifibrotic therapy in chronic liver disease. Clinical Gastroenterology And Hepatology.Clin Gastroenterol Hepatol 3, 95-107.

Rodin, S., Antonsson, L., Niaudet, C., Simonson, O.E., Salmela, E., Hansson, E.M., Domogatskaya, A., Xiao, Z., Damdimopoulou, P., Sheikhi, M., *et al*. (2014). Clonal culturing of human embryonic stem cells on laminin-521/E-cadherin matrix in defined and xeno-free environment. Nat Comms 5: 3195.

Rodin, S., Domogatskaya, A., Ström, S., Hansson, E.M., Chien, K.R., Inzunza, J., Hovatta, O., and Tryggvason, K. (2010). Long-term self-renewal of human pluripotent stem cells on human recombinant laminin-511. Nature Biotechnology 28, 611-615.

Rodríguez-Antona, C., Donato, M.T., Boobis, A., Edwards, R.J., Watts, P.S., Castell, J.V., and Gómez-Lechón, M. (2002). Cytochrome P450 expression in human hepatocytes and hepatoma cell lines: molecular mechanisms that determine lower expression in cultured cells. Xenobiotica 32, 505-520.

Roeb, E., Bosserhoff, A.K., and Hamacher, S. (2005). Enhanced migration of tissue inhibitor of metalloproteinase overexpressing hepatoma cells is attributed to gelatinases: relevance to intracellular signalling pathways. World J Gastroenterol 28, 1096-104.

Rogler, L.E. (1997). Selective bipotential differentiation of mouse embryonic hepatoblasts in vitro. Am J Pathol 150, 591-602.

Rosler, E.S., Fisk, G.J., Ares, X., Irving, J., Miura, T., Rao, M.S., and Carpenter, M.K. (2004). Long-term culture of human embryonic stem cells in feeder-free conditions. Dev. Dyn. 229, 259-74-274.

Rossant, J. (2008). Stem cells and early lineage development. Cell 132, 527-31.

Rossi, J.M., Dunn, N.R., and Hogan, B. (2001). Distinct mesodermal signals, including BMPs from the septum transversum mesenchyme, are required in combination for hepatogenesis from the endoderm. Genes Dev 15, 1998-2009

Rosu, L., Cascaval, C.N., Ciobanu, C., and Rosu, D. (2005). Effect of UV radiation on the semi-interpenetrating polymer networks based on polyurethane and epoxy maleate of bisphenol. J Photochem PhotoBiol Chem 169, 177-185

Rowe, C., Gerrard, D.T., Jenkins, R., Berry, A., and Durkin, K. (2013). Proteome-wide analyses of human hepatocytes during differentiation and dedifferentiation. Hepatology 58, 799-809.

Rowe, C., Goldring, C., and Kitteringham, N.R. (2010). Network analysis of primary hepatocyte dedifferentiation using a shotgun proteomics approach. J Proteome Res 7, 2658-68.

Ruoslahti, E. (1991). Integrins. J. Clin. Invest 87, 1-5.

Sachs, M., Brohmann, H., Zechner, D., and Müller, T. (2000). Essential role of Gab1 for signaling by the c-Met receptor in vivo. J Cell Biol 150, 1375-84

Satohisa, S., Chiba, H., Osanai, M., Ohno, S., Kojima, T., Saito, T., and Sawada, N. (2005). Behavior of tight-junction, adherens-junction and cell polarity proteins during HNF-4α-induced epithelial polarization. Experimental Cell Research 310, 66-78.

Schena, M., Shalon, D., Davis, R.W., and Brown, P.O. (1995). Quantitative monitoring of gene expression patterns with a complementary DNA microarray. Science 270, 467-70.

Schippers, I.J., Moshage, H., Roelofsen, H., and Müller, M. (1997). Immortalized human hepatocytes as a tool for the study of hepatocytic (de-) differentiation. Cell Biol Toxicol 13, 375-86.

Schlessinger, J. (2004). Common and Distinct Elements in Cellular Signaling via EGF and FGF Receptors. Science 306, 1506-1507.

Schmelzer, E., Wauthier, E., and Reid, L.M. (2006). The Phenotypes of Pluripotent Human Hepatic Progenitors. Stem Cells 24, 1852-1858.

Schmidt, C., Bladt, F., Goedecke, S., and Brinkmann, V. (1995). Scatter factor/hepatocyte growth factor is essential for liver development. Nature 373, 699.

Schmittgen, T.D., and Livak, K.J. (2008). Analyzing real-time PCR data by the comparative CT method. Nat Protoc 3, 1101-1108.

Schöler, H.R., Hatzopoulos, A.K., and Balling, R. (1989). A family of octamer-specific proteins present during mouse embryogenesis: evidence for germline-specific expression of an Oct factor. EMBO J 8, 2543-50.

Schwartz, M.A., and Schaller, M.D. (1995). Integrins: emerging paradigms of signal transduction. Annu Rev Cell Biol 11, 549-99.

Schwartz, R.E., and Linehan, J.L. (2005). Defined conditions for development of functional hepatic cells from human embryonic stem cells. Stem Cells Dev 14, 643-55.

Sekhon, S.S., Tan, X., Micsenyi, A., and Bowen, W.C. (2004). Fibroblast growth factor enriches the embryonic liver cultures for hepatic progenitors. The Am J Pathol 164, 2229-40.

Sekiya, S., and Suzuki, A. (2011). Direct conversion of mouse fibroblasts to hepatocyte-like cells by defined factors. Nature. 475, 390-3.

Semb, H. (2006). Human embryonic stem cells: origin, properties and applications. APMIS 113, 743-50-750.

Serls, A.E., Doherty, S., Parvatiyar, P., and Wells, J.M. (2005). Different thresholds of fibroblast growth factors pattern the ventral foregut into liver and lung. Development 132, 35-47.

Shan, J., Schwartz, R.E., Ross, N.T., Logan, D.J., Thomas, D., Duncan, S.A., North, T.E., Goessling, W., Carpenter, A.E., and Bhatia, S.N. (2013). Identification of small molecules for human hepatocyte expansion and iPS differentiation. Nature Chemical Biology 9, 514-520.

Sharma, R., and Greenhough, S. (2010). Three-dimensional culture of human embryonic stem cell derived hepatic endoderm and its role in bioartificial liver construction. J Biomed Biotechnol 2010: 236147.

Sharma, S., Cross, S.E., French, S., *et al.* (2009). Influence of substrates on hepatocytes: a nanomechanical study. J Scanning Probe Micros 4, 1-10.

Shay, J.W., and Wright, W.E. (2005). Senescence and immortalization: role of telomeres and telomerase. Carcinogenesis 26, 867-74.

Shen, C.N., Slack, J., and Tosh, D. (2000). Molecular basis of transdifferentiation of pancreas to liver. Nat. Cell Biol 2, 879-87.

Shi, Y., and Massagué, J. (2003). Mechanisms of TGF-β signaling from cell membrane to the nucleus. Cell 113, 685-700.

Shin, D., Shin, C.H., Tucker, J., Ober, E.A., Rentzsch, F., Poss, K.D., Hammerschmidt, M., Mullins, M.C., and Stainier, D.Y.R. (2007). Bmp and Fgf signaling are essential for liver specification in zebrafish. Development 134, 2041-2050.

Shiojiri, N., and Sugiyama, Y. (2004). Immunolocalization of extracellular matrix components and integrins during mouse liver development. Hepatology 40, 346-355.

Shirahashi, H., Wu, J., Yamamoto, N., and Catana, A. (2004). Differentiation of human and mouse embryonic stem cells along a hepatocyte lineage. Cell 13, 197-211.

Sinclair, E.M., Yusta, B., Streutker, C., Baggio, L.L., and Koehler, J. (2008). Glucagon receptor signaling is essential for control of murine hepatocyte survival. Gastroenterology 135, 2096-106.

Si-Tayeb, K., Noto, F.K., Nagaoka, M., Li, J., and Battle, M.A. (2010). Highly efficient generation of human hepatocyte–like cells from induced pluripotent stem cells. Hepatology 51, 297-305.

Sivertsson, L., Synnergren, J., and Jensen, J. (2012). Hepatic differentiation and maturation of human embryonic stem cells cultured in a perfused three-dimensional bioreactor. Stem Cells Dev 22, 581-94.

Skett, P., and Bayliss, M. (1996). Time for a consistent approach to preparing and culturing hepatocytes? Xenobiotica 26, 1-7.

Snykers, S., De Kock, J., Rogiers, V., and Vanhaecke, T. (2009). In Vitro Differentiation of Embryonic and Adult Stem Cells into Hepatocytes: State of the Art. Stem Cells 27, 577-605.

Soldatow, V.Y., LeCluyse, E.L., Griffith, L.G., and Rusyn, I. (2013). In vitro models for liver toxicity testing. Toxicol Res (Camb) 2, 23-39.

Song, Z., Cai, J., Liu, Y., Zhao, D and Yong, J. (2009). Efficient generation of hepatocyte-like cells from human induced stem cells. Cell Res 19, 1233-1242.

Soriano, H.E., Bilyeu, T.A., Juan, T., and Zhao, W. (1995). DNA binding by C/EBP proteins correlates with hepatocyte proliferation. In Vitro Cell Dev Biol Anim 31, 703-9.

Sosa, B., Wingle, TJ., Oliver, G. (2000). Hepatocyte migration during liver development requires Prox1. Nat. Genet 25, 254-5.

Späth, G.F., and Weiss, M.C. (1997). Hepatocyte nuclear factor 4 expression overcomes repression of the hepatic phenotype in dedifferentiated hepatoma cells. Mol Cell Biol 17, 1913-22.

Stadtfeld, M., Maherali, N., Breault, D.T., and Hochedlinger, K. (2008a). Defining molecular cornerstones during fibroblast to iPS cell reprogramming in mouse. Cell Stem Cell 2, 230-40..

Stanulović, V.S., Kyrmizi, I., and Julio, M.K. (2007). Hepatic HNF4α deficiency induces periportal expression of glutamine synthetase and other pericentral enzymes. Hepatology 45, 433-44.

Staudinger, J.L., Goodwin, B., and Jones, S.A. (2001). The nuclear receptor PXR is a lithocholic acid sensor that protects against liver toxicity. Proc Natl Avad Sci USA 98, 3369-74.

Steiner, D., Khaner, H., Cohen, M., and Even, S. (2010). Derivation, propagation and controlled differentiation of human embryonic stem cells in suspension. Nature 28, 361-4.

Su, T., and Waxman, D.J. (2004). Impact of dimethyl sulfoxide on expression of nuclear receptors and drug-inducible cytochromes P450 in primary rat hepatocytes. Arch Biochem Biophys 424, 226-34.

Sugimachi, K., Sosef, M.N., Baust, J.M., Fowler, A., Tompkins, R.G., and Toner, M. (2004). Long-term function of cryopreserved rat hepatocytes in a coculture system. Cell Transplant 13, 187-95.

Sullivan, G.J., Hay, D.C., Park, I., Fletcher, J., Hannoun, Z., Payne, C.M., Dalgetty, D., Black, J.R., Ross, J.A., Samuel, K., *et al*. (2009). Generation of functional human hepatic endoderm from human induced pluripotent stem cells. Hepatology 51, 329-335.

Suzuki, A., Iwama, A., Miyashita, H., and Nakauchi, H. (2003). Role for growth factors and extracellular matrix in controlling differentiation of prospectively isolated hepatic stem cells. Development 130, 2613-24.

Suzuki, T., Kanai, Y., Hara, T., Sasaki, J., Sasaki, T., Kohara, M., Maehama, T., Taya, C., Shitara, H., Yonekawa, H., *et al*. (2006). Crucial Role of the Small GTPase ARF6 in Hepatic Cord Formation during Liver Development. Molecular And Cellular Biology 26, 6149-6156.

Szabo, E., Rampalli, S., Risueno, R.M., and Schnerch, A. (2010). Direct conversion of human fibroblasts to multilineage blood progenitors. Nature 468, 521-6.

Szkolnicka, D., Farnworth, S.L., Lucendo-Villarin, B., Storck, C., Zhou, W., Iredale, J.P., Flint, O., and Hay, D.C. (2014). Accurate prediction of drug-induced liver injury using stem cell-derived populations. Stem Cells Transl Med 3, 141-148.

Takahashi, K., and Yamanaka, S. (2006). Induction of pluripotent stem cells from mouse embryonic and adult fibroblast cultures by defined factors. Cell 126, 663-76.

Takahashi, K., Ichisaka, T., and Yamanaka, S. (2006). Identification of genes involved in tumor-like properties of embryonic stem cells. Methods Mol Biol 329, 449-58.

Takahashi, K., Tanabe, K., Ohnuki, M., Narita, M., and Ichisaka, T. (2007). Induction of pluripotent stem cells from adult human fibroblasts by defined factors. Cell 30, 861-72.

Takahashi, R., Sonoda, H., and Tabata, Y. (2010). Formation of hepatocyte spheroids with structural polarity and functional bile canaliculi using nanopillar sheets. Tissue Eng Part A 16, 1983.

Takayama, K., Kawabata, K., Nagamoto, Y., Kishimoto, K., Tashiro, K., Sakurai, F., Tachibana, M., Kanda, K., Hayakawa, T., Furue, M.K., *et al*. (2013). 3D spheroid culture of hESC/hiPSC-derived hepatocyte-like cells for drug toxicity testing. Biomaterials 34, 1781-1789.

Takebe, T., Sekine, K., Enomura, M., Koike, H., Kimura, M., Ogaeri, T., Zhang, R., Ueno, Y., Zheng, Y., Koike, N., *et al*. (2013). Vascularized and functional human liver from an iPSC-derived organ bud transplant. Nature 499, 481-484.

Takeichi, M. (1995). Morphogenetic roles of classic cadherins. Current Opinion In Cell Biology 7, 619-27.

Takeuchi, JK., and Bruneau, BG. (2009) Directed transdifferentiation of mouse mesoderm to heart tissue by defined factors. Nature 459, 708-11.

Tan, X., Yuan, Y., Zeng, G., Apte, U., Thompson, M.D., Cieply, B., Stolz, D.B., Michalopoulos, G.K., Kaestner, K.H., and Monga, S.P.S. (2008). β-Catenin deletion in hepatoblasts disrupts hepatic morphogenesis and survival during mouse development. Hepatology 47, 1667-1679.

Tanimizu, N. (2004). Notch signaling controls hepatoblast differentiation by altering the expression of liver-enriched transcription factors. Journal Of Cell Science 117, 3165-3174.

Taraviras, S., Monaghan, A.P., and Schütz, G. (1994). Characterization of the mouse HNF-4 gene and its expression during mouse embryogenesis. Mech Dev 48, 67-79.

Tare, R.S., Khan, F., Tourniaire, G., Morgan, S.M., Bradley, M., and Oreffo, R.O.C. (2009). A microarray approach to the identification of polyurethanes for the isolation of human skeletal progenitor cells and augmentation of skeletal cell growth. Biomaterials 30, 1045-1055.

Teixeira, A.I., Abrams, G.A., Bertics, P.J., Murphy, C.J., and Nealey, P.F. (2003). Epithelial contact guidance on well-defined micro- and nanostructured substrates. Journal Of Cell Science 116, 1881-1892.

Tekkatte, C., Gunasingh, G.P., and Cherian, K.M. (2011). “Humanized” stem cell culture techniques: the animal serum controversy. Stem Cells 504723.

Thomas, H., Jaschkowitz, K., Bulman, M., Frayling, TM. (2001). A distant upstream promoter of the HNF—4alpha gene connects the transcription factors involved in maturity-onset diabetes of the young. Hum Mol Genet 10, 2089-97.

Thomson, J.A. (1998). Embryonic Stem Cell Lines Derived from Human Blastocysts. Science 282, 1145-1147.

Timchenko, N.A., Harris, T.E., and Wilde, M. (1997). CCAAT/enhancer binding protein alpha regulates p21 protein and hepatocyte proliferation in newborn mice.Mol Cell Biol 17, 7353-61.

Tomizawa, M., Garfield, S., and Factor, V. (1998). Hepatocytes deficient in CCAAT/enhancer binding protein α (C/EBPα) exhibit both hepatocyte and biliary epithelial cell character. Biochem Biophys Res Commun 10, 1-5.

Touboul, T., Vallier, L., and Weber, A. (2010). [Robust differentiation of fetal hepatocytes from human embryonic stem cells and iPS]. Med Sci (Paris) 26, 1061-6-1066.

Touboul, T., Vallier, L., and Weber, A. (2010). [Robust differentiation of fetal hepatocytes from human embryonic stem cells and iPS]. Med Sci (Paris) 26, 1061-6-1066.

Tourniaire, G., Collins, J., and Campbell, S. (2006). Polymer microarrays for cellular adhesion. Chem Commun (Camb) 28, 2118-20.

Tremblay, K.D., and Zaret, K.S. (2005). Distinct populations of endoderm cells converge to generate the embryonic liver bud and ventral foregut tissues. Developmental Biology 280, 87-99.

Trounson, A. (2006). The production and directed differentiation of human embryonic stem cells. Endocrine Reviews 27, 208-19.

Tsuchiya, A., Lu, W.Y., Weinhold, B., and Boulter, L. (2014). Polysialic acid/neural cell adhesion molecule modulates the formation of ductular reactions in liver injury. Hepatology 60, 1727-40.

Tsukita, S., Furuse, M., and Itoh, M. (2001). Multifunctional strands in tight junctions. Nat Rev Mol Cell Biol 2, 285-93.

Turner, R., Lozoya, O., Wang, Y., Cardinale, V., Gaudio, E., Alpini, G., Mendel, G., Wauthier, E., Barbier, C., Alvaro, D., *et al*. (2011). Human hepatic stem cell and maturational liver lineage biology. Hepatology 53, 1035-1045.

Tuschl, G., and Mueller, S.O. (2006). Effects of cell culture conditions on primary rat hepatocytes—cell morphology and differential gene expression. Toxicology 218, 205-15.

Ugele, B., Kempen, H.J., Kempen, J.M., and Gebhardt, R. (1991). Heterogeneity of rat liver parenchyma in cholesterol 7 alpha-hydroxylase and bile acid synthesis. Biochem J 276, 73-7.

Van de Kerkhove, M.P., and Di Florio, E. (2002). Phase I clinical trial with the AMC-bioartificial liver. Int J Artif Organs 25, 950-9.

Vazin, T., and Freed, W.J. (2010). Human embryonic stem cells: derivation, culture, and differentiation: a review. Restorative Neurology And Neuroscience 28, 589-603.

Venkatasubbarao, S. (2004). Microarrays–status and prospects. Trends Biotechnol 22, 630-7.

Verzi, M.P., Shin, H., Roman, A.S., and Liu, X.S. (2013). Intestinal master transcription factor CDX2 controls chromatin access for partner transcription factor binding.Mol Cell Biol 33, 281-92.

Vessey, C.J., and la M. Hall, de, P. (2001). Hepatic stem cells: a review. Pathology 33, 130-41.

Villa-Diaz, L.G., Brown, S.E., Liu, Y., and Ross, A.M. (2012). Derivation of mesenchymal stem cells from human induced pluripotent stem cells cultured on synthetic substrates. Stem Cells 30, 1174-81.

Villa-Diaz, L.G., Nandivada, H., Ding, J., Nogueira-de-Souza, N.C., Krebsbach, P.H., O'Shea, K.S., Lahann, J., and Smith, G.D. (2010). Synthetic polymer coatings for long-term growth of human embryonic stem cells. Nature Biotechnology 28, 581-583.

Villa-Diaz, L.G., Ross, A.M., Lahann, J., and Krebsbach, P.H. (2013). Concise review: the evolution of human pluripotent stem cell culture: from feeder cells to synthetic coatings. Stem Cells.

Vincent, S.D., Dunn, N.R., Hayashi, S., Norris, D.P., and Robertson, E.J. (2003). Cell fate decisions within the mouse organizer are governed by graded Nodal signals. Genes &Amp; Development 17, 1646-62-1662.

Vinken, M., Papeleu, P., and Snykers, S. (2006). Involvement of cell junctions in hepatocyte culture functionality. Crit Rev Toxicolo 36, 299-318.

Visk, D.A. (2015). Will advances in preclinical in vitro models lower the costs of drug development? Applied In Vitro Toxicology. doi; 10.1089/aivt.2015.1503

Visse, R., and Nagase, H. (2003). Matrix metalloproteinases and tissue inhibitors of metalloproteinases structure, function, and biochemistry. Cir Res 92, 827-39.

Vosough, M., Omidinia, E., Kadivar, M., Shokrgozar, M., Pournasr, B., Aghdami, N., and Baharvand, H. (2013). Generation of functional hepatocyte-like cells from human pluripotent stem cells in a scalable suspension culture. Stem Cells Dev. 22, 2693-2705.

Vuoristo, S., Toivonen, S., Weltner, J., Mikkola, M., Ustinov, J., Trokovic, R., Palgi, J., Lund, R., Tuuri, T., and Otonkoski, T. (2013). A novel feeder-free culture system for

human pluripotent stem cell culture and induced pluripotent stem cell derivation. Plos ONE 8, e76205.

Wall, D.A., Wilson, G., and Hubbard, A.L. (1980). The galactose-specific recognition system of mammalian liver: the route of ligand internalization in rat hepatocytes. Cell 21, 79-93-93.

Wang, N.D., Finegold, M.J., Bradley, A., and Ou, C.N. (1995). Impaired energy homeostasis in C/EBP alpha knockout mice. Science 269, 1108.

Ware, B.R., Berger, D.R., and Khetani, S.R. (2015). Prediction of drug-induced liver injury in micropatterned co-cultures containing iPSC-derived human hepatocytes. Toxicol Sci 145, 252-62.

Webster, D.C. (2008). Combinatorial and High-Throughput Methods in Macromolecular Materials Research and Development. Macromol Chem Phys 209, 237-246.

Weinstein, D.C., Altaba, A.I., Chen, W.S., and Hoodless, P. (1994). The winged-helix transcription factor HNF-3β is required for notochord development in the mouse embryo. Cell 78, 575-588.

Wells, J.M., and Melton, D.A. (1999). Vertebrate endoderm development. Ann Rev Cell Dev 25, 221-251.

Werner, A., Duvar, S., and Müthing, J. (1999). Cultivation and characterization of a new immortalized human hepatocyte cell line, HepZ, for use in an artificial liver support system. Ann N Y Acad Sci 18, 346-8.

Wobus, A.M., and Boheler, K.R. (2005). Embryonic stem cells: prospects for developmental biology and cell therapy. Physiol Rev 85, 635- 78.

Wong, N., Lai, P., Pang, E., Leung, T., and Lau, J. (2000). A comprehensive karyotypic study on human hepatocellular carcinoma by spectral karyotyping. Hepatology 32, 1060-8.

Xu, C., Inokuma, M.S., Denham, J., Golds, K., and Kundu, P. (2001). Feeder-free growth of undifferentiated human embryonic stem cells. Nature Biotechnology 19, 971.

Xu, Y., Zhu, X., Hahm, H.S., Wei, W., and Hao, E. (2010). Revealing a core signaling regulatory mechanism for pluripotent stem cell survival and self-renewal by small molecules. Proc Natl Acad Sci USA 107, 8129-34.

Yamanaka, S., and Blau, H.M. (2010). Nuclear reprogramming to a pluripotent state by three approaches. Nature 465, 704-12.

Yamasaki, H., Sada, A., Iwata, T., Niwa, T., Tomizawa, M., Xanthopoulos, K.G., Koike, T., and Shiojiri, N. (2006). Suppression of C/EBP expression in periportal hepatoblasts may stimulate biliary cell differentiation through increased Hnf6 and Hnf1b expression. Development 133, 4233-4243.

Yamauchi, M., Mizuhara, Y., and Toda, G. (1993). Serum vitronectin receptor in alcoholic liver disease: correlation with fibronectin receptor and morphological features. Alcohol Alcoho Supple 1A, 37-43.

Yamazoe, T., Shiraki, N., and Toyoda, M. (2013). A synthetic nanofibrillar matrix promotes in vitro hepatic differentiation of embryonic stem cells and induced pluripotent stem cells. J Cell Sci 126, 5391-9.

Yan, S., Chen, G.M., Yu, C.H., Zhu, G.F., and Li, Y.M. (2005). Expression pattern of matrix metalloproteinases-13 in a rat model of alcoholic liver fibrosis. Pancreat Dis Int 4, 569-572.

Yanai, M., Tatsumi, N., Hasunuma, N., Katsu, K., Endo, F., and Yokouchi, Y. (2008). FGF signaling segregates biliary cell-lineage from chick hepatoblasts cooperatively with BMP4 and ECM components in vitro. Dev. Dyn. 237, 1268-1283.

Yang, X.F., Tallman, D.E., Bierwagen, G.P., and Croll, S.G. (2002). Blistering and degradation of polyurethane coatings under different accelerated weathering tests. Polym Degrad Stab 77, 103-9.

Yang, Y., Bolikal, D., Becker, M.L., and Kohn, J. (2008). Combinatorial Polymer Scaffold Libraries for Screening Cell-Biomaterial Interactions in 3D. Adv. Mater. Weinheim 20, 2037-2043.

Yim, E., and Leong, K.W. (2005). Significance of synthetic nanostructures in dictating cellular response. Nanomedicine 1, 10-21.

Yonemura, S., Itoh, M., and Nagafuchi, A. (1995). Cell-to-cell adherens junction formation and actin filament organization: similarities and differences between non-polarized fibroblasts and polarized epithelial cells. J Cell Sci 108, 127-42.

Yoshioka, N., Gros, E., Li, H.R., Kumar, S., and Deacon, D.C. (2013). Efficient generation of human iPSCs by a synthetic self-replicative RNA. Cell Stem Cell 13, 246-54.

YU, J., Hu, K., and Smuga, K. (2009). Human induced pluripotent stem cells free of vector and transgene sequences. Science 324, 797-801.

Zaret, K.S. (2001). Hepatocyte differentiation: from the endoderm and beyond. Curr Opin Genet Dev 11, 568-74.

Zaret, K.S. (2002). Regulatory phases of early liver development: paradigms of organogenesis. Nat Rev Genet 3, 499-512.

Zaret, K.S. (2008). Genetic programming of liver and pancreas progenitors: lessons for stem-cell differentiation. Nat Rev Genet 9, 329-340.

Zaret, K.S., and Grompe, M. (2008). Generation and regeneration of cells of the liver and pancreas. Science 322, 1490-4.

Zhang, R., Liberski, A., Sanchez-Martin, R., and Bradley, M. (2009b). Microarrays of over 2000 hydrogels – Identification of substrates for cellular trapping and thermally triggered release. Biomaterials 30, 6193-6201.

Zhang, R., Mjoseng, H.K., Hoeve, M.A., Bauer, N.G., Pells, S., Besseling, R., Velugotla, S., Tourniaire, G., Kishen, R.E.B., Tsenkina, Y., *et al*. (2013). A thermoresponsive and chemically defined hydrogel for long-term culture of human embryonic stem cells. Nat Comms 4, 1335.

Zhao, R., and Duncan, S.A. (2005). Embryonic development of the liver. Hepatology 41, 956-967.

Zhao, T., Zhang, Z.N., Rong, Z., and Xu, Y. (2011). Immunogenicity of induced pluripotent stem cells. Nature 474, 212-5.

Zhou, Q., Brown, J., Kanarek, A., Rajagopal, J., and Melton, DA. In vivo reprogramming of adult pancreatic exocrine cells to beta-cells. Nature 455, 627-32.

Zhou, X., Sun, P., Lucendo-Villarin, B., Angus, A.G.N., Szkolnicka, D., Cameron, K., Farnworth, S.L., Patel, A.H., and Hay, D.C. (2014). Modulating innate immunity improves hepatitis C virus infection and replication in stem cell-derived hepatocytes. Stem Cell Reports 3, 204-14-214.

Znoyko, I., Trojanowska, M., and Reuben, A. (2006). Collagen binding α2β1 and α1β1 integrins play contrasting roles in regulation of Ets-1 expression in human liver myofibroblasts. Mol Cell Biochem 282, 89.

Zorn, A.M., and Wells, J.M. (2009). Vertebrate endoderm development and organ formation. Annu Rev Dev Biol 25, 221-51.

Zorn, A.M., Butler, K., and Gurdon, J.B. (1999). Anterior Endomesoderm Specification inXenopusby Wnt/β-catenin and TGF-β Signalling Pathways. Dev Bio 209, 282-97.

Zou, C., Luo, Q., Qin, J., Shi, Y., Yang, L. *et al* (2013). Osteopontin promotes mesenchymal stem cell migration and lessens cell stiffness via integrin β1, FAK, and ERK pathways. Cell Biochem and Biophy 65, 455-462.

SUPPLEMENTARY INFORMATION

A

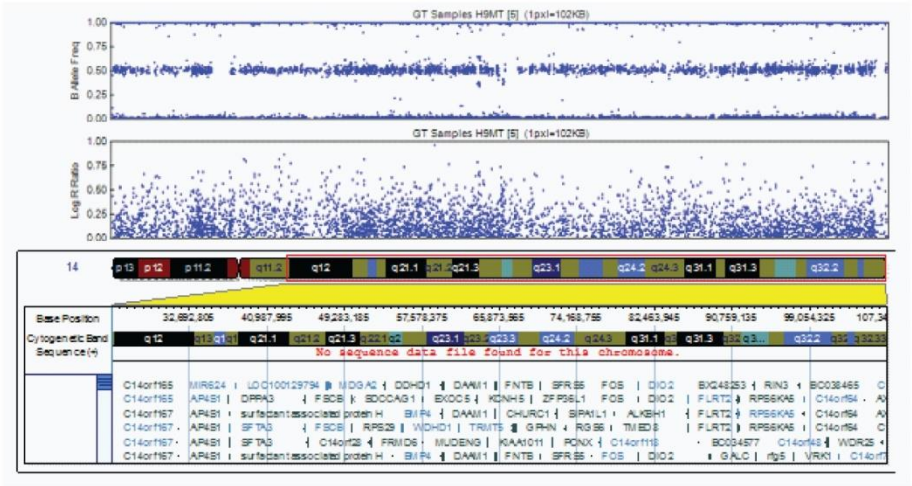

B

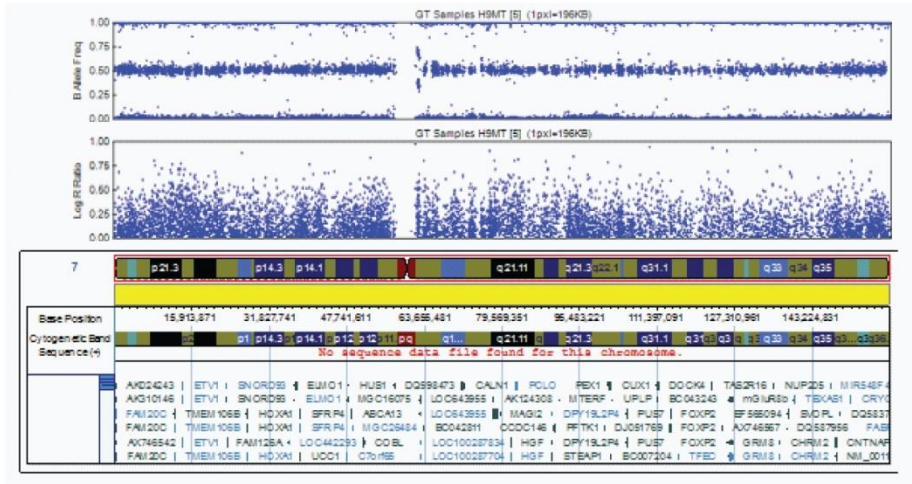

Supplementary Figure 1. SNP analysis of H9 cells. Log 2 ratio represents the allele signals from the probes by two channels (red and green), counting the intensities of these alleles, representing how much different or similar the alleles are. The B allele ratio counts how much of the B alleles contribute to the while alleles intensity, indicating if there is any change in the genotype. As indicated in the red boxes (Panels A and B), there is a split in the straight red line, indicating the presence of a microduplication in chromosome 7, q11.1 and in chromosome 14 q.23.1, but in a non-coding region.

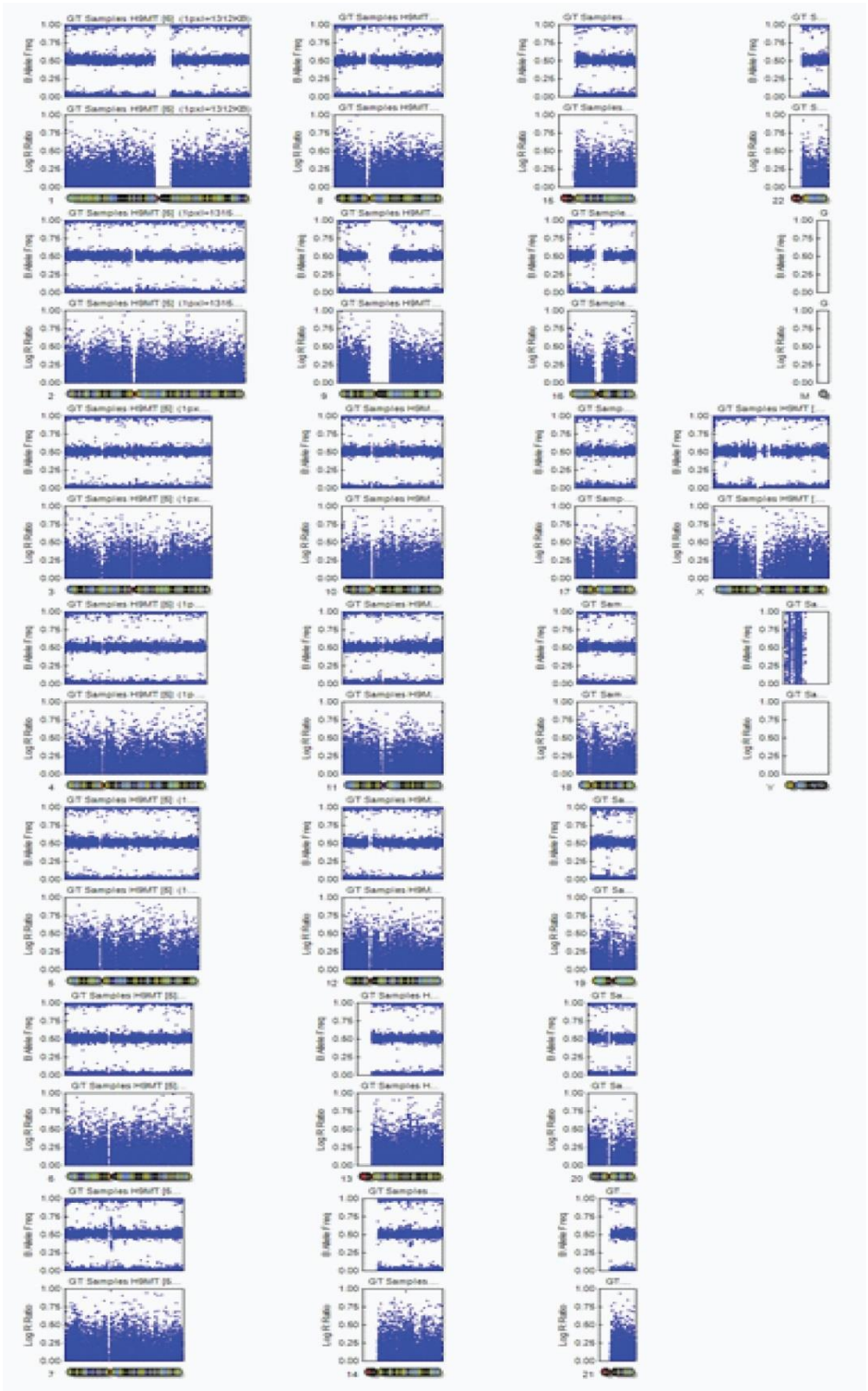

Supplementary Figure 2. Karyotyping analysis of H9 cells.

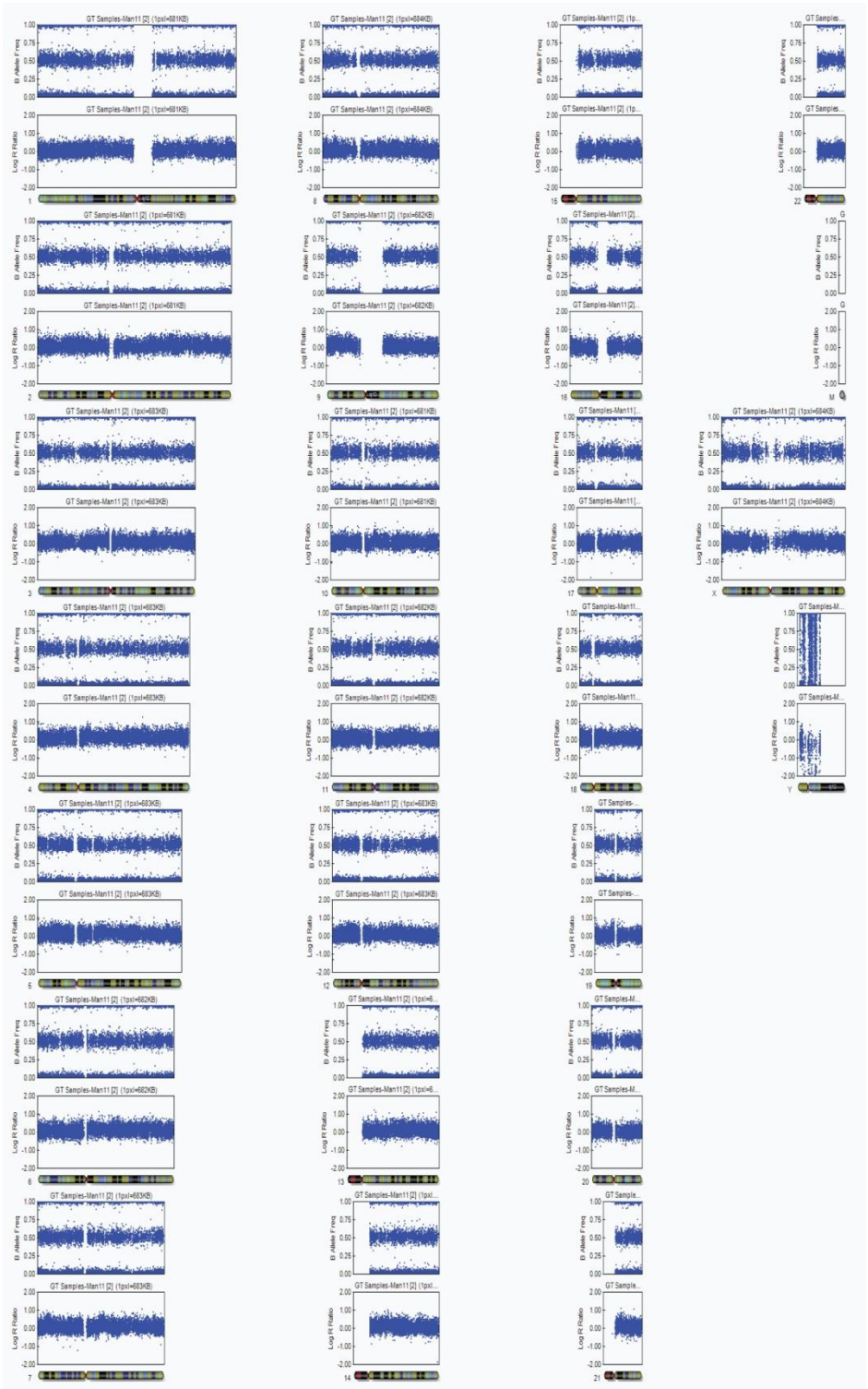

Supplementary Figure 3. Karyotyping analysis of Man 11 cells.

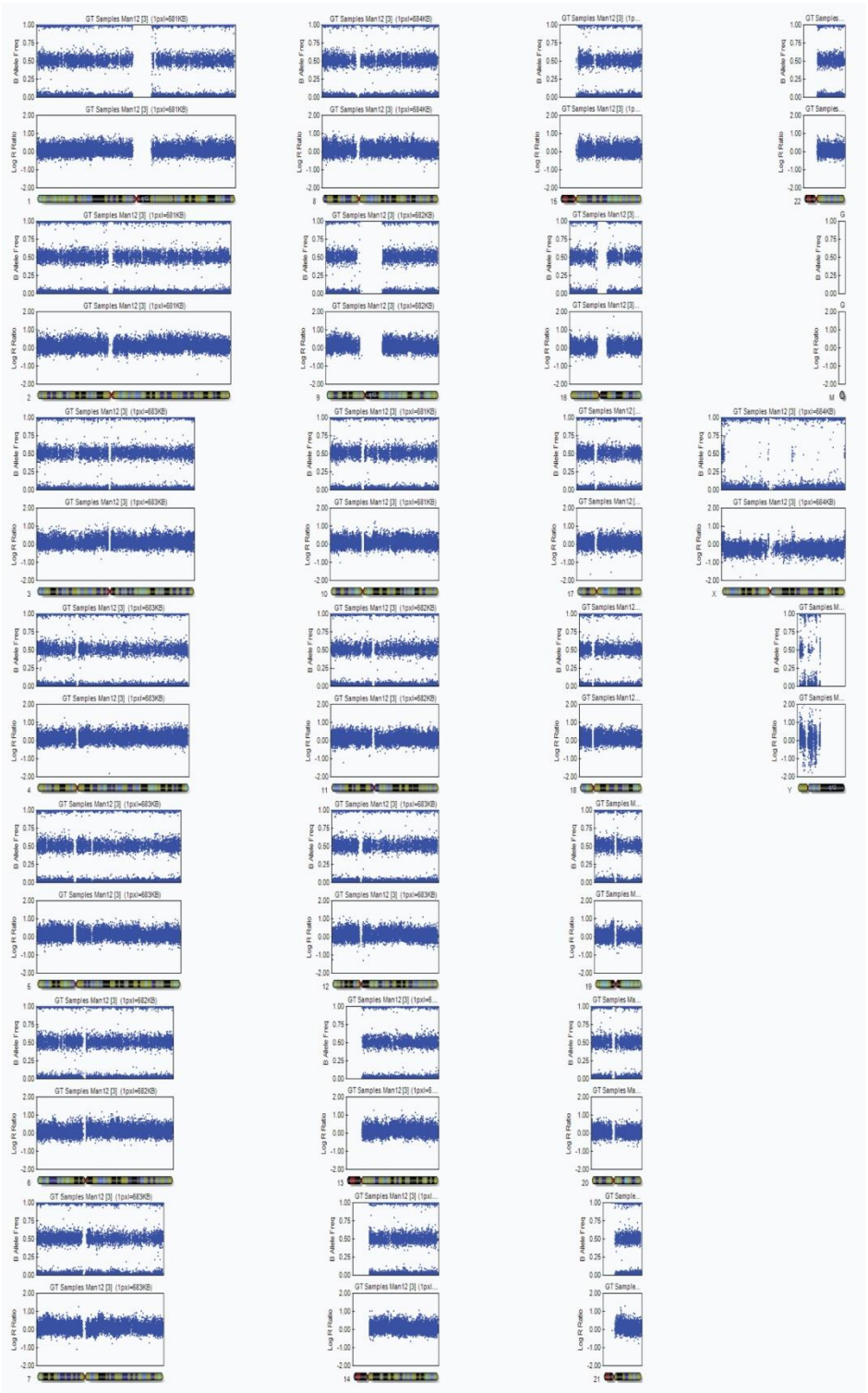

Supplementary Figure 4. Karyotyping analysis of Man 12 cells.

Supplementary Table 1. RT2 Profile PCR Array. The accuracy of the results depend on the threshold cycle for each of the genes. A- means that the gene's average threshold cycle is relatively high (> 30) in either the control or the test sample, and is reasonably low in the other sample (< 30). B- means that the gene's average threshold cycle is relatively high (> 30), meaning that its relative expression level is low. C-means that the gene's average threshold cycle is either not determined or greater than the defined cut-off value (default 35), meaning that its expression was undetected, making this fold-change erroneous.

RT2 PROFILER PCR ARRAY-HUMAN EXTRACELLULAR MEMBRANE COMPONENTS AND ASOCIATED MEMBRANE RECEPTORS (QIAGEN; PAHS-013Z)							
Gene Symbol	AVG Ct		2^(-Avg.(Delta(Ct))		Fold Change	Up-Down Regulation	
	Control Group (HLC-MG)	Group 1 (HLC-PU)	Control Group (HLC-MG)	Group 1 (HLC-PU)	Group 1 /Control Group	Group 1 /Control Group	Comments
ADAMTS1	4.854308	4.001948	0.034571	0.062416	1.8055	1.8055	OKAY
ADAMTS13	13.388739	11.440248	0.000093	0.00036	3.8597	3.8597	A
ADAMTS8	13.039285	12.644685	0.000119	0.000156	1.3146	1.3146	B
CD44	2.329808	2.078464	0.198911	0.236766	1.1903	1.1903	OKAY
CDH1	2.916024	3.118729	0.132492	0.115125	0.8689	-1.1509	OKAY
CLEC3B	13.426055	12.758982	0.000091	0.000144	1.5878	1.5878	B
CNTN1	11.391376	10.257768	0.000372	0.000817	2.1941	2.1941	OKAY
COL11A1	5.583059	4.272228	0.020861	0.051752	2.4808	2.4808	OKAY
COL12A1	9.282489	8.290053	0.001606	0.003195	1.9895	1.9895	OKAY
COL14A1	7.672686	6.592752	0.004901	0.010361	2.1139	2.1139	OKAY
COL15A1	6.734712	6.161742	0.00939	0.013968	1.4876	1.4876	OKAY
COL16A1	8.907474	8.309277	0.002082	0.003153	1.5138	1.5138	OKAY
COL1A1	1.132694	0.211449	0.456063	0.86367	1.8937	1.8937	OKAY
COL4A2	2.911102	2.773548	0.132945	0.146244	1.1	1.1	OKAY
COL5A1	3.318939	2.436436	0.100207	0.184739	1.8436	1.8436	OKAY
COL6A1	5.077306	4.200056	0.02962	0.054407	1.8369	1.8369	OKAY
COL6A2	5.631223	5.099271	0.020176	0.029172	1.4459	1.4459	OKAY
COL7A1	11.181996	10.160147	0.00043	0.000874	2.0305	2.0305	OKAY
COL8A1	14.978788	12.416075	0.000031	0.000183	5.9082	5.9082	B
CTGF	0.959471	2.259963	0.514245	0.208777	0.406	-2.4631	OKAY

CTNNA1	2.577209	2.426659	0.167565	0.185996	1.11	1.11	OKAY
CTNNB1	5.234586	5.110498	0.02656	0.028946	1.0898	1.0898	OKAY
CTNND1	3.981209	3.977116	0.063319	0.063499	1.0028	1.0028	OKAY
CTNND2	9.16369	7.130899	0.001744	0.007135	4.092	4.092	OKAY
ECM1	6.31031	6.862964	0.012601	0.008591	0.6818	-1.4668	OKAY
FN1	-2.255304	-2.806925	4.774349	6.997914	1.4657	1.4657	OKAY
HAS1	13.211213	12.82552	0.000105	0.000138	1.3065	1.3065	B
ICAM1	3.844587	4.14428	0.069609	0.056552	0.8124	-1.2309	OKAY
ITGA1	3.358126	2.431646	0.097522	0.185354	1.9006	1.9006	OKAY
ITGA2	3.342377	3.929539	0.098593	0.065628	0.6657	-1.5023	OKAY
ITGA3	4.061134	4.35002	0.059907	0.049036	0.8185	-1.2217	OKAY
ITGA4	10.700162	9.642069	0.000601	0.001252	2.0822	2.0822	OKAY
ITGA5	3.220991	2.462139	0.107247	0.181477	1.6921	1.6921	OKAY
ITGA6	3.877713	4.413846	0.068029	0.046914	0.6896	-1.4501	OKAY
ITGA7	10.503223	9.338918	0.000689	0.001544	2.2413	2.2413	OKAY
ITGA8	7.537291	8.061834	0.005383	0.003742	0.6952	-1.4385	OKAY
ITGAL	13.672973	11.856826	0.000077	0.00027	3.5214	3.5214	B
ITGAM	13.52038	13.701747	0.000085	0.000075	0.8819	-1.134	B
ITGAV	3.036623	3.060722	0.121867	0.119848	0.9834	-1.0168	OKAY
ITGB1	1.096662	1.166646	0.467597	0.445456	0.9526	-1.0497	OKAY
ITGB2	11.32439	12.098721	0.00039	0.000228	0.5847	-1.7104	A
ITGB3	6.709127	7.232763	0.009558	0.006648	0.6956	-1.4376	OKAY
ITGB4	7.782731	8.041465	0.004541	0.003796	0.8358	-1.1964	OKAY
ITGB5	5.040115	4.893022	0.030393	0.033655	1.1073	1.1073	OKAY
KAL1	7.871863	7.308391	0.004269	0.006309	1.4778	1.4778	OKAY
LAMA1	8.17998	9.575856	0.003448	0.00131	0.38	-2.6315	OKAY
LAMA2	7.747082	6.952568	0.004655	0.008074	1.7345	1.7345	OKAY
LAMA3	5.07801	5.165841	0.029605	0.027857	0.9409	-1.0628	OKAY
LAMB1	2.184283	2.253012	0.220022	0.209786	0.9535	-1.0488	OKAY
LAMB3	4.175411	5.211378	0.055345	0.026991	0.4877	-2.0505	OKAY
LAMC1	1.759972	1.754205	0.295254	0.296436	1.004	1.004	OKAY
MMP1	4.130322	4.224059	0.057102	0.05351	0.9371	-1.0671	OKAY
MMP10	7.803641	6.04239	0.004476	0.015173	3.3899	3.3899	OKAY
MMP11	8.765227	8.530261	0.002298	0.002705	1.1769	1.1769	OKAY
MMP12	12.335765	13.062276	0.000193	0.000117	0.6044	-1.6546	B
MMP13	10.509822	7.987264	0.000686	0.003941	5.746	5.746	OKAY
MMP14	5.926664	6.177311	0.01644	0.013818	0.8405	-1.1897	OKAY
MMP15	12.64461	12.920823	0.000156	0.000129	0.8258	-1.211	B

MMP16	7.416048	6.151237	0.005855	0.01407	2.403	2.403	OKAY
MMP2	6.498155	6.080997	0.011063	0.014772	1.3353	1.3353	OKAY
MMP3	9.541153	9.05852	0.001342	0.001875	1.3973	1.3973	OKAY
MMP7	6.158659	5.371202	0.013998	0.024161	1.726	1.726	OKAY
MMP8	16.815915	16.16106	0.000009	0.000014	1.5745	1.5745	B
MMP9	8.570126	8.25599	0.002631	0.003271	1.2433	1.2433	OKAY
NCAM1	6.78335	4.966589	0.009078	0.031982	3.5229	3.5229	OKAY
PECAM1	12.434322	11.80038	0.000181	0.00028	1.5518	1.5518	B
SELE	16.815915	16.550459	0.000009	0.00001	1.202	1.202	C
SELL	14.128418	13.71298	0.000056	0.000074	1.3337	1.3337	B
SELP	15.731125	16.286926	0.000018	0.000013	0.6803	-1.47	B
SGCE	5.702236	5.200974	0.019207	0.027186	1.4155	1.4155	OKAY
SPARC	1.04553	0.727454	0.484467	0.603969	1.2467	1.2467	OKAY
SPG7	6.86904	5.974256	0.008555	0.015906	1.8593	1.8593	OKAY
SPP1	1.415048	0.375946	0.374997	0.7706	2.0549	2.0549	OKAY
TGFBI	0.724891	0.330266	0.605043	0.79539	1.3146	1.3146	OKAY
THBS1	4.340047	4.292355	0.049376	0.051036	1.0336	1.0336	OKAY
THBS2	9.409283	7.760355	0.001471	0.004612	3.136	3.136	OKAY
THBS3	9.512634	8.843686	0.001369	0.002177	1.5899	1.5899	OKAY
TIMP1	0.672729	0.858124	0.627319	0.55167	0.8794	-1.1371	OKAY
TIMP2	2.515796	3.324184	0.174852	0.099844	0.571	-1.7513	OKAY
TIMP3	3.019186	2.478653	0.123349	0.179412	1.4545	1.4545	OKAY
TNC	2.482001	1.961975	0.178996	0.256677	1.434	1.434	OKAY
VCAM1	6.162104	5.560844	0.013964	0.021185	1.517	1.517	OKAY
VCAN	4.37732	4.08778	0.048117	0.058811	1.2223	1.2223	OKAY
VTN	1.465153	0.746327	0.362197	0.596119	1.6458	1.6458	OKAY
ACTB	-2.417753	-2.275571	5.34338	4.841894	0.9061	-1.1036	OKAY
B2M	-0.832032	-0.459519	1.780191	1.375083	0.7724	-1.2946	OKAY
GAPDH	-1.227067	-1.249671	2.340906	2.377873	1.0158	1.0158	OKAY
HPRT1	5.610511	5.330445	0.020468	0.024853	1.2143	1.2143	OKAY
RPLP0	-1.965691	-1.805202	3.905998	3.494781	0.8947	-1.1177	OKAY
HGDC	16.815915	15.867506	0.000009	0.000017	1.9297	1.9297	B
RTC	2.69829	2.468113	0.154076	0.180727	1.173	1.173	OKAY
RTC	2.700373	2.540182	0.153853	0.171921	1.1174	1.1174	OKAY
RTC	2.72024	2.576645	0.151749	0.16763	1.1047	1.1047	OKAY
PPC	0.666397	0.624545	0.630078	0.648624	1.0294	1.0294	OKAY
PPC	0.831618	0.607965	0.561899	0.656122	1.1677	1.1677	OKAY
PPC	0.830463	0.624092	0.562349	0.648828	1.1538	1.1538	OKAY